Characterisation of the Physiological, Biochemical and Molecular Responses of Sorghum to Drought Stress

Tatenda Goche

2015276153

Thesis submitted in fulfilment of the requirements for the degree PhD in Botany in the Faculty of Natural and Agricultural Sciences, Department of Plant Sciences - Qwaqwa Campus, University of the Free State

Supervisor: Dr. Rudo Ngara

Co-supervisor: Dr. Stephen Chivasa

November 2018

DECLARATION

I, Tatenda Goche, declare that the PhD research thesis that I herewith submit for the PhD qualification in Botany at the University of the Free State is my independent work and that I have not previously submitted it for a qualification at another institution of higher education.

I, Tatenda Goche, hereby declare that I am aware that the copyright is vested in the University of the Free State.

I, Tatenda Goche, hereby declare that all royalties as regards intellectual property that was developed during the course of and/ or in connection with the study at the University of the Free State will accrue to the University.

Tatenda Goche

DEDICATION

To my nieces, Layla and Liora.

ACKNOWLEDGEMENTS

I would like to express my sincere gratitude to my supervisor Dr. Rudo Ngara for allowing me the opportunity to pursue this degree. I would also like to thank my co-supervisor Dr. Stephen Chivasa at Durham University, United Kingdom for his support throughout my research and for the iTRAQ, osmolyte and gene expression analyses of my samples. My sincere gratitude to Colleen Turnbull, Sepideh Abedi, Adrian Brown and Mahsa Movahedi for your assistance and guidance during my 4.5 months research visit at Durham University in the United Kingdom. I am also grateful for the financial support I received from the National Research Foundation, the Royal Society and the University of the Free State tuition fee bursary. Lastly I would like to thank Sellwane Moloi and the Plant Biotechnology Research Group for being great friends and colleagues.

TABLE OF CONTENTS

LIST OF TABLES

LIST OF FIGURES

LIST OF ABBREVIATIONS

1D	One-dimensional
1D-SDS-PAGE	One-dimensional sodium dodecyl sulfate polyacrylamide gel electrophoresis
2D	Two-dimensional
2D-DiGE	Two dimensional-differential gel electrophoresis
ABA	Abscisic acid
APS	Ammonium persulfate
BSA	Bovine serum albumin
CAM	Crassulacean acid metabolism
CBB	Coomassie Brilliant Blue
CD	Cell death
CHAPS	3-[(3-Cholamidopropyl) dimethylammonio]-1 propanesulfonate
DNA	Deoxy-ribonucleic acid
DTT	Dithiothreitol Cleland's reagent
EDTA	Ethylenedinitrilo-tetraacetic acid
EGRIN	Environmental gene regulatory influence networks
ESI	Electronspray ionisation
FC	Field capacity
HILIC-MS	Hydrophilic interaction liquid chromatography – mass spectrometry
hrs	hours
iTRAQ	isobaric Tags for Relative and Absolute Quantitation
kDa	kilo Dalton
LC/MS	Liquid chromatography mass spectrometry
LEA	Late-embryogenesis abundant protein
MALDI	Matrix assisted laser desorption ionisation

mins	minutes
MOPS	3-(N-Morpholino)-propanesulfonic acid
MSMO	Murashige and Skoog Basal Salt with minimum organics
MW	Molecular weight
NAA	1-naphthaleneacetic acid
NCBI	National Centre for Biotechnology Information
PAGE	Polyacrylamide gel electrophoresis
PEP	Phospho-enoyl pyruvate
pmol	picomoles
PTM	Post-translational modification
qRT-PCR	quantitative real-time polymerase chain reaction
RNA	Ribonucleic acid
ROS	Reactive oxygen species
RuBisCo	Ribulose-1,5-biphosphate carboxylase/oxygenase
RWC	Relative water content
RWL	Relative water loss
SDS	Sodium dodecyl sulfate
TAE	Tris acetate-(ethylenedinitrilo)-tetraacetic acid
TAIR	The Arabidopsis Information Resource
TCA	Trichloroacetic acid
TEMED	N,N,N',N'-Tetramethylethylenediamine
v/v	volume to volume
Vhrs	Volt hours
w/v	weight to volume

ABSTRACT

Characterisation of the Physiological, Biochemical and Molecular Responses of Sorghum to Drought Stress

Tatenda Goche
PhD thesis, Department of Plant Sciences-Qwaqwa Campus, University of the Free State

Drought is a major threat to global food security due to its detrimental effects on plant growth, productivity and yield quality. Many climatic models are predicting the increasing duration and severity of drought episodes. Therefore, understanding plant adaptive responses to drought stress is important in developing new biotechnological solutions to avert crop yield losses to drought. Sorghum (*Sorghum bicolor*) is an African indigenous crop that is well-adapted to thrive on marginal lands. This makes the crop a suitable model plant for studying adaptive responses to drought. In this study, the physiological and biochemical responses of two sorghum varieties with contrasting phenotypic traits to drought stress was analysed under drought stress. The two sorghum varieties used were the drought susceptible ICSB 338 and the drought tolerant SA 1441. The sorghum plants were grown in soil until the V3 growth stage before withholding water for 8 days, re-watering and then assessing the physiological changes following the drought stress treatment. Physiological analyses of the plants revealed striking differences between the sorghum varieties. The growth parameters of both roots and shoots exhibited more tolerance related responses in the drought-tolerant variety, while the susceptible variety was adversely affected and had poor recovery after re-watering. The leaf relative water content, stomatal conductance and chlorophyll content, supported the observed physiological adaptations. The analysis of proline and glycine betaine

showed that there was an increase in the accumulation of the two omolytes in response to drought stress. The drought tolerant variety showed significantly higher osmolyte accumulation earlier than the drought susceptible variety in both root and shoot tissue. The isobaric tags for relative and absolute quantitation (iTRAQ) analysis was used to identify drought-stress responsive root proteins in the two sorghum varieties. In the root proteome, 1169 and 1043 proteins were positively identified for ICSB 338 and SA 1441 sorghum varieties, respectively. Of these proteins, 237 and 184 were drought responsive for ICSB 338 and SA 1441, respectively. A large proportion of the proteins are involved in disease/defence (26% for ICSB 338 and 23% for SA 1441) followed by metabolism (25% for ICSB 338 and 21% for SA 1441). To validate gene function, eight proteins with the highest fold-change in response to drought were selected for gene expression analysis using quantitative real time-polymerase chain reaction (qRT-PCR). The results showed that all the genes evaluated were drought stress responsive. In order to develop the eight target genes as drought markers, their expression was analysed in cell suspension cultures of White sorghum and ICSB 338 with and without sorbitol treatment. The gene expression analysis showed that seven of the eight drought responsive genes could distinguish between White sorghum and ICSB 338 in the cell suspension culture system without sorbitol treatment. In addition, all the eight genes could distinguish between White sorghum and ICSB 338 in response to the sorbitol-induced osmotic stress. Following this, the responses of the genes to heat stress was analysed in the White sorghum cell suspension cultures. The results showed that seven of the genes were also heat responsive. These genes are recommended for use as drought markers in marker assisted selection for drought tolerance. As proof-of-concept and to develop a workflow for the use of the drought markers in other crops, three published genes from our research group were used. Four Arabidopsis (*Arabidopsis thaliana*) homologues of each sorghum gene were selected for gene expression analysis. The results showed that there is differential gene expression

between homologues of the same gene in response to osmotic stress. In conclusion, the comparative sorghum physiological, biochemical, protein and gene expression data generated in this study forms a foundation for further sorghum molecular studies. Furthermore, the drought marker genes toolkit developed in this study can be utilised by plant breeders in marker assisted selection for the improvement of agriculturally important crops against drought.

Keywords: Sorghum, Arabidopsis, drought stress, proteomics, cell suspension culture, 2D-DiGE, iTRAQ, qRT-PCR, gene expression, drought markers.

CHAPTER 1

LITERATURE REVIEW

1.1 The Production, Uses and Importance of Cereal Crops

Cereals such as maize (*Zea mays*), sorghum (*Sorghum bicolor*), pearl millet (*Pennisetum glaucum*), wheat (*Triticum aestivum*) and rice (*Oryza sativa*) are the mainstay of diets in many countries, mostly in sub-Saharan Africa (Alexandratos *et al*., 2012). Their demand has increased with the corresponding increase in world population. The production quantity, harvested area and yield of cereal crops has subsequently increased by 2.5%, 0.5% and 1.8%, respectively from 2000 to 2013 (OECD/Food and Agriculture Organization of the United Nations, 2015). Subsequently, cereals make up the majority of crop sector production, worldwide with 106 million tons having been produced from 98.6 million ha in 2015 (Macauley, 2015).

1.2 Sorghum and its Uses

Sorghum (Figure 1.1) is an herbaceous annual short day plant with a C_4 photosynthetic pathway (Rosenow *et al.*, 1983). It is known by common names such as milo, kafir and guinea corn in different parts of the world. Plants with a C_4 photosynthetic pathway produce greater biomass and yield per unit of water transpired compared to C_3 plants (Erickson *et al*., 2012). One of the major strengths of sorghum is the ability to grow in tropical, sub-tropical, temperate and semi-arid regions (Nathan, 1978; Jackson and Arthur, 1980). This highly adaptive tolerance to multiple environments makes it a crop of universal value (Kimber *et al*., 2013). In order of importance and production among cereal crops, sorghum is ranked fifth in the world after wheat, rice, maize and barley (*Hordeum vulgare*) (Pocketbook, 2015).

Figure 1.1: Image of sorghum crop stand (PlantVillage, 2018).

The utility of sorghum is fairly diverse ranging from food, feed, fibre, biofuel to building material (Almolares *et al*., 1999; Kimber *et al*., 2013). As a food crop, sorghum has a good nutritional value consisting of 70-80% carbohydrates, 11-13% gluten free protein, 2-5% fat, 1-3% fibre and 1-2% ash (Plessis *et al*., 2015). It is a staple food of over 500 million people in more than 30 countries of the semi-arid tropics (Dahlberg *et al*., 2012). In addition, surplus sorghum is most suitable as animal feed owing to its low production cost and high nutrient quality in comparison to alternatives such as maize (Jackson and Arthur, 1980; Alexandratos and Bruinsma, 2012). Sorghum is naturally drought tolerant (Rosenow *et al*., 1983) with a wide genetic diversity (Motlhaodi *et al*., 2017). This makes the crop a potential model system in abiotic stress studies (Ngara and Ndimba, 2014).

1.3 Plant Abiotic Stresses

An abiotic stress is any factor exerted by the environment on the optimal functioning of an organism (Cramer and Nowak, 1992; Vahdati and Leslie, 2013). Examples of abiotic stresses that significantly affect plant growth and development are drought, temperature extremes, salinity, nutrient deficiency or toxicity, soil pH (Wang *et al*., 2003b; Ahmad and Prasad, 2011), excess light and increased soil hardness (Verslues *et al*., 2006). Generally, abiotic stresses on plants cause a combination of physiological, biochemical and molecular changes in plants that adversely affect growth (Jaleel *et al*., 2009; Vahdati and Leslie, 2013). The resulting low biomass production as well as reduced grain yield pose a major threat to agricultural productivity and food security.

1.4 The Complexity of Abiotic Stress Responses in Plants

Plant responses towards abiotic stresses are a complex phenomenon involving morphological, physiological, biochemical and molecular mechanisms at both cellular and whole plant levels (Farooq *et al*., 2009). Different abiotic stress response pathways can possess potential 'sites' for crosstalk. Crosstalk refers to a convergence in signalling or response pathways, which may include two pathways interacting to achieve a similar outcome in either an additive or negatively regulatory way (Knight and Knight, 2001; Roychoudhury *et al*., 2013). An example of crosstalk within drought and cold stress responses (Shinozaki *et al*., 2003) is illustrated in Figure 1.2 below. The diagram shows the gene expression regulatory network in response to drought and cold stresses. From the diagram, the open double-headed arrow is showing crosstalk between dehydration-responsive element binding proteins (DREB2) and abscisic acid-responsive element binding protein/ abscisic acid-responsive element binding factor (AREB/ABF). Both specific and interlinked pathways are shown in the abscisic acid (ABA)-dependent and ABA-independent drought and cold stress response networks.

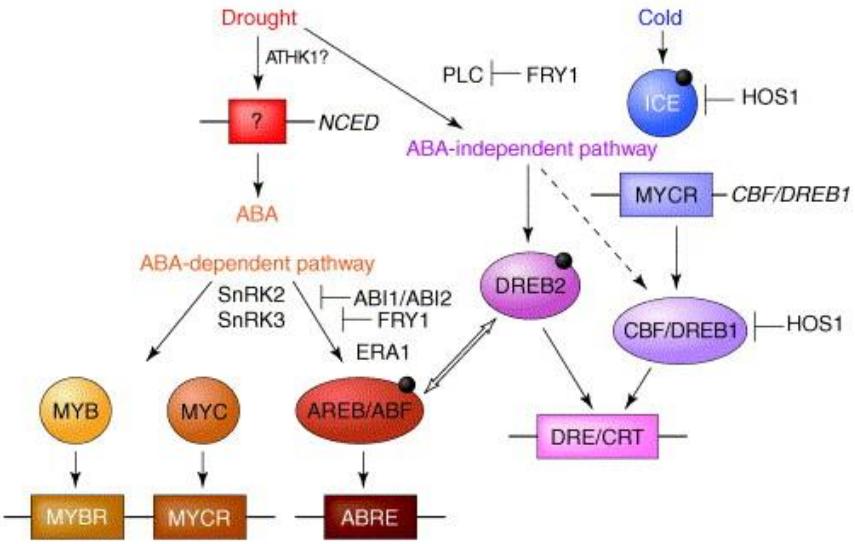

Figure 1.2: Gene expression regulatory network in response to drought and cold stress illustrating specificity and cross-talk. Transcription factors that control stress-inducible gene expression are shown in circles or ovals. Small shaded circles indicate the modification of transcription factors in response to stress signals for their activation, such as phosphorylation. The upper part of the figure shows transcription cascades that are involved in rapid and emergency responses to drought and cold stresses, such as those involving inducer of C-repeat binding factor expression (ICE), DREB2 or 9-cis-epoxycarotenoid dioxygenase (NCED). Lower parts of the figure show transcription cascades that are involved in slow and adaptive processes in stress responses, such as those involving AREB/ABF, MYB, MYC and CBF/DREB1. The open double-headed arrow suggests crosstalk between DREB2 and AREB/ABF that is based on DRE/CRT acting as a coupling element for ABRE (Shinozaki *et al*., 2003).

Wilkins *et al*. (2016), analysed environmental gene regulatory influence networks (EGRINs) in rice in response to different abiotic stresses and concluded that water deficits and high temperatures shared various pathways. In another study, more than half of the drought responsive genes were also triggered under both salinity and ABA treatments (Seki *et al*., 2001; Seki Motoaki *et al*., 2002). This suggests the possibility of similar responses to

different stresses. Furthermore, osmotic and oxidative stresses are secondary stresses common to drought, cold, salinity, heat and chemical pollution (Wang *et al*., 2003a). These secondary stresses disrupt the osmotic and ionic homeostasis of cells and also damage proteins, nucleic acids as well as membranes (Figure 1.3). In essence, it would be difficult to completely isolate unique stress response mechanisms due to this crosstalk between pathways. Nevertheless, plants respond to these stresses by synthesising genes involved in signalling perception and transduction, and the activation of stress responsive genes and proteins (Shinozaki and Yamaguchi-Shinozaki, 2000). This study focuses on drought stress and is effects on plants.

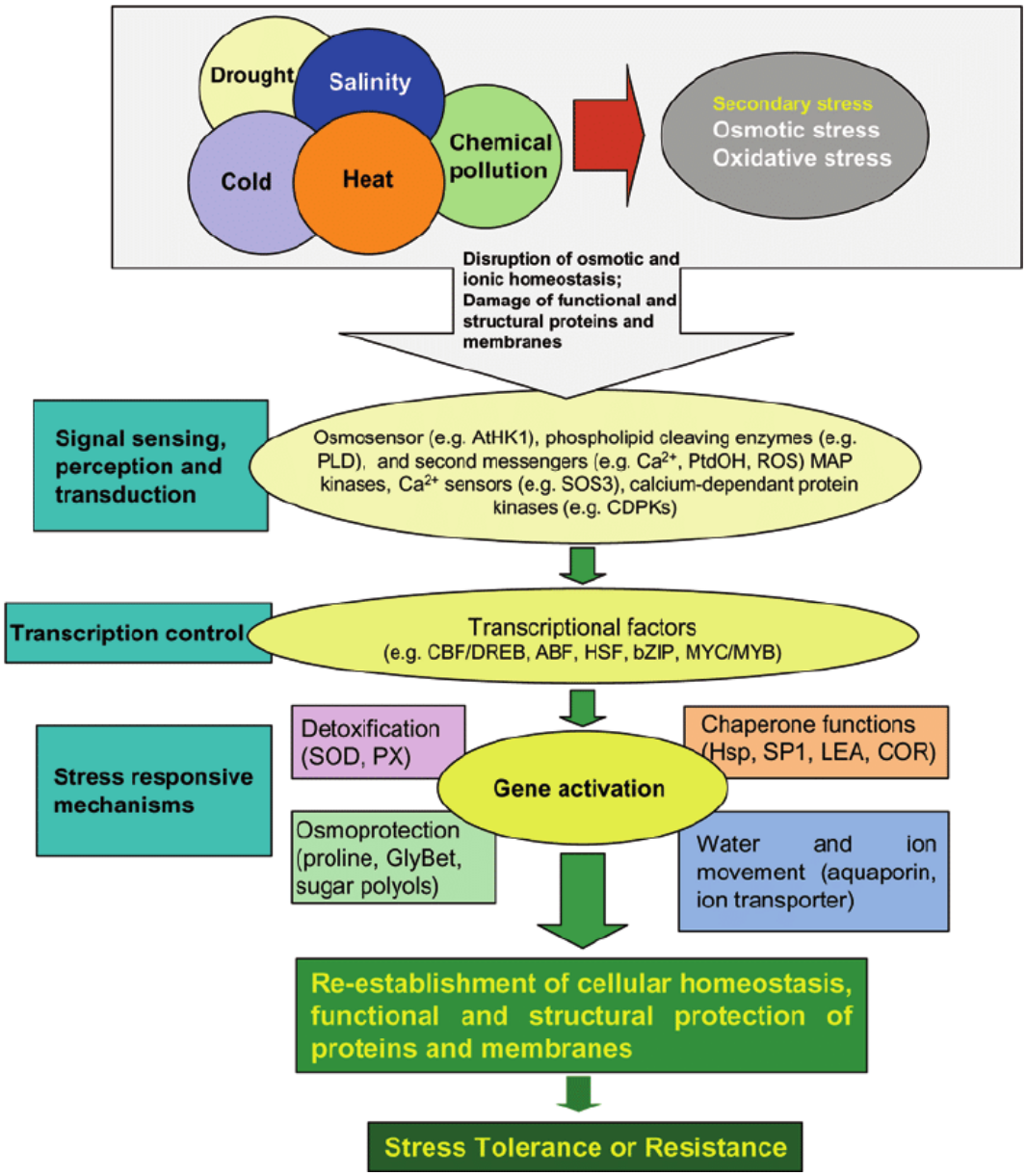

Figure 1.3: The complexity of plant responses to abiotic stresses (Wang, 2003a).

1.5 Drought Stress

Drought stress, sometimes referred to as water or osmotic stress, is defined as insufficient soil moisture to meet the needs of a crop at a particular time (Blum, 2009; Salekdeh *et al*., 2009). It occurs as a result of drastic temperature increases, drying up of previously moist areas, and low or erratic rainfall patterns. Many climatic models are predicting increased frequency and duration of drought episodes in the immediate to long-term future (Anjum *et al*., 2011; Pocketbook, 2015). Apart from water scarcity, climate change is also predicted to increase the incidence of floods and elevated surface temperatures (OECD-FAO Agricultural Outlook 2015-2024, 2015), which all negatively affect plant growth and development. Consequently, drought and other abiotic stress factors are major threats to global food security due to their detrimental effects on plant growth, productivity and yield quality (Yang *et al*., 2015b). Therefore, crops which are better adapted to these abiotic stresses are required to counter the negative effects of climate change and maintain adequate food provision for the growing population.

1.5.1 Plant Responses to Drought Stress

Plants are sessile organisms, which need to adjust to constantly changing environmental conditions. Plant responses to abiotic stresses are thus complex, involving morphological, physiological, biochemical and molecular changes at both cellular and whole plant levels (Farooq *et al*., 2009). In many cases, the molecular responses are synchronised across several cell layers in the same tissue or across different tissues and organs. Such coordinated responses require cell-to-cell communication, which is mediated by mobile signals transmitted through the plasmodesmata or secreted into the extracellular matrix (Isaacson *et al*., 2006).

During periods of water deficits, plants attempt to maintain essential processes at the expense of non-life threatening ones. This is because the plant functions as a system that self regulates in periods of stress. Generally, drought impairs seed germination (Harris *et al*., 2002), mainly because water is required for imbibition and activation of enzymes to initiate mitosis, cell expansion and elongation. The disruption of any of these processes translates to reduced plant growth, and yield (Harris *et al*., 2002). Furthermore, plants exhibit reduced leaf number and size, reduced stem elongation and increased root proliferation in response to drought stress (Farooq *et al*., 2009). The declining leaf area reduces the surface area for photosynthesis and ultimately plant growth. Conversely, an increase in root proliferation during periods of water stress is due to the plant's ability to allocate photo-assimilates towards root growth in order to capture soil moisture from deeper levels (Blum, 2005).

Plants also respond to the detrimental effects of drought stress by synthesising the stress-signalling phytohormone ABA (Ackerson and Radin, 1983; Davies *et al*., 1986). The accumulation of ABA results in stomatal closure, thus reducing transpirational water loss and its deleterious effects on plant growth (Ludlow and Muchow, 1990; Cornic and Massacci, 1996). Once the required response has been elicited, the ABA concentrations return to basal levels (Seiler *et al*., 2011). ABA dependent and ABA independent pathways operate in regulating the expression of osmotic stress responsive genes (Yamaguchi-Shinozaki and Shinozaki, 2006). These genes are responsible for the expression of stress response proteins, such as chaperones, enzymes for osmolyte biosynthesis, late embryogenesis abundant (LEA) proteins, channel and signalling proteins (Mahajan and Tuteja, 2005). Although stomatal closure leads to reduced transpirational water loss, it also reduces gaseous exchange, thus resulting in the reduction of photosynthesis as demonstrated by Baldocchi *et al*. (1985), in soybean (*Glycine max*). Reduced photosynthesis means that fewer photo-assimilates are produced, leading to an overall diminished plant growth (Anjum *et al*., 2011).

1.5.2 Osmolyte Accumulation in Stressed Plants

One of the plant responses to drought stress is the synthesis and accumulation of osmolytes. Osmolytes are low molecular weight metabolites synthesised as an inherent mechanism of osmotic adjustment in stressed plants (Di Martino *et al*., 2003). Plants accumulate either organic or inorganic solutes in the cytosol, primarily to lower water potential and maintain turgidity (Hamilton and Heckathorn, 2001). Inorganic solutes such as K^+, Na^+ and Cl^- are usually compartmentalised during osmotic stress because their accumulation interferes with cellular activities (Hasegawa *et al*., 1986). Solutes whose accumulation does not interfere with cellular function are termed compatible solutes. The most common compatible solutes synthesised by plants under abiotic stress include amino acids (proline, glycine), sugars (mannitol, sorbitol, sucrose, trehalose), polyols (glycerol, inositol, sorbitol) and their derivatives (methyl-inositol), quaternary ammonium compounds (glycine betaine) and tertiary sulphodium compounds (Di Martino *et al*., 2003; Valadez-Bustos *et al*., 2016).

Under drought stress, the accumulation of osmolytes maintains turgidity in plant cells, minimising interruption of cellular metabolism whilst sustaining growth (Blum, 2005; Amrhein *et al*., 2013). Various studies have been conducted to illustrate the change in osmolyte content in plants under drought stress. For example, Tully *et al*. (1979) observed increases in proline content under drought stress in barley leaf tissue. A comparative study between the leaf tissue of chickpea (*Cicer arietinum*) cultivars with contrasting responses to drought stress was carried out. The results showed that the drought tolerant variety accumulated higher proline content compared to the drought sensitive variety (Mafakheri *et al*., 2010). Other studies in leaf tissue of crops such as peanut (*Arachis hypogaea*) (Quilambo and Scott, 2004), and pea (*Pisum sativum*) (Alexieva *et al*., 2001) showed an increase in proline content in response to drought stress. In sorghum leaf tissue, drought tolerant varieties

accumulated higher proline levels compared to drought susceptible varieties in response to drought stress (Sivaramakrishnan *et al*., 1988).

1.5.3 Drought Induced Reactive Oxygen Species Accumulation in Plants

Plants have evolved an efficient enzymatic antioxidative system that protects cellular components against oxidative damage and maintains reactive oxygen species (ROS) at optimum levels for signal transduction (You and Chan, 2015). The enzymes responsible for ROS-scavenging and detoxification in plants include superoxide dismutase, ascorbate peroxidase, catalase, glutathione peroxidase, monodehydroascorbate reductase, dehydroascorbate reductase, glutathione reductase, glutathione S-transferase, and peroxiredoxin. All these enzymes function in detoxifying ROS in different sites where they are located (Noctor *et al*., 2014). Besides the enzymatic scavengers of ROS, non-enzymatic antioxidants such as glutathione, ascorbic acid, proline, carotenoids, tocopherols and flavonoids are also responsible for maintaining ROS homeostasis in plants (Gill and Tuteja, 2010). These systems are switched on following the onset of drought stress. There are many studies that illustrate increases in ROS accumulation in response to drought stress in crops such as rice (Boo and Jung, 1999), wheat (Loggini *et al*., 1999), pea (Moran *et al*., 1994) and sunflower (*Helianthus annuus*) (Sgherri and Navari-Izzo, 1995). Increases in non-enzymatic antioxidant systems such as ascorbic acid and glutathione in response to drought stress were reported in *Diosporus spp* root tissue (Wei *et al*., 2015), while glutathione reductase and superoxide dismutase were also shown to increase in response to salinity and drought stresses in monocots of the genus *Juncus* (Al Hassan *et al*., 2017).

1.5.4 Metabolic Adaptations of Plants to Drought Stress

Metabolic adaptation also plays an important role in maintaining plant cellular homeostasis in periods of drought. Plants which possess a C_4 photosynthetic pathway produce greater biomass and yield per unit of water transpired compared to C_3 plants (Erickson *et al*., 2012) and are thus better adapted to hot and dry environments. Such plants possess bundle sheath cells which accumulate CO_2 in the form of malate (Edwards and Walker, 1983). The C_4 photosynthetic pathway is also more efficient in CO_2 use because it utilises the enzyme phospho-enoyl pyruvate (PEP) carboxylase instead of the ribulose biphosphate carboxylase oxygenase (RuBisco) as the first CO_2 acceptor (Lambers *et al*., 2008). PEP carboxylase has a higher affinity for CO_2 compared to RuBisCO and does not fix O_2. Therefore, the energy consuming photorespiration process does not occur in C_4 plants (Stern *et al*., 2000). An example of a C_3 plant is rice whilst C_4 plants include sorghum and maize.

Another photosynthetic pathway that makes plants survive drought conditions is the crassulacean acid metabolism (CAM) pathway. In this pathway, carbon fixation occurs during the night when the stomata are open to form 4-carbon acids (Monson and Fall, 1989). During the day these acids are broken down to pyruvate and CO_2 in the presence of light and photosynthesis occurs (Monson and Fall, 1989). Plants with the CAM photosynthetic pathway are mainly succulent plants like cactus, which need to survive in semi-arid to arid environments. Compared to C_4 plants, however, CAM plants have extremely high rates of water use efficiency but lower photosynthetic rates (Stern *et al*., 2000). Some of the roles of signalling pathways are outlined in Section 4.1.

1.5.5 Sorghum Responses to Drought Stress

The responses of sorghum to drought stress are complex. Sorghum varieties in drought prone environments have more developed water saving mechanisms such as dense, extended root systems as a way of facilitating survival during periods of water scarcity (Schittenhelm and Schroetter, 2014). Drought tolerant and resistant sorghum varieties thus exhibit greater root weight, root volume, and root/shoot ratios compared to their drought susceptible counterparts (Nour and Weibel, 1978). The increase in shoot/root dry matter ratios, however, is not necessarily due to increased root mass but due to reduced shoot growth and mass (Blum, 2005).

According to Merrill and Rawlins (1979), the sorghum plant directs resources to deeper soil penetration through higher root density in the deeper soil profile during drought stress. This is in agreement with Blum and Arkin (1984), where a higher root concentration was observed at the shallow top soil layers in well-watered plants. In contrast, drought stressed sorghum plants, had a more homogeneous root distribution within all the soil layers. Reverse water flow is also an important mechanism in dry soils especially where plants need to access nutrients from the dry top soil. Xu and Bland (1993), demonstrated that sorghum can extract water from deep soil levels via an elongated root system and subsequently efflux the water to the dry upper soil layers before resuming uptake again. This adaptation ensures that the sorghum plants can access mineral nutrients even in hot and dry conditions.

Apart from root morphology and growth patterns, the plant's water status, and its photosynthetic and antioxidant capacity under drought stress are all important aspects to consider when evaluating a crop's tolerance to water stress. According to Zhang and Kirkham (1996), the chlorophyll content and relative leaf water content were higher for sorghum compared to sunflower under drought stress. Only after 7-8 days of withholding water was

the level of antioxidant enzymes, non-enzymatic antioxidants (ascorbate, glutathione, carotenoids) and malondialdehyde affected in sorghum. For sunflower, the responses were detected earlier at days 5-6 following drought stress. Although these changes were not consistently higher for sorghum compared to sunflower, the authors concluded that antioxidant responses differ between the two species and the onset of responses is much delayed for sorghum compared to sunflower (Zhang and Kirkham, 1996).

Sorghum has been shown to allocate water to younger, more productive upper leaves compared to older leaves during water stress as a way of using the limited water more efficiently during the vegetative stage (Blum and Arkin, 1984; Blum, 2010). Under drought stress with soil moisture below 20%, the rate of transpiration for sorghum is mainly controlled by the reduction in total leaf surface area through leaf senescence (Blum and Arkin, 1984). Furthermore, leaf rolling in sorghum causes partial shading of the leaf, thus reducing both the surface area exposed to light and the rate of transpiration.

The two most sensitive stages of sorghum to drought stress with respect to grain filling are the pre- and post-flowering stages (Borrell *et al*., 1999). Some sorghum varieties are thus pre-anthesis drought tolerant whilst others are post-anthesis drought tolerant. The ability of a sorghum plant to maintain a green leaf phenotype during grain filling is a vital drought adaptation trait (Borrell *et al*., 1999). Borrell *et al*. (1999), exposed sorghum hybrids to post-anthesis drought and concluded that hybrids possessing the stay green trait had a significant yield advantage over those which did not. However, the genetic and physiological mechanisms that form the basis for the stay green trait are yet to be fully understood.

Johnson *et al*. (2015), investigated gene expression differences between a stay green and a senescent sorghum variety using microarray analysis. They observed increased gene expression of delta1-pyrroline-5-carboxylate synthase 2 (*P5CS2*), a proline biosynthetic

enzyme in the stay green variety compared to the senescent variety. This correlated with higher proline levels in the stay green variety. Furthermore, the *P5CS2* gene was found to lie within the Stg1 QTL region (Johnson *et al*., 2015) and could possibly be a diagnostic marker gene for the stay green trait in sorghum.

The presence of the stay green (*stg*) quantitative trait loci (QTL) in sorghum leads to decreased tillering and reduced upper leaf size. Decreased tillering greatly reduces the canopy size at anthesis under terminal drought (Borrell *et al*., 1999). This strategy reduces transpirational leaf surface area resulting in soil water conservation for use during grain filling (Burch *et al*., 1978). Such responses ultimately results in higher biomass post anthesis and increased grain number and yield (Borrell *et al*., 1999). Another drought stress adaptation exhibited by sorghum is the use of lesser soil water before anthesis (Burch *et al*., 1978; Borrell *et al*., 1999). This physiological adaptation can be attributed to low axial hydraulic conductance due to the increased deposition of lignin and suberin in the hypoderm and endodermis of stressed sorghum plants (Cruz *et al*., 1992).

Sorghum also responds to drought stress through the accumulation of osmolytes and epicuticular wax. The most common compatible solutes found in sorghum in response to drought stress are soluble carbohydrates, amino acids, organic acids and betaines (Yang *et al*., 2003; Anjum *et al*., 2011). Sorghum varieties selected for osmotic adjustment gave high grain yield and also developed greater root length, higher soil water extraction ability and greater dry weight compared to those of low osmotic adjustment under drought stress (Santamaria *et al*., 1990). The epicuticular wax in sorghum accumulates on the abaxial or adaxial leaf surfaces, and lowers leaf surface temperatures due to their light reflectance ability (Johnson *et al*., 1983). Jordan *et al*. (1984), reported that an epicuticular wax load of greater than 0.067 g m^{-2} is an effective barrier against water loss in sorghum under any

condition. Furthermore, Hamissou and Weibel (2004), reported that the presence of epicuticular wax cover reduces transpirational water loss. Burow *et al.* (2009), successfully mapped the locus of *BLOOM-CUTICLE (BLMC)*, which is associated with high cuticular wax production. An increase in plant death rating was also observed in the mutants with less epicuticular wax production. An increase in plant death rating was also observed in the mutants with less epicuticular wax.

Plant responses to drought stress can also be analysed on a protein and/or gene level. The identification of drought responsive proteins and the functional validation of the corresponding genes could assist in the understanding the molecular mechanisms of drought response pathways in plants.

1.5.6 Combined Heat and Drought Stress

High temperatures accompanying drought leads to high plant tissue temperatures. This ultimately leads to heat stress due to the unavailability of water to meet the evaporative demand (Grill and Ziegler, 1998). Although heat and drought stress episodes almost always occur combined under field conditions, the majority of studies have focused on independent heat or drought stress (FAO, 2015). Due to the biological cross-talk between the two stress responses, mostly emanating from common responses such as closure of stomata, suppression of photosynthesis, increased leaf temperature and ROS accumulation, the plant responses to these stresses are similar. In spite of this study focusing on drought stress, the combined heat and osmotic stress analysis is performed *in vitro* in order to further develop heat and drought marker genes.

1.6 Proteomics

The proteome is defined as the entire protein complement of a cell, tissue or organism under defined conditions (Blackstock and Weir, 2003). Accordingly, proteomics refer to the

systematic analysis of protein populations in a tissue, cell or subcellular compartment (Van Wijk, 2001). Proteomics is a field of study which began with the introduction of two-dimensional gel electrophoresis (2DE) in 1975 (O'Farrell, 1975). There was relatively low activity in the field then until the sequencing of the human genome and the development of electrospray ionisation (ESI) and matrix assisted laser desorption ionisation (MALDI)-based mass spectrometry MS (Aebersold and Munn, 2003).

The improvements in the sensitivity of 2DE together with protein detection and quantification methods, mass spectrometry, genomics and bioinformatics led to an increase in proteome analyses (Salekdeh and Komatsu, 2007). Proteomics also assists in elucidating the role of post-translational modifications (PTMs), protein interactions and novel gene identifications thus making it a vital tool for global phenotypic characterisation (Hu *et al*., 2016). Although early efforts were focused on human and yeast studies mainly because of the availability of genomic data (Bradshaw, 2008), plant proteomics is also now advancing. With the genomic sequence of sorghum being complete (Paterson *et al*., 2009), it is expected that linked proteomic studies will also gradually increase.

1.6.1 Plant Proteomics

1.6.1.1 Gel Based Proteomics

The breadth of methods used to quantitatively study proteomes is increasing. However, 2DE remains the mostly used method (Klose *et al*., 2002). Proteomic changes during different growth and developmental stages of plants as well as the analysis of differentially expressed proteins under both biotic and abiotic stresses are some of the most widely studied.

The first dimension (1D) of protein analysis involves the separation of proteins according to their net charge through isoelectric focusing. The second dimension (2D) follows, which involves the separation of proteins according to molecular weight using SDS-PAGE. The

immobilised pH gradient (IPG) strips with resolved proteins previously used in the first dimension are applied to the second dimension gels and electrophoresed. Sodium dodecyl sulphate coats proteins according to their mass and proteins subsequently migrate as ellipsoids with a uniform negative mass charge to mass ratio (Garfin, 1995). In the 2D-based gel electrophoretic method, thousands of tissue or subcellular proteins can be separated in one gel run. Various protein spot visualisation methods are available and these range from visible stains such as Coomassie brilliant blue and silver to fluorescent stains such as Sypro Ruby. However, the major disadvantages of gel based proteomics remains the inability to detect low abundant proteins and gel-to-gel variation (Zhou *et al*., 2005).

In order to reduce these limitations in gel based proteomics, two dimensional-differential gel electrophoresis (2D-DiGE) was developed (Rabilloud and Lelong, 2011). 2D-DiGE allows the labelling of up to three samples with Cy dyes and thus reduces the gel-gel variation that exists in the traditional 2DE. 2D-DiGE has been performed in comparative proteome studies in sorghum (Jedmowski *et al*., 2014), maize (Vidal *et al*., 2015) and barley (Wendelboe-Nelson and Morris, 2012) among others. This method is however laborious and time consuming. The use of non-gel based methods for proteome analysis addresses some of the challenges of gel-based proteomics.

1.6.1.2 Non-gel Based Proteomics

1.6.1.2.1 Protein Labelling for Mass Spectrometry vs Label-free Approaches

Non-gel based approaches in proteomics utilise liquid chromatographic (LC) separation techniques coupled with tandem mass spectrometry (MS/MS). The samples may be labelled or unlabelled as in label free approaches. Various methods can be utilised in order to label samples by introducing isotopes at either protein or peptide level for mass spectrometry based analysis. These comprise of amino acid based labelling, N-terminal peptide labelling of the

epsilon-amino group of lysine residues and C-terminal peptide of glutamic or aspartic acid residue labelling (Goodlett *et al*., 2001). Amino acid based labelling consists of isotope coded affinity tag (ICAT), visible isotope coded affinity tag (VICAT), mass coded abundant tagging (MCAT) and quantitation using enhanced signal tags (QUEST). The N-terminal category of labelling are realised by utilising the N-hydroxysuccinimide (NHS) chemistry as well as active esters. The N-terminal labelling method consists of the isobaric tags for relative and absolute quantitation (iTRAQ) (Ross *et al*., 2004), tandem mass tags (TMT) (Thompson *et al*., 2003) and global internal standard technology (GIST). The C-terminal peptide labelling methods include esterification using deuterated alcohols (Goodlett *et al*., 2001).

The ICAT method was the first quantitative based approach to be introduced (Gygi *et al*., 1999). The ICAT method is perhaps the most characterised approach and consists of three components, namely thiol functional groups, a linkage group and a biotin moiety for affinity purification of the previously cysteine-derivatised peptides. The main disadvantage of ICAT is that only two sample labels are available. Therefore the analysis of various samples at the same time is impossible. Furthermore, ICAT is unsuitable for the analysis of samples which do not contain cysteine residues such as phosphopeptides (Ross *et al*., 2004). These challenges led to the development of the 2- or 4-plex isotope coded affinity tag (ICAT), 4- or 8-plex iTRAQ (Ross *et al*., 2004) and 2- or 6-plex tandem mass tag (TMT) (Thompson *et al*., 2003) based techniques.

Label-free based approaches of protein quantification represents a strategy which avoids the isotope labelling step. Two categories utilised in label-free based measurements are peak area and spectal counting. Peak area is a method that measures the quantity of analytes from the integrated peak area from the the extracted ion chromatogram (EIC). The method relies on the principle that the detected ion signal is positively proportional to the analyte

concentration by ESI within a certain range when coupling with LC. On the other hand, spectral counting represents a method based on the observation that there is typically positive correlation between protein abundance and the number of its proteolytic peptides and vice versa (Fan *et al*., 2010). Although MS/MS-based gel-free label-free approaches and isotopic labelling methods work equally well especially where accuracy is important, the former is generally underutilised (Leroy *et al*., 2012). This may be because isotopic labelling exhibits greater precision in comparison to label-free workflows. However, since MS-based label-free approaches have been adapted to support absolute quantitation (Silva *et al*., 2016), such approaches are expected to increase in utility. This study utilises the iTRAQ method, which is a gel-free label-based workflow.

1.6.1.2.2 iTRAQ Analysis

The iTRAQ method is based on the tagging of primary amines, that is, the N-terminal based labelling (Ross *et al*., 2004). The iTRAQ reagents are multiplexed, amine specific and of a stable isotope nature and allow both relative and absolute identification and quantitation (Martínez-Esteso *et al*., 2014). The iTRAQ reagents currently in use are the 4-plex (114, 115, 116 and 117) or 8-plex which includes the 113, 118, 119 and 121 in addition to the 4-plex reagents. This allows the tracking of multiple samples, up to eight, in an LC-MS run or the following of biological systems of a time course nature. An example of the iTRAQ workflow is shown in Figure 1.4 for rice root tissue (Wang *et al*., 2014). Protein is extracted from the samples followed by a series of steps where the precipitated protein is reduced, alkylated and digested. Sample labelling, pooling, fractionation by LC-MS/MS ensures protein identification and quantitation.

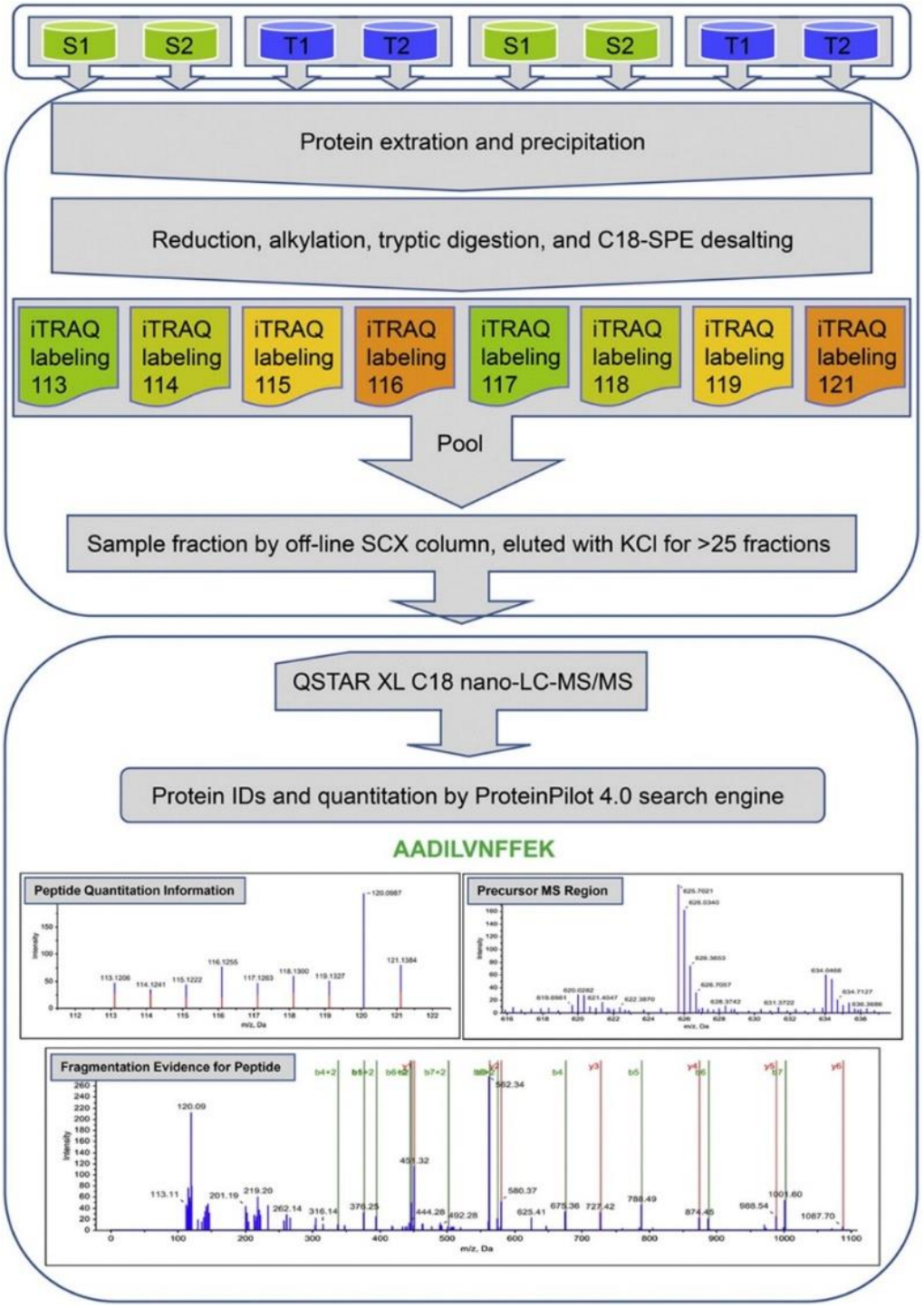

Figure 1.4: A workflow for analysis of protein expression in rice roots by 8-plex isobaric tagging (Wang *et al*., 2014).

1.6.1.2.3 iTRAQ Analysis in Plant Biotic and Abiotic Stress Studies

The iTRAQ method is being increasingly used in various plant biotic and abiotic stress studies. This is mainly because the technology is a more efficient way for protein identification and quantitation compared to the traditional 2DE. The 2DE is unable to identify proteins which are in low abundance, too hydrophobic, extremely small/large, as well as extremely acidic/basic (Zieske, 2006). Crops in which the iTRAQ technology has been applied include sorghum (Zhou *et al*., 2016), rice (Wang *et al*., 2014; Chen *et al*., 2016), tobacco (*Nicotiana tabacum*) (Zhong *et al*., 2017), soybean (Li *et al*., 2016a), maize (Yu *et al*., 2016), faba bean (*Vicia faba*) (Cao *et al*., 2017) among others. The increase in the use of this technology also lies in its accuracy at quantitation, ability to analyse from 4 up to 8 samples and its high resolution power (Bindschedler and Cramer, 2010).

1.6.2 Plant Root Proteomics and Gene Expression Analysis

The first plant organ to detect a deficit in water supply to the plant is the root system (Ghatak *et al*., 2016). Roots send both water and minerals through the xylem sap to aerial parts of the plant. In addition, it has been shown that roots also send molecular signals using the same mechanism (Davies *et al*., 1986). ABA, a vital root-shoot stress signal, is transmitted through the xylem sap (Hartung *et al*., 2002). When the signal reaches the leaf tissue, stomatal closure is effected as a water saving mechanism. However, gaseous exchange is also hindered in the process. For these reasons, it is important to study the responses of roots to drought stress.

Comparative differential root proteome expression analysis has been performed in tomato (*Solanum lycopersicum*), where cellular metabolic activity and protein biosynthesis was suppressed by drought stress (Zhou *et al*., 2013). Post-transcriptional regulation and protein translation were shown to be high in the drought resistant variety compared to the drought susceptible tomato variety. In another study, wild peanut (*Arachis duranensis*) was exposed

to drought stress and 31 root proteins unique to drought stress perception were identified (do Carmo *et al*., 2018). These included chitinase 2, an MLK like protein, a glycine-rich protein DOT 1-like, a muturase A and heat shock-related proteins. Gene expression analysis was also carried out for all the genes corresponding to the drought responsive proteins in root tissue using qRT-PCR. A total of 15 of the genes were up-regulated, while 14 genes were down-regulated in root tissue in response to drought stress (do Carmo *et al*., 2018).

In sorghum, previous investigations into the proteome profiles of drought susceptible and tolerant varieties have focused on the leaf tissue (Jedmowski *et al*., 2014). Currently, there are no comparative proteomic studies between the root tissue of sorghum varieties with contrasting responses to drought stress. This study will therefore provide information which could be useful in understanding sorghum root proteome changes under drought stress. Model plant systems such as Arabidopsis (*Arabidopsis thaliana*) are also important in drought stress studies. This is because model plant systems are easier to manipulate and have well characterised genetic tools.

1.7 The Use of Model Plant Systems in Plant Abiotic Stress Studies

Model plant systems have been used to obtain knowledge on the molecular and biochemical responses of plants to biotic and abiotic stresses (Ngara and Ndimba, 2014). Historically, Arabidopsis, maize and rice have been utilised as plant model systems in a range of studies. This has resulted in knowledge gains in numerous plant growth and developmental processes. Arabidopsis is currently still the leading model plant system in the plant 'omics' studies.

Arabidopsis is a flowering plant native to Eurasia. The plant is an important model system for gene identification and function (Rensink and Buell, 2004). The low content of repeated DNA, low level of methylation, efficient chemical and radiation mutagenesis, short generation time, large number of seeds and relatively smaller genome (Koornneef and

Meinke, 2010), makes Arabidopsis an appropriate model for molecular biology. Since the publication of the complete genome sequence of Arabidopsis (The Arabidopsis Genome Initiative, 2000), it has been easier to manipulate the sequenced genome for gene functional studies. More importantly, there are many gene knockout mutant lines available to the scientific community. The availability of vast numbers of natural accessions adapted to varying environments also contributes to the advantages of using Arabidopsis in stress response studies (Weigel, 2012).

The utilisation of a model plant system, such as Arabidopsis, is an invaluable method for validating crop gene function. Over-expression analyses have been successfully done to validate gene function. For instance, Yu *et al*. (2006) over-expressed the sorghum gene *SbSTS1*, responsible for defence responses, in transgenic Arabidopsis in order to determine the gene function *in planta*. Yan *et al*. (2013), also utilised Arabidopsis to validate the sorghum basic helix-loop-helix (*bHLH*) gene function. These studies demonstrate the importance of utilising a plant with well-known characteristics in validating gene expression and function.

Although Arabidopsis is a model plant system widely utilised, the plant is naturally drought susceptible and agriculturally unimportant. This has led to suggestion of adopting sorghum as a model plant system in abiotic stress studies (Ngara and Ndimba, 2014). Sorghum is a good plant system for abiotic stress studies because it is naturally drought tolerant (Rosenow *et al*., 1983) and possesses great diversity in its gene pool (Motlhaodi *et al*., 2017).

1.8 Aim and Objectives of this Study

The goal of this study is to identify sorghum proteins and genes recruited in sorghum adaptive responses to drought stress. A few of these proteins will be selected for functional validation with the possibility of developing drought markers for assisting plant breeders in the selection process during classical plant breeding programs for drought tolerance. These genes could also be used in improving crop productivity under drought stress through conventional breeding or genetic engineering. This will help increase food security in this time of uncertainty in weather patterns.

The global aim of the research was:

To evaluate the physiological, biochemical and molecular responses of two sorghum varieties to drought stress with the ultimate goal of working towards the development of drought markers.

The specific objectives were:

i. To characterise the physiological and biochemical responses of two sorghum varieties with contrasting phenotypic drought traits after exposure to drought stress,

ii. To perform a comparative quantitative analysis of the root proteome in response to drought stress and validate the expression of selected gene targets, and

iii. To develop molecular markers for drought tolerance.

CHAPTER 2

MATERIALS AND METHODS

2.1 Plant Material

2.1.1 Sorghum Germplasm

Five sorghum (*Sorghum bicolor* L. Moench) varieties were initially used in the study in order to select two with contrasting tolerance to drought stress. The seeds were obtained from the Agricultural Research Council (ARC) - Grain Crops Institute (GCI), Potchefstroom, South Africa; Capstone Seeds, Howick, South Africa; and Agricol, Pretoria, South Africa as shown in Table 2.1.

Table 2.1: Sorghum varieties used in the study.

Variety	Source	Phenotypic trait
SA 1441	ARC-GCI	Drought tolerant
ICSV 210	ARC-GCI	Drought resistant
ICSB 338	ARC-GCI	Drought susceptible
Ns 5511	Agricol	Unknown
Cap 1003	Capstone seeds	Unknown

2.1.2 Sorghum and Arabiopsis Cell Suspension Cultures

White sorghum (Ngara *et al*., 2008), Arabidopsis (*Arabidopsis thaliana* var. Landsberg *erecta*) (May and Leaver, 1993), and ICSB 338 sorghum cell suspension cultures (Ramulifho, 2017) were used as *in vitro* systems for studying the effects of osmotic stress in plants. The sorghum cell suspension cultures were maintained on sorghum cell suspension culture medium [4.4g/L Murashige and Skoog Basal Salt with minimum organics (MSMO) medium, 3% (w/v) sucrose; adjusted to pH 5.8 using 1 M NaOH. Arabidopsis cell suspension cultures were maintained in MSMO medium with an addition of 3% (w/v) sucrose and 1 mg/mL each of NAA and kinetin growth hormones; adjusted to pH 5.7. The sorghum cell suspension cultures were maintained at 30°C in dark conditions, while the Arabidopsis cell suspension cultures were maintained at 22-23°C under both dark and light conditions with agitation at 130 rpm on an orbital shaker. Arabidopsis cell cultures were maintained by weekly subculturing into fresh growth medium using 10% (v/v) ratio inoculum. Sorghum cell cultures were maintained by fortnightly subculturing into fresh medium using 10% (v/v) ratio inoculum. Early-mid log phase cells were used for the experiments, equating to 4 days after subculturing of Arabidopsis cell cultures and 8 days for sorghum cell cultures.

2.2 Plant Growth Conditions and Drought Stress Treatment

2.2.1 Determination of Field Capacity

The field capacity (FC) of the soil was determined using a protocol adapted from Vineeth *et al*., (2016). Ten plastic pots of 10 cm diameter and depth were used in this experiment. Each pot was filled with 150 g of potting soil mix (Culterra, Muldersdrift, South Africa) and then saturated with water. The excess water was allowed to drip from the pots for three hrs. The pots were then weighed to obtain the saturated soil weight (SW). After weighing, the soil was oven-dried at 40°C and weighed daily until constant dry weight was reached (DW). The FC was estimated using the following equation:

FC = SW – DW

Where FC = field capacity, SW = saturated soil weight, DW = dry soil weight.

The field capacity of the soil was noted and used in devising a daily watering regime for the germination and drought stress experiments.

2.2.2 Measurement of Growth and Physiological Parameters

Sorghum seeds were imbibed in distilled water for 30 min and ten seeds per variety were sown in plastic pots. The pots were saturated with Nitrosol® nutrient solution [Envirogreen (Pty) Ltd, Braamfontein, South Africa] with standardised macro and micro nutrient content [N (80 g/kg); P (20 g/kg); K (58 g/kg); Ca (6 g/kg); Mg (7 g/kg); S (4 g/kg); Mn (40 mg/kg); Mo (15 mg/kg); Fe (60 mg/kg); Cu (1 mg/kg); Zn (1 mg/kg); Bo (23 mg/kg)], allowed to drip for three hrs and placed in a growth chamber (Model: GC-539DH, Already Enterprises Inc., Taipei, Taiwan). The soil was kept moist by irrigating daily to field capacity with distilled water. The seeds were grown on a 27/19°C day/night temperature cycle in the growth chamber with a 16/8 hrs light/dark cycle. Germination was recorded by counting the emerging seedlings every second day until the sixth day.

2.2.3 Drought Stress Treatment Experiments

2.2.3.1 Seedling Growth for Physiological Measurements and Protein Extraction

ICSB 338 (drought susceptible) and SA 1441 (drought tolerant) sorghum seeds were germinated as described above and well-watered until the V3 growth stage (three fully expanded leaves with a fourth emerging leaf). Thereafter, drought stress was imposed by withholding water for 8 days. The control plants were maintained at 100% FC throughout the experiment. Following drought stress, some plants were re-watered for 24 hrs. These plants were used as the re-watered plants in subsequent physiological and growth measurements.

2.2.3.2 Seedling Growth for Osmolyte and Gene Expression Analysis

Seedlings for osmolyte content analysis as well as gene expression analysis were grown at Durham University, United Kingdom. The seeds were germinated on moist filter paper in petri dishes and incubated in a 30°C dark room for 72 hrs. After germination, the seedlings were transplanted into Levington F2 + sand compost and sand mix (ICL Everris Ltd, Ipswich, United Kingdom) in square plastic pots (6.5 x 6.5 x 6.5 cm^3). The seedlings were well-watered until the V3 growth stage.

At the V3 growth stage, water was withheld and root and leaf samples were collected at days 0, 4, 8 and 12 as follows. For osmolyte content analysis, each biological replicate was a pool of three leaf discs, each derived from an independent plant. At each sampling time-point, the roots were washed to remove soil, blotted dry, and about 100 mg placed in an Eppendorf tube and snap-frozen in liquid nitrogen prior to storage at -80°C. A total of three biological replicates were generated for the root samples, with each replicate consisting of tissue from a single plant. For gene expression analysis, the third leaf was excised from the plant at the leaf point of attachment with the plant whilst the roots were washed over running water and quickly blotted dry with filter paper. The samples were quickly wrapped in aluminium foil, flash frozen in liquid nitrogen and stored at -80°C until further use.

2.2.4 Osmotic Stress Treatment of Cell Suspension Cultures

Early-mid log phase sorghum and Arabidopsis cell cultures were aliquoted into 10 mL cultures, using sterile 25 mL Erlenmeyer flasks. Both light-grown and dark-grown Arabidopsis cell cultures were used in this experiment, which gave rise to four cell types/series – white sorghum, ICSB 338 sorghum, dark-grown Arabidopsis, and light-grown Arabidopsis. Cell cultures of both sorghum lines were grown in complete darkness as they cannot withstand light (Ngara *et al.*, 2008). Control cultures were mock-treated by addition of

2 mL sterilised MilliQ-water. The cells were harvested immediately, flash frozen in liquid nitrogen and stored at -80°C. The remaining flasks were treated by addition of 2 mL of 2 M sorbitol stock solution to achieve a final sorbitol concentration of 0.4 M. The cell suspension cultures were then returned to their respective incubation conditions and harvested at 6, 24, 48 or 72 hrs later. Cell cultures were filtered through 2 layers of Miracloth and the cells were immediately flash frozen in liquid nitrogen and stored at -80°C.

2.3 Measurement of Growth and Physiological Parameters

2.3.1 Growth Measurements

After 8 days of drought stress (Section 2.2.3.1), the root and shoot length of ICSB 338 and SA 1441 sorghum varieties were measured in both control and drought-stressed plants and 24 hrs after re-watering. The shoot length was measured from the point of attachment of the stem with the roots to the tip of the longest leaf. The root length was measured from the point of attachment with the stem to the tip of the longest root. Five biological replicates were used per treatment for all measurements per sorghum variety.

The fresh and dry weight measurements were taken after 8 days of drought stress and 24 hrs after re-watering. The same measurements were taken for the respective controls. Briefly, the intact root system of harvested sorghum plants was gently shaken to remove all the soil lumps, washed under running water and blotted dry on paper towel. The plants were excised at the point of attachment with the roots. Each shoot and root tissue sample was then weighed to obtain the fresh weight. The shoot and root tissues were separately oven-dried at 60°C for 48 hrs and weighed to obtain the dry weight. Five biological replicates were used per treatment for all measurements per sorghum variety.

2.3.2 Physiological Measurements

2.3.2.1 Measurement of Relative Water Content

Relative water content (RWC) was estimated as previously described (Barrs and Weatherley, 1962). Briefly, the third leaf was excised from the plants and immediately weighed to determine the fresh weight (FW) for five biological replicates. The leaf samples were saturated in distilled water in 50 mL Falcon tubes in the dark for 24 hrs at 4°C, blotted dry between filter paper and weighed to determine the turgid weight (TW). The leaf samples were then wrapped with paper towel and oven dried at 60°C for 24 hrs to obtain the dry weight (DW).

The RWC was be calculated using the formula

$$RWC = \frac{FW - DW}{TW - DW} * 100$$

Where RWC = relative water content, FW = fresh weight, DW = dry weight, TW= turgid weight.

2.3.2.2 Leaf Chlorophyll Content

The chlorophyll content of sorghum plants was measured on the third leaf using a CCM 200 Plus Chlorophyll Content Meter (Opti-Science, ADC BioScientific Ltd., Hoddesdon, UK) according to the manufacturer's instructions. The measurements were taken daily at the same time of the day for the eight days of drought stress so as to reduce technical variation and 24 hrs after re-watering. Ten biological replicates were used per treatment for each sorghum variety and the chlorophyll content was expressed as Chlorophyll Content Index (CCI).

2.3.2.3 Leaf Stomatal Conductance and Surface Temperature

The leaf stomatal conductance and surface temperature of the sorghum plants was measured using an SC-1 Leaf Porometer (Decagon Devices, Inc., Washington, USA) according to the manufacturer's instructions with minor modifications. The leaf abaxial conductance and surface temperature measurements were taken simultaneously on a daily basis at the same time on the third leaf for eight days and 24 hrs after re-watering. Ten biological replicates were used per treatment for each sorghum variety.

2.3.2.4 Relative Cell Death

The root and leaf relative cell death was determined using the Evans blue method as previously described (Ngara, 2009). Firstly, 100 mg of the control and drought stressed sorghum root tissue or 1 cm x 1 cm leaf discs was weighed. Separate leaf discs and root samples were boiled to kill all cells and used as the 100% cell death samples. The plant samples were each submerged in 1 mL of 0.25% (w/v) Evans blue solution in 10 mL centrifuge tubes. The tubes were incubated on a horizontal shaker with gentle shaking for 20 min. The plant samples were then transferred to a 2 mL Eppendorf tube and washed at least three times with distilled water to remove all the Evans blue solution on the surface of the samples. After washing, 1.2 mL of 1% (w/v) sodium dodecyl sulphate (SDS) in 50% (v/v) methanol was added to the samples before grinding using a plastic pestle. Thereafter, the samples were vortexed and centrifuged at 7 300 × g for three min. A 0.8 mL aliquot from the supernatant was taken and its optical density was determined spectrophotometrically at 600 nm. For the calculation of the relative cell death the following equation was used:

$$CD = (y - z)/(z - x)$$

Where CD % = cell death percentage

x = optical density value for the control sample

y = optical density value for the drought stressed sample

z = optical density value for the boiled sample

2.4 Osmolyte Content Analysis

The proline and glycine betaine contents of sorghum leaf and root tissue in control and drought stressed samples were determined using Hydrophilic Interaction Liquid Chromatography-Mass Spectrometry (HILIC-MS). For leaf tissue, three 7 mm diameter biological replicate discs per control and drought stressed treatment were used, while for roots, approximately 100 mg of ground sample was used. Three biological replicates were harvested at days 0, 4, 8 and 12 after drought stress (Section 2.2.3.2) and weighed. Thereafter, 125 µL of 0.25 N HCl was added to each sample and incubated at 60°C on a heat block for 5 min as previously described (González-Torralva *et al*., 2017). After the incubation period, the liquid extract was collected and stored at -80°C pending osmolyte content analysis.

2.4.1 Proline Content Analysis

The chromatographic separation of leaf extract samples for proline content analysis was performed on an Acquity UPLC BEH Amide column (2.1×100 mm, 1.7 µL particle size) (Waters, Milford, USA) as previously described (Prinsen *et al*., 2016). A volume of 2 µL of the leaf extracts was diluted by a factor of 100, injected into the column and the column

temperature was maintained at 35°C. The same volume of root extract was injected into the column with no dilution. For optimal chromatographic separation, a gradient with two solvents, namely A (10 mM ammounium formate in 85% acetonitrile containing 0.15% formic acid) and B (10 mM ammounium formate in MilliQ-water containing 0.15% formic acid pH 3.0) was established at a flow rate of 200 µL/min as follows. Initially solvent A was maintained at 100% for 6 min. A gradient was then started for 0.1 min at which solvent A was decreased to 94.1% whilst solvent B was increased to 5.9%. Following this, solvent A was further decreased to 82.4% whilst solvent B was increased to 17.6% from 6.1 to 10 min. From 10 to 12 min, solvent A was set at 70.6% and solvent B at 29.4%. This was followed by the equilibration of the column for 6 min in the initial conditions (100% solvent A) giving a total run time of 18 min including the calibration process. The column was then coupled to a QTRAP 6500 mass spectrometer (AB Sciex, Redwood city, USA) for the Multiple Reaction Monitoring (MRM) analysis of proline content. The MRM transition was 116→70. Peaks of interest were integrated using Analyst software (AB Sciex) and quantified with reference to external standards.

2.4.2 Glycine Betaine Content Analysis

The chromatographic separation of the leaf extract samples for glycine betaine content analysis was performed on an Acquity UPLC BEH Amide column (2.1×100 mm, 1.7 µL particle size) (Waters). A volume of 2 µL of the leaf and root extracts (Section 2.4) was injected into the column and the temperature of the column was maintained at 30 °C. Only the leaf extracts were diluted by a factor of 100. For optimal chromatographic separation, a gradient with two solvents, namely A (10 mM ammounium formate in 85% acetonitrile containing 0.15% formic acid) and B (10 mM ammounium formate in MilliQ-water containing 0.15% formic acid pH 3.0) was established at a flow rate of 200 µL/min as follows. Initial conditions were 100% solvent A for 6 min. A hold step was maintained for 2

min. Thereafter, solvent B was ramped to 100% at 5 min. This was followed by a hold step for 5 min and equilibration at 100% solvent A for 5 min. The column was then coupled to a QTRAP 6500 hybrid triple quadruple mass spectrometer system (AB Sciex) for the MRM analysis of glycine betaine content. The MRM transitions were ES+ 118→58, 118→59.

2.5 Protein Extraction and Quantification

2.5.1 Protein Extraction from Sorghum Root and Leaf Tissue

Total soluble protein (TSP) extraction was performed as previously described (Ngara, 2009). Approximately 1 g fresh weight of sorghum root and leaf samples (Section 2.2.3.1) were ground to a fine powder using sterile frozen pestle and mortar. Five biological replicates were used for control and drought-stressed root and leaf tissues. The ground plant tissue was transferred to 1.5 mL Eppendorf tubes and precipitated in 1 mL of 10% (w/v) trichloroacetic acid (TCA) on ice. The homogenate was then briefly vortexed and centrifuged at 15 000 × g for 10 min at room temperature. Following centrifugation, the supernatant was discarded and the pellet was washed thrice with 1.5 mL of ice-cold 80% (v/v) acetone by centrifugation at 15 000 × g for 10 min per wash. The pellet was air-dried at room temperature for 5 min and re-suspended in 1 mL and 1.4 mL of urea extraction buffer [9 M urea, 2 M thiourea and 4% 3-(3-Cholamidopropyl) dimethylammonio]-1-propanesulfonate (CHAPS)] for the root and leaf sample, respectively. The TSP was extracted in the urea extraction buffer overnight at room temperature with vigorous vortexing before centrifugation at 15 000 × g for 10 min. The supernatant containing the TSP was then carefully collected and stored at -20°C pending protein analysis.

2.5.2 Protein Quantification

The concentration of all protein extracts was determined using a Bradford assay (Bradford, 1976) with minor modifications as previously described (Ngara, 2009). Bovine serum

albumin (BSA) standards were prepared in duplicate from a 5 mg/mL BSA stock solution in 2 mL plastic cuvettes as shown in Appendix, Table A1. Protein samples were also prepared in duplicate in 2 mL plastic cuvettes by mixing 10 µL of each respective protein extract with 10 µL of 0.1 M HCl and 80 µL distilled water. The Protein Assay Dye Reagent Concentrate (BIO-RAD, Hercules, California, USA) was diluted in the ratio 1 part Bradford reagent to 4 parts distilled water. A volume of 900 µL of the dilute Bradford reagent was then added to all the BSA standards as well as the protein samples, mixed and incubated for 5 min at room temperature before reading the absorbance at 595 nm. The 0 mg/mL BSA standard solution was used as a blank. The standards were used to plot a standard curve from which the concentrations of the unknown protein samples were estimated.

2.6 Protein Gel Electrophoresis

2.6.1 One Dimensional (1D) Polyacrylamide Gel Electrophoresis (PAGE)

Protein extracts were separated on a 1D SDS-PAGE as previously described (Laemmli, 1970). The 1D gels were cast on 10.1 cm (width) x 8.3 cm (height) spacer glass plates mounted with 1 mm thick spacers using the Mini – PROTEAN® Tetra cell (BIO-RAD) gel casting system following manufacturer's instructions. Stacking and resolving gels of 5% (v/v) and 12% (v/v), respectively were prepared as shown in Appendix, Table A2.

The protein samples were prepared by combining each sample with 2X SDS sample loading buffer [100 mM Tris HCl, pH 6.8, 4% (w/v) SDS, 20% (v/v) glycerol, 200 mM DTT, and a tint of bromophenol blue] in equal amounts in a 1.5 mL Eppendorf tube, pulse vortexed and pulse centrifuged. The protein samples were heated on a heat block at 100°C for 5 min and pulse centrifuged prior to loading 2.5 µg for root and 10 µg for leaf samples and onto the 1D SDS-PAGE gels. A volume of 6 µL of an unstained protein marker (New England Biolabs, Hertfordshire, UK) was loaded in the first well. Gel electrophoresis was carried out in

electrode running buffer [25 mM Tris, 192 mM glycine and 0.1% (w/v) SDS] on a Mini-PROTEAN® Tetra System (BIO-RAD) using a Power Pac™ Basic (BIO-RAD). Initially the gels were run at 100 V for 30 min before increasing the voltage to 150 V until the bromophenol blue dyes reached the bottom of the gels.

2.6.1.1 Coomassie Brilliant Blue (CBB) Staining

The proteins separated by 1D SDS-PAGE were detected and visualised by staining using a modified CBB R-250 staining procedure in three stages. Three staining solutions, namely, Coomassie I [0.025% (w/v) CBB R-250, 10% (v/v) glacial acetic acid and 25% (v/v) propan-2-ol], Coomassie II [0.003% (w/v) CBB R-250, 10% (v/v) glacial acetic acid and 10% (v/v) propan-2-ol] and Coomassie III [0.003% (w/v) CBB R-250 and 10% (v/v) glacial acetic acid], were prepared from a 1.25% (w/v) CBB stock solution and used as follows: The gels were immersed in warm Coomassie I for 30 mins with gentle shaking. This was followed by Coomassie II and Coomassie III. The gels were then immersed in a de-staining solution [10% (v/v) acetic acid and 1% (v/v) glycerol] until the bands were clearly distinct against a clear background. The gels were scanned and imaged on a Gel Doc™ XR+ Molecular imager with Image Lab ™ software version 5.2.1 (BIO-RAD).

2.6.1.2 Protein Precipitation

The protein samples were transferred to 10 mL centrifuge tubes and precipitated in 80% (v/v) acetone overnight at -20°C. The samples were then centrifuged at 3000 × *g* for 10 min and the supernatant was discarded. The resulting pellets were washed three times with ice-cold 80% (v/v) acetone, centrifuged at 3000 × *g* for 10 min and the acetone was discarded. The pellets were then covered with 50 µL of 80% (v/v) acetone and couriered to Durham University, United Kingdom for use in two dimensional differential gel electrophoresis (2D-DiGE) and isobaric Tags for Relative and Absolute Quantitation (iTRAQ) analysis.

2.6.2 Two Dimensional - Differential Gel Electrophoresis (2D-DiGE)

The precipitated root and leaf samples couriered to Durham University were re-solubilised as follows. The protein samples were centrifuged at 15 000 × *g* for 10 min, the acetone was discarded and the protein samples were briefly air-dried. Thereafter, 400 µL of extraction buffer was added to the protein samples and vortexed for 5 min before centrifugation at 15 000 × *g* for 10 min. The supernatant was then transferred to fresh 1.5 mL Eppendorf tubes and quantified using the Bradford assay (Section 2.5.2). Approximately 2.5 and 10 µg of root and leaf samples, respectively were run on a 1D SDS-PAGE (Section 2.6.1) to determine protein quality.

The gels were stained with a SYPRO Ruby fluorescent stain as follows. The gels were fixed with a solution of 40% (v/v) methanol and 10% (v/v) acetic acid for 30 min before staining with a Lonza SYPRO Ruby protein gel stain (Scientific Laboratory Supplies, Nottingham, UK), for at least 90 min with gentle shaking in the dark. After the staining procedure, the gels were destained in 10% (v/v) methanol and 6% (v/v) acetic acid for 30 min and imaged using the Typhoon 9100 Variable Mode Imager (Amersham Biosciences, California, USA).

2.6.2.1 Sample Preparation and Labelling for 2D-DiGE

Root and leaf protein sample preparation for 2D-DiGE labelling began with adding 2 µL of 1.5 M Tris-HCl, pH 8.8 to 98 µL of protein sample. The mixture was pulse vortexed, pulse centrifuged and adjusted to pH 8-9 by adding 0.1 M NaOH before storage at -20°C. The pH was monitored using pH Test Strips 4.5-10.0 (SIGMA, St Louis, USA). The pH adjusted samples were thawed, pulse-vortexed, pulse-centrifuged and stored in a light protected ice-bath. Subsequently, a protein sample volume equivalent to 50 µg was topped up to a volume of 48 µL with extraction buffer. The control and drought-stressed protein samples were then labelled with 800 pmol of Cy3 and Cy5 fluorescent dyes, respectively, pulse vortexed and

returned to the light protected ice-bath for 30 min. After exactly 30 min, 1 µL of 10 mM lysine was added to stop the labelling reaction. The labelled samples were then stored at -20°C pending 1D and 2D SDS-PAGE analysis.

2.6.2.2 1D Gel Electrophoresis for DiGE Labelled Samples

Following the root and leaf protein sample DiGE fluorescent labelling procedure, 1D SDS-PAGE was performed as described in Section 2.6.1 to check the loading quality and confirm successful labelling of the proteins. Approximately 2.5 µg of labelled sample was electrophoresed. After electrophoresis, the gels were fixed in solution 40% (v/v) methanol, 10% (v/v) glacial acetic acid for 30 min in the dark with gentle shaking. The gels were then imaged using the Typhoon 9400 Variable Mode Imager (Amersham Biosciences).

2.6.2.3 2D Gel Electrophoresis for DiGE Labelled Samples

2.6.2.3.1 Rehydration of 7 cm Immobilised pH Gradient (IPG) Strips

Protein extracts of 15 µg were mixed with 0.8% (w/v) DTT, 0.2% (v/v) ampholytes (BIO-RAD), a tint of bromophenol blue and topped up to 125 µL with extraction buffer. The samples were pulse vortexed and centrifuged before being placed in different wells of an Immobiline™ Dry Strip Re-swelling Tray (GE Healthcare, Amersham, UK). Linear, 7 cm ReadyStrip™ IPG strips of pH range 4-7 (GE Healthcare) were placed on top of the sample, gel side down without trapping air bubbles. The strips were then completely covered with paraffin oil to prevent the evaporation of the sample and left to passively re-hydrate overnight at room temperature.

2.6.2.3.2 Isoelectric Focusing (IEF) of IPG Strips

For the first dimension IEF, the rehydrated IPG strips were removed from the re-swelling tray, briefly rinsed with distilled water and blotted dry on moist filter paper. The strips were then placed on the focusing platform of the Ettan™ IPGPhor 3 (GE Healthcare) and damp

electrode wicks were placed on each end of the gel to collect salts from the samples during the focusing process. The IPG strips were then covered with paraffin oil to avoid sample evaporation during the IEF run. Isoelectric focusing was performed in three stages for the IPG strips as shown in Table 2.2. After IEF, the IPG strips were equilibrated prior to the second dimension gel electrophoresis.

Table 2.2: Isoelectric focusing programme for 7 cm IPG strips.

Step	Volts	Duration volt hrs (Vhrs)
1	200	10
2	3500	2800
3	3500	3700

2.6.2.3.3 Equilibration of IPG Strips

After IEF, the IPG strips were equilibrated in 2.5 mL of 2% (w/v) DTT containing equilibration buffer [6 M urea, 2% (w/v) SDS, 50 mM Tris/HCl, pH 8.8, 20% (v/v) glycerol], followed by 2.5% (w/v) iodoacetamide containing equilibration buffer for 15 min each with gentle shaking. The strips were then ready for the second dimension SDS-PAGE.

2.6.2.3.4 Second Dimension SDS-PAGE

The mini format 2D SDS-PAGE gels were prepared using 12% (v/v) resolving gel as described in Appendix, Table A2. Dimensions of 10.1 cm (width) × 8.3 cm (height) spacer glass plates (BIO-RAD) mounted with 1 mm thick spacers were used. Six microliters of unstained SDS7 protein marker was spotted on separate small square pieces of filter paper and air-dried. The equilibrated 7 cm IPG strips were rinsed with MilliQ-water and placed on

top of mini format 12% (v/v) SDS-PAGE resolving gels avoiding trapping bubbles in the process. The dry filter paper with the unstained SDS7 protein marker was placed on the anodic side of each IPG strip. The IPG strips were then overlaid with 1 mL of 0.5% (w/v) molten agarose sealing solution prepared in electrode running buffer containing a tint of bromophenol blue. Electrophoresis was then performed using the Mini-PROTEAN® system (BIO-RAD) using a Power Pac™ basic (BIO-RAD) as described in Section 2.6.1. After electrophoresis, the gels were scanned and imaged using the Typhoon 9400 Variable Mode Imager (Amersham Biosciences).

2.7 iTRAQ Analysis

2.7.1 Sample Preparation for iTRAQ Analysis

The sorghum re-solubilised root TSP (Section 2.6.2) were prepared for iTRAQ analysis as follows. MilliQ-water was added to 50 µg of protein extracts to make a total volume of 100 µL. This was followed by the addition of 5 µL of 1.5 M Tris HCl pH 8.8 and 400 µL of 100% acetone and pulse vortexing. The protein samples were left to stand at room temperature for 2 hrs and centrifuged at 15 000 × *g* for 10 min. The resulting pellet was washed twice with 500 µL 80% (v/v) acetone. Five microliters of 2% (w/v) SDS was added and the samples were incubated at 60°C on a heat block for 1 hr.

Samples were labelled using 8-plex iTRAQ kit (AB Sciex) as follows. A volume of 95 µL of dissolution buffer (500 mM Triethylammonium bicarbonate) was added and the samples were incubated for 20 min on a shaker. The protein samples were reduced by adding 2 µL of reducing agent [1mM Tris(2-carboxyethyl)phosphine)] and incubating the samples at 60°C on a heat block for 1 hr. After reduction, 1 µL of blocking agent (methyl methanethiosulfonate) was added to alkylate the proteins and the samples were incubated at room temperature for 10 min. Thereafter, the proteins were digested by adding 10 µL of 0.5

µg/µL of trypsin (PROMEGA, Madison, USA). The proteins were incubated at 37°C overnight and vacuum freeze dried before sample labelling with an 8-plex iTRAQ reagent kit (AB Sciex) according to manufacturer's instructions.

2.7.2 Sample Labelling and iTRAQ Analysis

The protein samples were re-suspended in 50 µL of sterile MilliQ-water before the addition of the label and isopropanol. The control samples were labelled with tags of molecular weights 113, 114, 115 and 116 whilst the drought stressed treatment samples were labelled with 117, 118, 119 and 121 molecular weight tags. The pH of the labelled samples was adjusted to 7.5 by adding dissolution solution and the pH range was checked using pH Test Strips 4.5-10.0 (SIGMA). All the eight samples of control and drought stressed samples of each sorghum variety were separately combined into one tube to make one composite sample, redistributed back in equal amounts into eight portions and vacuum-dried.

Samples were cleaned-up using HILIC SPE cartridges (PolyLC Inc.), containing 300 mg of 12 µm polyhydroxyethyl-A, to remove unincorporated label and buffer salts. The cartridges were equilibrated by sequential addition of 4 × 3 mL releasing solution (5% ACN, 30 mM ammonium formate pH 3.0) followed by 4 × 3 mL binding solution (85% ACN, 30 mM ammonium formate pH 3.0). The dried iTRAQ-labelled peptide residue was dissolved in 75 µL of 3% acetonitrile (ACN), 0.1% formic acid (FA) followed by 150 µL of 0.3 M ammonium formate, pH 3. The pH of the mixture was checked and adjusted to 3.0 using trifluoroacetic acid (TFA). After clarifying by centrifugation (10,000 × g, 10 mins), the samples were mixed with 1275 µL ACN. The resulting 1.5 mL sample was added to the SPE cartridge and the flow-through retained and passed through a second time. The column was then washed twice with 2 mL binding solution. Finally, the peptides were eluted with 2 × 1

mL releasing solution. The eluate was freeze-dried and re-suspended in 3% ACN, 0.1% formic acid for liquid chromatography-mass spectrometry (LC-MS).

After freeze-drying, and subsequent resuspension, the samples were separated into 56 fractions on the Poly-LC strong cation exchange column (200 × 2.1 mm) at 200 µL/min on an Ettan LC (GE Healthcare) high pressure liquid chromatography system. A biphasic gradient of 0-150 mM KCI over 11.25 column volumes and 150-500 mM KCI in buffer A over 3.25 column volumes was used for performing peptide separation. Over this gradient, 56 fractions were collected and reduced to a total of 30 fractions by pooling those with low peptide concentration. The 30 fractions were dried and re-suspended in 90 µL of 2% acetonitrile/0.1% formic acid of which 20 µL of each fraction was analysed by LC-MS/MS using a nano-flow Ettan MDLC system (GE Healthcare) attached to a hybrid quadrapole-TOF mass spectrometer (QStar Pulsar *i*, Applied Biosystems, Foster City) coupled to a nanospray source (Protana) and a PicoTip silica emitter (New Objective, Woburn, MA). Samples were loaded and washed on a Zorbax 300SB-C18, 5 mm, 5 × 0.3 mm trap column (Agilent, Stockport, UK) and online chromatographic separation performed over 2 hrs on a Zorbax 300SB-C18 capillary column (3.5 × 75 µm) with a linear gradient of 0 – 40% acetonitrile, 0.1% formic acid at a flow rate of 200 nl/min. Applied Biosystems Analyst software version 1.1 was used acquire all MS and MS/MS data switching between the survey scan (1 × 1 s MS) and three product ion scans (3 × 3 s MS/MS) every 10 sec. Ions in the range of 2^+ to 4^+ charge state and with TIC > 10 counts selected for fragmentation.

2.7.3 Mass Spectra Data Analysis

Data analyses for mass spectrometry were performed as previously described (Smith *et al*., 2015) with minor modifications. Briefly, ProteinPilot™ 5.0.1 software version 4895 incorporating the Paragon™ Algorithm 5.0.1.0.4874 (AB Sciex) was used for data analysis against a TrEMBL database (downloaded October 2013) sequences of *Sorghum bicolor* only. An iTRAQ 8-plex (peptide-labelled). For each identified peptide, a minimum threshold of 1.3 at 95% confidence interval was set whilst a minimum protein score threshold of 2.0 at 99% confidence interval was set for protein identification. Proteins identified on the basis of a single peptide were removed from the dataset. For quantitative analysis, the abundance of each protein per sample was obtained as a ratio to the 113-tagged sample. Across the four biological replicates, the averages of the ratios for each protein in control and drought stressed samples were calculated. The fold-change in protein expression was denoted by the ratio of control average to drought stressed sample average. A negative sign denoted down-regulation for the drought stress responsive proteins and the drought stress sample averages were the numerators with the controls as the denominators. The Student's t-test was used for computing the probability values for the comparison of control averages and drought stress sample averages.

2.7.4 Bioinformatic analysis

The mass spectrometry identified proteins were functionally annotated using the UniProt database (http://www.uniprot.org). The database was used to search for the Gene Ontology (GO) analysis using three key terms, Biological Process, Biological Function and Cellular Component. The conserved domains and family names of the identified proteins were determined using the Interpro database (http://www.ebi.ac.uk/interpro/). The Arabidopsis homologues of the sorghum genes were obtained from the Arabidopsis Information Resource

(TAIR) (www.arabidopsis.org/Blast) using the sorghum protein sequence to query the Arabidopsis protein sequences.

2.8 Gene Expression Analysis

2.8.1 Total RNA Extraction and Analysis

Total RNA was extracted from sorghum root and leaf samples and sorghum and Arabidopsis cell suspension cultures using the Spectrum™ Plant Total RNA Kit (SIGMA) according to the manufacturer's instructions. Briefly, 500 µL of Lysis solution was added to 100 mg of ground sample and immediately vortexed vigorously for at least 30 sec. The sample was incubated at 56°C for 3-5 min and centrifuged at 15 000 × *g* for 3 min to pellet cellular debri. The lysate supernatant was collected by filtering through a filtration column. The RNA was bound by adding 500 µL of Binding Solution to the lysate supernatant, gently mixing by pipetting and briefly vortexing.

The mixture was passed through a binding column and centrifuged at 15 000 × *g*. The bound RNA was washed with 300 µL of Wash Solution 1 to remove impurities and the DNA in-column digestion was performed as follows. A mixture of DNase 1 (10 µL) and DNase digestion buffer (70 µL) was placed directly onto the binding column and incubated for 15 min at room temperature. Thereafter, Wash Solution 2 was passed through the column twice by centrifugation at 15 000 × *g* to remove the digested DNA. This was followed by centrifugation at 15 000 × *g* for 1 min to dry the column and the addition of 50 µL of the Elution Solution directly onto the centre of the binding matrix, centrifuging at 15 000 × *g* for 1 min and collecting the purified total RNA. The RNA was quantified using a Nano Drop® ND 1000 Spectrophotometer (NanoDrop Technologies, Inc., Wilmington, USA).

2.8.2 Agarose Gel Electrophoresis of RNA

A total of 300 ng of RNA was electrophoresed on 1.2% (w/v) agarose gels in 3-(N-Morpholino)-propanesulfonic acid (MOPS) buffer [20 mM MOPS pH 7.0, 2 mM sodium acetate pH 7.0, 1 mM (Ethylenedinitrilo)-tetraacetic acid (EDTA) pH 8.0]. The RNA samples were prepared by adding 5 µL of RNA loading buffer [63.7% (v/v) formamide, 1.14 M formaldehyde, 6.4% (v/v) MOPS buffer, 50 µg/mL ethidium bromide] to 300 ng of RNA and incubating at 65°C for 10 min on a heat block. The mixture was then pulse centrifuged and loaded on the agarose gel and run at 50V for 20 min in MOPS buffer. The gel image was taken using the Ingenius Bio-Imager (SynGene, Cambridge, UK).

2.8.3 Complementary Deoxy-ribonucleic Acid (cDNA) Synthesis

First strand cDNA synthesis was performed using the GoScript™ Reverse Transcriptase System (PROMEGA) according to the manufacturer's instructions. Briefly, 2 µg of total RNA, 1 µL of Oligo(dt) and nuclease free water were mixed to a total volume of 11.8 µL and incubated on a heat block at 70°C for 5 min. The mixture was chilled on ice water for at least 5 min, centrifuged at 15 000 × *g* for 10 sec and stored on ice whilst the reverse transcriptase mixture was being prepared. A total volume of 8.2 µL of the reverse transcriptase mixture was made by combining 1 µL of GoScript™ 5X Reaction buffer, 1.8 µL of 1.5-5.0 mM $MgCl_2$, 1 µL of 0.5 M dNTPs, 0.4 µL of Recombinant RNasin® Ribonuclease inhibitor and 1 µL of GoScript™ Reverse Transcriptase. The reverse transcription mixture was added to 11.8 µL of the RNA reaction mixture, annealed at 25°C for 5 min, extended at 42°C for 1 hr and denatured at 70°C for 15 min in a thermal cycler. The cDNA was diluted in the ratio 1:7 with sterile MilliQ-water and stored at -20°C prior to polymerase chain reaction (PCR) analysis.

2.8.4 Primer Designing

The primers of target genes were designed on the National Centre for Biotechnology Information (NCBI) database using the Primer-BLAST software (Ye *et al*., 2012) with the following specifications: the primers were selected from the *Sorghum bicolor* (taxid:4558) database, GC clamp 1, maximum primer size 150 bp, where the primer must span an exon-exon junction. All the genes tested in this study, as well as their specific primers used are shown in Tables 2.3 and 2.4. Two sets of genes were used in this study. The first set consisted of 10 genes selected from drought stress responsive gene identities (Table 2.3) in the iTRAQ experiment and two reference genes. The second set consisted of three sorghum genes selected from a sorbitol-induced osmotic stress experiment (Ngara *et al*., 2018), their Arabidopsis homologues and two reference genes (Table 2.4). The Arabidopsis genes were selected by blasting the three sorghum genes from the sorbitol-induced osmotic stress experiment on the Arabidopsis Information Resource (TAIR) database and selecting four homologues with the highest sequence identities per sorghum gene identity.

Table 2.3: List of sorghum target genes and primer sequences used in qRT-PCR analysis.

Target Gene Identity	Gene name	Primer Name	Forward Primer (5'>3')	Reverse Primer(5'>3')
SORBI_3009G190800	Thioredoxin	Thioredoxin	TCAGCTTCTCAAGCGGTAGC	CTGTTGGCCTCCTCGATCTG
SORBI_3007G172100	Peptidase	Peptidase	TCCTACCCCGTCAAGACCTC	ATGCGATTCAGAGCTCGTCG
SORBI_3002G302000	Xyloglucanase	Xyloglucanase	GCGTATCGCCAACAAAGTGG	ATGAATCATGGACGCTTGCC
SORBI_3008G134700	Aspartic peptidase	SORBI_3008G134700	CCCATCCACTGGAACGAGAC	ACTGCGTCCAGATGAGGTTG
SORBI_3001G514200	Thioredoxin	SORBI_3001G514200	GGAACATCCTGGCGCATTTG	AGAGCCAGACCGACACAAAC
SORBI_3002G217200	Peptidase	SORBI_3002G217200	GCCCAGAAATGGCTAGTGTTC	AATTCTGGCTCCGCCACTAC
SORBI_3003G136200	Germin	SORBI_3003G136200	TGCCACGCACAGAATACGAG	TACACATGCCGGAGAATCGG
SORBI_3006G135500	Galactose oxidase	SORBI_3006G135500	AGGGAAATGGTTGTACGGGC	GTGCTGGTGCACAAAATATATAGC
SORBI_3007G149600	Histone H2B	SORBI_3007G149600	TGCTCTCGTGAGATCGCTTG	GCAATACCACTGCGTATCTGTTG
SORBI_3001G313200	Histone H4	SORBI_3001G313200	GGATCCCTGGATCTTCTGGAG	TTTGGTGGCTCTGTGGTCAG
SORBI_3001G073900	Malate dehydrogenase	SORBI_3001G073900	CTTCTTCAACACACGCGACC	GTGTGGTGACGGATGGTAGG
SORBI_3003G322400	Ribosomal protein S25	SORBI_3003G322400	AACGAGTATATGCATCCCCG	AGCAGGCTCTAGGGTTTTGAG
SORBI_3002G049300	Ribosomal protein S25	SORBI_3002G049300	GGTCAAAACAGCCCGTTCAG	TAGTTGGGAGGGTGATGGGG
*Ref. Sb910	Sb03g038910	Uncharacterised protein	TCCTGAAGCATCTTTCCCTCC	ACAGCCTGATTAGTTGGGGG
*Ref. EIF4A	Sb04g003390	Eukaryotic initiation factor-4A	GATGAGATGCTCTCCCGTGG	TGATCTCTAGGGCCTCTGGG

*Reference genes

Table 2.4: List of Arabidopsis target genes and primer sequences used in qRT-PCR analysis.

Target Gene Identity	Gene name	Primer Name	Forward Primer (5'>3')	Reverse Primer(5'>3')
AT5G42980.1	Thioredoxin	TRX3	ACCTTGCCGTTTCATTGCAC	TCAGCAACAGTGTTCAATTCGTC
AT1G45145.1	Thioredoxin	TRX5	GATTGCTTGCCATACCCTCG	AAGTCTATCACAATCAGTTTCTTGG
AT3G51030.1	Thioredoxin	TRX1	ATTGAAGTCGGTGGCAAGTG	AGCCAAGTGTTTGGCAATGG
AT1G19730.1	Thioredoxin	ATTRX4	TGTTGATGAACTTCAGAGTGTTGC	GCTTATCCACAACTTCGCCG
AT5G50260.1	Peptidase	CEP1	TGCTCCGGTAGTTTCAATCG	CCGGTAAACACTCCCTCGG
AT3G48340.1	Peptidase	CEP2	TGGGCATGAAGATGTACCCG	TCCCGTAAACACTCCCTCTG
AT4G36880.1	Peptidase	XCP1	AATTTCGACCGGTGGTCTCC	CGCTGATTGTCACACGTTCC
AT1G20850.1	Peptidase	XCP2	TTACAGGGACGTCGAAGCTG	CGCCCAACAACTTCCACAAG
AT2G36870.1	Xyloglucanase	XTH32	AGCCCTAGAGAAATCATATTTTTGG	TTACCGTCTTCCGTTGCCC
AT3G44990.1	Xyloglucanase	XTH31	TACCCGAGTTCCCGAGTACC	CCCACTCCCAGTGGATTTGTC
AT1G14720.1	Xyloglucanase	XTH28	CGCCTTTTATTTATCAAATGGGGAC	TCTGCCCAAGTGTGTGCTTC
AT1G10550.1	Xyloglucanase	XTH33	CGACAAATCCTCCGGAGCTG	AATCCAGCGGGAAGCTTGAG
*AT3G13920	Eukaryotic Initiation Factor 4A	eIF4A	ATGAGAGGATGCTCTGCCTTCG	GCAGAGCAAACACAGCAACAG
*AT3G18780	Actin 2	Actin 2	GTGGTCGTACAACCGGTATTG	TCACGTCCAGCAAGGTCAAG

*Reference genes

2.8.5 Polymerase Chain Reaction for Primer Testing

PCR analysis was used to test primer specificity. A reaction mix was prepared with 25mM $MgCl_2$, 10mM dNTPs, 10 µM forward primer, 10 µM reverse primer, 1:7 dilution cDNA and 5 u/µL Taq polymerase topped up to 25 µL with MilliQ-water. The mixtures were transferred to the thermal block of a PCR machine and the program shown on Table 2.5 was run.

Table 2.5: Thermal cycling conditions for PCR.

Step	Temperature (°C)	Time (sec)	Cycles
Initial denaturation	95	60	1
Denaturation	94	30	40
Annealing	56	60	
Elongation	72	60	

2.8.6 Agarose Gel electrophoresis of PCR products

The PCR products were resolved on a 3.5% (w/v) agarose gel. The gels were prepared adding in tris acetate-(Ethylenedinitrilo)-tetraacetic acid (TAE) buffer (40 mM Tris acetate, 1 mM EDTA, 20 mM glacial acetic acid) with 0.5 µg/mL of ethidium bromide. The gels were cast and left to solidify before loading the samples and a HyperLadder™ 25 bp DNA marker (BIOLINE). After loading the samples, the gel was run at 50V for 10-20 min in 1X TAE running buffer. Following electrophoresis, the gel image was taken using the Ingenius Bio-Imager (SynGene).

2.8.7 Quantitative Real Time-Polymerase Chain Reaction (qRT-PCR) analysis

The qRT-PCR reactions were performed using the SensiFAST™ SYBR No-ROX Kit (BIOLINE). Briefly, 5 µL of the 8-fold dilution cDNA was added to PCR tubes in triplicate. A master mix containing 10 µL SensiFAST reagent, 0.3 nM of each of the forward primer and reverse primers and 3.4 µL nuclease free water was prepared for each cDNA sample. A volume of 15 µL of the master mix was added to each 5 µL of the 8-fold dilution cDNA. The qRT-PCR was performed on a Corbett Rotor-Gene 6000 (QIAGEN, Cambridge, UK) using the thermal cycling conditions shown in Table 2.6. Data analysis was done using the Relative Expression Software Tool 2009 (REST2009) version 2.0.13 (QIAGEN) using SbEIF4A and Sb910 as the constitutive reference control gene for sorghum samples and Actin and EIF4A for Arabidopsis. For the sorghum gene expression analyses, the relative fold changes between the respective varieties were determined and displayed graphically. For the Arabidopsis gene expression analyses, the cell suspension culture samples under osmotic stress were compared to control samples maintained under optimum conditions.

The REST2009 is based on the Pfaffl equation with the formula:

$$\text{Gene expression ratio} = (E_{goi})^{\Delta Ct\ goi} / (E_{rg})^{\Delta Ct\ rg}$$

Where E_{goi} = the real-time PCR efficiency of target gene transcript, E_{rg} = the real-time PCR efficiency of a referene gene and Ct = cycle threshold.

The results obtained from the Rotor-Gene comparative quantitation analysis were used rather than standard curves and Ct results. The software takes into account the different PCR efficiencies of the gene of interest and reference genes. In this study, two reference genes were used for normalisation in order to improve the reliability of results. For efficiency,

REST2009 uses amplification which has a value between 1 and 2. In addition, the randomisation algorithm uses take-off rather than the Ct values. The method used utilises relative gene expression rather than probes for which R-squared values are part of the output.

The genes were analysed by copying the take off and amplification control values of the reference gene and pasting it in the reference gene section of the REST2009 RG mode. This was followed by entering the corresponding treatment values of the reference gene in the treatment rows of the software. The control sample gene of interest values were then added to the control rows whilst the treatment values were entered in the corresponding treatment rows. Two reference genes were used per analysis in this study. In cases where the relative gene expression of two varieties was required, one variety was used as a baseline control to standardise the gene expression. The output gene expression values were then exported to Microsoft Excel and the Student's t-test was used to compare the gene expression means at a 5% level of significance.

Table 2.6: Thermal cycling conditions for qRT-PCR.

Step	Temperature (°C)	Time (sec)	Cycles
Initial denaturation	95	90	1
Denaturation	95	10	45
Annealing	56	15	
Elongation	72	25	

2.9 Statistical Analyses

For statistical analysis, a Mann-Whitney test was used to compare the means for physiological and biochemical results at a 5% level of significance, using the GraphPad Prism 5.00 software. The REST2009 software version 2.0.13 was used for gene expression analysis. The Student's t-test was used to compare the gene expression means at a 5% level of significance, using Microsoft Excel.

CHAPTER 3

COMPARATIVE PHYSIOLOGICAL AND BIOCHEMICAL RESPONSES OF SORGHUM TO DROUGHT STRESS

3.1 Introduction

When exposed to drought stress, synthesis of the phytohormone abscisic acid (ABA) increases, which triggers stomatal closure and numerous physiological responses. Stomatal closure in periods of drought stress reduces water loss through the leaves. However, stomatal closure also reduces the assimilation of CO_2 resulting in low rates of photosynthesis (Chaves *et al*., 2009). Plants also respond to drought stress by synthesising osmolytes such as proline, trehalose and glycine betaine (Valadez-Bustos *et al*., 2016). Osmolytes are low molecular weight metabolites synthesised as an inherent mechanism of osmotic adjustment in stressed plants (Hamilton and Heckathorn, 2001). Under drought stress, the accumulation of osmolytes maintains turgidity in leaf cells, minimising interruption of cellular metabolism whilst sustaining growth (Blum, 2005; Amrhein *et al*., 2013). Proline is also responsible for scavenging reactive oxygen species (ROS) in plants (Smirnoff and Cumbes, 1989). Proline content increases to a higher degree in drought tolerant plants compared to susceptible ones under the same drought stress conditions (Palfi and Juhász, 1971).

In a previous study, proline content was shown to increase significantly in drought resistant sorghum (*Sorghum bicolor*. L) crops grown in the semi-arid tropics whilst the susceptible varieties showed no significant increase (Sivaramakrishnan *et al*., 1988). Five days after re-watering, the proline content levels were restored to that of the well-watered controls. Waldren and Teare (1974), observed an increase in proline content under only extreme drought stress in sorghum and soybean (*Glycine max*) in comparison to mild stress. In a

sorghum callus culture experiment, the proline levels of both drought tolerant and susceptible sorghum samples significantly increased (Bhaskaran *et al*., 1985). However, the magnitude of increase was not correlated to the tolerance or susceptibility of the sorghum varieties in that callus study.

Sorghum is one of the naturally drought tolerant grain crops with a wide genetic diversity. As such, the crop is an invaluable model system for abiotic stress studies. A comparative evaluation of various parameters from such a crop may offer a better understanding of the mechanisms of plant drought stress responses. This chapter therefore aims to comparatively evaluate the physiological and biochemical differences between two sorghum varieties with contrasting phenotypes to drought stress, namely, ICSB 338 (drought susceptible) and SA 1441 (drought tolerant) under drought stress and following re-watering.

3.2.1 Field Capacity and Seed Germination Experiment

The field capacity (FC) of the potting mix soil was calculated using the formula shown in Section 2.2.1. The calculated FC value of 175.5 mL was utilized to devise an irrigation regime for maintaining the soil at field capacity before the drought stress treatment. For the germination experiment, five sorghum varieties (SA 1441, ICSV 210, ICSB 338, Ns 5511, Cap 1003, Table 2.1) were sown and germinated on potting soil mix in 10 cm diameter plastic pots at field capacity for the duration of the experiment. The germination rates of the sorghum varieties are shown in Figure 3.1. The varieties ICSB 338, Ns5511 and Cap 1003 had germination percentages of greater than 95% whilst ICSV 210 had the lowest value of 66%. The varieties ICSB 338 and SA 1441 were selected for further experiments on the basis of both germination percentage and contrasting phenotypic traits to drought stress (Table 2.1).

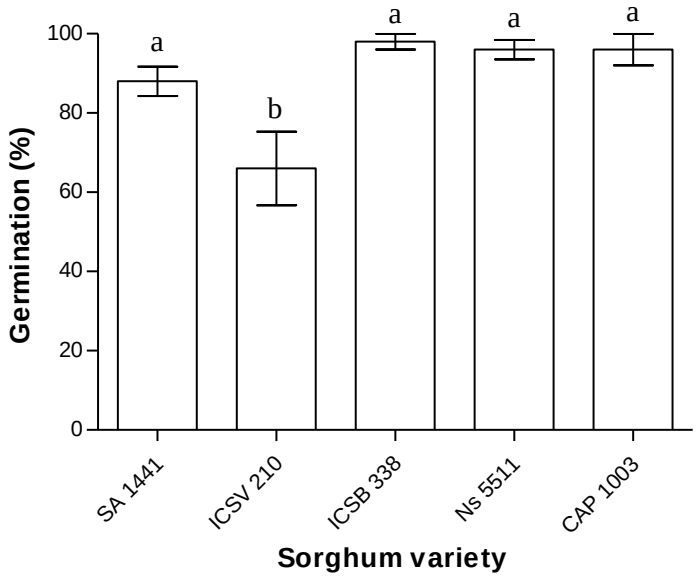

Figure 3.1: Germination rates of different sorghum varieties. The sorghum seeds were sown and grown on potting mix soil and germination counts were taken 6 days after sowing. Bars represent mean ±SE (n = 5). Bars with the same letter are not significantly different at $p \leq 0.05$ according to the Mann-Whitney test.

3.2.2 Effects of Drought Stress on Growth Parameters

The ICSB 338 and SA 1441 sorghum plants were drought stressed by withholding water at the V3 growth stage for 8 days. The plants were then re-watered to field capacity for 24 hrs. The plants began wilting and leaf rolling at day 4 of drought stress. The SA 1441 plants showed signs of wilting first compared to ICSB 338 (Figure 3.2A). However, ICSB 338 showed signs of chlorosis at day 6 of drought stress whilst for SA 1441 this symptom was observed at day 7. At day 8, the ICSB plants were highly chlorotic and smaller in overall size compared to SA 1441. SA 1441 however, showed more intense wilting at day 8 of drought

stress. Both sorghum varieties recovered to the same physiological status as the respective control plants 24 hrs after re-watering (Figure 3.2B).

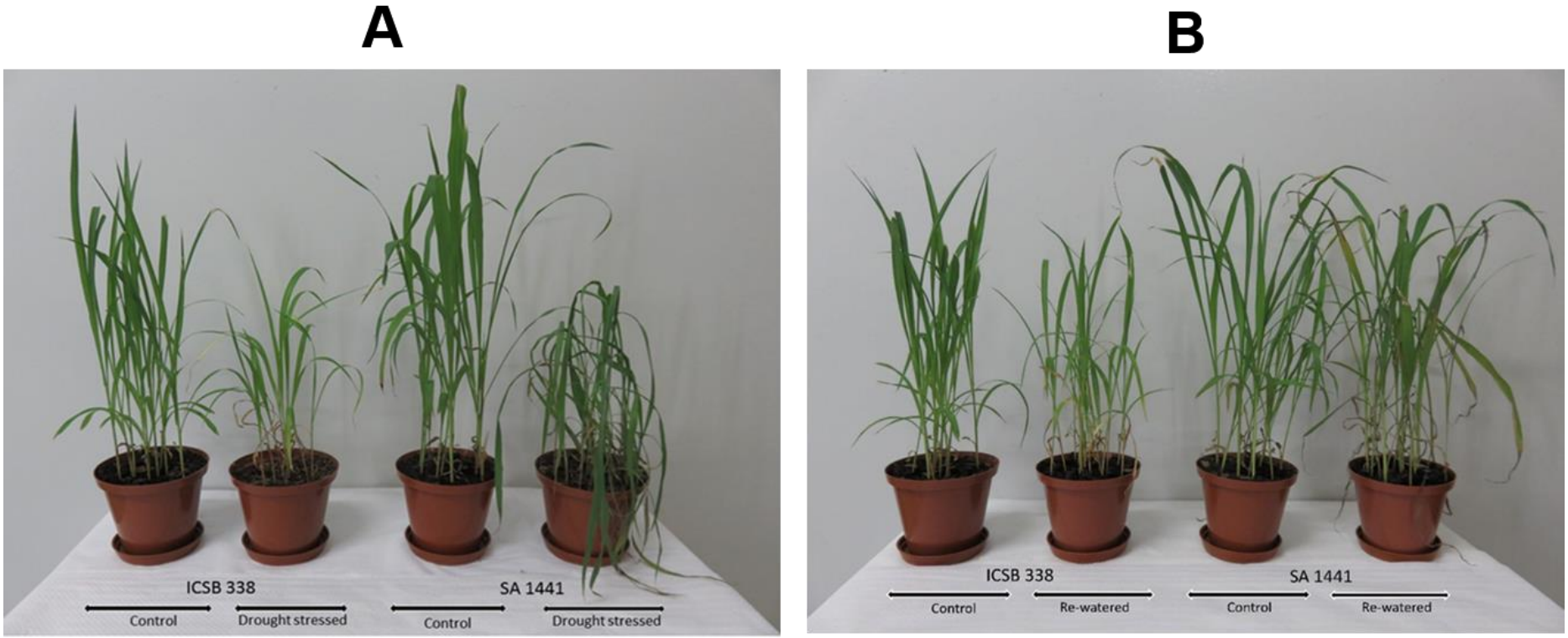

Figure 3.2: The effects of drought on sorghum plant morphology. Picture A shows control and drought stressed and B shows control and re-watered ICSB 338 (drought susceptible) and SA 1441 (drought tolerant) sorghum varieties. Ten plants per pot were sown. The sorghum plants were watered until the V3 growth stage. Water was withheld for 8 days to induce drought stress. The plants were re-watered for 24 hrs.

The effects of drought stress on sorghum root and shoot length as well as 24 hrs after re-watering were evaluated in both ICSB 338 and SA 1441 sorghum varieties (Figure 3.3). Generally, the root length increased significantly in both sorghum varieties following drought stress and remained constant after re-watering (Figure 3.3A). In contrast, the shoot length decreased for the ICSB 338 drought stressed samples in comparison to the well-watered controls, and remained constant after re-watering as illustrated on Figure 3.3B. For SA 1441, there was no significant difference in shoot length between the controls, drought stressed and re-watered samples.

Both ICSB 338 and SA 1441 showed significantly reduced root and shoot fresh and dry weight for both the drought-stressed and re-watered samples compared to their respective controls as shown in Figure 3.4. The only exception was SA 1441 root fresh weight which showed no significant reduction in weight after drought stress (Figure 3.4A).

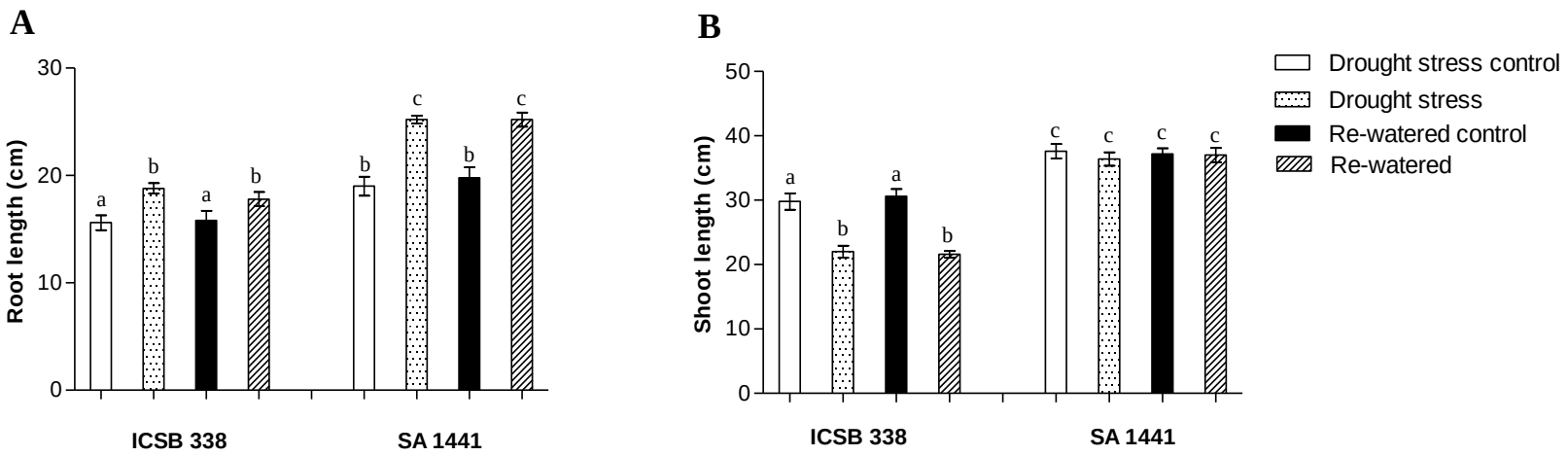

Figure 3.3: Effects of drought on sorghum shoot and root growth. Root (A) and shoot (B) length for the control, drought stressed and re-watered ICSB 338 (drought susceptible) and SA 1441 (drought tolerant) sorghum varieties. Plants were watered until the V3 growth stage. Water was withheld to induce drought stress and root and shoot length was measured for the control and drought stressed samples on the 8th day of drought stress. The plants were re-watered and the same measurements were repeated after 24 hrs. Bars represent mean ±SE (n = 5). Bars with the same letter are not significant different at $p \leq 0.05$ according to the Mann-Whitney test.

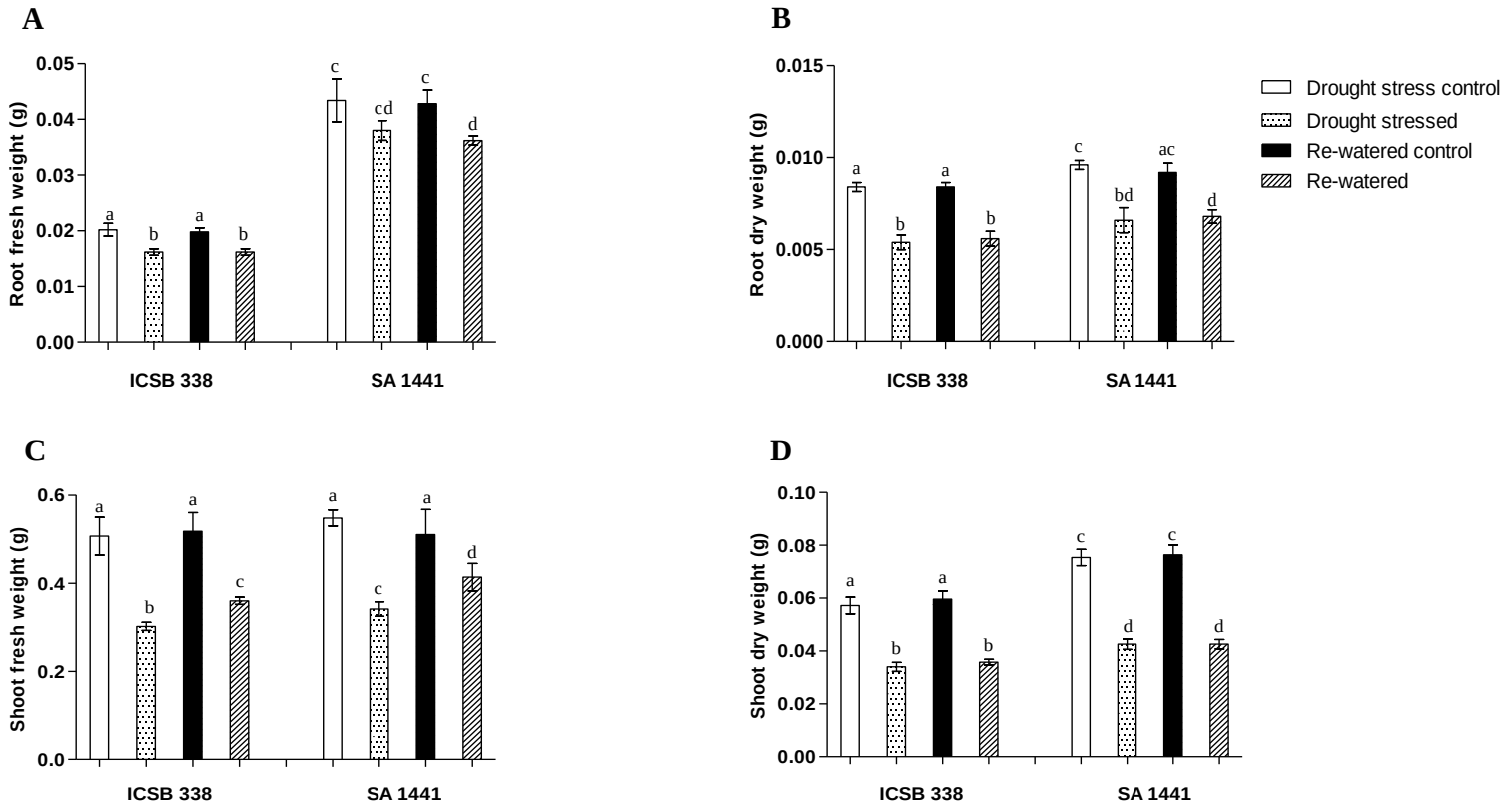

Figure 3.4: The effects of drought on sorghum root and shoot weight. Root fresh weight (A), root dry weight (B), shoot fresh weight (C) and shoot dry weight (D) for the control, drought stressed and re-watered ICSB 338 (drought susceptible) and SA 1441 (drought tolerant) sorghum varieties. Plants were well-watered until the V3 growth stage. Water was withheld and fresh weight readings for the control and drought stressed samples were taken on the 8th day of drought stress. The samples were then oven-dried to determine the dry weight. The plants were re-watered and readings were repeated after 24 hrs. Bars represent mean ±SE (n = 5). Bars with the same letter are not significantly different at $p \leq 0.05$ according to the Mann-Whitney test.

3.2.3 Leaf Relative Water Content

The 8 day drought stress treatment negatively affected the leaf relative water content (RWC) of both ICSB 338 and SA 1441 sorghum varieties (Figure 3.5). This was shown by the statistically significant reduction in RWC from 100% to 61% and 90% for ICSB 338 and SA 1441 drought-stressed samples, respectively. However, 24 hrs after re-watering the plants, the initial RWC for both sorghum varieties was restored to the levels of the controls.

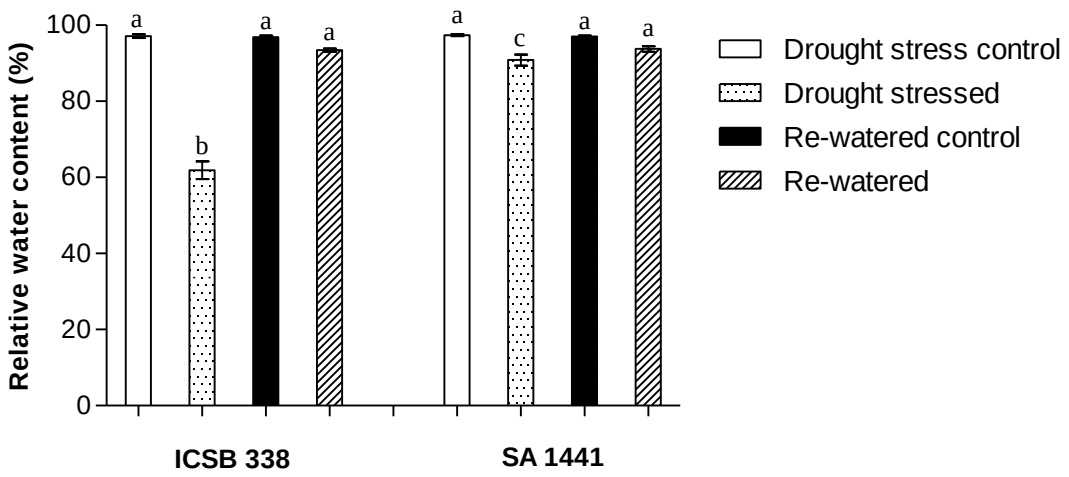

Figure 3.5: The effects of drought stress on RWC of sorghum. The RWC for the control, drought stressed and re-watered leaf samples of ICSB 338 (drought susceptible) and SA 1441 (drought tolerant) sorghum varieties. Seedlings were well-watered until the V3 growth stage. Water was withheld to induce drought stress and the RWC was estimated for the control and drought-stressed samples on the 8th day of drought stress. The seedlings were re-watered and the measurements were repeated after 24 hrs. Bars represent mean ±SE (n = 5). Bars with the same letter are not significantly different at $p \leq 0.05$ according to the Mann-Whitney test.

3.2.4 Leaf Stomatal Conductance and Surface Temperature

The stomatal conductance remained constant until day 3 of drought stress for both sorghum varieties (Figure 3.6A). Thereafter, the drought-stressed samples experienced a significant reduction in stomatal conductance for both varieties. An increase in stomatal conductance was exhibited by only SA 1441, 24 hrs after re-watering.

There was no significant difference between the control and drought-stressed leaf surface temperature of ICSB 338 for the first 4 days of drought stress. For SA 1441, the increase in leaf surface temperature began at day 3 of drought stress (Figure 3.6B). The leaf surface temperature then gradually increased for both varieties until day 8 of drought stress. The rate of temperature increase was however greater for SA 1441 compared to ICSB 338. After re-watering, the leaf surface temperatures for both sorghum varieties significantly dropped to the level of the control plants.

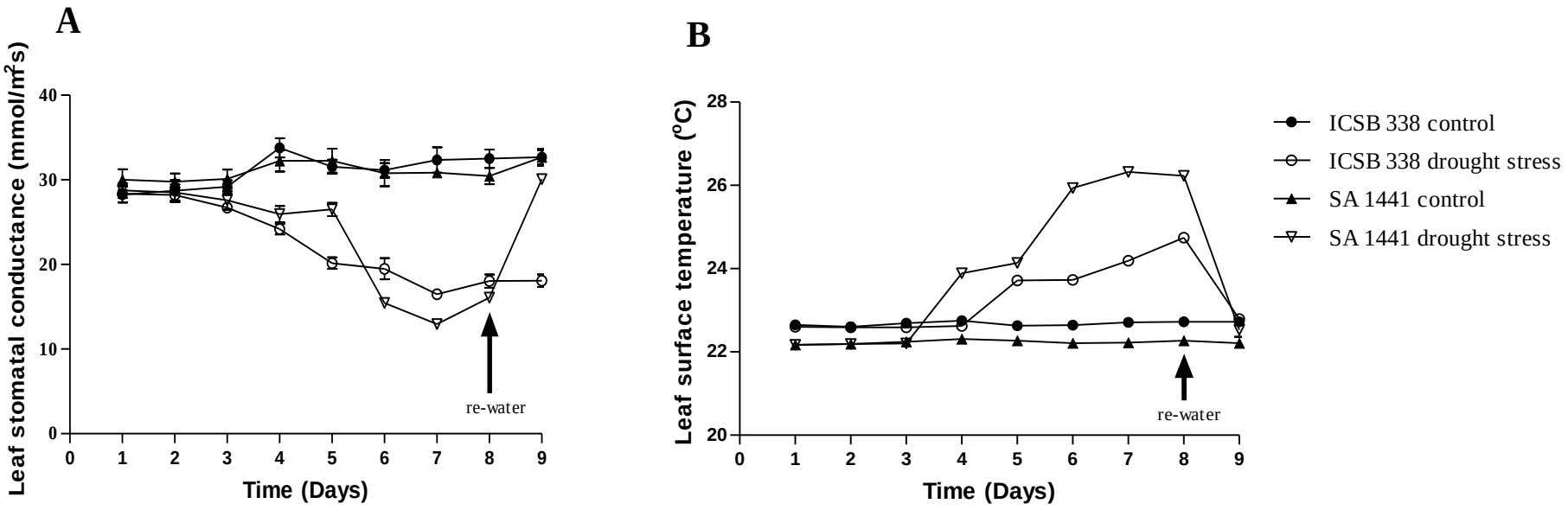

Figure 3.6: The effects of drought on sorghum leaf stomatal conductance and surface temperature. Leaf stomatal conductance (A) and leaf surface temperature (B) for the control, drought-stressed and re-watered third leaf of ICSB 338 (drought susceptible) and SA 1441 (drought tolerant) sorghum varieties. Both parameters were taken simultaneously using a portable leaf porometer. Plants were well watered until the V3 growth stage. Water was withheld to induce drought stress and readings for the control and drought stressed samples were taken on the 8th day of drought stress. The plants were re-watered and the same measurements were repeated after 24 hrs. Bars represent ± SE (n = 10). Bars with the same letter are not significantly different at $p \leq 0.05$ according to the Mann-Whitney test.

3.2.5 Leaf Chlorophyll Content

The chlorophyll content indices for the drought-stressed ICSB 338 and SA 1441 sorghum varieties showed no significant differences with their respective controls for the first 3 days of drought stress treatment (Figure 3.7). Decreases in chlorophyll content were observed for both sorghum varieties from day 3 after the induction of drought stress. The chlorophyll content of ICSB 338 decreased at a faster rate compared to SA 1441. Twenty four hrs after re-watering, the chlorophyll content of SA 1441 increased significantly while that of ICSB 338 remained constant.

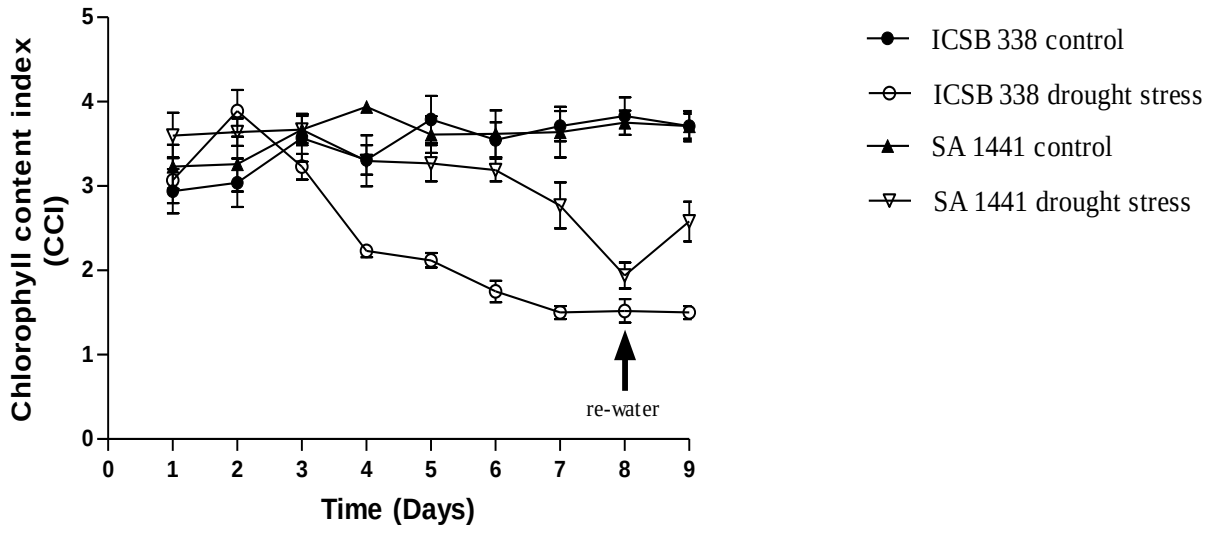

Figure 3.7: The effects of drought on sorghum leaf chlorophyll content. Leaf chlorophyll content index for the control, drought-stressed and re-watered third leaf of ICSB 338 (drought susceptible) and SA 1441 (drought tolerant) sorghum varieties. The readings were taken using chlorophyll content meter. Plants were watered until the V3 growth stage. Water was withheld to induce drought stress and readings for the control and drought stressed samples were taken on the 8th day of drought stress. The plants were re-watered and readings were repeated after 24 hrs. Bars represent ± SE (n = 10).

3.2.6 Root and Leaf Relative Cell Death

The root and leaf relative cell death was estimated using the Evans blue assay. The drought susceptible variety ICSB 338 exhibited higher root and leaf relative cell death under drought stress compared to the drought tolerant SA 1441 as shown in Figure 3.8.

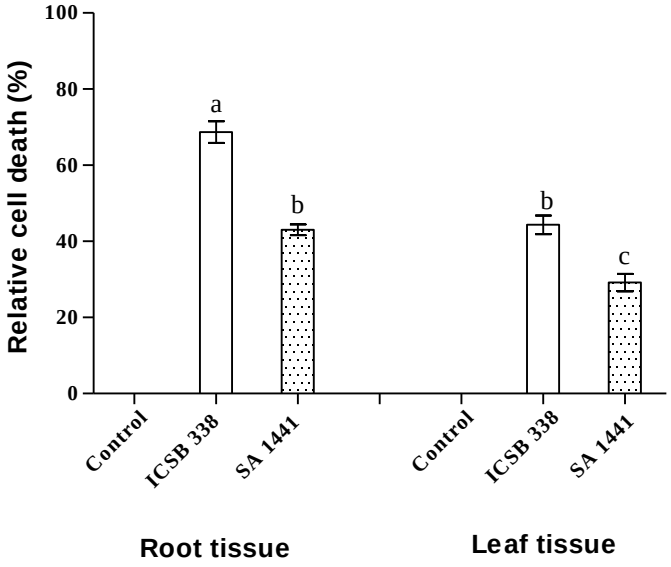

Figure 3.8: The effects of drought on root and leaf cell death. Cell death percentage for the root and leaf tissue of the control and drought stressed ICSB 338 (drought susceptible) and SA 1441 (drought tolerant) sorghum samples. Plants were well-watered until the V3 growth stage. Water was withheld for 8 days to induce drought stress and the Evans blue assay was carried out using 50 mg for each of the samples. Bars represent mean ± SE (n = 3). Bars with the same letter are not significantly different at $p \leq 0.05$ according to the Mann-Whitney test.

3.2.7 Osmolyte Content Analysis

3.2.7.1 Proline and Glycine Betaine (GB) Content Analysis

The proline and glycine betaine content analysis was performed using Hydrophilic Interaction Liquid Chromatography-Mass Spectrometry (HILIC-MS) at 0, 4, 8 and 12 days post drought stress. The root and leaf tissue proline content (Figures 3.9A and C, respectively) remained constant for both sorghum for the first 4 days of drought stress treatment. At day 8, there was a significant increase in proline content in SA 1441 for both root and leaf tissue whilst it remained low for ICSB 338. The root and leaf glycine betaine content (Figures 3.9B and D, respectively) showed a significant difference between ICSB 338 and SA 1441 at days 4 and 8 of drought stress for both root and leaf tissue. At day 8 of drought stress, SA 1441 exhibited significantly higher glycine betaine content for both root and leaf tissue (Figures 3.9B and D, respectively).

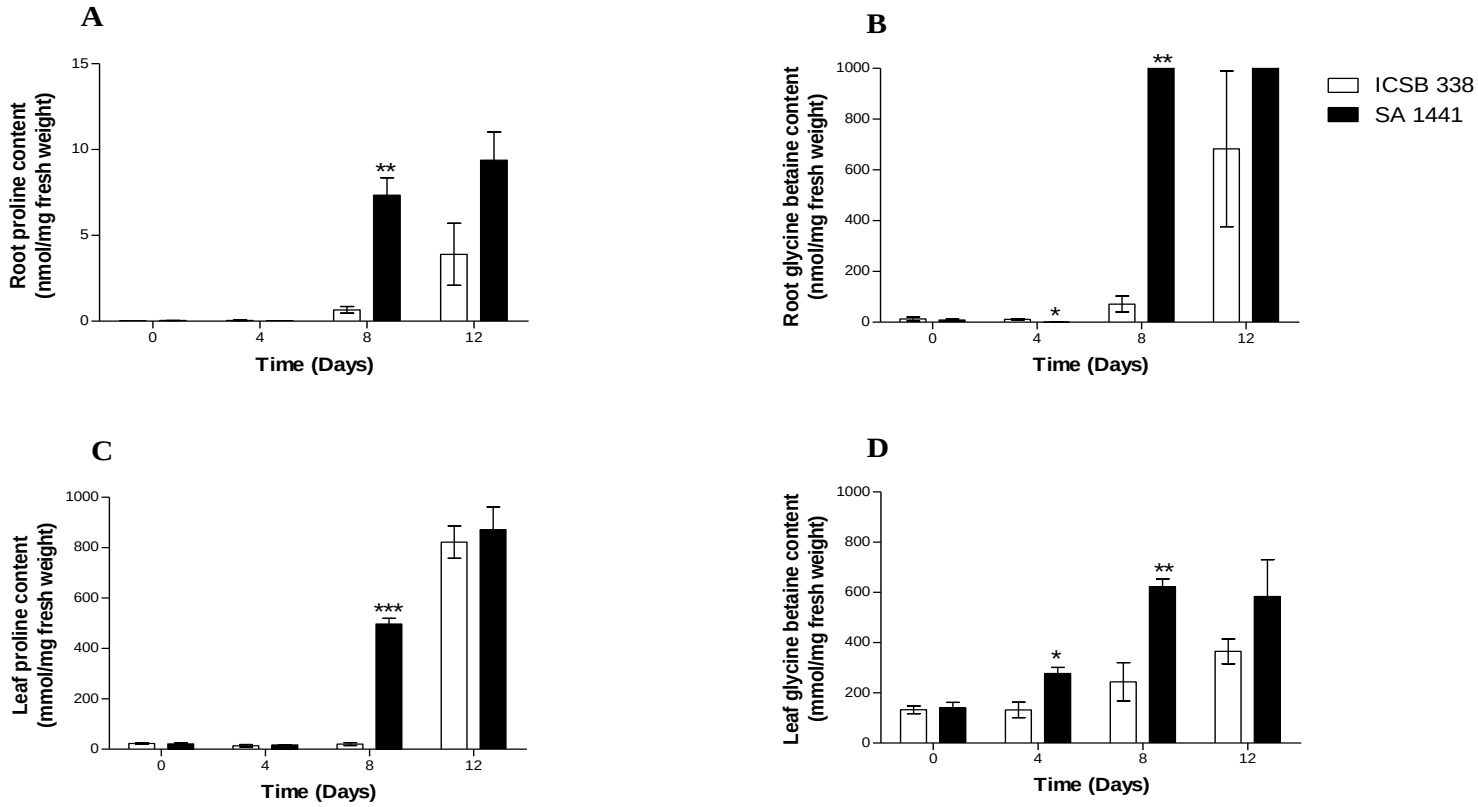

Figure 3.9: Effects of drought stress on sorghum leaf proline and glycine betaine content. Sorghum root proline (A) and root glycine betaine (B) content and leaf proline (C) and leaf glycine betaine (D) content for ICSB 338 (drought susceptible) and SA 1441 (drought tolerant) sorghum varieties, respectively are shown above. Seedlings were well-watered until the V3 growth stage. Water was withheld to induce drought stress and samples were collected at 0, 4, 8 and 12 days of drought stress. HILIC-MS was used for osmolyte content analysis. Bars represent ± SE (n = 3). *, ** and *** = significance between ICSB 338 and SA 1441 at each time point at $p \leq 0.05$, 0.01 and 0,001, respectively.

3.3 Discussion

The effects of drought stress occur at morphological, biochemical and molecular levels and may be evident at any phenological stage at which the stress is imposed (Farooq *et al*., 2009). Drought stress causes osmotic and oxidative stress which results in undesirable effects on plant growth. Cell division, elongation, enlargement and differentiation are the main processes necessary for growth and depend on water availability to effect growth. Any disruption of these vital plant processes can lead to stunted growth whilst severe water deprivation can result in plant death.

In this study, two sorghum varieties described by plant breeders as drought susceptible and drought tolerant (Table 2.1) were used to comparatively analyse their physiological and biochemical responses to drought stress. These were the drought susceptible ICSB 338 and drought tolerant SA 1441. Currently, there is no published data confirming the drought response phenotype of these sorghum varieties. The two sorghum varieties were grown in a soil-potted experiment at field capacity and drought stress was imposed by withholding water for 8 days. Following drought stress, the plants were re-watered and measurements were repeated after 24 hrs. This allowed the evaluation of the abilities of the two varieties to recover from the imposed drought stress. The sorghum plants for osmolyte content analysis were harvested in a time course drought stress experiment at 0, 4, 8 and 12 days.

The RWC of a leaf estimates the current water status of the sampled tissue relative to the maximal water content it can hold at full turgidity (Barrs and Weatherley, 1962). In essence, the RWC value reflects a measure of water balance or deficit in the leaf (González and González-Vilar, 2001). The leaf RWC decreased for both seed varieties following drought stress (Figure 3.5). Similar results were observed in both drought resistant and susceptible sorghum varieties grown in the semi-arid tropics (Sivaramakrishnan *et al*., 1988) as well as in

another study in wheat (Siddique *et al*., 2000). In this study, the leaf RWC was higher for the drought stressed SA 1441 compared to ICSB 338 (Figure 3.5). The RWC increased significantly for both varieties 24 hrs after re-watering which may signify the possibility of the ability of the sorghum varieties to restore leaf water status after a period of water stress before permanent cell damage occurs.

One of the first responses of plants to osmotic stress is the production of the endogenous growth regulator ABA (Ackerson and Radin, 1983). ABA controls stomatal closure thus reducing transpirational water loss and its deleterious effects (Ludlow and Muchow, 1990). In this study, stomatal conductance (Figure 3.6A) and chlorophyll content (Figure 3.7) of both sorghum varieties decreased with an increase in drought stress over the 8 days of stress treatment. Significant differences between the two sorghum varieties and their respective controls were exhibited beginning at day 4 after withholding water. A corresponding increase in leaf surface temperature was observed beginning at day 3 (Figure 3.6B). The increase in leaf surface temperature can be attributed to stomatal closure which reduces gaseous exchange and ventilation thereby increasing the amount of heat available within the leaf that can be dissipated (Yokota *et al*., 2002). A similar increase in leaf surface temperature in response to drought stress was reported in wheat (Siddique *et al*., 2000).

Stomatal closure possibly reduced the rate of photosynthesis since CO_2 and O_2 were hindered from diffusing in and out of the leaves, respectively. This was reflected by the low plant total biomass as estimated by root and shoot fresh and dry weights of the drought stressed plants compared to the well-watered controls (Figure 3.4). The chlorophyll content was also reduced with an increase in the duration of drought stress for both sorghum varieties (Figure 3.8). Similar results were reported in a sorghum drought stress experiment by Jagtap *et al*. (1998) in varieties with differing drought stress tolerances.

In this study, the drought tolerant variety SA 1441 had higher total chlorophyll content compared to the drought susceptible variety ICSB 338. There was significant recovery in both chlorophyll (Figure 3.7) and stomatal conductance (Figure 3.6A) of SA 1441 after re-watering. Beardsell and Cohen (1975) also observed the same trend in stomatal conductance in maize and sorghum after re-watering. Contrary to this result, ICSB 338 showed no significant change in the chlorophyll content and stomatal conductance 24 hrs after re-watering indicating the inability of the drought susceptible variety to increase the biosynthesis of photosynthetic pigments immediately after water supply to the plant is restored. This could have been because of the excessive oxidative damage of photosynthetic machinery due the accumulation of ROS in ICSB 338 leaf tissue during drought stress. This damage was reflected partly in higher relative cell death of ICSB 338 root and leaf tissues in comparison to SA 1441 (Figure 3.8). However, ROS levels in both root and leaf tissue would need to be measured to ascertain the level of oxidative stress in the two sorghum varieties.

The plant root and shoot weight was significantly reduced for both sorghum varieties compared to their respective controls following drought stress (Figure 3.4). This could have been due to the limited production and translocation of photo-assimilates. This result is in contrast to the increased root weight in drought resistant sorghum varieties observed by Nour and Weibel, (1978). Stomatal closure could have also contributed to this phenomenon since it ultimately reduced the rate of photosynthesis. Furthermore, the increased relative cell death (Figure 3.8) due to drought stress could have also reduced the total surface area available for photosynthesis.

In contrast to the observed reduced root weight (Figure 3.4A and B), root length increased significantly (Figure 3.3A) for both sorghum varieties in response to drought stress. This could have been due to the extension of roots by the sorghum plant in search of water. This

could possibly have been facilitated by ABA which maintains cell expansion in roots under dry conditions whilst halting that in shoots (Munns and Sharp, 1993). Nour and Weibel (1978), also observed increased root length in drought resistant sorghum varieties compared to the less drought resistant varieties whilst Merrill and Rawlins (1979), reported that sorghum plants direct resources to deeper soil penetration through higher root density in the deeper soil profile during drought stress. Furthermore, Xu and Bland (1993), demonstrated that sorghum can extract water from deep soil via an elongated root system and subsequently efflux the water to the dry upper soil layers before resuming uptake again. This adaptation ensures that the sorghum plants can access both moisture and mineral nutrients even in hot and dry conditions.

Apart from the growth and physiological changes observed in ICSB 338 and SA 1441 sorghum varieties in response to drought stress, the proline and glycine betaine contents of the two varieties also differed. Proline is a compatible osmolyte that functions as an osmo-protectant involved in various important functions in osmotic balancing during stress (Di Martino *et al*., 2003). In this study, proline content was significantly higher for the drought tolerant variety SA 1441 compared to the drought susceptible variety ICSB 338 from day 8 of drought stress in both root and leaf tissue (Figures 3.9A and C). The same results were obtained in a comparative study using drought resistant and drought susceptible sorghum varieties (Sivaramakrishnan *et al*., 1988). The higher proline content reflects the ability of SA 1441 to synthesise compatible osmolytes required for osmotic adjustment and membrane protection earlier in the course of drought stress. This means that SA 1441 can better protect cellular components under drought stress compared to ICSB 338.

Increases in proline content in response to drought stress were also observed in sorghum and soybean (Waldren and Teare, 1974) as well as wheat (*Triticum vulgare*), plantago (*Plantago*

ovata), papavar (*Papaver somnifera*) and mustard (*Brassica juncea*) (Patel and Vora, 1985). Proline is also known for its role in ROS scavenging (Hare and Cress, 1997). Reactive oxygen species are chemically reactive molecules or free radicals which contain oxygen (Hayyan *et al*., 2016). The ROS are synthesised in high quantities in response to drought stress and this is detrimental to plant growth since they degrade proteins and nucleic acids (Vranova *et al*., 2002).

The quaternary ammonium compound glycine betaine, whose main function in plants is osmotic adjustment, increased gradually in root and leaf tissue for both sorghum varieties with an increase in the duration of drought stress (Figures 3.9B and D). There was a higher increase in the glycine betaine content of SA 1441 compared to ICSB 338 in both root and leaf tissue. This is in agreement with Quan *et al*. (2004) who transformed maize plants with the *betA* gene encoding a key enzyme in glycine betaine biosynthesis and treated the plants with drought stress (Quan *et al*., 2004). Maize plants expressing the *betA* gene accumulated more glycine betaine and were more drought tolerant. Glycine betaine has also been shown to increase in abundance under dehydration stress in sorghum (Yang *et al*., 2003; Fracasso *et al*., 2016) The observed increase in both proline and glycine betaine content represent an important adaptive response of sorghum to drought stress, in particular SA 1441, the drought tolerant variety. Furthermore, the overall higher levels of proline in leaf tissue compared to roots and the inverse for glycine betaine possibly indicates the tissue specific responses of sorghum to drought stress.

Based on the physiological and biochemical data obtained in this study, generally the drought susceptible variety ICSB 338 was more adversely affected by drought stress and exhibited poor recovery after re-watering compared to the drought tolerant variety. Having confirmed

the tolerance status of these two sorghum varieties to drought stress, they were further utilized in a sorghum drought stress proteomic study as described in the following chapter.

CHAPTER 4

IDENTIFICATION OF DROUGHT STRESS RESPONSIVE PROTEINS FROM SORGHUM ROOT TISSUE AND GENE EXPRESSION ANALYSIS OF SELECTED TARGETS

4.1 Introduction

Under environmental stresses, plants undergo physiological and biochemical changes to restore cellular homeostasis. Drought stress also triggers gene and protein expression changes in plants. Some of these molecular responses are involved in signal transduction pathways and in the re-activation of gene expression for cellular protective functions and osmotic balance (Shinozaki *et al*., 2003; Shinozaki and Yamaguchi-Shinozaki, 2007). For example protein kinases and phosphatases are involved in cell signalling processes during stress response. In addition, enzymes involved in the biosynthesis of osmolytes are activated to maintain osmotic homeostasis during periods of stress.

Dehydrins, late embryogenesis abundant, responsive to abscisic acid (RABs) and vegetative storage proteins are some of the known drought stress responsive proteins (Artlip and Funkhouser, 1995). However, the level of tolerance of a plant species to drought depends on its genetic make-up and the level of selective evolution to survive adverse environmental conditions. Sorghum, for instance is naturally drought tolerant (Rosenow *et al*., 1983). This attribute may be credited to the continuous exposure of the crop to harsh environmental conditions during its evolutionary history.

Proteomics studies have been performed in various plant species using different technologies with the aim of understanding stress adaptive mechanisms. These methods range from the classical two dimensional gel electrophoresis (2DE) based methods coupled with mass

spectrometry (MS) to the label and label-free liquid chromatography (LC-MS) and LC-MS/MS based methods. For example, 2DE has been applied in the proteomic analysis of rice (*Oryza sativa*) leaf tissue (Ji *et al*., 2012), sugar beet (*Beta vulgaris*) leaf tissue (Hajheidari Mohsen *et al*., 2005) and wheat (*Triticum aestivum*) leaf and root tissues (Peng *et al*., 2009) under drought stress. Although 2DE is relatively inexpensive and easy to perform, it has its own limitations such as the inability to resolve hydrophobic proteins and its non-quantitative nature (Haynes and Yates III, 2000). With the development of non-gel based proteomics, an improvement in the proteome coverage is possible with high accuracy and efficiency. Examples of such gel free techniques include the isobaric Tags for Relative and Absolute Quantitation (iTRAQ) (Ross *et al*., 2004). In iTRAQ analysis, 4 or 8 samples can be labelled and analysed simultaneously (Pierce *et al*., 2008).

The iTRAQ method has been used to study proteome changes in tobacco (*Nicotiana tabacum*) leaf tissue (Xie *et al*., 2016), wheat leaf tissue (Ford *et al*., 2011) and white clover (*Trifolium repens*) leaf tissue (Li *et al*., 2016b) under drought stress. Recently, proteomic changes in sorghum cell suspension cultures under sorbitol-induced osmotic stress have also been investigated (Ngara *et al*., 2018). Collectively, some of the differentially expressed drought responsive proteins identified in these studies were involved in photosynthesis, metabolism, and stress and defence-related processes. Currently there are a limited number of studies in root proteomics. Root proteomics is important in enhancing our knowledge on plant responses to water stress. This is because of the central roles played by roots in water stress perception and also in search for water deep down into the soil profile (Ghatak *et al*., 2016) during periods of drought.

The objective of this chapter was to perform a comparative iTRAQ analysis of the root proteome of two sorghum varieties under drought stress followed by gene expression analysis

of a few selected targets. The sorghum varieties used, ICSB 338 and SA 1441 had contrasting phenotypic traits to drought.

4.2. One Dimensional Protein Profiles of Sorghum Root and Leaf

Two sorghum varieties, ICSB 338 and SA 1441 were grown on soil and drought stressed by withholding water for 8 days as described in Section 2.2.3.1. Control plants were maintained at field capacity for the duration of the experiment. Root and leaf protein extracts were prepared and 2.5 µg and 10 µg of the root and leaf samples was electrophoresed on one dimensional sodium dodecyl sulfate-polyacrylamide gel electrophoresis (1D SDS-PAGE) for quality and quantity checks (Figures 4.1 and 4.2). For all protein samples, both the quality and loading quantities of the extracts was good with no visible signs of streaking. The protein samples were acetone precipitated and re-solubilised in extraction buffer for two dimensional-differential gel electrophoresis (2D-DiGE).

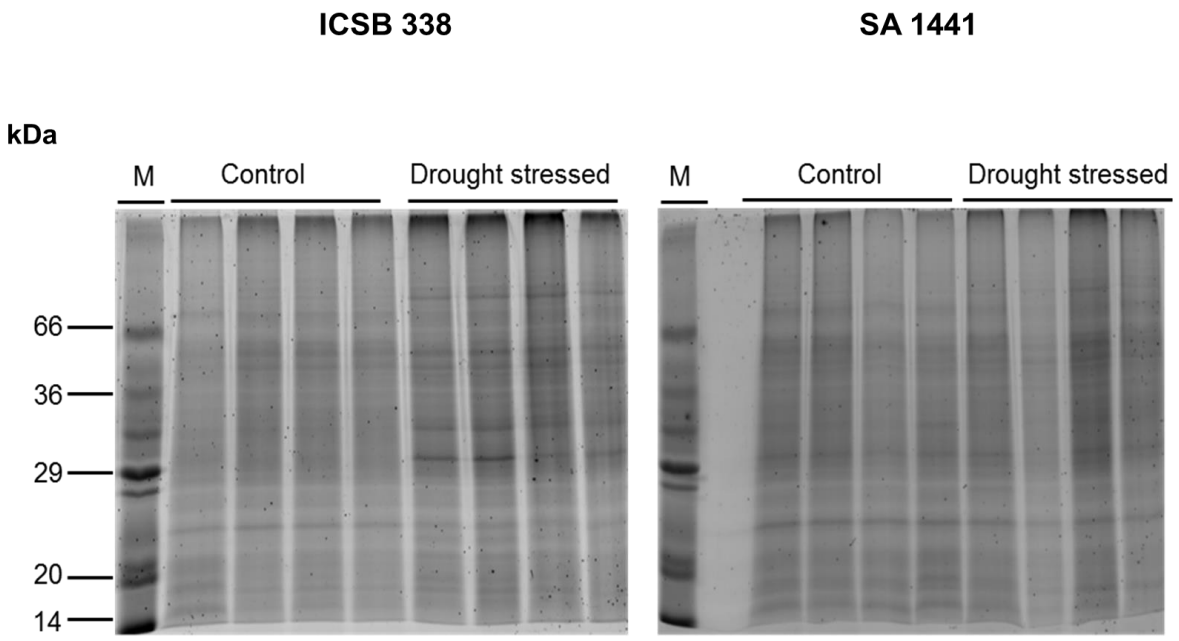

Figure 4.1: One dimensional SDS-PAGE analysis of sorghum root tissues. ICSB 338 is the drought susceptible variety, while SA 1441 is drought tolerant. Approximately 2.5µg of root protein of each sample was loaded on 12% (v/v) SDS-PAGE gels. Lane M is the molecular weight marker. The gels were stained with a SYPRO Ruby gel stain and images were taken using a Typhoon 9400 Variable Mode Imager. The first 4 lanes on each gel represent biological replicate protein extracts for the control root samples whilst the second 4 lanes represent the drought stressed biological replicate root protein extracts.

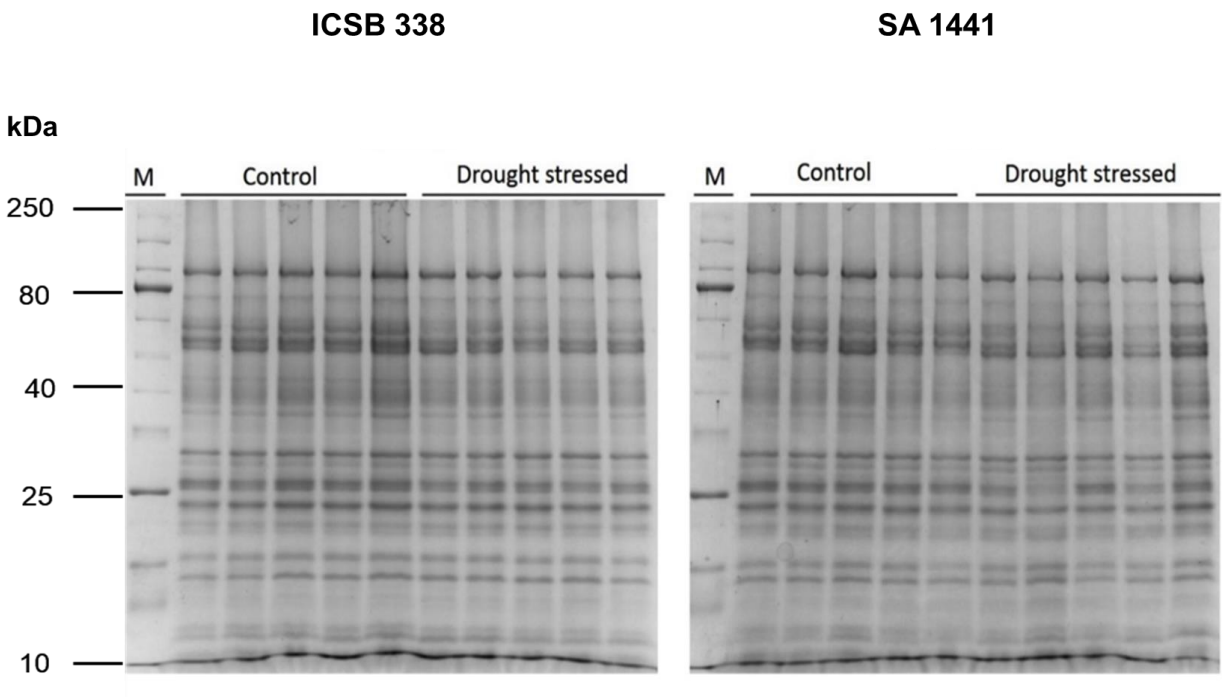

Figure 4.2: One dimensional SDS-PAGE analysis of sorghum leaf tissues. ICSB 338 is the drought susceptible variety, while SA 1441 is drought tolerant. Approximately 10µg of leaf protein of each sample was loaded on 12% (v/v) SDS-PAGE gels. Lane M is the molecular weight marker. The first 5 lanes on each gel represent biological replicate protein extracts for the control leaf samples whilst the second 5 lanes represent the drought stressed biological replicate leaf protein extracts. The gels were stained with Coomassie Brilliant Blue (CBB) R-250 stain and visualised using the Gel Doc Molecular imager.

4.3 2D-DiGE Profiles of Sorghum Root and Leaf Samples

Following the acetone precipitation and re-solubilisation of the sorghum root and leaf samples in extraction buffer, the samples were labelled with Cy fluorescent dyes for 2D-DiGE analysis. The controls were labelled with Cy3 (red) whilst the drought stress samples were labelled with Cy5 (green). The quality of the labelling was assessed using 1D SDS PAGE. The results showed that the labelling was successful (data not shown). This was followed by 2D-DiGE as described in Section 2.6.2. The root and leaf proteome profiles are

shown in Figures 4.3 and 4.4, respectively. These profiles showed some differential protein expression on the gel overlays, while some spots remained unchanged. For example, the green spots on the gel overlay represent protein spots that were up-regulated following drought stress, while the red spots represent down-regulated proteins. The orange spots are those that remained unchanged following the stress treatment. The purpose of 2D-DiGE was to visualise the proteins and confirm their differential expression in the two sorghum tissues before proceeding with iTRAQ analysis. Due to the high cost of iTRAQ analysis and the fact that a number of studies have been performed on leaf tissue, only the root samples were analysed in this study.

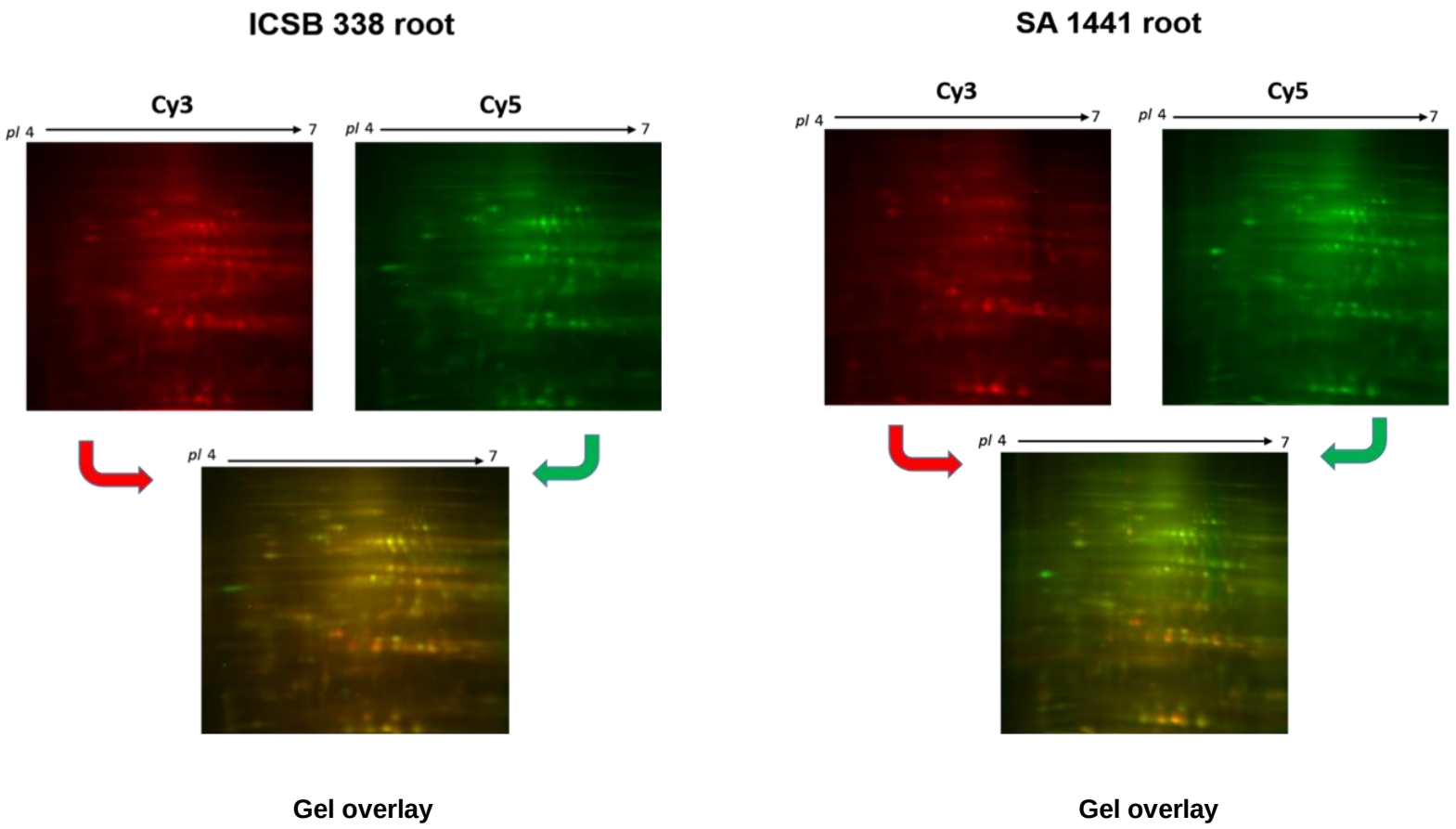

Figure 4.3: 2D-DiGE analysis of sorghum root total soluble protein. ICSB 338 is the drought susceptible variety, while SA 1441 is drought tolerant. Approximately 20 µg of root protein of each sample was separated on IPG strips of pH range 4-7. The control and drought stress samples were labelled with Cy3 and Cy5 fluorescent dyes, respectively. The gel images of control and drought samples were overlaid and imaged using the Typhoon Variable Mode Imager. The green and red spots in the gel overlay indicate protein up-regulation and down-regulation, respectively whilst the orange spots represent unchanged proteins following drought stress.

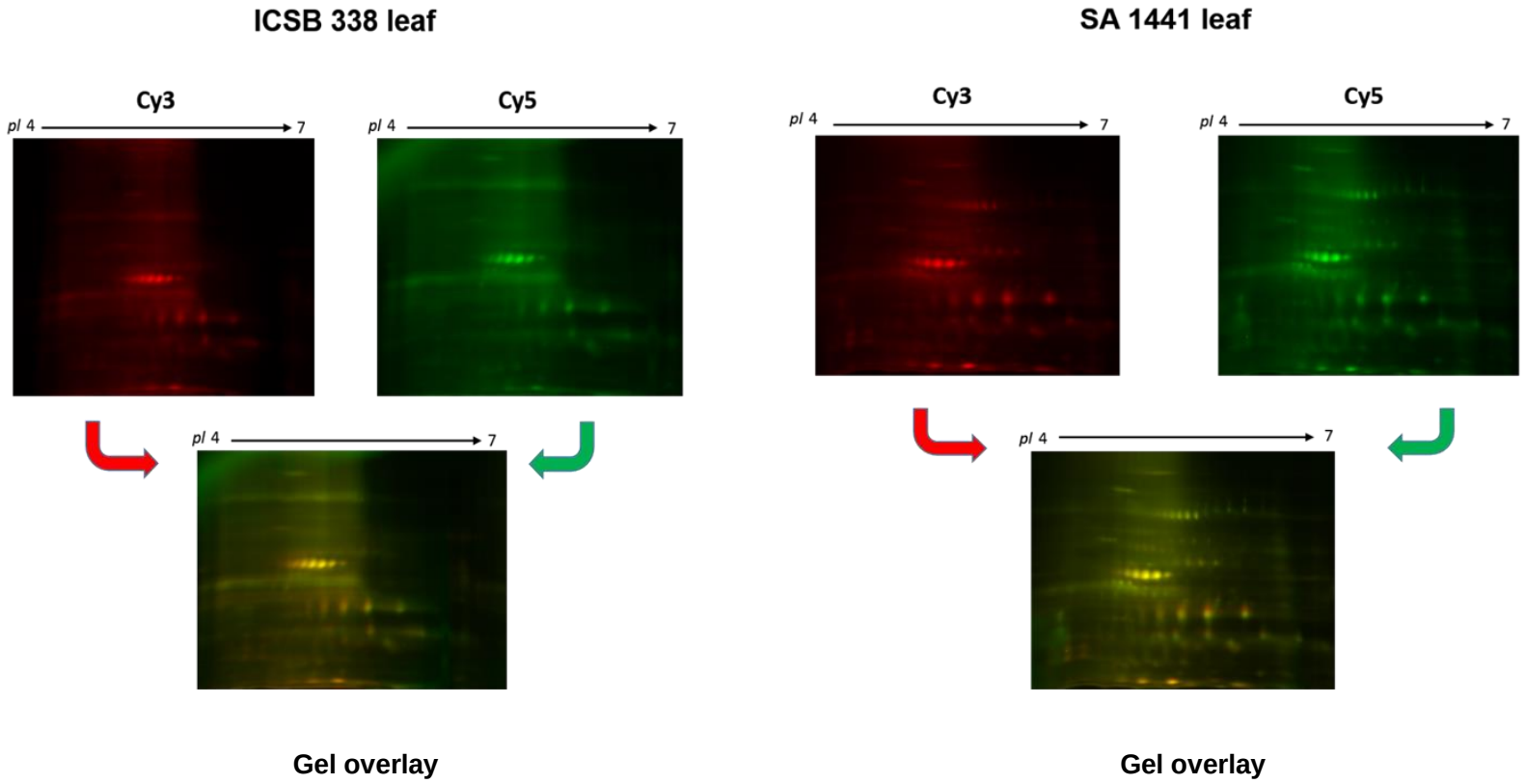

Figure 4.4: 2D-DiGE analysis of sorghum leaf total soluble protein. ICSB 338 is the drought susceptible variety, while SA 1441 is drought tolerant. Approximately 20 µg of leaf protein of each sample was separated on IPG strips of pH range 4-7. The control and drought stress samples were labelled with Cy3 and Cy5 fluorescent dyes, respectively. The gel images of control and drought samples were overlaid and imaged using the Typhoon Variable Mode Imager. The green and red spots in the gel overlay indicate protein up-regulation and down-regulation, respectively whilst the orange spots represent unchangedproteinsfollowingdroughtstress

.

4.4 iTRAQ Analysis of the Sorghum Drought Stress Responsive Root Proteins

Fifty micrograms each of root samples of ICSB 338 and SA 1441 sorghum varieties were digested with trypsin and prepared for iTRAQ analysis (Section 2.7.1). The four biological control replicates were labelled with tags of molecular weights 113, 114, 115, and 116, while the drought stress samples were labelled with 117, 118, 119, and 121 molecular weight tags. The samples were subsequently fractionated and analysed by LC-MS/MS. Only proteins identified with a minimum of two sequenced peptides with a statistical confidence threshold of greater than or equal to 95% were regarded as positively identified. This gave rise to a total of 1169 and 1043 positively identified root proteins in ICSB 338 and SA 1441 sorghum varieties, respectively. A large proportion of 76% and 72% of the proteins were uncharacterised for ICSB 338 and SA 1441 sorghum varieties, respectively.

A combined total of 1 341 unique proteins were identified in both sorghum varieties. Of these proteins, 871 were common to both sorghum varieties as illustrated in Figure 4.5 while 298 and 172 were unique to ICSB 338 and SA 1441, respectively The comparative fold-changes of the 871 root proteins common to both sorghum varieties is shown in Appendix, Figure A1 in the form of a heatmap. Of the 871 proteins common to both sorghum varieties, 174 and 172 were significant at 95% significance level for ICSB 338 and SA 1441, respectively. A total of 312 proteins significantly responded in at least one of the two sorghum varieties whilst there was an overlap of 34 significant proteins between ICSB 338 and SA 1441. Within the 312 significantly responding proteins in at least one sorghum variety, the highest fold change was approximately 2-fold. However, due to the large number of drought stress responsive proteins identified in this study, the heatmap (Appendix, Figure A1) does not include the actual protein names.

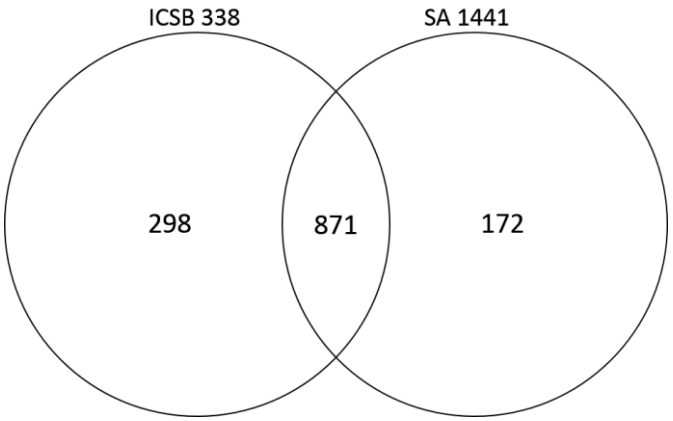

Figure 4.5: The relationship between ICSB 338 and SA 1441 identified drought stress responsive root proteins.

Of the positively identified root proteins, 237 and 184 were differentially expressed in response to drought stress in ICSB 338 and SA 1441, respectively (Tables 4.1 and 4.2). For ICSB 338, 111 (47%) proteins were up-regulated whilst 126 (53%) proteins were down-regulated. For SA 1441, 113 (61%) proteins were up-regulated whilst 74 (39%) proteins were down-regulated. For ICSB 338, fold change ranged from 1.06 (protein no. 250) to 2.93 (protein no. 868) for up-regulated proteins and -3.62 (protein no 1218) to -1.06 (protein no. 76) for down-regulated proteins. For SA 1441, fold change ranged from 1.10 (protein no. 158) to 2.72 (protein no. 1798) for up-regulated proteins and -1.52 (protein no. 161) to -1.07 (protein no. 157) for down-regulated proteins.

4.4.1 Bioinformatic Analyses on the Identified Drought Stress Responsive Sorghum Root Proteins

All the 237 and 184 differentially expressed drought stress responsive root proteins for ICSB 338 and SA 1441 respectively, were subjected to gene ontology annotation on the UniProt (http://www.uniprot.org/) database. Obsolete proteins on the UniProt database were annotated using the Morokoshi (http://sorghum.riken.jp/morokoshi/Home.htmL) database. This resulted in the determination of the cellular component, biological process, and functional process as shown in Tables 4.1 and 4.2. The conserved domains and protein family names were identified for all the drought responsive root proteins of the two sorghum varieties using the InterPro database (https://www.ebi.ac.uk/interpro/). Conserved domains assist in characterising proteins because they are distinct functional regions on proteins that can carry out a function independently (Marchler-Bauer *et al*., 2010). Family names on the other hand, link the proteins to their ancestral origins with the same protein structure, sequence and function (Finn *et al*., 2013).

Table 4.1: List of drought stress responsive proteins identified from ICSB 338 root samples using the iTRAQ and database searches.

Prot No[a]	Accession[b]	Prot Name	Scor[c]	% Cov[d]	Seq Pep[e]	Ratio[h]	SD[g]	p-val[f]	GO Analysis[i]			Conserved domains and family name[j]
									P	F	C	
Metabolism												
1	C9DHL2	Lipoxygenase OS=*Sorghum bicolor*	66.79	46.64	39	-1.53	0.05	9.0E-06	Oxylipin biosynthetic process	Oxidoreductase activity	None predicted	Lipoxygenase, C-terminal domain; lipoxygenase family
5	H2ET77	Sucrose synthase OS=*Sorghum bicolor* GN=SUSY2	49.35	35.29	30	-1.69	0.04	2.7E-05	Sucrose metabolic process	Sucrose synthase activity	None predicted	Sucrose synthase domain; sucrose synthase, plant/cyanobacteria family
6	C5WNU8	Lipoxygenase OS=*Sorghum bicolor* GN= SORBI_3001G125800	48.96	40.20	29	-1.31	0.06	5.9E-04	Fatty acid biosynthetic process	Dioxygenase activity	None predicted	Lipoxygenase, C-terminal domain; lipoxygenase family
13	A0A1B6Q6S1	Uncharacterized protein OS=*Sorghum bicolor* GN=SORBI_3003G336000	41.68	46.33	25	-1.16	0.07	9.7E-03	Glucose catabolic process	Phosphoglycerate mutase activity	Cytoplasm	BPG-independent PGAM, N-terminal domain; phosphoglycerate mutase, 2,3-bisphosphoglycerate-independent family
21	A0A1B6QE21	Uncharacterized protein OS=*Sorghum bicolor* GN= SORBI_3002G291200	36.63	46.85	23	-1.20	0.09	1.4E-02	UDP-glucose metabolic process	UTP:glucose-1-phosphate uridylyltransferase activity	None predicted	Domain not predicted; UTP--glucose-1-phosphate uridylyltransferase family
17	C5XES4	Lipoxygenase OS=*Sorghum bicolor* GN=SORBI_3003G385500	37.7	26.15	23	-1.41	0.01	4.1E-06	Fatty acid biosynthetic process	Dioxygenase activity	None predicted	Lipoxygenase, C-terminal domain; lipoxygenase family
31	A0A1B6QI05	Uncharacterized protein OS=*Sorghum bicolor* GN= SORBI_3001G089100	30.52	33.17	21	1.37	0.02	9.9E-06	Carbohydrate metabolic process	Hydrolase activity, hydrolyzing O-glycosyl compounds	None predicted	Glycoside hydrolase family 3 C-terminal domain and superfamily
34	C5X3X5	Uncharacterized protein OS=*Sorghum bicolor* GN= SORBI_3002G247600	29.92	47.92	33	1.40	0.15	4.6E-03	Glycosyl compound metabolic process	Hydrolase activity, acting on glycosyl bonds	None predicted	Domain not predicted; glycoside hydrolase family 1 family
40	A0A1B6QL52	Uncharacterized protein OS=*Sorghum bicolor* GN=SORBI_3001G260800	28.21	43.18	18	-1.28	0.06	1.7E-03	Biosynthetic process	Pyridoxal phosphate binding	None predicted	Aminotransferase, class I/classII domain; pyridoxal phosphate-dependent transferase, major domain
44	C5YIC1	Aconitate hydratase OS=*Sorghum bicolor* GN=SORBI_3007G068100	27.11	21.99	18	-1.07	0.05	3.4E-02	Metabolic process	Aconitate hydratase activity	None predicted	Aconitase A/isopropylmalate dehydratase small subunit, swivel domain; aconitase/Iron-responsive element-binding protein 2 family

48	A0A1B6PRR1	Uncharacterized protein OS=*Sorghum bicolor* GN=SORBI_3005G112800	26.66	31.71	17	-1.22	0.08	1.2E-02	One-carbon metabolic process	Hydrolase activity	None predicted	S-adenosyl-L-homocysteine hydrolase, NAD binding domain; adenosylhomocysteinase-like family
58	C5YZJ4	S-adenosyl methionine synthase OS=*Sorghum bicolor* GN=SORBI_3009G033600	25.03	54.04	21	1.45	0.11	1.6E-03	S-adenosyl methionine biosynthetic process	Methionine adenosyl transferase activity	Cytosol	S-adenosyl methionine synthetase, central domain; s-adenosyl methionine synthetase family
60	A0A194YGV9	Uncharacterized protein OS=*Sorghum bicolor* GN=SORBI_3010G023700	24.58	22.03	15	-1.19	0.05	1.4E-03	Metabolic process	Transketolase activity	None predicted	Transketolase, C-terminal domain; transketolase family
72	C5WXJ1	Sucrose synthase OS=*Sorghum bicolor* GN=SORBI_3001G344500	22.8	27.57	21	-1.37	0.10	3.6E-02	Sucrose metabolic process	Sucrose synthase activity	None predicted	Sucrose synthase domain; sucrose synthase, plant/cyanobacteria family
76	C5Z7L1	Pyrophosphate--fructose 6-phosphate 1-phosphotransferase subunit beta OS=*Sorghum bicolor* GN=PFP-BETA	22.34	31.15	14	-1.06	0.03	3.3E-02	Fructose 6-phosphate metabolic process	Diphosphate-fructose-6-phosphate 1-phosphotransferase activity	Cytoplasm	Phosphofructokinase domain; ATP-dependent 6-phosphofructokinase family
87	C5Y2F0	6-phosphogluconate dehydrogenase, decarboxylating OS=*Sorghum bicolor* GN=SORBI_3005G115600	20.89	27.18	16	-1.19	0.04	2.3E-03	D-gluconate metabolic process	Phosphogluconate dehydrogenase (decarboxylating) activity	None predicted	6-phosphogluconate dehydrogenase, NADP-binding domain; 6-phosphogluconate dehydrogenase family
96	A0A194YT53	Uncharacterized protein OS=*Sorghum bicolor* GN=SORBI_3004G345800	20.14	33.91	14	-1.11	0.03	1.5E-03	Metabolic process	Transferase activity, transferring acyl groups other than amino-acyl groups	None predicted	Thiolase, N-terminal domain; thiolase family
109	A0A1B6Q7Z8	Uncharacterized protein OS=*Sorghum bicolor* GN=SORBI_3003G410500	18.42	28.04	10	-1.15	0.05	1.5E-02	Carbohydrate metabolic process	Sedoheptulose-7-phosphate:D-glyceraldehyde-3-phosphate glyceronetransferase activity	Mitochondrion	Domain not predicted; transaldolase/Fructose-6-phosphate aldolase family
110	A0A1B6PEZ5	Uncharacterized protein OS=*Sorghum bicolor* GN=SORBI_3007G014700	18.4	34.73	11	-1.25	0.10	1.6E-02	Fructose metabolic process	Phosphotransferase activity, alcohol group as acceptor	Cytosol	Carbohydrate kinase PfkB domain; ribokinase-like superfamily
111	C5Z0G8	Uncharacterized protein OS=*Sorghum bicolor* GN=SORBI_3009G048100	18.39	22.67	18	1.13	0.05	4.6E-03	Lipid metabolic process	Hydrolase activity	None predicted	Fungal lipase-like domain; Alpha/Beta hydrolase fold superfamily
115	Q9XE77	Patatin OS=*Sorghum bicolor*	18.2	31.04	13	-1.47	0.10	4.9E-03	Lipid catabolic process	Hydrolase activity	None predicted	Patatin-like phospholipase domain; acyl transferase/acyl hydrolase/lysophospholipase superfamily
128	A0A194YKZ5	Uncharacterized protein OS=*Sorghum bicolor* GN=SORBI_3010G227400	17.68	17.58	8	1.18	0.08	1.1E-02	Carbohydrate metabolic process	Hydrolase activity, hydrolyzing O-glycosyl compounds	Extracellular	Domain not predicted; Glycosyl hydrolases family 31

131	Q94EL4	Chitinase-B (Fragment) OS=Sorghum arundinaceum	17.56	43.89	18	1.55	0.24	6.9E-03	Chitin catabolic process	Chitin binding	None predicted	Chitin-binding, type 1 domain; glycoside hydrolase, family 19
133	C5Y397	Alpha-mannosidase OS=*Sorghum bicolor* GN=SORBI_3005G132400	17.32	9.42	9	1.18	0.12	2.8E-02	Mannose metabolic process	Alpha-mannosidase activity	Apoplast	Glycoside hydrolase family 38, central domain and superfamily
138	C5YSN7	Beta-galactosidase OS=*Sorghum bicolor* GN=SORBI_3008G052200	16.71	13.87	10	1.23	0.09	2.1E-03	Carbohydrate metabolic process	Hydrolase activity, acting on glycosyl bonds	Vacuole	Glycoside hydrolase 35, catalytic domain; glycoside hydrolase, family 35
155	C5Y1P4	Uncharacterized protein OS=*Sorghum bicolor* GN=SORBI_3005G099000	16.08	38.78	10	-2.10	0.06	2.1E-02	Chitin catabolic process	Chitin binding	Extracellular region	Glycoside hydrolase family 18, catalytic domain; glycoside hydrolase superfamily
162	C5YB69	Uncharacterized protein OS=*Sorghum bicolor* GN=SORBI_3006G000100	15.74	17.04	14	-1.21	0.06	9.7E-03	Metabolic process	4 iron, 4 sulfur cluster binding	None predicted	Aconitase A/isopropylmalate dehydratase small subunit, swivel domain; aconitase/Iron-responsive element-binding protein 2 family
178	C5Y4G6	Uncharacterized protein OS=*Sorghum bicolor* GN=SORBI_3005G030100	14.66	19.19	9	-1.17	0.07	1.0E-02	Carboxylic acid metabolic process	Transferase activity, transferring acyl groups, acyl groups converted into alkyl on transfer	None predicted	2-isopropylmalate synthase LeuA, allosteric (dimerisation) domain; 2-isopropylmalate synthase, bacterial-type family
187	C5WWZ1	Uncharacterized protein OS=*Sorghum bicolor* GN=SORBI_3001G498500	14.16	19.48	9	-1.11	0.07	4.3E-02	L-serine biosynthetic process	O-phospho-L-serine:2-oxoglutarate aminotransferase activity	None predicted	Aminotransferase class V domain; phosphoserine aminotransferase family
197	C5Y093	Formate dehydrogenase, mitochondrial OS=*Sorghum bicolor* GN=SORBI_3004G265000	13.73	26.04	9	-1.28	0.04	1.6E-03	Formate catabolic process	Formate dehydrogenase (NAD+) activity	Mitochondrion	D-isomer specific 2-hydroxyacid dehydrogenase, NAD-binding domain; NAD-dependent formate dehydrogenase family
229	A0A194YR85	Uncharacterized protein OS=*Sorghum bicolor* GN=SORBI_3004G166700	12.37	17.88	7	1.10	0.04	2.9E-02	Carbohydrate metabolic process	Hydrolase activity, hydrolyzing O-glycosyl compounds	None predicted	Glycosyl hydrolase family 32, N-terminal domain; glycoside hydrolase, family 32
240	C5Y8Y2	Uncharacterized protein OS=*Sorghum bicolor* GN=SORBI_3006G235600	12.07	12.52	8	1.28	0.06	7.2E-04	Carbohydrate metabolic process	Hydrolase activity, hydrolyzing O-glycosyl compounds	None predicted	Glycoside hydrolase, family 3, N-terminal domain; glycoside hydrolase superfamily
249	C5XES7	Lipoxygenase OS=*Sorghum bicolor* GN=SORBI_3003G385900	11.83	13.40	9	-1.16	0.02	1.6E-03	Oxylipin biosynthetic process	Oxidoreductase activity	None predicted	Lipoxygenase, C-terminal domain; lipoxygenase family
250	A0A1B6Q495	Uncharacterized protein OS=*Sorghum bicolor*	11.83	21.74	6	1.06	0.03	4.2E-03	Metabolic process	IAA-Ala conjugate hydrolase activity	Plasma membrane	Domain not predicted; Sec1 family

		GN=SORBI_3003G190500										
258	C5Y5U9	Uncharacterized protein OS=*Sorghum bicolor* GN=SORBI_3005G177500	11.58	33.88	8	-1.97	0.01	1.9E-02	Chitin catabolic process	Chitin binding	Extracellular region	Glycoside hydrolase family 18, catalytic domain; Glycoside hydrolase superfamily
289	C5YYX0	Beta-hexosaminidase OS=*Sorghum bicolor* GN=SORBI_3009G017500	10.86	12.64	5	1.22	0.11	1.7E-02	Carbohydrate metabolic process	Beta-N-acetylhexosaminidase activity	Cytosol	Beta-hexosaminidase, eukaryotic type, N-terminal domain; Beta-hexosaminidase family
294	B5B9V8	Glutamine synthetase OS=*Sorghum bicolor* GN=gs	10.77	28.01	12	-1.60	0.06	3.4E-04	Glutamine biosynthetic process	Glutamate-ammonia ligase activity	None predicted	Glutamine synthetase, catalytic domain; Glutamine synthetase, N-terminal domain superfamily
319	C5Z1E3	ATP-dependent 6-phosphofructokinase OS=*Sorghum bicolor* GN=PFK	10.27	9.77	4	-1.18	0.08	1.7E-02	Fructose 6-phosphate metabolic process	6-phosphofructokinase activity	Cytoplasm	Phosphofructokinase domain; ATP-dependent 6-phosphofructokinase family
325	A0A1B6QG06	Uncharacterized protein OS=*Sorghum bicolor* GN=SORBI_3002G402700	10.11	4.14	5	-1.28	0.10	1.4E-02	Glutamate biosynthetic process	Glutamate synthase activity	None predicted	Glutamine amidotransferase type 2 domain; Glutamate synthase, alpha subunit, C-terminal domain superfamily
327	C5YMM3	Patatin OS=*Sorghum bicolor* GN=SORBI_3007G158600	10.1	20.69	6	-1.42	0.08	1.7E-03	Lipid catabolic process	Acylglycerol lipase activity	Membrane	Patatin-like phospholipase domain; Acyl transferase/acyl hydrolase/lysophospholipase superfamily
414	C5XZW8	Uncharacterized protein OS=*Sorghum bicolor* GN=SORBI_3004G261500	8.25	23.19	5	-1.25	0.04	1.5E-04	Nucleotide biosynthetic process	Ribose phosphate diphosphokinase activity	Cytosol	Ribose-phosphate pyrophosphokinase, N-terminal domain; Ribose-phosphate pyrophosphokinase family
449	C5XKA7	3-methyl-2-oxobutanoate hydroxymethyltransferase OS=*Sorghum bicolor* GN=SORBI_3003G011600	7.74	16.58	7	1.27	0.10	1.2E-02	Pantothenate biosynthetic process	3-methyl-2-oxobutanoate hydroxymethyltransferase activity	None predicted	Domain not predicted; Ketopantoate hydroxymethyltransferase family
482	C5XCA6	Amine oxidase OS=*Sorghum bicolor* GN=SORBI_3002G347300	7.32	7.89	3	1.24	0.18	4.4E-02	Amine metabolic process	Primary amine oxidase activity	None predicted	Copper amine oxidase, catalytic domain; Copper amine oxidase family
621	C5XHG5	Uncharacterized protein OS=*Sorghum bicolor* GN=SORBI_3003G265400	5.72	10.19	3	-1.26	0.13	1.8E-02	Cellular amino acid metabolic process	Threonine synthase activity	Cytoplasm	Domain not predicted; Pyridoxal-phosphate dependent enzyme
647	C5YD28	Glutamate dehydrogenase OS=*Sorghum bicolor* GN=SORBI_3006G165400	5.4	14.84	5	-1.38	0.07	2.7E-02	Cellular amino acid metabolic process	Glutamate dehydrogenase (NAD+) activity	Vacuolar membrane	NAD(P) binding domain of glutamate dehydrogenase domain; Glutamate dehydrogenase family
711	A0A1B6QME4	Uncharacterized protein	4.72	3.74	3	-1.22	0.09	2.2E-02	Pyruvate metabolic	Pyruvate, phosphate	None predicted	Pyruvate phosphate

		OS=*Sorghum bicolor* GN=SORBI_3001G326900							process	dikinase activity		dikinase, PEP/pyruvate-binding domain; Pyruvate/Phosphoenolpyruvate kinase-like domain superfamily
729	C5YUA1	Phosphotransferase OS=*Sorghum bicolor* GN=SORBI_3009G069800	4.52	8.28	2	-1.75	0.18	1.1E-02	Glucose 6-phosphate metabolic process	Phosphotransferase activity, alcohol group as acceptor	Cytosol	Hexokinase, C-terminal domain; Hexokinase family
735	C5YMI0	Uncharacterized protein OS=*Sorghum bicolor* GN=SORBI_3007G023700	4.44	5.19	3	-1.26	0.10	1.7E-02	None predicted	Modified amino acid binding	None predicted	Initiation factor eIF-4 gamma, MA3 domain; MIF4G-like domain superfamily
767	C5YBH7	Uncharacterized protein OS=*Sorghum bicolor* GN=SORBI_3006G135500	4.19	6.39	2	1.56	0.19	3.1E-03	None predicted	None predicted	None predicted	Galactose oxidase-like, Early set domain; Galactose oxidase, central domain superfamily
774	C5XY71	Nitrilase OS=*Sorghum bicolor* GN=nit	4.15	9.70	3	1.13	0.05	2.8E-02	Nitrogen compound metabolic process	Hydrolase activity, acting on carbon-nitrogen (but not peptide) bonds	None predicted	Carbon-nitrogen hydrolase domain; Carbon-nitrogen hydrolase superfamily
783	C5WV22	Chalcone-flavonone isomerase family protein OS=*Sorghum bicolor* GN=SORBI_3001G035600	4.1	14.29	2	1.31	0.20	3.2E-02	Flavonoid biosynthetic process	Chalcone isomerase activity	Endoplasmic reticulum	Chalcone isomerase domain; Chalcone isomerase superfamily
791	C5YN64	Uncharacterized protein OS=*Sorghum bicolor* GN=SORBI_3007G167800	4.07	5.75	2	-1.17	0.03	4.1E-02	Branched-chain amino acid biosynthetic process	Dihydroxy-acid dehydratase activity	Chloroplast stroma	Domain not predicted; Dihydroxy-acid dehydratase family
814	A0A1B6Q8W1	Uncharacterized protein OS=*Sorghum bicolor* GN=SORBI_3002G026300	4	5.66	2	-1.47	0.08	9.5E-03	Fructose 6-phosphate metabolic process	6-phosphofructokinase activity	Cytoplasm	Phosphofructokinase domain; ATP-dependent 6-phosphofructokinase family
828	C5Z263	Uncharacterized protein OS=*Sorghum bicolor* GN=SORBI_3010G005000	4	4.85	3	1.16	0.09	1.1E-02	Carbohydrate metabolic process	Hydrolase activity, acting on glycosyl bonds	Extracellular region	Domain not predicted; Glycoside hydrolase, family 28 family
924	C5YYK2	Uncharacterized protein OS=*Sorghum bicolor* GN=SORBI_3009G014600	3.27	11.27	2	-1.71	0.22	3.1E-02	Lipid metabolic process	Phosphatidylcholine 1-acylhydrolase activity	None predicted	Fungal lipase-like domain; Phospholipase A1-II family
933	C5YMM5	Patatin OS=*Sorghum bicolor* GN=SORBI_3007G158800	3.16	9.95	4	1.26	0.14	3.2E-02	Lipid metabolic process	Hydrolase activity	None predicted	Ca2+-independent phospholipase A2 domain; Patatin-like phospholipase
975	Q41290	Dhurrinase OS=*Sorghum bicolor*	2.82	5.31	3	1.15	0.07	3.3E-02	Carbohydrate metabolic process	Hydrolase activity, acting on glycosyl bonds	None predicted	Domain not predicted; Glycoside hydrolase family 1
1010	C5XEU4	Uncharacterized protein OS=*Sorghum bicolor* GN=SORBI_3003G388200	2.6	4.21	2	1.26	0.08	2.4E-02	RNA catabolic process	RNA binding	None predicted	Domain not predicted; Ribonuclease T2 family
1029	C5WP07	Aldose 1-epimerase OS=*Sorghum bicolor* GN=SORBI_3001G265600	2.5	5.93	2	1.29	0.19	4.6E-02	Hexose metabolic process	Aldose 1-epimerase activity	Cytosol	Domain not predicted; Aldose 1-epimerase family

Disease/defence												
10	C5XX52	Glyceraldehyde-3-phosphate dehydrogenase OS=*Sorghum bicolor* GN=SORBI_3004G205100	44.17	75.07	48	-1.59	0.01	3.3E-04	Oxidation-reduction process	Oxidoreductase activity	None predicted	Glyceraldehyde 3-phosphate dehydrogenase, domain and family
25	C5XXT8	Phenylalanine ammonia-lyase OS=*Sorghum bicolor* GN=SORBI_3004G220300	33.23	28.84	19	1.40	0.18	6.2E-03	L-phenylalanine catabolic process	Phenylalanine ammonia-lyase activity	Cytoplasm	Domain not predicted; phenylalanine ammonia-lyase family
43	C5WNL8	Uncharacterized protein OS=*Sorghum bicolor* GN=SORBI_3001G410200	27.28	27.28	25	1.31	0.06	5.2E-04	Hydrogen peroxide catabolic process	L-ascorbate peroxidase activity	Chloroplast	Haem peroxidase, plant domain; class I peroxidase family
11	A0A1B6PQR2	Uncharacterized protein OS=*Sorghum bicolor* GN=SORBI_3005G074400	42.68	42.68	22	-1.18	0.10	3.7E-02	Cell redox homeostasis	Protein disulfide isomerase activity	Endoplasmic reticulum lumen	Thioredoxin domain; protein disulphide isomerase family
43	C5WNL8	Uncharacterized protein OS=*Sorghum bicolor* GN=SORBI_3001G410200	27.28	62.40	25	1.31	0.06	5.2E-04	Hydrogen peroxide catabolic process	L-ascorbate peroxidase activity	Chloroplast	Haem peroxidase, plant domain; class I peroxidase family
53	C5WWQ2	Uncharacterized protein OS=*Sorghum bicolor* GN=SORBI_3001G342600	25.79	31.16	13	-1.17	0.09	1.7E-02	Cellular oxidant detoxification	Thioredoxin-disulfide reductase activity	Cytoplasm	Thioredoxin domain; thioredoxin-like superfamily
70	C5X1Q1	Uncharacterized protein OS=*Sorghum bicolor* GN=SORBI_3001G385900	23.37	45.58	17	1.23	0.17	4.1E-02	None predicted	None predicted	None predicted	Domain not predicted; ricin B-like lectins family
82	C5XGS0	Uncharacterized protein OS=*Sorghum bicolor* GN=SORBI_3003G258800	21.42	8.04	11	-1.21	0.02	1.9E-03	Oxidation-reduction process	Oxidoreductase activity, acting on the CH-NH2 group of donors, NAD or NADP as acceptor	Cytoplasm	FAD/NAD(P)-binding domain; Glutamate synthase, NADH/NADPH, small subunit 1 family
83	A0A1B6Q513	Uncharacterized protein OS=*Sorghum bicolor* GN=SORBI_3003G241500	21.09	30.43	13	-1.13	0.04	2.9E-02	Oxidation-reduction process	Magnesium ion binding	Plasma membrane	Isocitrate/isopropylmalate dehydrogenase family
93	C5Y949	Uncharacterized protein OS=*Sorghum bicolor* GN=SORBI_3006G243400	20.57	22.42	10	-1.17	0.06	4.3E-03	Oxidation-reduction process	Oxidoreductase activity, acting on the CH-OH group of donors, NAD or NADP as acceptor	None predicted	D-isomer specific 2-hydroxyacid dehydrogenase, NAD-binding domain; D-3-phosphoglycerate dehydrogenase family
95	C5YB27	Peroxidase OS=*Sorghum bicolor* GN=SORBI_3006G277800	20.25	44.22	18	-1.27	0.06	5.0E-03	Hydrogen peroxide catabolic process	Peroxidase activity	Extracellular region	Secretory peroxidase domain; plant peroxidase family
101	O82430	Putative alcohol dehydrogenase 1 OS=*Sorghum bicolor* GN=Adh1	19.05	31.66	11	-1.64	0.03	3.4E-03	Oxidation-reduction process	Oxidoreductase activity	None predicted	Alcohol dehydrogenase, N-terminal domain; NAD(P)-binding domain superfamily
108	C5XFP2	Uncharacterized protein OS=*Sorghum bicolor* GN=SORBI_3003G110200	18.43	38.61	12	-1.12	0.06	2.4E-02	Oxidation-reduction process	Oxidoreductase activity	None predicted	Alcohol dehydrogenase, C-terminal domain; NAD(P)-binding domain superfamily

126	A0A1B6QM42	Uncharacterized protein OS=*Sorghum bicolor* GN=SORBI_3001G310300	17.77	35.37	10	1.23	0.10	1.4E-02	None predicted	Protein binding	None predicted	Glutathione S-transferase, C-terminal-like domain; thioredoxin-like superfamily
134	A0A1B6Q818	Uncharacterized protein OS=*Sorghum bicolor* GN=SORBI_3003G416300	17.27	68.04	15	-1.31	0.11	8.2E-03	None predicted	Protein binding	None predicted	Glutathione S-transferase, C-terminal and superfamily
148	C5YB22	Peroxidase OS=*Sorghum bicolor* GN=SORBI_3006G277500	16.29	33.70	11	-1.37	0.05	2.1E-03	Hydrogen peroxide catabolic process	Peroxidase activity	Extracellular region	Secretory peroxidase domain; Plant peroxidase family
149	A0A194YU12	Uncharacterized protein OS=*Sorghum bicolor* GN=SORBI_3004G341200	16.29	21.01	8	1.07	0.02	4.1E-03	Cellular oxidant detoxification	Oxidoreductase activity, acting on a sulfur group of donors, NAD(P) as acceptor	Peroxisome	FAD/NAD(P)-binding domain; Glutathione-disulphide reductase family
173	C5Z864	Peroxidase OS=*Sorghum bicolor* GN=SORBI_3010G232500	14.82	25.98	8	1.23	0.13	1.5E-02	Hydrogen peroxide catabolic process	Peroxidase activity	Extracellular region	Secretory peroxidase domain; Plant peroxidase family
232	C5XIX9	Peroxidase OS=*Sorghum bicolor* GN=SORBI_3003G151900	12.33	19.95	7	1.16	0.11	3.3E-02	Hydrogen peroxide catabolic process	Peroxidase activity	Extracellular region	Secretory peroxidase domain; plant peroxidase family
234	C5WZ12	Uncharacterized protein OS=*Sorghum bicolor* GN=SORBI_3001G514400	12.3	34.88	12	1.40	0.12	1.5E-03	Glutathione metabolic process	Glutathione transferase activity	Cytoplasm	Glutathione S-transferase, C-terminal domain; thioredoxin-like superfamily
235	C5Z469	Peroxidase OS=*Sorghum bicolor* GN=SORBI_3010G161600	12.25	33.12	8	1.66	0.28	4.2E-03	Hydrogen peroxide catabolic process	Peroxidase activity	Extracellular region	Secretory peroxidase domain; plant peroxidase family
259	A0A1B6PL71	Uncharacterized protein OS=*Sorghum bicolor* GN=SORBI_3006G096400	11.53	20.85	7	1.25	0.13	1.2E-02	Oxidation-reduction process	Oxidoreductase activity	None predicted	NADP-dependent oxidoreductase domain; Aldo/keto reductase family
273	C5WNE0	Uncharacterized protein OS=*Sorghum bicolor* GN=SORBI_3001G264300	11.31	32.55	7	1.21	0.15	3.7E-02	None predicted	None predicted	None predicted	Alpha crystallin/Hsp20 domain; Small heat shock protein HSP20 family
292	C5Y1X4	Uncharacterized protein OS=*Sorghum bicolor* GN=SORBI_3005G103300	10.79	26.39	11	-2.60	0.00	2.8E-04	Oxidation-reduction process	Oxidoreductase activity	None predicted	Alcohol dehydrogenase, N-terminal domain; NAD(P)-binding domain superfamily
295	A0A1B6QJR7	Uncharacterized protein OS=*Sorghum bicolor* GN=SORBI_3001G189000	10.77	18.95	7	1.16	0.07	4.9E-02	Hydrogen peroxide catabolic process	Peroxidase activity	Extracellular region	Secretory peroxidase domain; Plant peroxidase family
298	C5XWZ7	Uncharacterized protein OS=*Sorghum bicolor* GN=SORBI_3004G069900	10.76	23.36	6	1.23	0.16	3.7E-02	Response to stress	None predicted	Endoplasmic reticulum	Domain not predicted; Putative cyclase family
329	C5WZ08	Uncharacterized protein OS=*Sorghum bicolor* GN=SORBI_3001G514200	10.05	30.53	5	1.77	0.35	1.0E-02	Glutathione metabolic process	Glutathione transferase activity	Cytoplasm	Glutathione S-transferase, N-terminal domain; Thioredoxin-like superfamily
354	C5XKN3	Uncharacterized protein	9.41	17.94	5	1.15	0.08	2.1E-02	Ubiquinone-6	NADH	None predicted	NAD-dependent

		OS=*Sorghum bicolor* GN=SORBI_3003G166500							biosynthetic process	dehydrogenase activity		epimerase/dehydratase domain; NAD(P)-binding domain superfamily
360	C5XHV4	Uncharacterized protein OS=*Sorghum bicolor* GN=SORBI_3003G426000	9.28	23.79	5	-1.14	0.06	4.9E-02	Glutathione metabolic process	Glutathione transferase activity	Cytoplasm	Glutathione S-transferase, N-terminal domain; Thioredoxin-like superfamily
367	C5XF87	Ketol-acid reductoisomerase OS=*Sorghum bicolor* GN=SORBI_3003G239900	9.06	10.02	9	-1.20	0.04	3.3E-04	Oxidation-reduction process	Ketol-acid reductoisomerase activity	None predicted	Ketol-acid reductoisomerase, N-terminal domain; Ketol-acid reductoisomerase family
389	A0A1B6Q6I7	Uncharacterized protein OS=*Sorghum bicolor* GN=SORBI_3003G319700	8.73	46.31	12	1.47	0.21	4.4E-03	Oxidation-reduction process	NAD(P)H dehydrogenase (quinone) activity	None predicted	NADPH-dependent FMN reductase-like domain; Flavoprotein WrbA-like family
400	A0A1B6PEV7	Uncharacterized protein OS=*Sorghum bicolor* GN=SORBI_3007G009100	8.52	12.59	4	-1.11	0.06	4.2E-02	Oxidation-reduction process	Oxidoreductase activity	Mitochondrion	Polyketide synthase, enoylreductase domain; NAD(P)-binding domain superfamily
443	C5Z240	Uncharacterized protein OS=*Sorghum bicolor* GN=SORBI_3010G003100	7.85	11.36	5	1.12	0.03	2.2E-02	Oxidation-reduction process	Oxidoreductase activity, oxidizing metal ions	None predicted	Ascorbate oxidase homologue, first cupredoxin domain; Cupredoxin superfamily
446	C5Z0N9	Peroxidase OS=*Sorghum bicolor* GN=SORBI_3009G055300	7.77	17.63	10	-1.19	0.09	1.9E-02	Hydrogen peroxide catabolic process	Peroxidase activity	Extracellular region	Secretory peroxidase domain; Plant peroxidase family
454	C5WZ26	Inosine-5'-monophosphate dehydrogenase OS=*Sorghum bicolor* GN=SORBI_3001G069900	7.69	16.17	4	-1.09	0.06	4.7E-02	Oxidation-reduction process	Oxidoreductase activity	Cytoplasm	CBS domain; Inosine-5'-monophosphate dehydrogenase family
466	C5XVU9	S-(hydroxymethyl)glutathione dehydrogenase OS=*Sorghum bicolor* GN=SORBI_3004G343200	7.5	14.70	4	1.25	0.09	1.4E-02	Oxidation-reduction process	S-(hydroxymethyl) glutathione dehydrogenase activity	None predicted	Alcohol dehydrogenase, C-terminal domain; Alcohol dehydrogenase class III family
532	C5Z0L4	Uncharacterized protein OS=*Sorghum bicolor* GN=SORBI_3009G052600	6.59	38.32	4	-1.26	0.10	1.2E-02	Response to stress	None predicted	None predicted	UspA domain; Universal stress protein A family
558	C5YD83	Uncharacterized protein OS=*Sorghum bicolor* GN=SORBI_3006G031200	6.28	24.09	5	1.29	0.17	2.0E-02	None predicted	None predicted	None predicted	Thioredoxin-like fold domain; Thioredoxin-like superfamily
592	A0A1B6QGT1	Uncharacterized protein OS=*Sorghum bicolor* GN=SORBI_3001G012500	6	21.40	7	-1.43	0.04	4.4E-03	None predicted	Protein binding	None predicted	Glutathione S-transferase, C-terminal-like domain; Thioredoxin-like superfamily
623	C5X768	Uncharacterized protein OS=*Sorghum bicolor* GN=SORBI_3002G005600	5.64	10.86	3	-1.25	0.07	7.4E-03	Response to oxidative stress	Catalytic activity	Cytosol	Domain not predicted; Dirigent-like protein family

631	A0A1B6QKQ9	Uncharacterized protein OS=*Sorghum bicolor* GN=SORBI_3001G243100	5.58	19.89	3	-1.23	0.08	2.2E-02	Oxidation-reduction process	Acireductone dioxygenase [iron(II)-requiring] activity	Cytoplasm	Domain not predicted; Acireductone dioxygenase ARD family
689	C5WRM3	Uncharacterized protein OS=*Sorghum bicolor* GN=SORBI_3001G443100	4.92	11.49	3	-1.58	0.09	3.2E-03	Oxidation-reduction process	3"-deamino-3"-oxonicotianamine reductase activity	None predicted	NADP-dependent oxidoreductase domain; Aldo/keto reductase family
708	C5YGF5	Peroxidase OS=*Sorghum bicolor* GN=SORBI_3006G079300	4.73	14.33	3	-1.51	0.06	8.8E-04	Hydrogen peroxide catabolic process	Peroxidase activity	Extracellular region	Secretory peroxidase domain; Plant peroxidase family
715	A0A1B6QNZ7	Uncharacterized protein OS=*Sorghum bicolor* GN=SORBI_3001G412800	4.7	12.37	2	1.14	0.10	5.0E-02	None predicted	Protein binding	None predicted	Glutathione S-transferase, C-terminal-like domain; Thioredoxin-like superfamily
731	C5WXD7	Uncharacterized protein OS=*Sorghum bicolor* GN=SORBI_3001G209300	4.47	29.33	6	1.41	0.16	1.1E-02	Defence mechanism against pathogens	None predicted	None predicted	Domain not predicted; Uncharacterised protein family, basic secretory protein family
766	C5X763	Dirigent protein OS=*Sorghum bicolor* GN=SORBI_3002G005100	4.21	18.11	3	1.20	0.13	2.3E-02	Biosynthetic process	Enzyme regulator activity	None predicted	Domain not predicted; Dirigent-like protein
777	A0A1B6PQP5	Uncharacterized protein OS=*Sorghum bicolor* GN=SORBI_3005G073000	4.14	12.27	2	1.35	0.17	1.0E-02	None predicted	None predicted	None predicted	Domain not predicted; Ricin B-like lectins superfamily
780	C5YF15	Uncharacterized protein OS=*Sorghum bicolor* GN=SORBI_3006G198800	4.1	9.52	2	1.23	0.08	3.5E-03	Defence response	None predicted	None predicted	Bet v I/Major latex protein domain; START-like domain superfamily
785	C5WMM0	Uncharacterized protein OS=*Sorghum bicolor* GN=SORBI_3001G400900	4.08	70.63	18	-1.30	0.12	1.1E-02	Defence response	None predicted	None predicted	Bet v I/Major latex protein domain; Bet v I type allergen family
794	C5Y360	Peroxidase OS=*Sorghum bicolor* GN=SORBI_3005G011300	4.05	11.59	3	1.17	0.08	1.1E-02	Hydrogen peroxide catabolic process	Peroxidase activity	Extracellular region	Secretory peroxidase domain; Plant peroxidase family
831	A0A194YQ30	Uncharacterized protein OS=*Sorghum bicolor* GN=SORBI_3004G159000	4	10.41	5	1.37	0.18	1.1E-02	Oxidation-reduction process	Oxidoreductase activity, acting on diphenols and related substances as donors	Membrane	Rieske [2Fe-2S] iron-sulphur domain; Rieske iron-sulphur protein family
845	A0A194YLK4	Uncharacterized protein OS=*Sorghum bicolor* GN=SORBI_3010G258500	3.9	2.75	2	-1.21	0.05	5.9E-03	Oxidation-reduction process	Prephenate dehydrogenase (NAD+) activity	None predicted	Prephenate dehydrogenase domain; NAD(P)-binding domain superfamily
876	C5X4Y7	Uncharacterized protein OS=*Sorghum bicolor* GN=SORBI_3002G412800	3.66	8.91	2	1.26	0.08	4.1E-02	Lipid particle organisation	None predicted	Lipid droplet	Domain not predicted; rubber elongation factor family
880	A2SXR8	Uricase OS=*Sorghum bicolor*	3.62	7.52	2	-1.34	0.10	7.4E-03	Urate catabolic process	Urate oxidase activity	Peroxisome	Domain not predicted; uricase family
918	C5YWZ7	Uncharacterized protein OS=*Sorghum bicolor* GN=SORBI_3009G255200	3.3	11.67	3	1.31	0.10	3.6E-03	None predicted	None predicted	None predicted	Alpha crystallin/Hsp20 domain; HSP20-like chaperone superfamily

977	C5X765	Dirigent protein OS=*Sorghum bicolor* GN=SORBI_3002G005300	2.82	23.67	3	1.27	0.13	1.9E-02	None predicted	None predicted	None predicted	Domain not predicted; Dirigent protein family
1051	C5XMC9	Uncharacterized protein OS=*Sorghum bicolor* GN=SORBI_3003G322100	2.35	3.68	2	1.22	0.15	3.3E-02	Oxidation-reduction process	Catechol oxidase activity	None predicted	Polyphenol oxidase, central domain; Polyphenol oxidase family
1102	C5Z026	Uncharacterized protein OS=*Sorghum bicolor* GN=SORBI_3009G043600	2.13	11.06	4	-1.33	0.16	3.3E-02	Glutathione metabolic process	Glutathione transferase activity	Cytoplasm	Glutathione S-transferase, N-terminal domain; Thioredoxin-like superfamily
1216	Q4VQB5	Pathogenesis-related protein 10a OS=*Sorghum bicolor* GN=PR10	2	76.88	23	-1.43	0.13	1.7E-02	Response to biotic stimulus	None predicted	None predicted	Bet v I/Major latex protein domain; Bet v I type allergen family
1218	A0A1B6PRF2	Uncharacterized protein OS=*Sorghum bicolor* GN=SORBI_3005G103500	2	31.72	10	-3.62	0.04	5.2E-03	Oxidation-reduction process	None predicted	None predicted	Alcohol dehydrogenase, C-terminal domain; NAD(P)-binding domain superfamily
1228	A0A1B6QQQ9	Uncharacterized protein OS=*Sorghum bicolor* GN=SORBI_3001G517700	2	9.15	4	-1.61	0.16	2.4E-02	Hydrogen peroxide catabolic process	Peroxidase activity	None predicted	Catalase core domain; Catalase, mono-functional, haem-containing family
Energy												
3	A0A194YGY2	Uncharacterized protein OS=*Sorghum bicolor* GN=SORBI_3010G027000	52.35	78.48	60	-1.29	0.10	5.8E-03	Glycolytic process	Phosphopyruvate hydratase activity	Cytosol	Enolase, C-terminal TIM barrel domain; enolase family
12	A0A194YMV2	Uncharacterized protein OS=*Sorghum bicolor* GN=SORBI_3004G055200	42.27	63.43	37	-1.27	0.07	4.4E-03	Glycolytic process	ATP binding	None predicted	Domain not predicted;Phosphoglycerate kinase family
14	C5XYZ9	Uncharacterized protein OS=*Sorghum bicolor* GN=SORBI_3004G106900	40.48	26.67	24	-1.20	0.01	3.6E-06	Tricarboxylic acid cycle	Phosphoenolpyruvate carboxylase activity	Chloroplast	Domain not predicted;Phosphoenolpyruvate carboxylase family
15	C5XFH6	Fructose-bisphosphate aldolase OS=*Sorghum bicolor* GN=SORBI_3003G393900	39.96	65.92	40	-1.64	0.03	4.9E-04	Glycolytic process	Fructose-bisphosphate aldolase activity	None predicted	Domain not predicted; fructose-bisphosphate aldolase, class-I family
37	C5WSL1	Uncharacterized protein OS=*Sorghum bicolor* GN=SORBI_3001G449700	28.63	34.58	18	-1.24	0.02	4.3E-03	Electron transfer activity	Ion-ion binding	Mitochondrion	Domain not predicted; Cytochrome P450 family
121	C5XQ07	Uncharacterized protein OS=*Sorghum bicolor* GN=SORBI_3003G072300	18	62.06	15	-1.32	0.10	4.1E-03	Glyceraldehyde-3-phosphate biosynthetic process	Triose-phosphate isomerase activity	Cytosol	Domain not predicted; triosephosphate isomerase family
135	C5XY37	Acetyltransferase component of pyruvate dehydrogenase complex OS=*Sorghum bicolor* GN=SORBI_3004G093600	17.2	20.04	11	-1.14	0.06	2.0E-02	Pyruvate metabolic process	Transferase activity, transferring acyl groups	Mitochondrion	2-oxoacid dehydrogenase acyltransferase, catalytic domain; dihydrolipoyllysine-residue acetyltransferase component of pyruvate dehydrogenase complex family

144	A0A1B6QHQ8	Uncharacterized protein OS=*Sorghum bicolor* GN=SORBI_3001G071800	16.45	17.81	9	-1.08	0.04	3.1E-02	Gluconeogenesis	Glucose-6-phosphate isomerase activity	None predicted	Phosphoglucose isomerase, SIS domain 1; phosphoglucose isomerase (PGI) family
147	C5XZ73	Pyruvate dehydrogenase E1 component subunit alpha OS=*Sorghum bicolor* GN=SORBI_3004G244000	16.3	25.13	8	-1.07	0.04	3.5E-02	Acetyl-CoA biosynthetic process from pyruvate	Pyruvate dehydrogenase (acetyl-transferring) activity	Intracellular membrane-bounded organelle	Dehydrogenase, E1 component domain; pyruvate dehydrogenase (acetyl-transferring) E1 component, alpha subunit, subgroup y family
181	C5YAI8	Pyruvate kinase OS=*Sorghum bicolor* GN=SORBI_3006G267200	14.61	15.40	8	-1.27	0.02	5.4E-04	Glycolytic process	Pyruvate kinase activity	Cytoplasm	Pyruvate kinase, C-terminal domain; pyruvate kinase family
191	A0A1B6P9F4	Uncharacterized protein OS=*Sorghum bicolor* GN=SORBI_3009G188000	14.03	50.49	18	1.25	0.14	1.6E-02	Oxidation-reduction process	FMN protein binding	None predicted	Flavodoxin/nitric oxide synthase domain; flavoprotein WrbA-like family
206	C5X2Z4	Glucose-6-phosphate isomerase OS=*Sorghum bicolor* GN=SORBI_3002G230600	13.36	14.96	7	-1.08	0.02	2.2E-02	Gluconeogenesis	Glucose-6-phosphate isomerase activity	None predicted	Phosphoglucose isomerase, SIS domain 1; phosphoglucose isomerase (PGI) family
220	A0A1B6PFE9	Uncharacterized protein OS=*Sorghum bicolor* GN=SORBI_3007G038600	12.68	21.23	7	-1.11	0.07	4.2E-02	Oxidation-reduction process	Flavin adenine dinucleotide protein binding	Chloroplast	FAD/NAD(P)-binding domain; FAD/NAD(P)-binding domain superfamily
261	A0A1B6QIA3	Uncharacterized protein OS=*Sorghum bicolor* GN=SORBI_3001G098500	11.52	37.56	7	-1.16	0.09	3.3E-02	Glycolytic process	None predicted	Cytoplasm	CBS domain; family not predicted
436	C5XH93	Pyruvate kinase OS=*Sorghum bicolor* GN=SORBI_3003G130800	7.94	12.97	6	-1.31	0.15	4.2E-02	Glycolytic process	Pyruvate kinase activity	Cytoplasm	Pyruvate kinase, C-terminal domain; Pyruvate kinase
503	C5Z6W2	Uncharacterized protein OS=*Sorghum bicolor* GN=SORBI_3010G086800	6.99	24.64	4	1.98	0.36	1.8E-03	Electron transport chain	Electron transfer activity	Anchored component of plasma membrane	Phytocyanin domain; Cupredoxin superfamily
525	C5WY84	Ferredoxin--NADP reductase OS=*Sorghum bicolor* GN=SORBI_3001G067100	6.75	10.00	4	-1.21	0.07	7.8E-03	Oxidation-reduction process	Ferredoxin-NADP+ reductase activity	Chloroplast	Ferredoxin reductase-type FAD-binding domain; Ferredoxin--NADP reductase family
543	C5WWE9	Uncharacterized protein OS=*Sorghum bicolor* GN=SORBI_3001G202400	6.46	34.53	4	1.11	0.07	4.6E-02	None predicted	Heme protein binding	None predicted	Cytochrome b5-like heme/steroid binding domain; Cytochrome b5-like heme/steroid binding domain superfamily
549	C5YPW0	Uncharacterized protein OS=*Sorghum bicolor* GN=SORBI_3008G132700	6.41	10.43	4	-1.24	0.13	3.4E-02	Acetyl-CoA biosynthetic process	ATP citrate synthase activity	Cytosol	ATP-citrate synthase, citrate-binding domain; Succinyl-CoA synthetase-like superfamily
594	C5XW40	Uncharacterized protein	6	24.68	4	1.11	0.05	3.0E-02	Glycine	ATP binding	Mitochondrion	Biotin/lipoyl attachment

		OS=*Sorghum bicolor* GN=SORBI_3004G055700							decarboxylation via glycine cleavage system			domain; Glycine cleavage system H-protein family
806	C5Y4L1	Pyruvate kinase OS=*Sorghum bicolor* GN=SORBI_3005G034400	4	20.30	8	-1.51	0.06	2.9E-03	Glycolytic process	Pyruvate kinase activity	Cytoplasm	Pyruvate kinase, barrel domain; Pyruvate kinase family
1110	C5XD18	Uncharacterized protein OS=*Sorghum bicolor* GN=SORBI_3002G356400	2.1	38.22	2	1.29	0.16	2.2E-02	Electron transport chain	Oxidoreductase activity, acting on NAD(P)H	None predicted	Domain not predicted; NADH dehydrogenase ubiquinone Fe-S protein 4, mitochondrial family
Protein destination and storage												
166	C5Y8M5	Uncharacterized protein OS=*Sorghum bicolor* GN=SORBI_3006G082000	15.66	20.75	10	1.24	0.19	4.9E-02	Proteolysis	Serine-type endopeptidase activity	None predicted	Peptidase S8/S53 domain; peptidase S8, subtilisin-related family
196	C5YBS5	Uncharacterized protein OS=*Sorghum bicolor* GN=SORBI_3006G011400	13.76	11.11	6	-1.30	0.08	1.5E-02	Proteolysis	Serine-type endopeptidase activity	None predicted	Peptidase S8/S53 domain; Peptidase S8, subtilisin-related family
225	C5XVC9	Uncharacterized protein OS=*Sorghum bicolor* GN=SORBI_3004G047200	12.54	15.54	6	-1.23	0.05	3.8E-02	Chaperone-mediated protein folding	Unfolded protein binding	Chaperonin-containing T-complex	Domain not predicted; chaperonin Cpn60/TCP-1 family
242	C5WW86	Uncharacterized protein OS=*Sorghum bicolor* GN=SORBI_3001G196700	12.01	9.15	9	1.29	0.16	1.5E-02	Proteolysis	Dipeptidyl-peptidase activity	None predicted	Peptidase S28; alpha/Beta hydrolase fold superfamily
272	C5WV27	Uncharacterized protein OS=*Sorghum bicolor* GN=SORBI_3001G036300	11.31	15.71	6	-1.21	0.05	5.0E-03	Peptide catabolic process	Metalloaminopeptidase activity	Cytosol	Peptidase M1, membrane alanine aminopeptidase, N-terminal domain; Peptidase M1, alanine aminopeptidase/leukotriene A4 hydrolase family
293	C5XDR4	Uncharacterized protein OS=*Sorghum bicolor* GN=SORBI_3002G217200	10.78	17.36	14	1.69	0.51	3.7E-02	Proteolysis	Cysteine-type endopeptidase activity	Extracellular space	Peptidase C1A, papain C-terminal domain; Peptidase C1A family
304	C5XUD0	Uncharacterized protein OS=*Sorghum bicolor* GN=SORBI_3004G326600	10.7	11.38	5	-1.14	0.06	9.3E-03	Chaperone-mediated protein folding	Unfolded protein binding	Chaperonin-containing T-complex	Domain not predicted; Chaperonin Cpn60/TCP-1 family
315	C5X455	Carboxypeptidase OS=*Sorghum bicolor* GN=SORBI_3002G401200	10.42	15.59	5	1.24	0.13	1.5E-02	Proteolysis	Serine-type carboxypeptidase activity	None predicted	Domain not predicted; Serine carboxypeptidase family
363	C5XXJ0	Uncharacterized protein OS=*Sorghum bicolor* GN=SORBI_3004G081800	9.2	16.83	5	1.13	0.06	1.4E-02	Proteolysis	Aspartic-type endopeptidase activity	Cytosol	Aspartic peptidase, DDI1-type domain; DNA damage-inducible protein 1 family
369	A0A1B6PNM7	Uncharacterized protein OS=*Sorghum bicolor* GN=SORBI_3006G242000	9.01	18.22	11	1.26	0.08	4.0E-03	Proteolysis	Cysteine-type peptidase activity	None predicted	Peptidase C1A, papain C-terminal domain; Peptidase C1A family
392	C5Y171	Uncharacterized protein OS=*Sorghum bicolor* GN=SORBI_3004G142800	8.71	16.71	5	1.43	0.21	8.4E-03	Proteolysis involved in cellular protein catabolic process	Cysteine-type endopeptidase activity	Extracellular space	Peptidase C1A, papain C-terminal domain; Peptidase C1A family

404	A0A1B6Q8T4	Uncharacterized protein OS=*Sorghum bicolor* GN=SORBI_3002G024400	8.41	16.30	5	1.11	0.03	3.7E-02	Proteolysis	Serine-type carboxypeptidase activity	Vacuole	Domain not predicted; Serine carboxypeptidase family
582	C5Z8D3	Uncharacterized protein OS=*Sorghum bicolor* GN=SORBI_3010G239400	6.1	10.33	9	-2.06	0.04	6.5E-04	Proteolysis involved in cellular protein catabolic process	Cysteine-type endopeptidase activity	Extracellular space	Peptidase C1A, papain C-terminal domain; Peptidase C1A family
627	C5YRI0	Uncharacterized protein OS=*Sorghum bicolor* GN=SORBI_3008G161800	5.61	10.09	3	-1.14	0.03	6.2E-03	Proteasome assembly, ubiquitin-dependent protein catabolic process	Protein binding	Proteasome regulatory particle, lid subcomplex	Proteasome component (PCI) domain; Tetratricopeptide-like helical domain superfamily
722	C5Z8D2	Uncharacterized protein OS=*Sorghum bicolor* GN=SORBI_3010G239300	4.62	6.99	5	-1.41	0.10	5.3E-03	Proteolysis	Cysteine-type endopeptidase activity	Extracellular space	Peptidase C1A, papain C-terminal domain; Peptidase C1A family
790	A0A1B6P5Q3	Uncharacterized protein OS=*Sorghum bicolor* GN=SORBI_3009G008800	4.07	14.61	4	1.29	0.08	6.4E-04	Proteolysis	Cysteine-type peptidase activity	None predicted	Peptidase C1A, papain C-terminal domain; Peptidase C1A family
841	C5XZT7	Uncharacterized protein OS=*Sorghum bicolor* GN=SORBI_3004G257700	3.95	8.95	3	1.37	0.13	2.1E-03	Protein catabolic process	Aspartic-type endopeptidase activity	None predicted	Peptidase family A1 domain; Aspartic peptidase A1 family
868	C5YPX8	Uncharacterized protein OS=*Sorghum bicolor* GN=SORBI_3008G134700	3.74	8.91	2	2.93	0.54	4.3E-04	Protein catabolic process	Aspartic-type endopeptidase activity	None predicted	Peptidase family A1 domain; Aspartic peptidase A1 family
934	A0A1B6QEG2	Uncharacterized protein OS=*Sorghum bicolor* GN=SORBI_3002G315800	3.16	8.73	3	1.31	0.20	3.3E-02	Proteolysis	Cysteine-type endopeptidase activity	None predicted	Peptidase C1A, papain C-terminal domain; Peptidase C1A family
980	C5XUD8	Uncharacterized protein OS=*Sorghum bicolor* GN=SORBI_3004G327500	2.8	4.39	2	-1.37	0.14	1.5E-02	Proteolysis	Dipeptidyl-peptidase activity	Cytoplasm	G-patch domain; Family not predicted
Protein synthesis												
80	A0A194YLC1	Uncharacterized protein OS=*Sorghum bicolor* GN=SORBI_3010G251100	21.66	23.99	14	-1.41	0.15	2.3E-02	rRNA maturation	Nucleotide binding	Intracellular	Domain not predicted; DEAD-box superfamily
246	A0A1B6Q0S3	Uncharacterized protein OS=*Sorghum bicolor* GN=SORBI_3003G012200	11.92	13.16	6	-1.11	0.04	3.4E-02	Translation	Aminoacyl-tRNA ligase activity	Cytoplasm	Aminoacyl-tRNA synthetase, class II domain; aspartate-tRNA synthetase, type 2 family
330	C5YIU0	Uncharacterized protein OS=*Sorghum bicolor* GN=SORBI_3007G212600	10.05	39.23	6	1.13	0.07	3.9E-02	Translation	Structural constituent of ribosome	Ribosome	Ribosomal protein S8 domain and superfamily
355	A0A1B6PQ87	Uncharacterized protein OS=*Sorghum bicolor* GN=SORBI_3005G050500	9.31	12.08	6	-1.38	0.04	2.6E-03	Translation	Structural constituent of ribosome	Ribosome	Domain not predicted; Ribosomal protein L3 family
396	C5XE07	Uncharacterized protein OS=*Sorghum bicolor* GN=SORBI_3002G373800	8.59	25.99	5	-1.15	0.07	2.1E-02	Translation	Translation elongation factor activity	Eukaryotic translation elongation factor 1 complex	Translation elongation factor EF1B, beta/delta subunit, guanine nucleotide exchange domain; translation elongation factor eEF-1beta-like

												superfamily
483	C5XIN8	Uncharacterized protein OS=*Sorghum bicolor* GN=SORBI_3003G436700	7.31	30.17	5	1.15	0.06	1.8E-02	Ribosomal small subunit assembly	Structural constituent of ribosome	Cytosolic small ribosomal subunit	Plectin/S10, N-terminal domain; 40S Ribosomal protein S10
520	C5XGD3	60S ribosomal protein L13 OS=*Sorghum bicolor* GN=SORBI_3003G408100	6.81	24.04	4	-1.29	0.04	8.3E-03	Translation	Structural constituent of ribosome	Cytosolic large ribosomal subunit	Domain not predicted; Ribosomal protein L13e family
522	C5YAR4	Uncharacterized protein OS=*Sorghum bicolor* GN=SORBI_3006G121100	6.77	9.23	3	1.24	0.11	2.2E-02	Translational initiation	Translation initiation factor activity	None predicted	Domain not predicted; Plant specific eukaryotic initiation factor 4B family
707	C5Z466	Uncharacterized protein OS=*Sorghum bicolor* GN=SORBI_3010G161500	4.75	8.78	2	1.16	0.03	8.6E-03	Translation	Structural constituent of ribosome	Large ribosomal subunit	Ribosomal protein L1/ribosomal biogenesis protein domain; Ribosomal protein L1-like superfamily
816	C5XDZ7	Uncharacterized protein OS=*Sorghum bicolor* GN=SORBI_3002G372400	4	15.17	2	-1.66	0.06	1.4E-03	Cytoplasmic translation	Structural constituent of ribosome	Cytosolic large ribosomal subunit	Ribosomal protein L18e/L15P domain; Ribosomal protein L15 family
930	C5YZW6	Uncharacterized protein OS=*Sorghum bicolor* GN=SORBI_3009G177700	3.2	14.91	2	-1.48	0.13	5.0E-03	Translation	Structural constituent of ribosome	Cytosolic large ribosomal subunit	TRASH domain; Ribosomal protein L24e-related family
958	C5XPN5	60S ribosomal protein L36 OS=*Sorghum bicolor* GN=SORBI_3003G351000	2.95	16.96	2	-1.30	0.06	9.7E-03	Translation	Structural constituent of ribosome	Cytosolic large ribosomal subunit	Domain not predicted; Ribosomal protein L36e family
964	C5YNS4	40S ribosomal protein S6 OS=*Sorghum bicolor* GN=SORBI_3008G098800	2.91	9.56	2	-1.28	0.07	4.7E-02	Ribosomal small subunit biogenesis	Structural constituent of ribosome	Cytosolic small ribosomal subunit	Domain not predicted; Ribosomal protein S6e family
1022	C5Z5W5	Ribosomal protein L19 OS=*Sorghum bicolor* GN=SORBI_3010G069400	2.52	15.87	3	-1.38	0.09	2.3E-02	Translation	Structural constituent of ribosome	Cytosolic large ribosomal subunit	Ribosomal protein L19/L19e domain and superfamily
1074	C5WRR1	Uncharacterized protein OS=*Sorghum bicolor* GN=SORBI_3001G447300	2.22	5.30	2	-1.23	0.13	4.7E-02	Translational initiation	Ribosomal small subunit binding	Intracellular	RNase L inhibitor RLI, possible metal-binding domain; RLI1 family
1077	A0A1B6QMW1	Uncharacterized protein OS=*Sorghum bicolor* GN=SORBI_3001G354600	2.21	3.55	2	-1.24	0.08	1.7E-02	None predicted	Nucleic acid binding	Cytosol	Acinus, RNA recognition motif domain; RNA-binding domain superfamily
1223	C5YMC5	Uncharacterized protein OS=*Sorghum bicolor* GN=SORBI_3007G019000	2	34.44	5	1.43	0.29	3.3E-02	Translation	Small ribosomal subunit rRNA binding	Cytosolic small ribosomal subunit	Ribosomal protein S13/S15, N-terminal domain; Ribosomal protein S15 family
1410	A0A194YL15	Uncharacterized protein OS=*Sorghum bicolor* GN=SORBI_3010G230700	1.72	8.33	2	-1.57	0.27	4.9E-02	Translation	Structural constituent of ribosome	Ribosome	KOW domain; Ribosomal protein L27e family
1454	C5WZW1	Uncharacterized protein OS=*Sorghum bicolor* GN=SORBI_3001G517600	1.51	7.62	2	-1.21	0.06	1.3E-02	Ribosomal large subunit assembly	5S rRNA binding	Cytosolic large ribosomal subunit	Ribosomal protein L5 eukaryotic/L18 archaeal, C-terminal domain; Ribosomal protein L5

												eukaryotic/L18 archaeal family
Transporters												
4	C5Y9I0	Plasma membrane ATPase OS=*Sorghum bicolor* GN=SORBI_3006G247100	50.02	31.44	26	-1.18	0.02	8.0E-03	Proton export across plasma membrane	Proton-exporting ATPase activity	Plasma membrane	Cation-transporting P-type ATPase, N-terminal domain; P-type ATPase family
64	C5XHF1	Uncharacterized protein OS=*Sorghum bicolor* GN=SORBI_3003G136200	24.05	67.12	47	1.65	0.15	2.7E-04	Plasmodesmata-mediated intercellular transport	Manganese ion binding	Extracellular region	Cupin 1 domain; germin family
189	C5WNH9	Uncharacterized protein OS=*Sorghum bicolor* GN=SORBI_3001G405500	14.11	14.92	10	-1.71	0.04	3.2E-04	None predicted	Thiamine pyrophosphate binding, magnesium ion binding	Intracellular	Thiamine pyrophosphate enzyme, central domain; thiamine pyrophosphate (TPP)-dependent enzyme family
290	C5XSW1	Uncharacterized protein OS=*Sorghum bicolor* GN=SORBI_3004G310300	10.81	17.52	6	-1.14	0.07	3.1E-02	Phosphate ion transmembrane transport	Phosphate ion transmembrane transporter activity	Mitochondrial inner membrane	Domain not predicted; Mitochondrial carrier domain superfamily
299	C5XFB9	Uncharacterized protein OS=*Sorghum bicolor* GN=SORBI_3003G244200	10.75	22.61	5	1.52	0.30	1.6E-02	ATP hydrolysis coupled proton transport	Proton-transporting ATPase activity, rotational mechanism	Membrane	Domain not predicted; V-type ATPase subunit E family
332	C5XXV1	Uncharacterized protein OS=*Sorghum bicolor* GN=SORBI_3004G222000	10.04	25.26	5	-1.22	0.06	7.6E-03	Ion transmembrane transport	Water channel activity	Integral component of plasma membrane	Domain not predicted; Aquaporin transporter family
346	A0A1B6Q2N0	Uncharacterized protein OS=*Sorghum bicolor* GN=SORBI_3003G112200	9.72	18.67	5	1.33	0.20	1.7E-02	None predicted	Manganese ion binding	Extracellular region	Cupin 1 domain; Germin family
448	C5YUI7	Uncharacterized protein OS=*Sorghum bicolor* GN=SORBI_3009G212400	7.74	33.70	6	1.32	0.07	8.6E-03	Anion transmembrane transport	Voltage-gated anion channel activity	Mitochondrial outer membrane	Domain not predicted; Porin, eukaryotic type family
463	C5Y1D9	Uncharacterized protein OS=*Sorghum bicolor* GN=SORBI_3004G288700	7.51	22.15	9	-1.16	0.07	1.2E-02	Ion transmembrane transport	Water channel activity	Integral component of plasma membrane	Domain not predicted; Aquaporin transporter family
523	C5YBI6	Uncharacterized protein OS=*Sorghum bicolor* GN=SORBI_3006G136400	6.76	4.17	3	1.18	0.12	3.6E-02	Transport of virus in host, cell to cell	RNA binding	None predicted	Initiation factor eIF-4 gamma, MA3 domain; MIF4G-like domain superfamily
585	C5XHX2	Uncharacterized protein OS=*Sorghum bicolor* GN=SORBI_3003G427700	6.04	31.25	4	1.41	0.07	1.9E-02	Plasmodesmata-mediated intercellular transport	Manganese ion binding	Extracellular region	Cupin 1 domain; Germin family
680	C5YSH7	Uncharacterized protein OS=*Sorghum bicolor* GN=SORBI_3008G179500	5.09	56.32	3	1.22	0.08	2.7E-03	Metal ion transport	Metal ion binding	Cytoplasm	Heavy metal-associated domain, HMA; Heavy metal-associated domain

												superfamily
704	C5YIX1	Mitochondrial pyruvate carrier OS=*Sorghum bicolor* GN=SORBI_3007G078100	4.76	35.45	3	1.32	0.17	2.0E-02	Mitochondrial pyruvate transmembrane transport	Pyruvate transmembrane transporter activity	Mitochondrial inner membrane	Domain not predicted; Mitochondrial pyruvate carrier family
846	C5XHX3	Uncharacterized protein OS=*Sorghum bicolor* GN=SORBI_3003G427800	3.89	18.22	3	1.34	0.12	1.3E-03	Plasmodesmata-mediated intercellular transport	Manganese ion binding	Extracellular region	Cupin 1 domain; Germin family
Signal transduction												
7	A0A1B6QGY0	Uncharacterized protein OS=*Sorghum bicolor* GN=SORBI_3001G021300	48.46	30.96	32	-1.39	0.03	2.2E-06	None predicted	GTP binding	None predicted	Small GTP-binding protein domain; translation protein, beta-barrel domain superfamily
33	A0A1B6Q7A0	Uncharacterized protein OS=*Sorghum bicolor* GN=SORBI_3003G373500	29.94	38.81	21	1.13	0.05	4.7E-03	Phosphorylation	Phosphatidylinositol phosphate kinase activity	Cytoplasm	Phosphatidylinositol-4-phosphate 5-kinase, core domain; Chaperonin Cpn60/TCP-1 family
77	C5XES8	Uncharacterized protein OS=*Sorghum bicolor* GN=SORBI_3003G386000	22.33	48.92	12	-1.20	0.12	4.8E-02	Phosphorylation	Phosphotransferase activity, alcohol group as acceptor	None predicted	Carbohydrate kinase PfkB domain; ribokinase/fructokinase family
92	A0A1B6PIK2	Uncharacterized protein OS=*Sorghum bicolor* GN=SORBI_3007G190200	20.66	21.73	17	1.36	0.23	2.0E-02	Dephosphorylation	acid phosphatase activity	None predicted	Domain not predicted; Calcineurin-like phosphoesterase family
190	A0A194YKQ5	Uncharacterized protein OS=*Sorghum bicolor* GN=SORBI_3010G221800	14.05	52.12	22	-1.30	0.05	2.4E-02	Phosphorylation	Phosphoglycerate kinase activity	None predicted	Domain not predicted; Phosphoglycerate kinase family
199	A0A1B6P7A4	Uncharacterized protein OS=*Sorghum bicolor* GN=SORBI_3009G070800	13.6	31.35	11	1.55	0.34	1.8E-02	Dephosphorylation	Acid phosphatase activity	None predicted	Domain not predicted; acid phosphatase, plant family
262	A0A1B6PBB3	Uncharacterized protein OS=*Sorghum bicolor* GN=SORBI_3009G259200	11.5	24.69	6	1.23	0.04	3.6E-04	Nucleoside diphosphate phosphorylation	Nucleoside diphosphate kinase activity	None predicted	Nucleoside diphosphate kinase-like domain; Nucleoside diphosphate kinase family
526	C5XQD5	Uncharacterized protein OS=*Sorghum bicolor* GN=SORBI_3003G214900	6.72	8.99	4	1.25	0.07	4.6E-03	Protein phosphorylation	Protein kinase activity	Integral component of membrane	Protein kinase domain; Protein kinase-like domain superfamily
638	C5Y2R8	Uncharacterized protein OS=*Sorghum bicolor* GN=SORBI_3005G126200	5.52	16.60	4	1.28	0.12	6.8E-03	Protein phosphorylation	Transmembrane receptor protein serine/threonine kinase activity	Plasma membrane	Leucine-rich repeat-containing N-terminal, plant-type domain; Leucine-rich repeat domain superfamily
776	A0A1B6PPB3	Uncharacterized protein OS=*Sorghum bicolor* GN=SORBI_3006G276700	4.14	12.15	2	-1.27	0.07	2.5E-02	Phosphate-containing compound metabolic process	Inorganic diphosphatase activity	Cytoplasm	Inorganic pyrophosphatase domain; Inorganic pyrophosphatase superfamily

921	C5XR62	Uncharacterized protein OS=*Sorghum bicolor* GN=SORBI_3003G225200	3.28	5.71	4	-1.14	0.09	4.5E-02	Protein autophosphorylation	Calmodulin-dependent protein kinase activity	Cytoplasm	Protein kinase domain; Protein kinase-like domain superfamily
1393	C5YAK6	Uncharacterized protein OS=*Sorghum bicolor* GN=SORBI_3006G268900	1.84	6.31	2	1.38	0.14	1.3E-02	Clathrin-dependent endocytosis	Clathrin heavy chain binding, structural molecule activity	Membrane	Domain not predicted; Clathrin light chain family
1425	C5XTL6	UMP-CMP kinase OS=*Sorghum bicolor* GN=SORBI_3004G318100	1.65	14.55	2	1.20	0.10	1.8E-02	Phosphorylation	Kinase activity	Nucleus	Domain not predicted; Adenylate kinase/UMP-CMP kinase family
Transcription												
57	C5Y220	Uncharacterized protein OS=*Sorghum bicolor* GN=SORBI_3005G107900	25.17	37.16	24	1.26	0.07	2.7E-03	Methylation	O-methyltransferase activity	None predicted	Plant methyltransferase dimerization domain; o-methyltransferase COMT-type family
395	C5Z4W3	Uncharacterized protein OS=*Sorghum bicolor* GN=SORBI_3010G052200	8.63	24.90	5	1.43	0.16	4.7E-03	Methylation	O-methyltransferase activity	None predicted	Domain not predicted; O-methyltransferase, family 3
518	A0A1B6QMW0	Uncharacterized protein OS=*Sorghum bicolor* GN=SORBI_3001G354200	6.81	21.83	5	-2.02	0.07	1.2E-02	Methylation	O-methyltransferase activity	None predicted	Plant methyltransferase dimerization domain; O-methyltransferase COMT-type family
533	C5Y9F6	Uncharacterized protein OS=*Sorghum bicolor* GN=SORBI_3006G244400	6.59	11.72	3	1.29	0.12	5.8E-03	Nucleic acid phosphodiester bond hydrolysis	Endonuclease activity	None predicted	S1/P1 nuclease domain; Phospholipase C/P1 nuclease domain superfamily
702	C5Z0T1	Uncharacterized protein OS=*Sorghum bicolor* GN=SORBI_3009G193800	4.77	29.17	4	1.25	0.07	2.7E-03	Pseudouridine synthesis	Pseudouridine synthase activity	Nucleus	Zinc finger, RING-H2-type domain; Zinc finger, RING/FYVE/PHD-type superfamily
787	A0A1B6Q2Y5	Uncharacterized protein OS=*Sorghum bicolor* GN=SORBI_3003G134000	4.08	5.22	2	-1.32	0.12	2.4E-02	RNA editing	Protein binding	None predicted	Pentacotripeptide-repeat region of PRORP domain; Tetratricopeptide-like helical domain superfamily
836	C5WVZ7	Uncharacterized protein OS=*Sorghum bicolor* GN=SORBI_3001G041100	4	23.85	2	-1.41	0.07	3.4E-02	mRNA splicing, via spliceosome	RNA binding	Nucleus	RNA recognition motif domain; RNA-binding domain superfamily
865	C5YH53	Uncharacterized protein OS=*Sorghum bicolor* GN=SORBI_3007G179900	3.74	17.96	3	1.25	0.06	1.8E-03	RNA modification	RNA binding	Intracellular	C2 domain; C2 domain superfamily
Cell structure												
563	C5YYR1	Uncharacterized protein OS=*Sorghum bicolor* GN=SORBI_3009G153000	6.24	26.06	7	-1.18	0.07	4.6E-02	None predicted	ATP binding	None predicted	Domain not predicted; Actin family
804	A0A1B6PBJ7	Uncharacterized protein OS=*Sorghum bicolor* GN=SORBI_3008G047000	4	57.56	31	1.22	0.17	4.8E-02	None predicted	ATP binding	None predicted	Domain not predicted; Actin family
907	C5YXZ2	Uncharacterized protein OS=*Sorghum bicolor*	3.41	7.02	2	1.53	0.31	1.6E-02	Regulate the actin and microtubule	Protein binding	None predicted	Leucine-rich repeat-containing N-terminal,

		GN=SORBI_3009G002400							cytoskeleton			plant-type; leucine-rich repeat domain superfamily
1127	A0A1B6PCX7	Uncharacterized protein OS=*Sorghum bicolor* GN=SORBI_3008G106700	2.07	5.41	2	1.66	0.44	2.5E-02	Lignan biosynthetic process	None predicted	Plasmodesmata	NmrA-like domain; NAD(P)-binding domain superfamily
1378	A0A1B6Q2X9	Uncharacterized protein OS=*Sorghum bicolor* GN=SORBI_3003G135400	1.89	33.18	24	1.87	0.39	5.6E-03	Cytoskeleton organization	Structural constituent of cytoskeleton	Cytoskeleton	Tubulin/FtsZ, GTPase domain; Tubulin family
Unclear classification												
19	C5YBP8	Uncharacterized protein OS=*Sorghum bicolor* GN=SORBI_3006G009000	36.79	55.68	32	-1.25	0.05	8.3E-04	None predicted	None predicted	None predicted	E2F/DP family winged-helix DNA-binding domain; von Willebrand factor A-like domain superfamily
75	C5YBP9	Uncharacterized protein OS=*Sorghum bicolor* GN=SORBI_3006G009100	22.35	24.11	12	-1.19	0.06	9.5E-03	None predicted	Protein binding	None predicted	Domain not predicted; six-bladed beta-propeller, TolB-like superfamily
251	A0A1B6PH65	Uncharacterized protein OS=*Sorghum bicolor* GN=SORBI_3007G112100	11.83	20.75	6	1.15	0.10	4.4E-02	None predicted	None predicted	None predicted	Domain not predicted domain; Short-chain dehydrogenase/reductase SDR family
286	C5YWC5	Uncharacterized protein OS=*Sorghum bicolor* GN=SORBI_3009G104100	10.93	18.37	7	-1.10	0.03	2.7E-02	None predicted	None predicted	None predicted	Peptidase M24 domain; Peptidase M24, methionine aminopeptidase family
303	C5WMM5	Uncharacterized protein OS=*Sorghum bicolor* GN=SORBI_3001G535400	10.71	35.36	8	1.08	0.03	2.6E-02	None predicted	None predicted	None predicted	Remorin, C-terminal domain; family not predicted family
384	C5WY51	Uncharacterized protein OS=*Sorghum bicolor* GN=SORBI_3001G063500	8.84	12.03	4	1.42	0.22	8.6E-03	None predicted	None predicted	Cytoplasm	Fasciclin domain and superfamily
465	C5YAK8	Uncharacterized protein OS=*Sorghum bicolor* GN=SORBI_3006G269200	7.5	17.87	4	-1.29	0.06	4.2E-03	None predicted	None predicted	Cytoplasm	Domain of unknown function DUF3700; Nucleophile aminohydrolases, N-terminal
467	C5XJI8	Uncharacterized protein OS=*Sorghum bicolor* GN=SORBI_3003G003000	7.49	37.67	5	1.19	0.06	6.6E-03	None predicted	None predicted	Cytosol	Domain not predicted; Nucleic acid-binding, OB-fold superfamily
514	C5XKH1	Uncharacterized protein OS=*Sorghum bicolor* GN=SORBI_3003G017700	6.88	25.64	7	1.23	0.13	4.5E-02	None predicted	None predicted	Vacuole	Domain not predicted; DJ-1/PfpI family
601	C5X978	Uncharacterized protein OS=*Sorghum bicolor* GN=SORBI_3002G307600	5.96	47.37	9	1.42	0.13	9.3E-03	None predicted	None predicted	None predicted	C2 domain domain; C2 domain superfamily
609	C5XNE6	Uncharacterized protein OS=*Sorghum bicolor* GN=SORBI_3003G050200	5.89	28.04	7	1.57	0.38	4.2E-02	None predicted	Protein binding	None predicted	Domain not predicted; Embryo-specific ATS3 family

652	C5XHE5	Uncharacterized protein OS=*Sorghum bicolor* GN=SORBI_3003G135600	5.35	11.03	2	-1.28	0.06	6.3E-03	None predicted	None predicted	Cytoplasm	Domain not predicted; trimeric LpxA-like superfamily
723	C5XTT3	Uncharacterized protein OS=*Sorghum bicolor* GN=SORBI_3004G028400	4.62	32.06	4	1.20	0.09	2.2E-02	None predicted	Protein binding	None predicted	SWIB domain; SWIB/MDM2 domain superfamily
818	C5YI64	Uncharacterized protein OS=*Sorghum bicolor* GN=SORBI_3007G198000	4	15.89	2	1.52	0.08	2.7E-04	None predicted	None predicted	Membrane	DOMON domain; family not predicted
1173	C5WPI6	Uncharacterized protein OS=*Sorghum bicolor* GN=SORBI_3001G132100	2.02	15.35	2	1.30	0.17	3.1E-02	None predicted	None predicted	None predicted	Domain not predicted; Protein of unknown function DUF4370
1412	A0A1B6QD95	Uncharacterized protein OS=*Sorghum bicolor* GN=SORBI_3002G244300	1.72	9.66	2	1.48	0.13	5.0E-03	None predicted	None predicted	Cytoplasm	FAS1 domain; FAS1 domain superfamily

[a] Protein number assigned in ProteinPilot software.

[b] Protein accession numbers obtained from the TrEMBL database [incorporated within the UniProt database (http://www.uniprot.org)] searches against sequences of *Sorghum bicolor* only.

[c] Protein score generated by ProteinPilot software relating to the confidence of protein identification. A protein identification threshold of 1.3 was applied to the data, which only retains proteins identified with a 95% confidence.

[d] Percentage coverage is determined by the number of amino acids of sequenced peptides against the total length of the protein, with a threshold of at least 95% confidence.

[e] Sequenced peptide refers to the number of peptide that were sequenced and gave rise to protein identity. All proteins that were identified by means of a single peptide were filtered out of the dataset.

[f] Probability value of the quantitative difference between the treatment and control protein abundance being due to chance alone.

[g]Standard deviation of the ratios of drought stressed samples (n=4).

[h] Ratio represents the average fold-change (n = 4) induced by treatment relative to control. Positive values indicate an up-regulation.

[i] Gene ontology analysis as predicted on the IntePro database (https://www.ebi.ac.uk/interpro/) and UniProt database (http://www.uniprot.org). P denotes Biological Process, F denotes Functional Process, and C denotes Cellular Component.

[j] Conserved domains and family name as predicted by InterPro database (http://www.ebi.ac.uk/interpro/).

Table 4.2: List of drought stress responsive proteins identified from SA 1441 root samples using the iTRAQ and database searches.

Prot No[a]	Accession[b]	Protein Name	Scor[c]	% Cov[d]	Seq Pep[e]	Ratio[h]	SD[g]	p-val[f]	GO Analysis[i]			Conserved domains and family name[j]
									P	F	C	
Disease/defence												
5	C5YPZ1	Uncharacterized protein OS=*Sorghum bicolor* GN=SORBI_3008G136000	41.13	41.14	29	-1.25	0.03	1.16E-04	None predicted	ATP binding	None predicted	Domain not predicted, heat shock protein 70 family
36	C5WNL8	Uncharacterized protein OS=*Sorghum bicolor* GN=SORBI_3001G410200	26.13	56	20	1.21	0.05	2.71E-02	Cellular response to oxidative stress	Peroxidase activity	Chloroplast	Haem peroxidase, plant domain, class I peroxidase family
38	C5XIN9	Peroxidase OS=*Sorghum bicolor* GN=SORBI_3003G436800	25.77	43.24	34	1.33	0.14	8.38E-03	Cellular oxidant detoxification	Oxidoreductase activity	Extracellular region	Haem peroxidase, plant domain; plant peroxidase family
46	A0A1B6QHY1	Uncharacterized protein OS=*Sorghum bicolor* GN=SORBI_3001G084100	24.35	31.25	16	-1.27	0.10	3.41E-02	Oxidation-reduction process	Oxidoreductase activity, acting on the CH-OH group of donors, NAD or NADP as acceptor	None predicted	UDP-glucose/GDP-mannose dehydrogenase, N-terminal domain; UDP-glucose 6-dehydrogenase, eukaryotic type family
57	Q4VQB2	Pathogenesis-related protein 10b OS=*Sorghum bicolor* GN=PR10	22.93	89.38	33	1.38	0.21	1.63E-02	None predicted	Defence response	None predicted	Bet v I/Major latex protein domain; Bet v I type allergen family
66	C5YB27	Peroxidase OS=*Sorghum bicolor* GN=SORBI_3006G277800	21.8	42.49	26	-1.26	0.03	3.52E-03	Response to oxidative stress	Oxidoreductase activity	Extracellular region	Secretory peroxidase domain, plant peroxidase family
78	A0A194YLC1	Uncharacterized protein OS=*Sorghum bicolor* GN=SORBI_3010G251100	20.1	22.84	11	-1.14	0.04	1.03E-02	None predicted	Hydrolase activity	Cytoplasm	Ubiquitin-conjugating enzyme family
97	C5Z475	Peroxidase OS=*Sorghum bicolor* GN=SORBI_3010G162000	18.25	48.31	20	1.28	0.12	3.81E-03	Oxidation-reduction process	Peroxidase activity	Extracellular region	Secretory peroxidase domain; plant peroxidase family
102	C5YU67	Uncharacterized protein OS=*Sorghum bicolor* GN=SORBI_3009G067000	17.35	12.23	9	-1.14	0.03	1.85E-02	None predicted	ATP binding	None predicted	Domain not predicted; heat shock protein 70 family
119	C5Y2Z7	Uncharacterized protein OS=*Sorghum bicolor* GN=SORBI_3005G004400	16.38	12.45	10	-1.17	0.05	5.66E-03	Ubiquitin-dependent protein catabolic process	Ubiquitin activating enzyme activity	Cytoplasm	Ubiquitin-activating enzyme E1, FCCH domain; Ubiquitin/SUMO-activating enzyme E1 family
130	C5XI24	Peroxidase OS=*Sorghum bicolor* GN=SORBI_3003G140700	15.35	33.52	15	1.11	0.06	4.98E-02	Hydrogen peroxide catabolic process	Peroxidase activity	Extracellular region	Secretory peroxidase domain; plant peroxidase family
131	J7FJG8	Late embryogenesis	15.33	47.29	10	2.15	0.92	4.85E-02	Positive	None predicted	None predicted	Domain not predicted; late

		abundant protein 3 OS=*Sorghum bicolor* GN=Lea3							regulation of response to water deprivation			embryogenesis abundant protein family
159	C5XGH3	Peroxidase OS=*Sorghum bicolor* GN=SORBI_3003G121100	13.41	23.05	7	1.18	0.07	1.15E-02	Cellular oxidant detoxification	Peroxidase activity	Extracellular region	Secretory peroxidase domain; plant peroxidase family
161	C5Y1X4	Uncharacterized protein OS=*Sorghum bicolor* GN=SORBI_3005G103300	13.34	25.86	8	-1.52	0.07	1.01E-02	Oxidation-reduction process	Oxidoreductase activity	None predicted	Alcohol dehydrogenase domain; NAD(P)-binding domain superfamily
187	C5XMX0	Peroxidase OS=*Sorghum bicolor* GN=SORBI_3003G183300	12.12	42.27	13	1.16	0.08	2.21E-02	Hydrogen peroxide catabolic process	Peroxidase activity	Extracellular region	Secretory peroxidase domain; plant peroxidase family
207	C5Z864	Peroxidase OS=*Sorghum bicolor* GN=SORBI_3010G232500	11.43	25.68	8	1.15	0.03	5.76E-03	Hydrogen peroxide catabolic process	Peroxidase activity	Extracellular region	Secretory peroxidase domain; plant peroxidase family
214	C5WNE0	Uncharacterized protein OS=*Sorghum bicolor* GN=SORBI_3001G264300	11.17	32.08	7	1.20	0.08	1.39E-02	None predicted	None predicted	None predicted	Alpha crystallin/Hsp20 domain; small heat shock protein HSP20 family
267	C5YYX3	Uncharacterized protein OS=*Sorghum bicolor* GN=SORBI_3009G017800	9.89	33.18	5	1.31	0.10	1.72E-02	Glutathione metabolic process	Glutathione transferase activity	Cytoplasm	Glutathione S-transferase, N and C-terminal domain; Thioredoxin-like superfamily
287	C5YZI4	Peroxidase OS=*Sorghum bicolor* GN=SORBI_3009G032600	9.48	22.87	6	1.19	0.07	3.64E-03	Hydrogen peroxide catabolic process	Peroxidase activity	Extracellular region	Secretory peroxidase domain; plant peroxidase family
306	U5U008	Betaine-aldehyde dehydrogenase 2 OS=*Sorghum bicolor* GN=BADH2	9.12	20.79	5	-1.10	0.05	3.15E-02	Oxidation-reduction process	Oxidoreductase activity	Cytoplasm	Aldehyde dehydrogenase domain; Aldehyde/histidinol dehydrogenase superfamily
307	C5Z469	Peroxidase OS=*Sorghum bicolor* GN=SORBI_3010G161600	9.06	28.34	7	1.29	0.15	3.09E-02	Hydrogen peroxide catabolic process	Peroxidase activity	Extracellular region	Secretory peroxidase domain; plant peroxidase family
324	C5WPD8	Uncharacterized protein OS=*Sorghum bicolor* GN=SORBI_3001G418200	8.61	32.97	20	1.24	0.16	3.75E-02	None predicted	None predicted	None predicted	Ginkbilobin-2-homologous domain and superfamily
336	C5XF22	Uncharacterized protein OS=*Sorghum bicolor* GN=SORBI_3003G105700	8.39	22.11	4	1.40	0.18	5.74E-03	None predicted	None predicted	None predicted	Ricin B-related lectin domain and family
371	C5XVU9	S-(hydroxymethyl)glutathione dehydrogenase OS=*Sorghum bicolor* GN=SORBI_3004G343200	7.94	14.7	4	-1.22	0.02	2.29E-02	Oxidation-reduction process	S-(hydroxymethyl) glutathione dehydrogenase activity	None predicted	Alcohol dehydrogenase, N-terminal domain; alcohol dehydrogenase class III family
385	C5WZ12	Uncharacterized protein OS=*Sorghum bicolor* GN=SORBI_3001G514400	7.71	25.25	10	1.24	0.07	8.95E-03	Glutathione metabolic process	Glutathione transferase activity	Cytoplasm	Glutathione S-transferase, C-terminal-like domain; thioredoxin-like superfamily
403	A0A1B6P5R2	Uncharacterized protein OS=*Sorghum bicolor* GN=SORBI_3009G009600	7.44	29.11	3	1.68	0.30	4.26E-03	Negative regulation of endopeptidase activity	Serine-type endopeptidase inhibitor activity	None predicted	Domain not predicted; proteinase inhibitor I13, potato inhibitor I superfamily

412	C5YD83	Uncharacterized protein OS=*Sorghum bicolor* GN=SORBI_3006G031200	7.29	28.18	7	1.57	0.09	3.80E-05	None predicted	None predicted	None predicted	Thioredoxin-like fold; thioredoxin-like superfamily
429	A0A1B6QJR7	Uncharacterized protein OS=*Sorghum bicolor* GN=SORBI_3001G189000	7.05	11.97	4	1.19	0.09	3.67E-02	Hydrogen peroxide catabolic process	Peroxidase activity	Extracellular region	Secretory peroxidase domain; plant peroxidase family
437	C5XIY0	Peroxidase OS=*Sorghum bicolor* GN=SORBI_3003G152000	6.85	15.66	12	1.18	0.10	4.48E-02	Hydrogen peroxide catabolic process	Peroxidase activity	Extracellular region	Secretory peroxidase domain; plant peroxidase family
468	C5WQF6	Uncharacterized protein OS=*Sorghum bicolor* GN=SORBI_3001G147300	6.42	47.18	5	1.17	0.08	3.06E-02	None predicted	None predicted	None predicted	Vicinal oxygen chelate (VOC) domain; glyoxalase/Bleomycin resistance protein/Dihydroxybiphenyl dioxygenase superfamily
569	C5Z0G0	Uncharacterized protein OS=*Sorghum bicolor* GN=SORBI_3009G188300	5.32	15	3	1.27	0.19	4.76E-02	Response to stress	None predicted	None predicted	UspA domain; universal stress protein A family
622	C5XIY1	Peroxidase OS=*Sorghum bicolor* GN=SORBI_3003G152100	4.6	9.244	4	1.45	0.27	2.76E-02	Hydrogen peroxide catabolic process	Peroxidase activity	Extracellular region	Secretory peroxidase domain; plant peroxidase family
630	C5X760	Uncharacterized protein OS=*Sorghum bicolor* GN=SORBI_3002G004700	4.5	15.74	3	-1.14	0.04	2.61E-02	Oxidation-reduction process	Oxidoreductase activity, NAD(P)H dehydrogenase (quinone) activity	Cytoplasm	NADPH-dependent FMN reductase-like domain; flavoprotein WrbA-like family
641	C5XIY2	Peroxidase OS=*Sorghum bicolor* GN=SORBI_3003G152200	4.32	13.21	8	1.27	0.13	1.13E-02	Hydrogen peroxide catabolic process	Peroxidase activity	Extracellular region	Secretory peroxidase domain; plant peroxidase family
742	C5YXZ4	Uncharacterized protein OS=*Sorghum bicolor* GN=SORBI_3009G002600	3.93	5.865	3	1.24	0.03	1.41E-02	None predicted	Protein binding	None predicted	Leucine-rich repeat-containing N-terminal, plant-type domain; leucine-rich repeat domain superfamily
779	C5X040	Peroxidase OS=*Sorghum bicolor* GN=SORBI_3001G080300	3.58	10.18	2	1.24	0.11	1.72E-02	Hydrogen peroxide catabolic process	Peroxidase activity	Extracellular region	Secretory peroxidase domain; plant peroxidase family
794	C5X764	Dirigent protein OS=*Sorghum bicolor* GN=SORBI_3002G005200	3.48	10.95	2	1.27	0.07	3.87E-04	None predicted	None predicted	None predicted	Domain not predicted; dirigent protein family
885	A0A1B6QFH9	Uncharacterized protein OS=*Sorghum bicolor* GN=SORBI_3002G371400	2.78	10.42	2	1.22	0.09	4.41E-02	None predicted	None predicted	None predicted	Stress responsive alpha-beta barrel domain; dimeric alpha-beta barrel superfamily
909	A0A1B6P5R5	Uncharacterized protein OS=*Sorghum bicolor* GN=SORBI_3009G009700	2.56	43.66	2	1.31	0.17	3.38E-02	Negative regulation of endopeptidase activity	Serine-type endopeptidase inhibitor activity	None predicted	Domain not predicted; proteinase inhibitor I13, potato inhibitor I family
972	Q8W0Q8	Small heat shock-like protein OS=*Sorghum*	2.19	8.503	2	1.44	0.12	1.11E-03	None predicted	None predicted	None predicted	Alpha crystallin/Hsp20 domain; HSP20-like

		bicolor GN=SB32H17.11										chaperone superfamily
998	A0A1B6PJ81	Uncharacterized protein OS=*Sorghum bicolor* GN=SORBI_3007G225300	2.11	6.548	2	1.73	0.33	1.06E-02	Oxidation-reduction process	Nitronate monooxygenase activity	None predicted	Nitronate monooxygenase domain; aldolase-type TIM barrel superfamily
1014	A0A1B6QKE9	Uncharacterized protein OS=*Sorghum bicolor* GN=SORBI_3001G226000	2.08	5.133	2	-1.36	0.14	2.11E-02	Protein ubiquitination	Ubiquitin-protein transferase activity	Prp19 complex	Pre-mRNA-splicing factor 19 domain; pre-mRNA-processing factor 19 family
Metabolism												
2	C9DHL2	Lipoxygenase OS=*Sorghum bicolor*	51.44	37.51	33	-1.35	0.04	7.90E-03	Oxylipin biosynthetic process	Oxidoreductase activity	None predicted	Lipoxygenase, C-terminal domain; lipoxygenase family
9	C5WNU8	Lipoxygenase OS=*Sorghum bicolor* GN=SORBI_3001G125800	37.53	28.94	20	-1.25	0.04	1.66E-02	Oxylipin biosynthetic process	Oxidoreductase activity	None predicted	Lipoxygenase, C-terminal domain; lipoxygenase family
19	A0A1B6QC86	Uncharacterized protein OS=*Sorghum bicolor* GN=SORBI_3002G189100	32.99	32.11	20	-1.16	0.04	2.48E-03	None predicted	Glucan endo-1,3-beta-glucanase activity	None predicted	Domain not predicted, endo-1,3(4)-beta-glucanase family
21	A0A1B6QI05	Uncharacterized protein OS=*Sorghum bicolor* GN=SORBI_3001G089100	31.2	37.36	27	1.36	0.08	2.21E-04	Carbohydrate metabolic process	Hydrolase activity	None predicted	Glycoside hydrolase family 3 C-terminal domain; glycoside hydrolase superfamily
32	C5XES4	Lipoxygenase OS=*Sorghum bicolor* GN=SORBI_3003G385500	28.09	20.85	17	-1.33	0.05	2.59E-02	Oxylipin biosynthetic process	Oxidoreductase activity	None predicted	Lipoxygenase, C-terminal domain; lipoxygenase family
34	C5XYP5	Uncharacterized protein OS=*Sorghum bicolor* GN=SORBI_3004G233700	26.35	22.58	14	1.19	0.12	2.60E-02	Carbohydrate metabolic process	Hydrolase activity, hydrolyzing O-glycosyl compounds	None predicted	Glycoside hydrolase family 3 C-terminal domain,; glycoside hydrolase superfamily
45	A0A125QUG5	Uncharacterized protein OS=*Sorghum bicolor* GN= SORBI_3006G070298	24.43	24.22	12	1.23	0.10	6.47E-03	Carbohydrate metabolic process	Hydrolase activity, hydrolyzing O-glycosyl compounds	None predicted	Glycosyl hydrolase family 32, C-terminal domain; glycoside hydrolase, family 32
70	C5XRJ6	L-lactate dehydrogenase OS=*Sorghum bicolor* GN=SORBI_3004G004400	21.32	39.89	12	-1.23	0.13	4.52E-02	Carbohydrate metabolic processes	Oxidoreductase activity, acting on the CH-OH group of donors, NAD or NADP as acceptor	Cytoplasm	Lactate/malate dehydrogenase, N-terminal domain and family
76	C5WXJ1	Sucrose synthase OS=*Sorghum bicolor* GN=SORBI_3001G344500	20.21	25.25	21	-1.35	0.04	3.49E-02	Sucrose metabolic process	Sucrose synthase activity	None predicted	Sucrose synthase/ glycosyl transferase, family 1 domain; sucrose synthase, plant/cyanobacteria family
81	A0A1B6PEZ5	Uncharacterized protein	19.86	37.72	13	-1.28	0.05	2.07E-02	Fructose	Fructokinase	Cytosol	Carbohydrate kinase PfkB

		OS=*Sorghum bicolor* GN=SORBI_3007G014700							metabolic process	activity		domain; ribokinase-like superfamily
99	C5XB38	Uncharacterized protein OS=*Sorghum bicolor* GN=SORBI_3002G055600	18	36.48	12	1.35	0.13	2.82E-03	Chitin catabolic process	Chitin binding	Extracellular region	Glycoside hydrolase family 18, catalytic domain; glycoside hydrolase superfamily
142	C5XY37	Acetyltransferase component of pyruvate dehydrogenase complex OS=*Sorghum bicolor* GN=SORBI_3004G093600	14.42	16.51	9	-1.12	0.04	6.00E-03	Pyruvate metabolic process	Dihydrolipoyllysine-residue acetyltransferase activity	Mitochondrial matrix	2-oxoacid dehydrogenase acyltransferase, catalytic domain; dihydrolipoyllysine-residue acetyltransferase component of pyruvate dehydrogenase complex family
157	A0A194YT53	Uncharacterized protein OS=*Sorghum bicolor* GN=SORBI_3004G345800	13.51	23.11	9	-1.07	0.03	3.37E-02	Metabolic process	Transferase activity, transferring acyl groups other than amino-acyl groups	None predicted	Thiolase domain and family
158	A0A194YQ33	Uncharacterized protein OS=*Sorghum bicolor* GN=SORBI_3004G166700	13.44	11.88	6	1.10	0.02	8.84E-04	Carbohydrate metabolic process	Hydrolase activity, hydrolyzing O-glycosyl compounds	None predicted	Glycosyl hydrolase family domain 32; N-terminal glycoside hydrolase, family 32
166	C5YF84	Uncharacterized protein OS=*Sorghum bicolor* GN=SORBI_3006G058100	13.1	9.446	7	-1.13	0.02	5.27E-03	Protein metabolic process	ATP binding	None predicted	Domain not predicted; ClpA/B family
231	C5XAC2	Uncharacterized protein OS=*Sorghum bicolor* GN=SORBI_3002G045800	10.71	16.12	6	1.29	0.11	3.27E-03	Carbohydrate metabolic process	Hydrolase activity, hydrolyzing O-glycosyl compounds	Anchored component of plasma membrane	X8 domain; glycoside hydrolase family 17
247	C5XWE5	Uncharacterized protein OS=*Sorghum bicolor* GN=SORBI_3004G197600	10.32	10.76	6	-1.16	0.07	1.63E-02	Lipid metabolic process	Phosphoric diester hydrolase activity	None predicted	Glycerophosphodiester phosphodiesterase domain; family not predicted
276	C5WNH9	Uncharacterized protein OS=*Sorghum bicolor* GN=SORBI_3001G405500	9.71	11.48	6	-1.29	0.09	1.07E-02	None predicted	Thiamine pyrophosphate binding	Intracellular	Thiamine pyrophosphate enzyme, N-terminal TPP-binding domain; thiamine pyrophosphate (TPP)-dependent enzyme family
285	C5XF87	Ketol-acid reductoisomerase OS=*Sorghum bicolor* GN=SORBI_3003G239900	9.49	12.61	6	-1.34	0.03	1.37E-02	Branched-chain amino acid biosynthetic process	Ketol-acid reductoisomerase activity	None predicted	Ketol-acid reductoisomerase, N and C-terminal domain and family
288	C5Y4R7	Glycosyltransferase OS=*Sorghum bicolor* GN=SORBI_3005G156500	9.45	14.17	4	-1.20	0.07	4.77E-02	Metabolic process	Transferase activity, transferring glycosyl groups	Intracellular membrane-bounded organelle	UDP-glycosyltransferase family, conserved site domain; UDP-glucuronosyl/UDP-glucosyltransferase family
338	C5XSC5	Uncharacterized protein	8.33	28.05	14	-1.15	0.07	2.20E-02	UDP-glucose	dUTP:glucose-1-	Cytoplasm	Domain not predicted; UTP--

		OS=*Sorghum bicolor* GN=SORBI_3004G013500							metabolic process	phosphate uridylyltransferase activity		glucose-1-phosphate uridylyltransferase family
382	C5YBH7	Uncharacterized protein OS=*Sorghum bicolor* GN=SORBI_3006G135500	7.78	10.48	4	1.57	0.23	2.75E-03	None predicted	None predicted	None predicted	Galactose oxidase-like, early set domain; galactose oxidase, central domain superfamily
390	C5Z1D3	Phosphotransferase OS=*Sorghum bicolor* GN=SORBI_3009G203500	7.64	12.03	4	-1.29	0.10	7.09E-03	Glucose 6-phosphate metabolic process	Phosphotransferase activity, alcohol group as acceptor	Mitochondria	Hexokinase, N- and C-terminal domain; hexokinase family
422	C5Z1F9	Uncharacterized protein OS=*Sorghum bicolor* GN=SORBI_3009G209100	7.13	19.18	6	1.29	0.19	2.38E-02	None predicted	Quercetin 3-O-glucosyltransferase activity	Intracellular membrane-bounded organelle	Domain and family not predicted
463	C5X255	Uncharacterized protein OS=*Sorghum bicolor* GN=SORBI_3002G220200	6.47	8.788	4	-1.22	0.08	1.12E-02	Cellular amino acid metabolic process	Formate-tetrahydrofolate ligase activity	Intracellular	Domain not predicted; Tetrahydrofolate dehydrogenase/cyclohydrolase family
494	C5YMM3	Patatin OS=*Sorghum bicolor* GN=SORBI_3007G158600	6.13	12.41	3	-1.39	0.10	4.79E-03	Lipid catabolic process	Acylglycerol lipase activity, hydrolase activity	Cytoplasm	Patatin-like phospholipase domain; patatin family
568	C5YLQ3	D-3-phosphoglycerate dehydrogenase OS=*Sorghum bicolor* GN=SORBI_3007G145000	5.32	6.947	3	-1.19	0.06	2.60E-02	Cellular amino acid biosynthetic process	Phosphoglycerate dehydrogenase activity	None predicted	D-isomer specific 2-hydroxyacid dehydrogenase, NAD-binding domain; D-3-phosphoglycerate dehydrogenase family
649	A0A1B6PIY5	Uncharacterized protein OS=*Sorghum bicolor* GN=SORBI_3007G213300	4.28	3.728	2	1.25	0.09	2.25E-02	Carbohydrate metabolic process	Glycerophosphodiester phosphodiesterase activity	Plasmodesma	Glycerophosphoryl diester phosphodiesterase domain and family
691	A0A1B6PNS7	Uncharacterized protein OS=*Sorghum bicolor* GN=SORBI_3006G249400	4.05	14.09	7	-1.21	0.12	4.56E-02	Glutamine biosynthetic process	Glutamate-ammonia ligase activity	Chloroplast thylakoid membrane	Glutamine synthetase, catalytic domain; Glutamine synthetase, N-terminal domain superfamily
755	C5WTM9	UDP-glucose 6-dehydrogenase OS=*Sorghum bicolor* GN=SORBI_3001G459800	3.78	18.54	9	-1.25	0.06	2.13E-02	Glycosaminoglycan biosynthetic process	UDP-glucose 6-dehydrogenase activity	Cytosol	UDP-glucose/GDP-mannose dehydrogenase, dimerization domain; UDP-glucose 6-dehydrogenase, eukaryotic type family
785	A0A1B6P878	Uncharacterized protein OS=*Sorghum bicolor* GN=SORBI_3009G119200	3.54	13.33	2	1.51	0.07	5.95E-03	Carbohydrate metabolic process	Hydrolase activity, hydrolyzing O-glycosyl compounds	None predicted	Domain not predicted; glycoside hydrolase family 17
848	C5XL11	Uncharacterized protein OS=*Sorghum bicolor* GN=SORBI_3003G020500	3.03	6.562	2	1.37	0.13	5.48E-03	None predicted	Hydrolase activity, acting on ester bonds	None predicted	GDSL lipase/esterase-like, plant domain; SGNH hydrolase superfamily
851	C5YIY2	Uncharacterized protein OS=*Sorghum bicolor*	2.99	8.482	2	-1.20	0.04	3.00E-02	Fatty acid biosynthetic	Hydro-lyase activity	Cytoplasm	Beta-hydroxydecanoyl thiol ester dehydrase, FabA/FabZ

		GN=SORBI_3007G079600							process			domain; beta-hydroxyacyl-(acyl-carrier-protein) dehydratase FabZ family
856	C5XLZ0	ATP-dependent 6-phosphofructokinase OS=*Sorghum bicolor* GN=PFK	2.97	5.283	2	-1.26	0.09	2.37E-02	Fructose 6-phosphate metabolic process	6-phosphofructokinase activity	Cytoplasm	Phosphofructokinase domain; ATP-dependent 6-phosphofructokinase family
872	C5YDX7	Uncharacterized protein OS=*Sorghum bicolor* GN=SORBI_3006G177300	2.87	5.263	2	1.32	0.17	3.21E-02	Carbohydrate metabolic process	Alpha-L-fucosidase activity	Vacuole	Domain not predicted; Glycoside hydrolase, family 29
874	A0A1B6QHU0	Uncharacterized protein OS=*Sorghum bicolor* GN=SORBI_3001G073900	2.85	10.41	5	2.01	0.36	3.48E-03	Malate metabolic process	Malate dehydrogenase activity	None predicted	Lactate/malate dehydrogenase, N and C-terminal domain; malate dehydrogenase, type 1 family
942	A0A194YSX5	Uncharacterized protein OS=*Sorghum bicolor* GN=SORBI_3004G331700	2.34	6.972	2	-1.15	0.06	3.02E-02	Cellular amino acid metabolic process	Pyridoxal phosphate binding	None predicted	Aminotransferase, class I/classII domain; aspartate/other aminotransferase family
1294	C5XGS0	Uncharacterized protein OS=*Sorghum bicolor* GN=SORBI_3003G258800	1.73	1.063	2	-1.24	0.10	3.23E-02	Nitrogen compound metabolic process	Oxidoreductase activity, acting on the CH-NH2 group of donors	Cytoplasm	Glutamate synthase domain; glutamate synthase, NADH/NADPH, small subunit 1 family
Protein synthesis												
54	C5WW48	Uncharacterized protein OS=*Sorghum bicolor* GN=SORBI_3001G046300	23.5	47.08	17	1.53	0.07	5.48E-04	Translation	Structural constituent of ribosome	Cytosolic small ribosomal subunit	Ribosomal protein S5, N-terminal domain; ribosomal protein S5 family
118	C5YH46	Uncharacterized protein OS=*Sorghum bicolor* GN=SORBI_3007G178600	16.4	42.76	9	1.33	0.17	9.52E-03	Translation	Structural constituent of ribosome	Cytosolic small ribosomal subunit	Domain not predicted; ribosomal protein S19e family
133	C5Z622	Uncharacterized protein OS=*Sorghum bicolor* GN=SORBI_3010G076400	15.24	48.59	14	1.26	0.11	4.61E-03	Translation	Structural constituent of ribosome	Cytosolic small ribosomal subunit	Domain not predicted; ribosomal protein S17e family
134	C5Y9U0	Uncharacterized protein OS=*Sorghum bicolor* GN=SORBI_3006G106100	15.1	46	9	1.19	0.09	1.36E-02	Translation	Structural constituent of ribosome	Cytosolic small ribosomal subunit	Domain not predicted; ribosomal protein S11 family
255	C5X0P2	Uncharacterized protein OS=*Sorghum bicolor* GN=SORBI_3001G376600	10.17	39.39	5	1.29	0.16	2.77E-02	Translation	Structural constituent of ribosome	Cytosolic large ribosomal subunit	Domain not predicted; ribosomal protein L22e family
260	C5YR16	Uncharacterized protein OS=*Sorghum bicolor* GN=SORBI_3008G021100	10.08	38.93	6	1.36	0.18	1.44E-02	Translation	Structural constituent of ribosome	Cytosolic small ribosomal subunit	Domain not predicted; ribosomal protein S9 family
263	C5YF43	Uncharacterized protein OS=*Sorghum bicolor* GN=SORBI_3006G201500	10.03	36.14	6	1.25	0.17	3.82E-02	Translation	rRNA binding	Cytosolic large ribosomal subunit	Ribosomal protein L11 L and C terminal domains; Ribosomal protein L11/L12 family
290	C5XAE4	Uncharacterized protein OS=*Sorghum bicolor* GN=SORBI_3002G049300	9.44	32.24	5	1.79	0.39	1.23E-02	Translation	Structural constituent of ribosome	Small ribosomal subunit	Domain not predicted; ribosomal protein S13 family

291	C5YIU0	Uncharacterized protein OS=*Sorghum bicolor* GN=SORBI_3007G212600	9.43	39.23	7	1.29	0.11	2.18E-02	Translation	Structural constituent of ribosome	Ribosome	Domain not predicted; ribosomal protein S8 family
351	C5YGH8	Uncharacterized protein OS=*Sorghum bicolor* GN=SORBI_3006G081100	8.1	25.54	6	1.42	0.20	1.62E-02	Ribosomal small subunit assembly	Structural constituent of ribosome	Cytosolic small ribosomal subunit	Plectin/S10, N-terminal domain; 40S Ribosomal protein S10 family
374	C5YR01	Uncharacterized protein OS=*Sorghum bicolor* GN=SORBI_3008G153500	7.91	10.02	4	1.13	0.05	9.29E-03	None predicted	RNA binding	None predicted	K Homology domain, type 1 domain; K Homology domain, type 1 superfamily
419	C5YAD0	Uncharacterized protein OS=*Sorghum bicolor* GN=SORBI_3006G116700	7.2	29.22	8	1.25	0.03	2.70E-03	Translation	Structural constituent of ribosome	Cytosolic large ribosomal subunit	Domain not predicted; 60S ribosomal protein L6E
502	C5WYX6	Uncharacterized protein OS=*Sorghum bicolor* GN=SORBI_3001G225700	6.07	25.71	5	1.45	0.28	2.02E-02	Translation	Structural constituent of ribosome	Cytosolic large ribosomal subunit	Domain not predicted; ribosomal protein L14P family
525	C5XMD2	Uncharacterized protein OS=*Sorghum bicolor* GN=SORBI_3003G322400	5.93	35.19	5	1.82	0.57	3.17E-02	None predicted	None predicted	None predicted	Domain not predicted; Ribosomal protein S25 family
530	C5Z0J3	Uncharacterized protein OS=*Sorghum bicolor* GN=SORBI_3009G050300	5.86	18.09	3	1.22	0.12	2.93E-02	Translation	RNA binding structural constituent of ribosome	Cytosolic large ribosomal subunit	Ribosomal protein L18e/L15P domain; ribosomal protein L18e family
538	C5X548	Uncharacterized protein OS=*Sorghum bicolor* GN=SORBI_3002G124700	5.68	17.59	3	-1.47	0.10	1.36E-02	Translation	RNA binding structural constituent of ribosome	Cytosolic large ribosomal subunit	Ribosomal protein L18e/L15P domain; ribosomal protein L18e
563	C5WT03	Uncharacterized protein OS=*Sorghum bicolor* GN=SORBI_3001G016400	5.38	15.79	3	1.44	0.26	2.03E-02	Translation	Structural constituent of ribosome	Large ribosomal subunit	Domain not predicted; ribosomal protein L22/L17 family
611	C5XBK5	Elongation factor 1-alpha OS=*Sorghum bicolor* GN=SORBI_3002G339600	4.77	30.2	16	-1.19	0.10	4.83E-02	Translational elongation	Translation elongation factor activity	Cytoplasm	Transcription factor, GTP-binding domain; translation elongation factor EF1A, eukaryotic/archaeal family
648	C5Z466	Uncharacterized protein OS=*Sorghum bicolor* GN=SORBI_3010G161500	4.28	8.78	2	1.23	0.07	4.93E-02	Translation	RNA binding	Large ribosomal subunit	Domain not predicted; ribosomal protein L1/ribosomal biogenesis protein family
667	C5XQP0	Uncharacterized protein OS=*Sorghum bicolor* GN=SORBI_3003G078200	4.16	20.38	2	1.21	0.12	1.48E-02	Ribosomal large subunit biogenesis	RNA binding	Cytosolic large ribosomal subunit	KOW domain; ribosomal protein L26/L24, eukaryotic/archaeal family
793	C5XD92	40S ribosomal protein S3a OS=*Sorghum bicolor* GN=SORBI_3002G364500	3.48	26.24	5	1.23	0.06	2.34E-03	Cytoplasmic translation	Structural constituent of ribosome	Cytoplasm	Domain not predicted; 40S ribosomal protein S1/3, eukaryotes family
710	C5X7L1	Uncharacterized protein OS=*Sorghum bicolor* GN=SORBI_3002G286900	4	39.55	6	1.14	0.09	4.55E-02	Ribosomal large subunit biogenesis	RNA binding	Cytosolic large ribosomal subunit	Ribosomal protein L14e domain; translation protein SH3-like domain superfamily
806	A0A1B6PFH1	Uncharacterized protein OS=*Sorghum bicolor* GN=SORBI_3007G023400	3.38	6.59	4	-1.11	0.04	1.90E-02	None predicted	Structural constituent of ribosome	Cytoplasm	Domain not predicted; Ribosomal protein S14p/S29e family

883	C5Z0D7	Uncharacterized protein OS=*Sorghum bicolor* GN=SORBI_3009G185800	2.79	19.13	2	1.36	0.10	2.05E-02	Translational initiation	Translation initiation factor activity	None predicted	SUI1 domain; eukaryotic translation initiation factor SUI1 family
1103	C5WW47	Uncharacterized protein OS=*Sorghum bicolor* GN=SORBI_3001G046100	2	47.08	17	1.37	0.18	2.07E-02	Translation	RNA binding	Cytosolic small ribosomal subunit	Ribosomal protein S5, N and C-terminal domain; ribosomal protein S5 family
1186	C5XVB4	Uncharacterized protein OS=*Sorghum bicolor* GN=SORBI_3004G045400	2	17.39	3	1.18	0.08	1.84E-02	Translation	Structural constituent of ribosome	Ribosome	Domain not predicted; ribosomal protein L37ae family
Transporters												
12	C5Y9I0	Plasma membrane ATPase OS=*Sorghum bicolor* GN=SORBI_3006G247100	36.96	22.71	19	-1.24	0.03	1.50E-02	Proton export across plasma membrane	ATP binding	Plasma membrane	Cation-transporting P-type ATPase, N-terminal domain; P-type ATPase family
51	C5X0G5	Uncharacterized protein OS=*Sorghum bicolor* GN=SORBI_3001G236300	23.77	22.35	18	-1.17	0.06	1.53E-02	None predicted	Nucleotide binding	None predicted	AAA+ ATPase domain; AAA ATPase, CDC48 family
52	A0A194YJS5	Uncharacterized protein OS=*Sorghum bicolor* GN=SORBI_3010G172500	23.77	35.32	20	-1.15	0.07	3.70E-02	ATP hydrolysis coupled proton transport	ATP binding	Proton-transporting V-type ATPase, V1 domain	ATPase, F1/V1/A1 complex, alpha/beta subunit, N-terminal domain; V-type ATP synthase regulatory subunit B/beta family
61	C5XHF1	Uncharacterized protein OS=*Sorghum bicolor* GN=SORBI_3003G136200	22.39	59.82	66	1.53	0.14	2.66E-04	Plasmodesmata-mediated intercellular transport	Metal ion binding	Extracellular region	Cupin 1 domain; germin family
88	A0A194YRR0	Uncharacterized protein OS=*Sorghum bicolor* GN=SORBI_3004G259200	18.97	29.2	13	-1.36	0.10	4.65E-02	Transmembrane transport	Transmembrane transporter activity	Mitochondrial inner membrane, integral component of membrane	Domain not predicted; mitochondrial carrier protein family
156	C5WST3	Uncharacterized protein OS=*Sorghum bicolor* GN=SORBI_3001G457000	13.52	26.67	7	-1.24	0.08	1.00E-02	ATP hydrolysis coupled cation transmembrane transport	Proton-transporting ATP synthase activity, rotational mechanism	Proton-transporting ATP synthase complex, catalytic core F(1)	Domain not predicted; ATP synthase, F1 complex, gamma subunit family
215	C5XFB9	Uncharacterized protein OS=*Sorghum bicolor* GN=SORBI_3003G244200	11.14	26.52	6	1.29	0.10	1.81E-02	ATP hydrolysis coupled proton transport	Proton-transporting ATPase activity	Proton-transporting two-sector ATPase complex	Domain not predicted; V-type ATPase subunit family
346	C5XTE7	Uncharacterized protein OS=*Sorghum bicolor* GN=SORBI_3004G165300	8.18	18.22	4	1.24	0.17	4.02E-02	None predicted	Manganese ion binding	Extracellular region	Cupin 1 domain; Germin family
373	A0A1B6PAV5	Uncharacterized protein OS=*Sorghum bicolor* GN=SORBI_3008G003700	7.91	3.099	4	-1.30	0.10	9.46E-03	Intracellular protein transport	Clathrin light chain binding	Clathrin coat of trans-Golgi network vesicle	Clathrin, heavy chain, linker, core motif domain; clathrin, heavy chain family

381	C5XB21	Uncharacterized protein OS=*Sorghum bicolor* GN=SORBI_3002G053900	7.8	22.94	5	1.17	0.10	3.98E-02	Plasmodesmata-mediated intercellular transport	Manganese ion binding	Extracellular region	Cupin 1 domain; germin family
515	A0A1B6Q2N0	Uncharacterized protein OS=*Sorghum bicolor* GN=SORBI_3003G112200	6	16.14	5	1.49	0.28	1.53E-02	None predicted	Manganese ion binding	Extracellular region	Cupin 1 domain; germin family
516	C5YSH7	Uncharacterized protein OS=*Sorghum bicolor* GN=SORBI_3008G179500	6	56.32	3	1.20	0.14	4.24E-02	Metal ion transport	Transition metal ion binding	Cytoplasm	Heavy metal-associated domain, HMA; heavy metal-associated domain superfamily
657	C5YC92	Uncharacterized protein OS=*Sorghum bicolor* GN=SORBI_3006G018100	4.21	20.96	6	1.43	0.26	1.79E-02	None predicted	Manganese ion binding	Extracellular region	Cupin 1 domain; germin family
675	C5YG34	Uncharacterized protein OS=*Sorghum bicolor* GN=SORBI_3006G217100	4.13	30.04	8	1.19	0.12	2.54E-02	None predicted	Manganese ion binding	Extracellular region	Cupin 1 domain; germin family
693	C5Y1D9	Uncharacterized protein OS=*Sorghum bicolor* GN=SORBI_3004G288700	4.05	11.42	4	-1.32	0.09	2.25E-02	Ion transmembrane transport	Water channel activity	Integral component of plasma membrane	Domain not predicted; aquaporin transporter family
920	C5X999	Uncharacterized protein OS=*Sorghum bicolor* GN=SORBI_3002G309500	2.47	11.06	2	-1.33	0.09	6.51E-03	Intra-Golgi vesicle-mediated transport	GTP binding	Golgi apparatus	Small GTP-binding protein domain; small GTPase superfamily
1065	C5XHX2	Uncharacterized protein OS=*Sorghum bicolor* GN=SORBI_3003G427700	2.02	12.95	2	1.26	0.10	4.77E-02	Plasmodesmata-mediated intercellular transport	Manganese ion binding	Extracellular region	Cupin 1 domain; germin family
1107	C5WZZ8	Uncharacterized protein OS=*Sorghum bicolor* GN=SORBI_3001G522000	2	17.89	8	-1.18	0.03	1.66E-03	Regulation of mitochondrial membrane permeability	ATP:ADP antiporter activity	Mitochondrial inner membrane	Domain not predicted; mitochondrial carrier protein family
Energy												
4	A0A1B6Q5E4	Uncharacterized protein OS=*Sorghum bicolor* GN=SORBI_3003G260600	41.86	53.79	43	-1.24	0.08	3.07E-02	ATP biosynthetic process	ATP binding	Mitochondrial proton-transporting ATP synthase complex, catalytic core F(1)	AAA+ ATPase domain; ATP synthase, F1 complex, beta subunit family
27	C5WSL1	Uncharacterized protein OS=*Sorghum bicolor* GN=SORBI_3001G449700	28.85	36.85	21	-1.30	0.05	2.09E-03	Oxidation-reduction process	Electron transfer activity	Chloroplast	Domain not predicted; Cytochrome P450 family
121	C5XQ07	Uncharacterized protein OS=*Sorghum bicolor* GN=SORBI_3003G072300	16.17	57.31	13	-1.15	0.04	1.39E-02	Glycolytic process	Triose-phosphate isomerase activity	Cytosol	Domain not predicted; triosephosphate isomerase family
143	A0A1B6P9F4	Uncharacterized protein OS=*Sorghum bicolor*	14.41	47.55	15	1.21	0.08	1.69E-02	Oxidation-reduction process	FMN activity	None predicted	Flavodoxin/nitric oxide synthase domain;

		GN=SORBI_3009G188000										flavoprotein WrbA-like family
244	C5Y4L1	Pyruvate kinase OS=*Sorghum bicolor* GN=SORBI_3005G034400	10.35	14.99	6	-1.35	0.10	7.10E-03	Glycolytic process	Pyruvate kinase activity	Cytoplasm	Pyruvate kinase domain and family
277	A0A1B6Q6I7	Uncharacterized protein OS=*Sorghum bicolor* GN=SORBI_3003G319700	9.68	50.25	10	1.38	0.23	2.71E-02	Oxidation-reduction process	FMN binding	None predicted	Flavodoxin/nitric oxide synthase domain; flavoprotein WrbA-like family
297	A0A1B6QPV9	Uncharacterized protein OS=*Sorghum bicolor* GN=SORBI_3001G465400	9.34	15.26	6	-1.12	0.05	4.87E-02	Tricarboxylic acid cycle	Transferase activity, transferring acyl groups	Intracellular	Dihydrolipoamide succinyltransferase domain; Urb2/Npa2 family
304	C5XBD4	Uncharacterized protein OS=*Sorghum bicolor* GN=SORBI_3002G186900	9.16	15.06	6	-1.11	0.03	2.89E-03	Glycolytic process	Phosphopyruvate hydratase activity	Cytosol	Enolase, C and N-terminal TIM barrel domain; enolase family
359	C5Z7L1	Pyrophosphate--fructose 6-phosphate 1-phosphotransferase subunit beta OS=*Sorghum bicolor* GN=PFP-BETA	8.02	12.57	5	-1.40	0.07	1.16E-03	Glycolytic process through fructose-6-phosphate	Diphosphate-fructose-6-phosphate 1-phosphotransferase activity	Cytoplasm	Phosphofructokinase domain; pyrophosphate-dependent phosphofructokinase PfpB family
387	C5WN51	Uncharacterized protein OS=*Sorghum bicolor* GN=SORBI_3001G119000	7.69	38.28	9	1.36	0.20	1.28E-02	Electron transport chain	Electron transfer activity	Anchored component of plasma membrane	Phytocyanin domain; cupredoxin superfamily
489	C5Z8E7	Uncharacterized protein OS=*Sorghum bicolor* GN=SORBI_3010G110800 PE=4 SV=1	6.19	36.3	4	1.58	0.31	1.17E-02	Electron transport chain	Electron transfer activity	Anchored component of plasma membrane	Phytocyanin domain; cupredoxin superfamily
491	C5XWJ7	Uncharacterized protein OS=*Sorghum bicolor* GN=SORBI_3004G202100	6.17	16	3	-1.22	0.02	2.20E-02	Tricarboxylic acid cycle	Oxidoreductase activity	None predicted	Isopropylmalate dehydrogenase-like domain; isocitrate dehydrogenase NAD-dependent family
701	C5XC95	Uncharacterized protein OS=*Sorghum bicolor* GN=SORBI_3002G345800	4.02	18.95	6	1.42	0.25	3.02E-02	Electron transport chain	Electron transfer activity	Anchored component of plasma membrane	Phytocyanin domain; cupredoxin superfamily
871	C5Z0R1	Uncharacterized protein OS=*Sorghum bicolor* GN=SORBI_3009G189400	2.87	2.983	2	-1.23	0.03	1.02E-03	Sulfate reductions	Sulfite reductase (ferredoxin) activity	None predicted	Nitrite/Sulfite reductase ferredoxin-like domain; Sulphite reductase, ferredoxin dependent family
1111	A0A1B6PBV5	Uncharacterized protein OS=*Sorghum bicolor* GN=SORBI_3008G033600	2	12.22	5	-1.24	0.13	4.24E-02	Glycolytic process	Pyruvate kinase activity	None predicted	Pyruvate kinase, barrel domain; pyruvate kinase family
1114	C5WN52	Uncharacterized protein OS=*Sorghum bicolor* GN=SORBI_3001G119100	2	27.91	5	1.68	0.42	2.21E-02	Electron transport chain	Electron transfer activity	Anchored component of plasma membrane	Phytocyanin domain; cupredoxin superfamily

Transcription												
173	C5YM38	Histone H2B OS=*Sorghum bicolor* GN=SORBI_3007G149600	12.62	34.44	21	2.13	0.46	5.03E-03	None predicted	DNA binding	Nucleosome	Histone H2A/H2B/H3 domain; histone H2B family
184	C5YHS2	Uncharacterized protein OS=*Sorghum bicolor* GN=SORBI_3007G192700	12.34	42.51	10	1.12	0.06	2.33E-02	None predicted	None predicted	Cytoplasm	Nascent polypeptide-associated complex NAC domain; nascent polypeptide-associated complex subunit alpha family
196	C5XID4	Uncharacterized protein OS=*Sorghum bicolor* GN=SORBI_3003G279800	11.84	27.15	7	1.16	0.05	1.89E-03	None predicted	None predicted	None predicted	Hyaluronan/mRNA-binding protein domain, family not predicted
245	C5YL42	Uncharacterized protein OS=*Sorghum bicolor* GN=SORBI_3007G132900	10.34	24.24	5	1.36	0.20	1.43E-02	DNA-templated, nucleosome assembly	DNA binding	Nucleosome	Linker histone H1/H5, domain H15; high mobility group protein HMGA family
284	C5WYC3	Nascent polypeptide-associated complex subunit beta OS=*Sorghum bicolor* GN=SORBI_3001G216200	9.51	45.18	8	1.29	0.16	1.48E-02	Regulation of transcription, DNA-templated	None predicted	None predicted	Nascent polypeptide-associated complex NAC domain; NAC A/B domain superfamily
362	C5WTL6	Histone H4 OS=*Sorghum bicolor* GN=SORBI_3001G313200	8.01	42.72	5	2.06	0.33	7.98E-04	Nucleosome assembly	Histone binding	Nuclear nucleosome	CENP-T/Histone H4, histone fold domain; histone H4 family
500	C5XAT9	Histone H2A OS=*Sorghum bicolor* GN=SORBI_3002G330000	6.09	34.81	5	1.58	0.24	7.85E-03	Chromatin silencing	DNA binding	Nuclear chromatin	Histone H2A/H2B/H3 domain; histone H2A family
579	C5XX54	Histone H2A OS=*Sorghum bicolor* GN=SORBI_3004G205300	5.15	23.91	4	1.73	0.27	4.03E-03	Chromatin silencing	DNA binding	Nuclear chromatin	Histone H2A, C-terminal domain; histone H2A family
597	C5WMP6	Nascent polypeptide-associated complex subunit beta OS=*Sorghum bicolor* GN=SORBI_3001G537200	4.94	40.72	6	1.29	0.13	3.99E-03	Regulation of transcription, DNA-templated	None predicted	None predicted	Nascent polypeptide-associated complex NAC domain; NAC A/B domain superfamily
627	C5XYG2	Uncharacterized protein OS=*Sorghum bicolor* GN=SORBI_3004G096500	4.53	7.267	4	1.35	0.13	2.17E-03	None predicted	mRNA binding	Cytosol	K Homology domain; K Homology domain, type 1 superfamily
953	C5XAT8	Histone H2A OS=*Sorghum bicolor* GN=SORBI_3002G329900	2.3	29.85	3	1.42	0.20	6.61E-03	Chromatin silencing	DNA binding	Nuclear chromatin	Histone H2A, C-terminal domain; Histone H2A family
1112	C5WPC4	Histone H2A OS=*Sorghum bicolor* GN=SORBI_3001G416900	2	28.75	5	2.23	0.75	1.98E-02	Chromatin silencing	DNA binding	Nucleosome	Histone H2A, C-terminal domain; histone H2A family
Protein destination and storage												
90	A0A1B6PKJ4	Uncharacterized protein OS=*Sorghum bicolor* GN=SORBI_3006G062500	18.86	22.33	13	-1.17	0.02	4.88E-03	Protein folding	Unfolded protein binding	Endoplasmic reticulum, integral component of	Domain not predicted; calreticulin/calnexin family

											membrane	
135	C5WV27	Uncharacterized protein OS=*Sorghum bicolor* GN=SORBI_3001G036300	14.98	22.42	10	-1.14	0.01	2.38E-02	Proteolysis	Metalloaminopeptidase activity	Cytoplasm	Peptidase M1, membrane alanine aminopeptidase, N-terminal domain; peptidase M1, alanine aminopeptidase/leukotriene A4 hydrolase family
224	C5XDR4	Uncharacterized protein OS=*Sorghum bicolor* GN=SORBI_3002G217200	10.89	15.43	9	1.47	0.17	3.24E-03	Proteolysis	Cysteine-type endopeptidase activity	Extracellular space	Peptidase C1A, papain C-terminal; peptidase C1A family
233	C5Z4C7	Proteasome subunit beta type OS=*Sorghum bicolor* GN=SORBI_3010G042800	10.69	28.57	6	-1.22	0.07	4.62E-03	Proteolysis	Threonine-type endopeptidase activity	Cytoplasm	Domain not predicted; peptidase T1A, proteasome beta-subunit family
254	B3GQV9	Peptidyl-prolyl cis-trans isomerase OS=*Sorghum bicolor* GN=Cyp	10.19	34.3	11	1.12	0.05	1.51E-02	Protein peptidyl-prolyl isomerization	Peptidyl-prolyl cis-trans isomerase activity	None predicted	Cyclophilin-type peptidyl-prolyl cis-trans isomerase domain and family
272	A0A1B6PHE0	Uncharacterized protein OS=*Sorghum bicolor* GN=SORBI_3007G120800	9.8	7.306	5	-1.11	0.04	4.38E-02	Proteolysis	Aminopeptidase activity	None predicted	Peptidase M1, membrane alanine aminopeptidase, N-terminal domain; peptidase M1, alanine aminopeptidase/leukotriene A4 hydrolase family
296	C5XM19	Uncharacterized protein OS=*Sorghum bicolor* GN=SORBI_3003G037800	9.35	18.47	6	-1.21	0.04	1.55E-03	None predicted	Transferase activity, transferring acyl groups other than amino-acyl groups	None predicted	Domain not predicted; transferase family
311	C5XUD0	Uncharacterized protein OS=*Sorghum bicolor* GN=SORBI_3004G326600	8.97	10.83	4	-1.30	0.08	7.37E-03	Chaperone-mediated protein folding	ATP binding	Chaperonin-containing T-complex	Domain not predicted; chaperone tailless complex polypeptide 1 (TCP-1) family
319	C5Y8G7	Uncharacterized protein OS=*Sorghum bicolor* GN=SORBI_3005G224500	8.75	39.19	15	1.29	0.16	3.44E-02	Proteolysis	Aspartic-type endopeptidase activity	None predicted	Peptidase family A1 domain; aspartic peptidase A1 family
322	C5Y4Y9	Uncharacterized protein OS=*Sorghum bicolor* GN=SORBI_3005G163700	8.66	11.31	5	-1.09	0.05	3.10E-02	Chaperone-mediated protein folding	Protein binding involved in protein folding	Chaperonin-containing T-complex	Domain not predicted; chaperone tailless complex polypeptide 1 (TCP-1) family
536	C5WTN6	T-complex protein 1 subunit gamma OS=*Sorghum bicolor* GN=SORBI_3001G460500	5.7	5.376	3	-1.25	0.08	1.13E-02	Chaperone-mediated protein folding	Protein binding involved in protein folding	Chaperonin-containing T-complex	Domain not predicted; T-complex protein 1, gamma subunit family
668	C5X6A0	Uncharacterized protein OS=*Sorghum bicolor* GN=SORBI_3002G423500	4.16	5.607	2	-1.23	0.13	4.05E-02	Chaperone-mediated protein folding	Protein binding involved in protein folding	Chaperonin-containing T-complex	Domain not predicted; chaperonin Cpn60/TCP-1 family
Signal transduction												
42	A0A1B6PIK2	Uncharacterized protein OS=*Sorghum bicolor* GN=SORBI_3007G190200	24.58	21.73	18	1.17	0.09	1.11E-02	None predicted	Acid phosphatase activity	None predicted	Purple acid phosphatase domain; Calcineurin-like phosphoesterase family

43	A0A1B6Q0N0	Uncharacterized protein OS=*Sorghum bicolor* GN=SORBI_3003G005800	24.57	41.09	12	1.66	0.18	4.54E-03	Cellular response to stimulus	None predicted	Anchored component of plasma membrane	Domain not predicted; DREPP family
89	C5YU10	Uncharacterized protein OS=*Sorghum bicolor* GN=SORBI_3008G084600	18.89	43.15	12	1.30	0.12	9.71E-03	Nucleotide phosphorylation	Adenylate kinase activity	None predicted	Adenylate kinase, active site lid domain; adenylate kinase/UMP-CMP kinase family
150	A0A1B6P7A4	Uncharacterized protein OS=*Sorghum bicolor* GN=SORBI_3009G070800	13.98	31.35	12	1.37	0.10	6.51E-03	Dephosphorylation	Acid phosphatase activity	None predicted	Domain not predicted; acid phosphatase, class B-like family
252	A0A1B6PBB3	Uncharacterized protein OS=*Sorghum bicolor* GN=SORBI_3009G259200	10.2	20.99	5	1.19	0.03	8.22E-03	Nucleoside diphosphate phosphorylation	Nucleoside diphosphate kinase activity	None predicted	Nucleoside diphosphate kinase-like domain; nucleoside diphosphate kinase family
855	C5X044	Uncharacterized protein OS=*Sorghum bicolor* GN=SORBI_3001G080700	2.97	8.571	2	1.57	0.26	2.47E-02	Protein phosphorylation	Protein serine/threonine kinase activity, ATP binding	None predicted	Protein kinase domain; protein kinase-like domain superfamily
1039	C5YQC5	Purple acid phosphatase OS=*Sorghum bicolor* GN=SORBI_3008G140100	2.04	2.585	2	-1.23	0.07	1.65E-02	Dephosphorylation	Acid phosphatase activity	None predicted	Purple acid phosphatase domain; N-terminal family
20	C5WW94	Uncharacterized protein OS=*Sorghum bicolor* GN=SORBI_3001G197400	32.48	56.76	28	-1.24	0.11	1.46E-02	None predicted	ATP binding	None predicted	Domain not predicted; actin family
55	C5Z7S0	Tubulin beta chain OS=*Sorghum bicolor* GN=SORBI_3010G224900	23.35	37.22	23	-1.31	0.05	3.30E-02	Cytoskeleton organization	Structural constituent of cytoskeleton	Cytoplasm	Tubulin/FtsZ, GTPase domain; tubulin family
567	C5Z4B6	Profilin OS=*Sorghum bicolor* GN=SORBI_3010G041600	5.34	30.53	5	1.12	0.03	2.44E-02	Sequestering of actin monomers	Actin monomer binding	Cell cortex	Domain not predicted; profilin family
1104	C5WTY3	Uncharacterized protein OS=*Sorghum bicolor*	2	36.07	17	-1.37	0.19	4.76E-02	None predicted	ATP binding	None predicted	Domain not predicted; actin family
786	C5Z7L3	Uncharacterized protein OS=*Sorghum bicolor* GN=SORBI_3010G101800	3.53	2.629	2	1.12	0.09	5.00E-02	Mitochondrial fission	GTP binding	Cytoplasm	Dynamin-type guanine nucleotide-binding (G) domain; dynamin superfamily
Unclear classification												
50	C5YCX2	Uncharacterized protein OS=*Sorghum bicolor* GN=SORBI_3006G159300	23.79	50.47	11	1.74	0.23	1.23E-03	None predicted	None predicted	None predicted	Remorin, N-terminal domain; family not predicted
64	C5YBP8	Uncharacterized protein OS=*Sorghum bicolor*	22.2	37.19	16	-1.34	0.03	3.86E-03	None predicted	None predicted	None predicted	E2F/DP family winged-helix DNA-binding domain;

		GN=SORBI_3006G009000										family not predicted
175	A0A1B6Q9X2	Uncharacterized protein OS=*Sorghum bicolor* GN=SORBI_3002G082000	12.59	29.38	9	-1.13	0.06	1.79E-02	None predicted	Protein binding	None predicted	Domain not predicted; Kelch-type beta propeller superfamily
469	C5X978	Uncharacterized protein OS=*Sorghum bicolor* GN=SORBI_3002G307600	6.39	43.86	7	1.38	0.09	1.05E-03	None predicted	None predicted	None predicted	C2 domain; C2 domain superfamily
643	C5YVJ8	Uncharacterized protein OS=*Sorghum bicolor* GN=SORBI_3009G232200	4.32	8.633	2	1.11	0.06	4.54E-02	None predicted	None predicted	None predicted	FAS1 domain; FAS1 domain superfamily
808	C5XFL0	Uncharacterized protein OS=*Sorghum bicolor* GN=SORBI_3003G397500	3.34	20.65	3	2.00	0.48	8.56E-03	None predicted	None predicted	None predicted	Conserved hypothetical protein
824	C5XEU4	Uncharacterized protein OS=*Sorghum bicolor* GN=SORBI_3003G388200	3.22	4.207	2	1.38	0.03	3.83E-04	None predicted	RNA binding	None predicted	Ribonuclease T2 domain and family
956	A0A1B6PFS5	Uncharacterized protein OS=*Sorghum bicolor* GN=SORBI_3007G057100	2.29	26.76	2	1.47	0.16	2.16E-03	None predicted	None predicted	None predicted	Expressed protein

[a] Protein number assigned in ProteinPilot software.

[b] Protein accession numbers obtained from the TrEMBL database [incorporated within the UniProt database (http://www.uniprot.org)] searches against sequences of *Sorghum bicolor* only.

[c] Protein score generated by ProteinPilot software relating to the confidence of protein identification. A protein identification threshold of 1.3 was applied to the data, which only retains proteins identified with a 95% confidence.

[d] Percentage coverage is determined by the number of amino acids of sequenced peptides against the total length of the protein, with a threshold of at least 95% confidence.

[e] Sequenced peptide refers to the number of peptide that were sequenced and gave rise to protein identity. All proteins that were identified by means of a single peptide were filtered out of the dataset.

[f] Probability value of the quantitative difference between the treatment and control protein abundance being due to chance alone.

[g]Standard deviation of the ratios of drought stressed samples (n=4).

[h] Ratio represents the average fold-change (n = 4) induced by treatment relative to control. Positive values indicate an up-regulation.

[i] Gene ontology analysis as predicted on the IntePro database (https://www.ebi.ac.uk/interpro/) and UniProt database (http://www.uniprot.org). P denotes Biological Process, F denotes Functional Process, and C denotes Cellular Component.

[j] Conserved domains and family name as predicted by InterPro database (http://www.ebi.ac.uk/interpro/).

4.4.2 Gene ontology analysis

The 237 and 184 drought stress responsive differentially expressed proteins were submitted for GO annotation. This resulted in the determination of their cellular component, biological process and molecular function. From the results obtained, 50.2% and 44.6% of the root proteins had no predicted cellular component for ICSB 338 and SA 1441 sorghum varieties, respectively. These proteins comprised the greatest proportion for both sorghum varieties. The most highly represented cell components included the cytoplasm and cytosol with 17.7% and 15.2%, extracellular region with 8.9% and 12.5%, ribosome with 5.1% and 9.2%, mitochondrion with 4.2 and 2.7%, and chloroplast with 2.5% and 1.6% for ICSB 338 and SA 1441, respectively. Other cellular components such as the nucleus, plasma membrane, Golgi apparatus, endoplasmic reticulum, cytoskeleton were represented to a lower extent within each sorghum variety (Figure 4.6).

The 237 and 184 drought stress responsive root proteins identified for ICSB 338 and SA 1441 were annotated across a wide range of biological functions. Amongst the identified proteins, 15.6% and 22.8% had no predicted biological processes for ICSB 338 and SA 1441, respectively (Figure 4.7). Proteins predicted to be involved in metabolic processes comprised the largest proportion compared to other categories. In this category, ICSB 338 and SA 1441 totalled 17.7% and 13.6%, respectively. Other highly represented categories were oxidation reduction processes with 11.8% and 8.2%, catabolic processes with 12.2% and 7.1%, translation with 5.9% and 10.9%, biosynthetic processes with 8% and 4.9%, proteolysis with 5.9% and 2.7%, glycolytic processes 3% and 3.3%, phosphorylation with 3.4% and 2.7%, and transmembrane transport with 2.1% and 1.6% for ICSB 338 and SA 1441, respectively. The remaining proteins were distributed across several other biological processes (Figure 4.7).

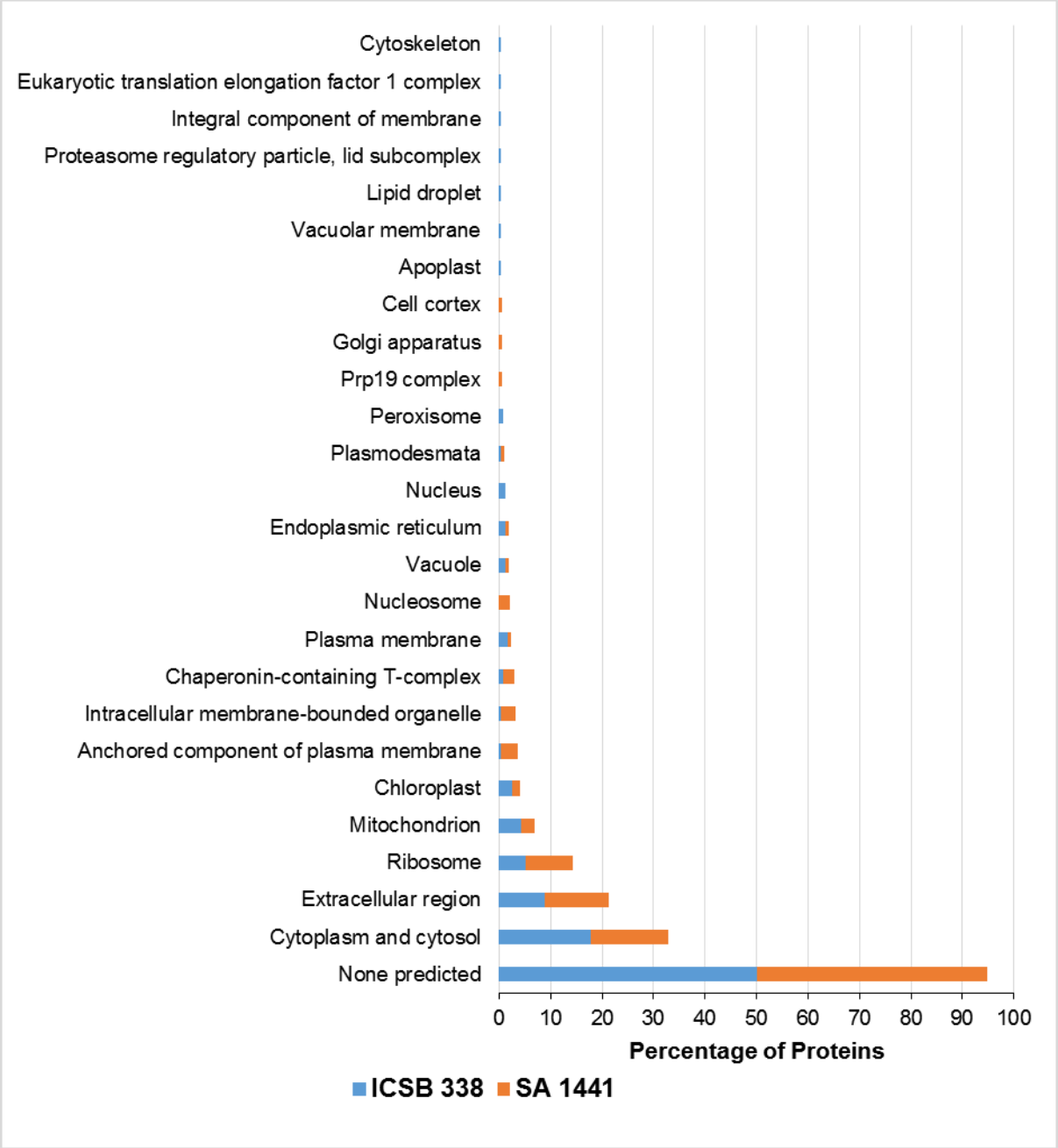

Figure 4.6: Cellular component predictions of the identified sorghum root drought stress responsive total soluble protein based on GO annotation.

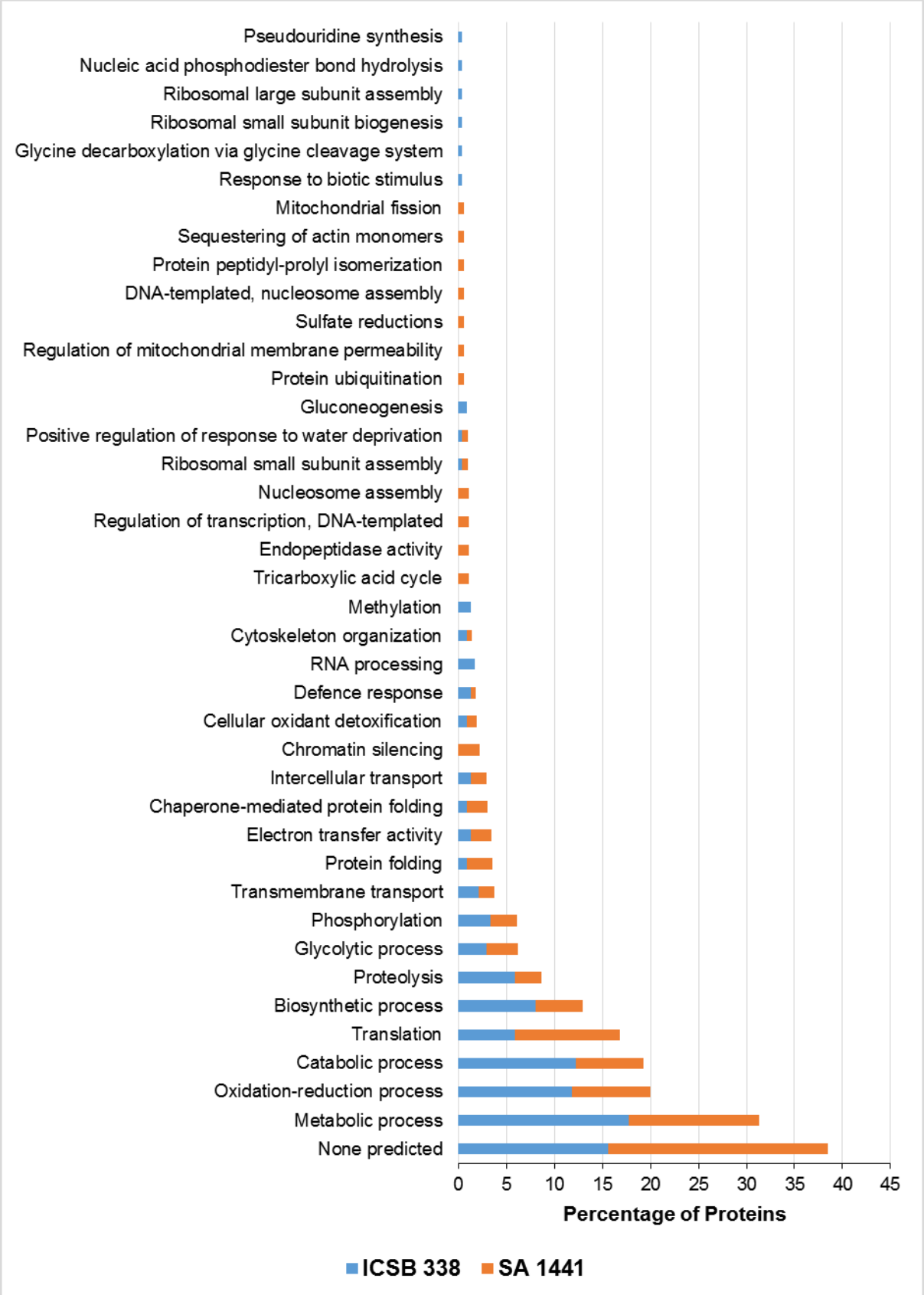

Figure 4.7: Biological process predictions of the identified sorghum root drought stress responsive protein based on GO annotation.

The identified drought stress responsive root proteins were annotated across a wide range of molecular functions as well (Figure 4.8). Proteins with binding activity which includes protein, nucleotide, ATP, GTP, ion-ion, FMN, heme- binding comprised 17.3% and 27.2% for ICSB 338 and SA 1441, respectively. Relatively high activity was also observed for electron transfer, peptidase, peroxidase, isomerase, kinase, dehydrogenase, hydrolase, transferase, synthase and oxidoreductase activity in both sorghum varieties.

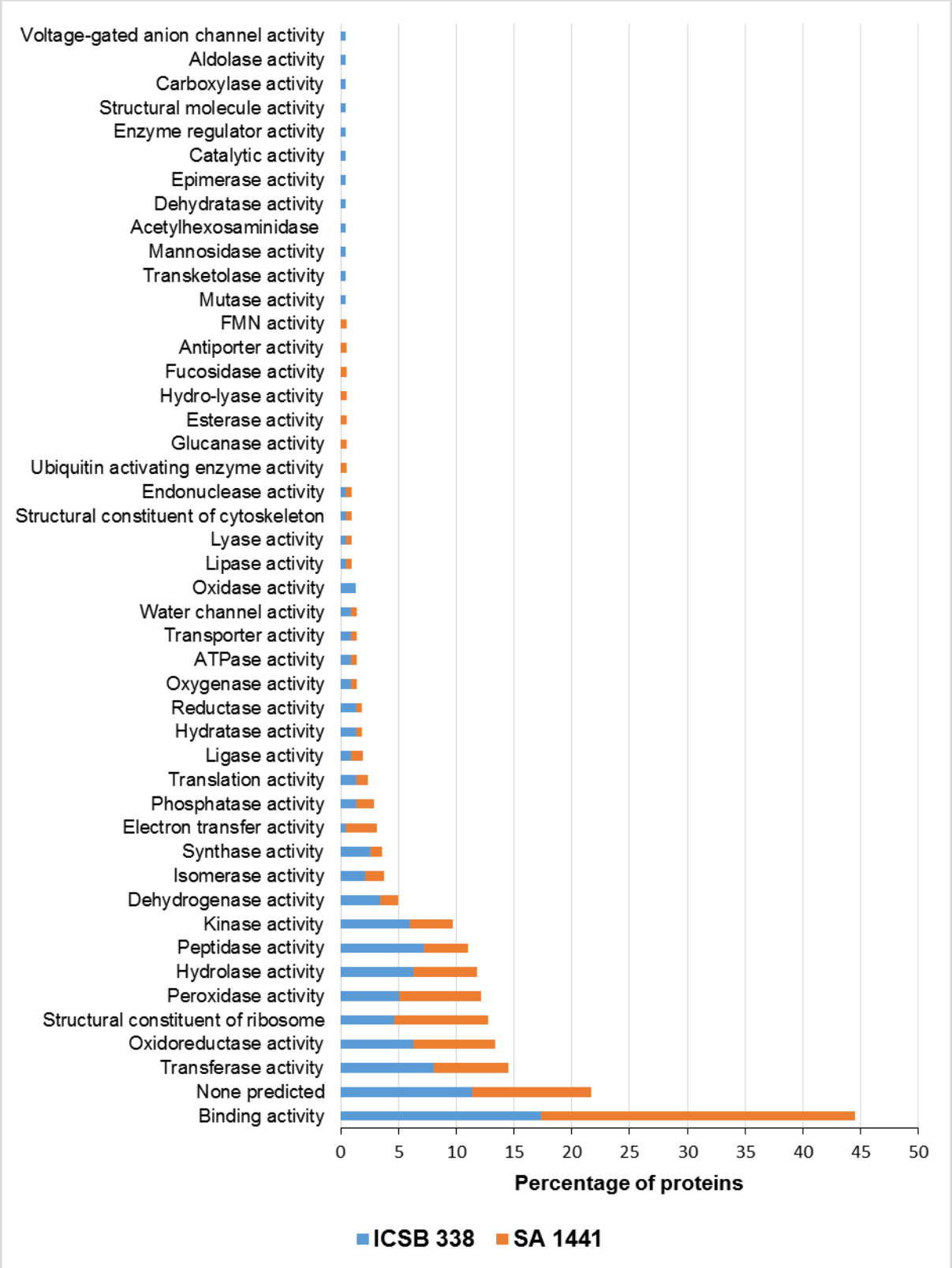

Figure 4.8: Molecular process predictions of the identified sorghum root drought stress responsive proteins based on GO annotation.

4.4.3 Functional Categories of Differentially Expressed Drought Responsive Proteins

The differentially expressed proteins in ICSB 338 and SA 1441 sorghum varieties were grouped into 11 functional categories according to Bevan *et al*. (1998) and other literature sources as shown in Tables 4.1 and 4.2, respectively. Functional classification was also carried out using GO datasets as well as the conserved domains/protein families, especially for the uncharacterized proteins. A graphical representation of the functional groups is shown in Fig 4.9. For ICSB 338, the most highly represented groups of differentially expressed root proteins in response to drought stress were disease/defense (26%), metabolism (25%), energy (9%), protein synthesis (8%) and protein destination and storage (8%). For SA 1441, disease/defense (23%), metabolism (21%), protein synthesis (14%), transporters (10%) and energy (9%) were highly represented. A brief description of some proteins in these functional groups is given below.

ICSB 338

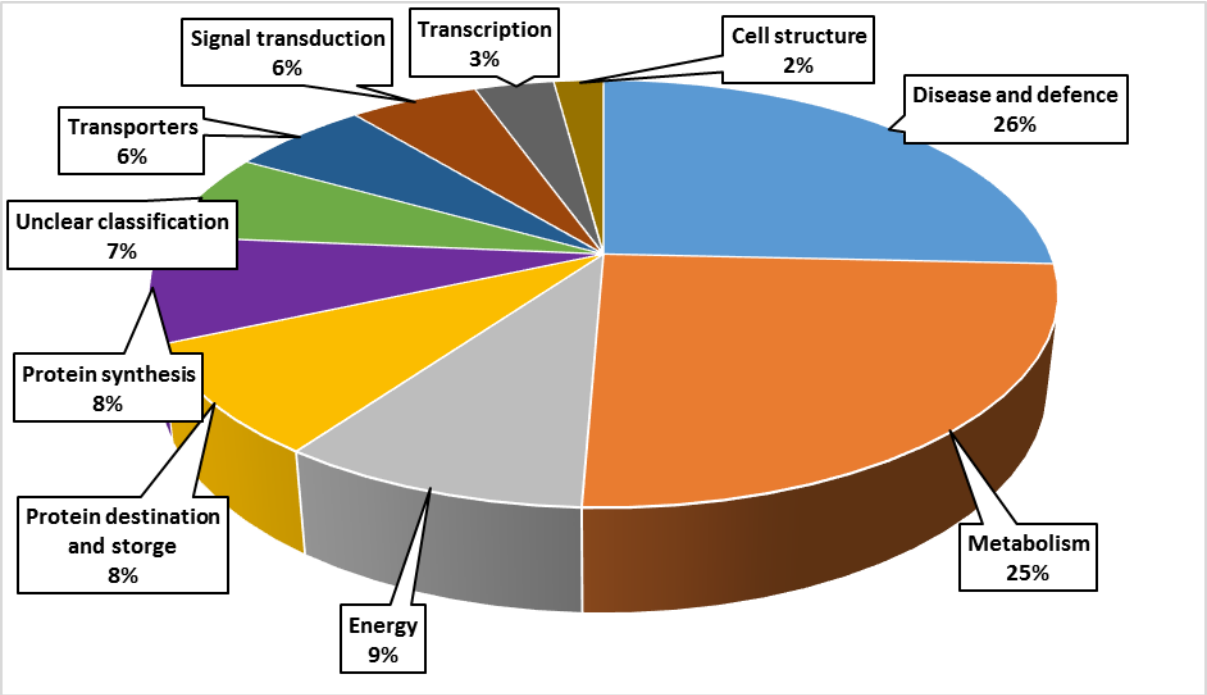

SA 1441

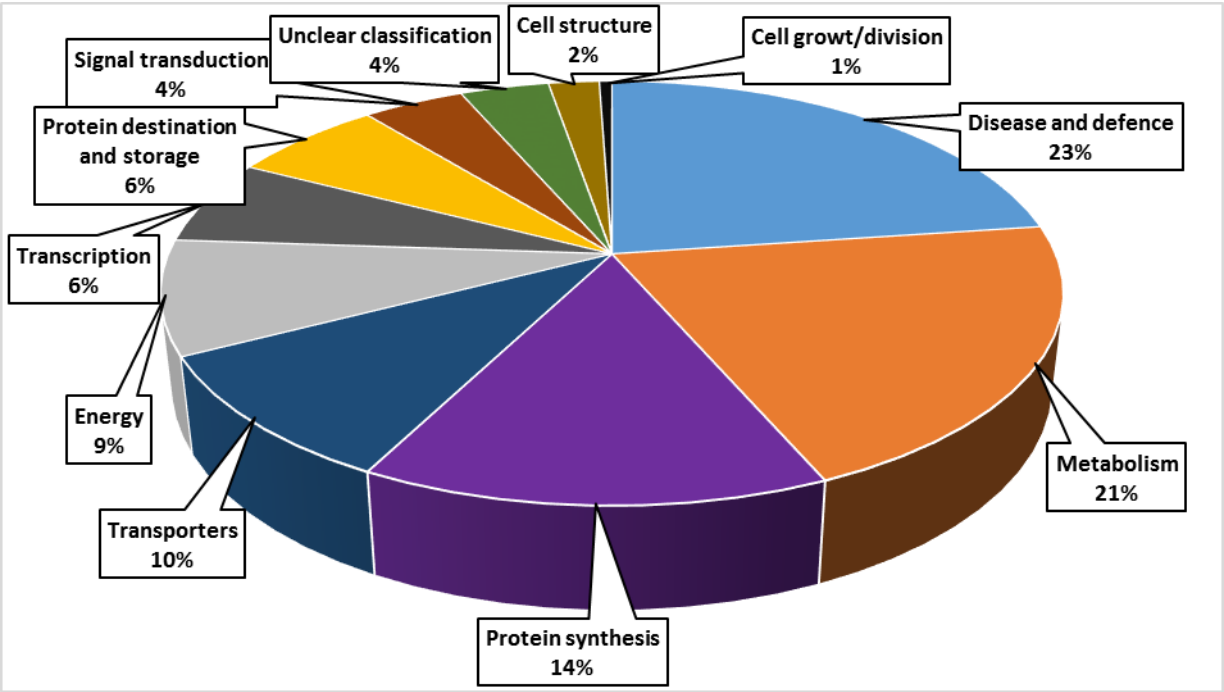

Figure 4.9: Functional classification of the differentially expressed sorghum root drought stress responsive proteins.

4.4.3.1 Metabolism

Of the 237 differentially expressed ICSB 338 sorghum drought stress responsive root proteins, 59 (25%) were involved in metabolism. For SA 1441, 38 (21%) proteins were assigned to the metabolism group out of a total of 184 drought responsive proteins (Figure 4.9). Of these proteins, a total of 30 and 25 were uncharacterised for ICSB 338 and SA 1441 sorghum varieties, respectively. The proteins with the highest fold change were protein no. 767 (1.56) and 874 (2.01) for ICSB 338 and SA 1441, respectively. Conversely, proteins with the lowest fold change were protein no. 155 (-2.1) and 494 (-1.39) for ICSB 338 and SA 1441, respectively.

Collectively some of the characterized proteins families in both sorghum varieties included lipoxygenase, sucrose synthase, aconitate hydratase, s-adenosyl methionine synthase, pyrophosphate--fructose 6-phosphate 1-phosphotransferase subunit beta, 6-phosphogluconate dehydrogenase, patatin, chitinase, alpha-mannosidase, beta-galactosidase, formate dehydrogenase, beta hexosaminidase, glutamine synthase, ATP-dependent 6-phosphofructokinase, 3-methyl-2-oxobutanoate hydroxymethyltransferase, amine oxidase, glutamate dehydrogenase, phosphotransferase, nitrilase, chalcone-flavonone, dhurrinase, aldose 1-epimerase, L-lactate dehydrogenase, acetyltransferase component of pyruvate dehydrogenase complex, ketol-acid reductoisomerase, glycosyltransferase, phosphotransferase, D-3-phosphoglycerate dehydrogenase and UDP-glucose 6-dehydrogenase (Table 4.1 and 4.2).

The group of proteins over-represented in both sorghum varieties was lipoxygenase (protein no. 1, 6, 17, 249 for ICSB 338 and protein no. 2, 9 and 32 for SA 1441). All the lipoxygenase proteins were down-regulated in both ICSB 338 and SA 1441. Lipoxygenases constitute a large gene family of non-heme, iron containing fatty acid dioxygenases which are ubiquitous

in plants (Brash, 1999; Feussner and Wasternack, 2002). They are involved in the catalysis of hydroperoxidation of polyunsaturated fatty acids in plants. Products of this pathway such as jasmonates function in signalling whilst leaf aldehydes have antimicrobial and antifungal properties (Feussner and Wasternack, 2002). Other proteins in this functional category were involved in the metabolism of a range of carbohydrates (protein no. 5, 72, 76, 87, 131, 133, 138, 289, 319, 319, 729, 975, and 109 for ICSB 338 and protein no. 70, 76, 142, 288, 390, 755 and 856 for SA 1441), lipids and fatty acids (protein no. 115 and 933 for ICSB 338 and protein no. 494 for SA 1441) and amino acids (protein no 58, 294, 482, 647 and 774 for ICSB 338 and 568, for SA 1441). Carbohydrate metabolism, amino acid metabolism and lipid metabolism proteins were also differentially expressed in tomato root tissue in a comparative study between a drought tolerant *Solanum chilense* and a susceptible *Solanum lycopersicum* tomato plants (Zhou *et al*., 2013).

4.4.3.2 Disease/defence

A total of 61 (26%) of the 237 ICSB 338 proteins that were responsive to drought stress were involved in the disease and defence (Figure 4.9). For SA 1441, 38 (21%) of the 184 drought responsive proteins were involved in this functional category. Of these proteins, 43 and 23 were uncharacterized for ICSB 338 and SA 1441, respectively (Table 4.1 and 4.2). The proteins with the highest fold change were protein no. 329 (1.77) and 998 (1.73) for ICSB 338 and SA 1441, respectively. Conversely, proteins with the lowest fold change were protein no. 1218 (-3.62) and 161 (-1.52) for ICSB 338 and SA 1441, respectively.

For ICSB 338, the peroxidase group of proteins (protein no. 95, 148, 173, 232, 235, 446, 708, 794) was most common. Of these, a total of 4 proteins (protein no. 173, 232, 235, 794) were up-regulated whilst the remaining 4 (protein no. 95, 148, 446, 708) were down-regulated. Peroxidases are known to utilize hydrogen peroxide as the optimal substrate although others

utilize organic hydroperoxides such as lipid peroxides (Elstner, 1987). The main function of peroxidases is in antioxidant defences by scavenging and detoxifying reactive oxygen species (ROS) present in plants. The major detoxification of hydrogen peroxide occurs through the ascorbate-glutathione cycle, in which the substrate is converted into water with the use of ascorbate as the electron donor (Elstner, 1987).

Other functions of peroxidases in plants include lignin biosynthesis, which renders the cell wall rigid thereby forming a defensive barrier against biotic and abiotic stress (Boudet, 1998; Kawano, 2003). Peroxidases were also up-regulated in wild wheat (*Triticum aestivum*) root tissue under drought stress (Liu *et al*., 2015). The other characterized proteins identified include the up-regulated proteins phenylalanine ammonia lyase (protein no. 25), S-(hydroxymethyl) glutathione dehydrogenase (protein no. 466), dirigent protein (protein 766 and 977), and the down-regulated glyceraldehyde-3-phosphate dehydrogenase (protein no. 10), putative alcohol dehydrogenase 1 (protein no. 101), ketol-acid reductoisomerase (protein no, 367), inosine-5'-monophosphate dehydrogenase (protein no. 454), uricase (protein no. 880) and the pathogenesis related protein 10a (protein no. 1216).

For SA 1441, the peroxidases (protein no. 38, 66, 97, 130, 159, 187, 207, 287, 307, 437, 622, 641, 779) were also the most common amongst the disease and defence functional group. Of these, a total of 12 proteins (protein no. 38, 97, 130, 159, 187, 207, 287, 307, 437, 622, 641, 779) were up-regulated whilst only one protein (protein no. 66) was down-regulated. This indicates that a larger number of peroxidase proteins responded to drought stress in SA 1441 in comparison to ICSB 338. An increase in abundance of peroxidases was also observed in Arabidopsis root tissue in response to salinity stress (Jiang *et al*., 2007). The other characterised up-regulated SA 1441 proteins were pathogenesis-related protein 10b (protein no. 57), late embryogenesis abundant protein (LEA) 3 (protein no. 131), dirigent protein

(protein no. 794), as well as small heat shock-like protein (protein no. 972). LEA proteins function as cellular protectants under water loss (Chakrabortee *et al*., 2007). Group 2 LEAs were up-regulated in maize (Benešová *et al*., 2012) and wheat (Ford *et al*., 2011) in response to drought stress. The down-regulated characterised SA 1441 proteins were betaine-aldehyde dehydrogenase 2 (protein no. 306) and S-(hydroxymethyl) glutathione dehydrogenase (protein no. 371).

4.4.3.3 Protein Destination and Storage

Figure 4.9 shows that 20 proteins (8%) of the 237 drought responsive root proteins function in protein destination and storage for ICSB 338. Im comparison, 12 proteins (6%) had functions in protein destination and storage for SA 1441. A total of 19 and 9 proteins were uncharacterised for ICSB 338 and SA 1441, respectively (Table 4.1 and 4.2). The protein with the highest fold change was protein no. 868 (2.93) and 224 (1.47) for ICSB 338 and SA 1441, respectively. Conversely, proteins with the lowest fold change were protein no. 582 (-2.06) and 311 (-1.3) for ICSB 338 and SA 1441, respectively. It is important to note that from this functional group, all the ICSB 338 proteins are involved in proteolysis except for protein no. 225 and 304 which are involved in chaperone mediated protein folding. Of the proteins involved in proteolysis, 70% were up-regulated with the remaining proportion being down-regulated. The two proteins involved in protein mediated protein folding were down-regulated. The only characterized ICSB 338 protein that was up-regulated was carboxypeptidase (protein no. 315), involved in protein catabolism and post-translational modification (Fraser *et al*., 2005).

For SA 1441, the down-regulated proteasome subunit beta type (protein no. 233), up-regulated peptidyl-prolyl cis-trans isomerase (protein no. 254) and the down-regulated T-complex protein 1 subunit gamma (protein no. 536) involved in proteolysis, protein

isomerisation and chaperone mediated protein folding, respectively were the only characterised proteins. The remaining proteins were uncharacterised and involved protein folding (protein no. 90, 311,322, 668), proteolysis (protein no, 135, 224, 233, 272, 319), protein binding and transferase activity (protein no. 296). All the proteins involved in protein folding were down-regulated whilst two of the five proteolysis proteins were up-regulated. Chaperonins play an important role in facilitating newly synthesised translocated proteins to obtain their native form (Wang *et al*., 2004). A chaperonin protein (chaperonin subunit beta) was down-regulated in response to drought stress in Kentucky bluegrass (*Poa pratenis*) leaf tissue in response to drought stress (Xu and Huang, 2010). In the current study, proteins involved in chaperone-mediated protein folding were also down-regulated.

4.4.3.4 Signal Transduction

A total of 13 (6%) proteins out of the 237 ICSB 338 and 7 (4%) of the total 184 SA 1441 drought responsive root proteins were signal transduction related proteins (Figure 4.9). A total of 12 and 6 of these proteins were uncharacterized for ICSB 338 and SA 1441, respectively (Table 4.1 and 4.2). The proteins with the highest fold change were protein no. 199 (1.55) and 43 (1.66) for ICSB 338 and SA 1441, respectively. Conversely, proteins with the lowest fold change were protein no. 1218 (-1.39) and 1039 (-1.23) for ICSB 338 and SA 1441, respectively.

In this functional category, only UMP-CMP kinase and purple acid phosphatase were characterised for ICSB 338 and SA 1441, respectively. UMP-CMP kinase was up-regulated whilst purple acid phosphatase was down-regulated. All the SA 1441 proteins were up-regulated except for purple acid phosphatase. The main function of UMP-CMP kinase is to catalyse the phosphorylation of pyrimidine nucleoside monophosphates using ATP. In this way, it plays a vital role in *de novo* pyrimidine nucleoside biosynthesis. Purple acid

phosphatase belongs to a family of dinuclear metalloenzymes (LeBansky *et al*., 1992), and catalyses phosphate ester hydrolysis. Kaida *et al*. (2010) showed that purple acid phosphatase can catalyse the dephosphorylation of cell wall proteins in tobacco.

The remaining ICSB 338 proteins were uncharacterized. These uncharacterized proteins were involved in kinase and phosphatase molecular activity except for protein no. 7 and 1393 whose function are GTP binding and clathrin heavy chain binding, respectively. Of the proteins involved in phosphorylation, 56% were up-regulated. The two proteins involved in dephosphorylation were both down-regulated. In SA 1441, the uncharacterized proteins were either kinases or phosphatases except for protein no. 43 which had no predicted molecular function but predicted to be involved in cellular response to stimuli. Protein kinases and phosphatases are responsible for signal transduction and regulation (Shinozaki and Yamaguchi-Shinozaki, 1997). Protein kinases were also up-regulated in sorghum leaf tissue in response to salt stress (Swami *et al*., 2011). The GTP binding protein was down-regulated in ICSB 338, whereas the protein was up-regulated in SA 1441. GTP binding proteins were also identified in Arabidopsis root tissue under salt stress (Jiang *et al*., 2007).

4.4.3.5 Energy

A total of 22 (9%) and 16 (9%) of the total drought responsive proteins for ICSB 338 and SA 1441 were annotated in the energy functional group (Figure 4.9). Of these proteins, 14 were uncharacterized for both ICSB 338 and SA 144 (Table 4.1 and 4.2). The protein with the highest fold change was protein no. 503 (1.98) and 1114 (1.68) for ICSB 338 and SA 1441, respectively. Conversely, proteins with the lowest fold change were protein no. 15 (-1.64) and 359 (-1.4) for ICSB 338 and SA 1441, respectively. In this functional category, the majority of the proteins were electron transport chain and glucose metabolism related for both sorghum varieties. These processes are responsible for the production of ATP required

for cellular function. All of the proteins involved in the glycolytic and gluconeogenesis processes were down-regulated in ICSB 338 and SA 1441. However, electron transport chain proteins were up-regulated in both sorghum varieties. The plasma membrane ATPase, involved in proton export across plasma membrane was down-regulated in both ICSB 338 and SA 1441.

All of the other characterised proteins in ICSB 338 were down-regulated. These include fructose-bisphosphate aldolase (protein no. 15), acetyltransferase component of pyruvate dehydrogenase complex (protein no. 135), pyruvate dehydrogenase E1 component subunit alpha (protein no. 147), pyruvate kinase (protein no. 181 and 806), glucose-6-phosphate isomerase (protein no. 206) and ferredoxin-NADP reductase (protein no. 525). In SA 1441, all the proteins under the energy functional group were uncharacterised except for pyruvate kinase (protein no. 244) and pyrophosphate-fructose 6-phosphate 1-phosphotransferase subunit beta (protein no. 359) which were down-regulated as well.

4.4.3.6 Protein Synthesis

Since their discovery in 1955, ribosomes are known as cell structures that synthesise proteins as directed by mRNA using aminoacyl-tRNA, GTP and ATP substrates (Zorca and Zorca, 2011). A total of 80 unique ribosomal proteins have been reported, with 32 being predicted to be present in the 40S ribosomal subunit whilst 48 are in the 60S subunit (Carroll *et al*., 2008; Chang *et al*., 2005). Figure 4.9 illustrates that 19 proteins (8%) and 26 (14%) of the total 237 and 184 proteins for ICSB 338 and SA 1441 drought responsive root proteins, respectively, were involved in protein synthesis. Of these, 15 and 24 proteins were uncharacterized for ICSB 338 and SA 1441, respectively (Table 4.1 and 4.2). The protein with the highest fold change was protein no. 1223 (1.43) and 525 (1.82) for ICSB 338 and SA

1441, respectively. Conversely, those with the lowest fold change were protein no. 816 (-1.66) and 538 (-1.47) for ICSB 338 and SA 1441, respectively.

In ICSB 338, 60S ribosomal protein L13 and L36 (protein no. 520 and 958), 40S ribosomal protein S6 (protein no. 964) and ribosomal protein L19 (protein no. 1022) all of which are involved in translation, were the only characterised proteins. For SA 1441 the elongation factor 1-alpha (protein no. 611) and 40S ribosomal protein S3a (protein no. 793) were the identified characterised proteins. Of all the characterised proteins for both sorghum varieties, only 40S ribosomal protein S3a (protein no. 793) was up-regulated. Ribosomal proteins were aslo down-regulated in Arabidopsis root tissue under salinity stress (Jiang *et al.*, 2007). In agreement to the findings in this study, the translation elongation factor 1-alpha was down-regulated in response to drought stress in barley leaf tissue (Śniegowska-Świerk *et al.*, 2015). The same protein was however up-regulated in sorghum leaf tissue in response to drought stress (Jedmowski *et al.*, 2014). The uncharacterised proteins were mainly involved in the translation and ribosomal large and small subunit biogenesis and assembly for both sorghum varieties. The results of this current study are consistent with Jiang *et al.* (2007) where translation related proteins were also identified in Arabidopsis root tissue under salinity stress.

In ICSB 338, 62% of the proteins involved in translation were up-regulated. The remaining uncharacterised proteins included those involved in rRNA maturation (protein no. 80) which was down-regulated, ribosomal small subunit assembly (protein no. 483) which was up-regulated and ribosomal large subunit assembly which was down-regulated. In SA 1441, all the uncharacterised proteins involved in translation were up-regulated except for protein no. 538. All the remaining uncharacterised proteins, that is, those involved in ribosomal small

subunit assembly (protein no. 35), ribosomal large subunit biogenesis (protein no. 667 and 710) were up-regulated.

4.4.3.7 Transporters

Of the 237 drought responsive root proteins for ICSB 338, 14 proteins (6%) with putative functions as transporters were identified (Figure 4.9). For SA 1441, 18 proteins (10%) were identified in this category. For ICSB 338, 12 proteins were uncharacterized (Table 4.1) whilst 17 proteins were uncharacterized for SA 1441 (Table 4.2). The protein with the highest fold change was protein no. 64 (1.65) and 61 (1.53) for ICSB 338 and SA 1441, respectively. Conversely, proteins with the lowest fold change were protein no. 189 (-1.71) and 88 (-1.36) for ICSB 338 and SA 1441, respectively.

The plasma membrane ATPase (protein no. 4) which was down-regulated, and the mitochondrial pyruvate carrier (protein no. 704) which was up-regulated, were the only characterised proteins in ICSB 338. These proteins are both important in transmembrane transport. In SA 1441, plasma membrane ATPase (protein no. 12), which was down-regulated, was the only characterised protein. Of the ICSB 338 uncharacterised proteins in this category, 67% were up-regulated and involved in various biological functions including intra- and inter-cellular transport. For SA 1441, 53% of the uncharacterised proteins were up-regulated and also involved in intra- and intercellular transport.

4.4.3.8 Other Functional Groups

The remaining functional groups with relatively low numbers of proteins were cell structure, transcription and cell growth/division (Tables 4.1 and 4.2). All the identified cell structure related proteins were uncharacterized for ICSB 338. SA 1441 had only two characterized proteins, namely, tubulin beta chain (protein no. 55) responsible for cytoskeleton organisation

and profilin (protein no. 567) important for sequestering actin monomers. Tubulin beta chain was down-regulated whilst profiling was up-regulated.

Amongst the five uncharacterized ICSB 338 cell structure proteins, protein no. 563 and 804 belonged to the actin family whilst the other three were involved in cytoskeleton organization. Only one protein (protein no. 563) was down-regulated in ICSB 338. Of the uncharacterized proteins, only one protein was also in the actin family for SA 1441. This protein was also down-regulated. This was in agreement with Śniegowska-Świerk *et al*. (2015) where actin was down-regulated in response to drought stress in barley leaf tissue. In contrast to this result, actin was up-regulated in response to drought stress in Kentucky bluegrass leaf tissue in response to drought stress (Xu and Huang, 2010).

All the transcription related proteins identified in ICSB 338 were uncharacterized. Two of the three proteins predicted to be involved in methylation (protein no. 57 and 395) were up-regulated. Proteins involved in nucleic acid phosphodiester bond hydrolysis (protein no. 533), pseudouridine synthesis (protein no.702) and RNA modification (protein no. 865) were also up-regulated. However, those involved in RNA editing (protein no. 787) and mRNA splicing (protein no. 836) were down-regulated. Proteins involved in RNA related processes were also down-regulated in Kentucky bluegrass leaf tissue in response to drought stress (Xu and Huang, 2010) as well as in the resurrection plant (*Xerophyta viscosa*) (Ingle *et al*., 2007). The RNA binding protein was down-regulated in sorghum leaf tissue in a drought sensitive sorghum variety (Jedmowski *et al*., 2014).

For SA 1441, histone H2B (protein no. 173), nascent polypeptide associated complex (protein no. 284), histone H4 (protein no. 362), histone H2A (protein no. 500, 579, 953 and 1112) were the SA 1441 characterised proteins. The most represented protein was histone H2A which is responsible for chromatin silencing (protein no. 500, 579,953 and 1112), all of

which were up-regulated. Chromatin silencing is an essential process in plants and it results in repression of transcription (Li *et al*., 2007). In order to initiate gene expression, chromatin must be modified to allow transcription factors, co-activators and RNA polymerase to access DNA (Thomas and Chiang, 2006). In other studies, histone H2Bs were down-regulated in rockrose (*Cistus albidus*) (Brossa *et al*., 2015) and oilseed rape (*Brassica napus*) (Koh *et al*., 2015) in response to drought stress.

Mitochondrial fission is a process that results in the formation of two daughter mitochondria. Mitochondrial fission and fusion are important processes because they allow the sharing of internal materials between mitochondria (Arimura *et al*., 2004a and b). One uncharacterized protein (protein no. 786) identified in SA 1441 was predicted to be responsible for mitochondrial fission. This protein is in the dynamin superfamily with a dynamin-type guanine nucleotide-binding domain. Dynamin-like proteins are a requirement in mitochondrial fission in Arabidopsis (Arimura *et al*., 2004a) and rice (Fujimoto *et al*., 2004). The protein was up-regulated in SA 1441, the drought tolerant variety.

4.4 Drought-Induced Gene Expression Analysis in Sorghum Root and Leaf Tissue

Five proteins with the highest fold-change were selected from each of the ICSB 338 and SA 1441 iTRAQ datasets (Tables 4.1 and 4.2) to make a total of 10 protein targets for gene expression analysis in sorghum plants (Table 4.3). Primers were designed for each of the genes using the Primer-BLAST tool on the NCBI database (https://www.ncbi.nlm.nih.gov). Following this, the two sorghum varieties were grown at field capacity until the V3 growth stage after which water was withheld for 12 days to impose drought stress (Figure 4.10). At 4 days of drought stress there were no visible signs of drought stress for both sorghum varieties. From 4 to 8 days of drought stress, SA 1441 showed a higher degree of wilting and leaf rolling compared to ICSB 338. ICSB 338 however showed greater leaf chlorosis during

this time period. From 8 to 12 days of drought stress the ICSB 338 leaf tissue became extremely chlorotic and the plants collapsed whilst SA 1441 plants maintained an upright position but the older leaves senesced whilst the new leaves experienced leaf rolling.

Table 4.3: Drought stress responsive proteins selected for primer designing.

Protein no.	Accession	Gene Identity	Fold Change	Protein Family
ICSB 338				
868	C5YPX8	SORBI_3008G134700	2.93	Aspartic peptidase
329	C5WZ08	SORBI_3001G514200	1.77	Thioredoxin
293	C5XDR4	SORBI_3002G217200	1.69	Peptidase
64	C5XHF1	SORBI_3003G136200	1.65	Germin
767	C5YBH7	SORBI_3006G135500	1.56	Galactose oxidase
SA 1441				
874	A0A1B6QHU0	SORBI_3001G073900	2.32	Malate dehydrogenase
173	C5YM38	SORBI_3007G149600	2.13	Histone H2B
362	C5WTL64	SORBI_3001G313200	2.06	Histone H4
525	C5XMD2	SORBI_3003G322400	1.82	Ribosomal protein S25
290	C5XAE4	SORBI_3002G049300	1.79	Ribosomal protein S25

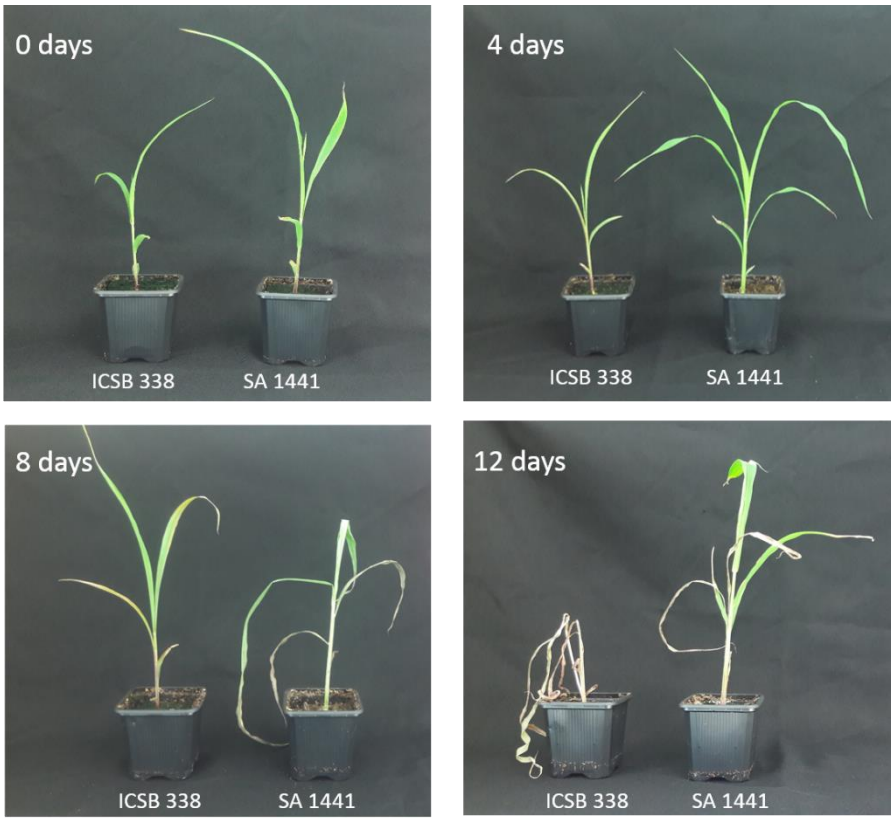

Figure 4.10: ICSB 338 and SA 1441 sorghum plants during the drought stress period. Seedlings were watered until the V3 growth stage. Water was withheld and root and leaf tissue samples were collected at 0, 4, 8 and 12 days after drought stress for gene expression analysis.

ICSB 338 and SA 1441 sorghum root and leaf samples were collected at 0, 4, 8 and 12 days after drought stress for RNA extraction and RNA gel electrophoresis (Figure 4.11). The RNA integrity was good for 0, 4 and 8 day time points for root and leaf tissue of both sorghum varieties. However, at 12 days of drought stress, RNA was somewhat degraded except for the SA 1441 root tissue. This could have possibly been due to leaf chlorosis observed in the plants during the drought stress treatment (Figure 4.10). This was followed by cDNA

synthesis and a standard PCR to assess the specificity of the 10 primers (*SORBI_3008G134700, SORBI_3001G514200, SORBI_3002G217200, SORBI_3003G136200, SORBI_3006G135500, SORBI_3007G149600, SORBI_3001G313200, SORBI_3001G073900, SORBI_3003G322400, SORBI_3002G049300*) to their intended targets **(**Figure 4.12). All the gene specific primers yielded PCR product except for *SORBI_3002G217200* (Figure 4.12) which was subsequently discarded from the study. The primer *SORBI_3002G049300* was also excluded because of non-specificity as observed in Fig 4.12 where no specific amplicon was observed, instead, multiple amplicons of the same resolution were observed. In addition, the melt curve of the gene showed two peaks, signifying the possibility of primer dimers (Appendix, Figure C9 and C12). Ultimately, eight genes were used in the study, four of which showed single amplicons (*SORBI_3001G514200, SORBI_3003G136200, SORBI_3006G135500* and *SORBI_3001G313200)* whilst the other four exhibited double amplicons (*SORBI_3008G134700, SORBI_3007G149600, SORBI_3001G073900 and SORBI_3003G322400).* Of the genes with double amplicons, it was noted that the most prominent amplicon was of the expected size and also, the melt curves showed specific products (Appendix, Figure C7, C8 and C9), therefore the primers were selected for further analyses. Consequently, qRT-PCR was used to analyse the expression of the selected target eight genes.

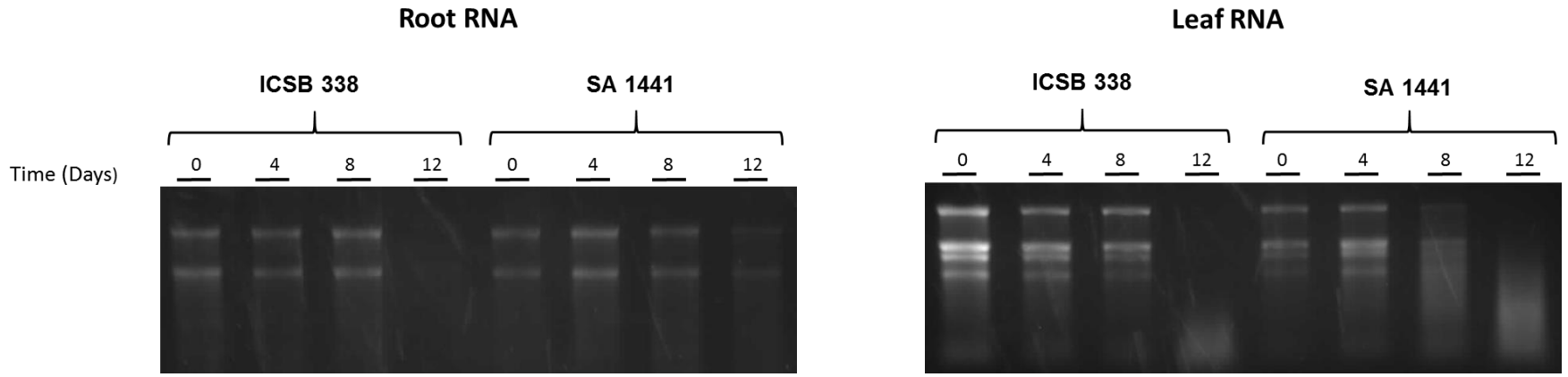

Figure 4.11: Sorghum root and leaf total RNA gel. Approximately 300 ng of RNA for each sample was loaded on a 1.2% agarose gel. Images were taken using an Ingenius Bio-Imager. Four lanes, each in succession, represent ICSB 338 and SA 1441 total RNA at 0, 4, 8 and 12 days of drought stress, respectively.

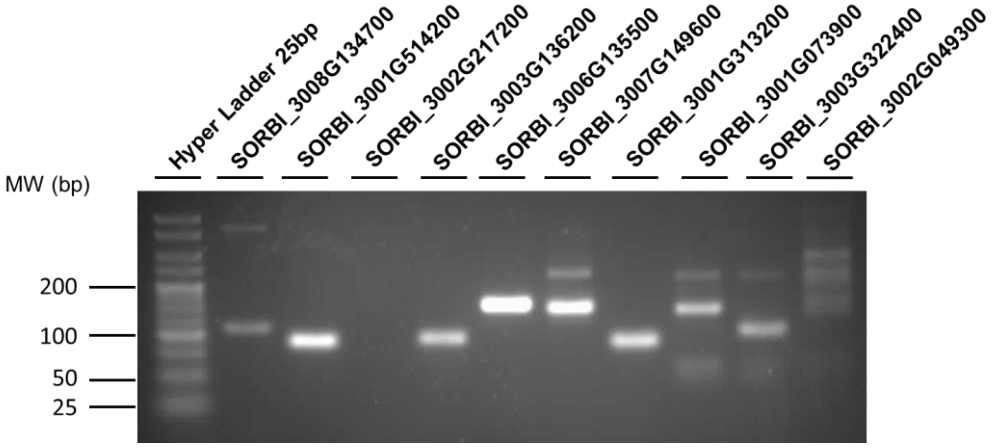

Figure 4.12: Primer analysis of sorghum root drought responsive genes. Sorghum PCR products were loaded on a 3.5% agarose gel. Images were taken using an Ingenius Bio-Imager. The first lane represent a HyperLadder™ 25 bp DNA marker. The following lanes represent amplicons of each of the drought responsive genes.

The gene expression values were generated by entering take off and amplification control values of the reference gene and pasting it in the reference gene section of the REST2009 RG mode. This was followed by entering the corresponding treatment values of the reference gene in the treatment rows of the software. The control sample gene of interest values were then added to the control rows whilst the treatment values were entered in the corresponding treatment rows. Two reference genes were used per analysis in this study. SA 1441 was used as a baseline control to standardise the gene expression for comparison with ICSB 338. The output gene expression values were then exported to Microsoft Excel and the Student's t-test was used to compare the gene expression means at a 5% level of significance. All the sorghum genes except for *SORBI_3003G136200* showed significant differences in expression on at least one time point between ICSB 338 and SA 1441 root tissue in response to drought stress (Figure 4.13). There was a significantly higher expression of *SORBI_3001G073900* and *SORBI_3003G322400* in SA 1441 compared to ICSB 338 at 12 hrs of drought stress. In contrast, *SORBI_3008G134700*, *SORBI_3006G135500* and *SORBI_3001G313200* showed significantly higher expression levels in ICSB 338 compared to SA 1441 at the same time point. Of the 8 genes analysed, 6 showed a peak in gene expression in root tissue at 12 days of drought stress (Figure 4.13).

In the sorghum leaf tissue, a consistent trend of gradual increase in gene expression peaking at 12 days of drought stress was exhibited by all the 8 genes (Figure 4.14). Most of the genes showed a gradual decrease in expression in both sorghum varieties until day 8 of drought stress. This was followed by a massive increase in gene expression at day 12 of drought stress (Figure 4.14).

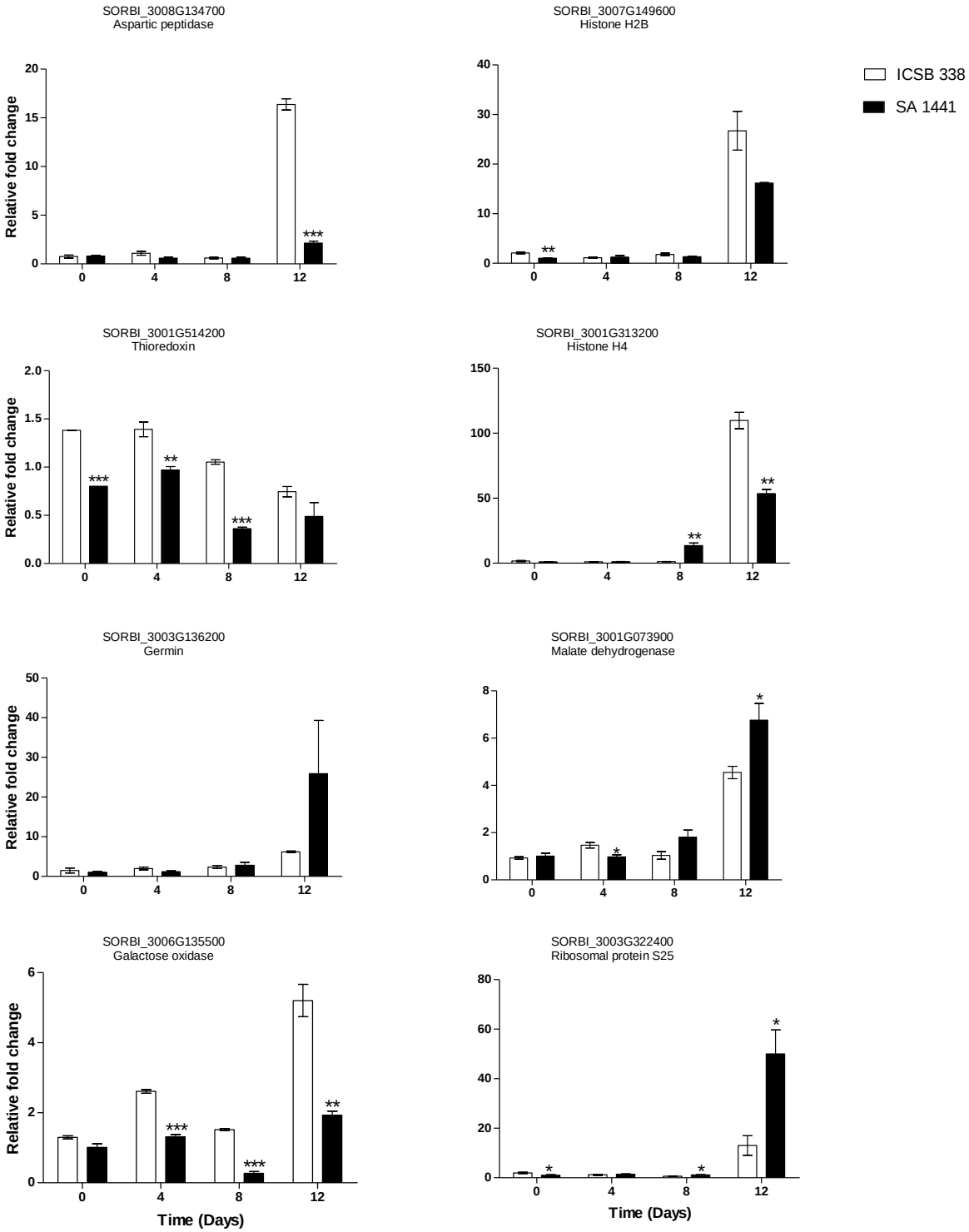

Figure 4.13: Drought stress-induced gene expression in sorghum root tissue. ICSB 338 (drought susceptible) and SA 1441 (drought tolerant) sorghum plants were exposed to drought by withholding water for 12 days. The root samples were harvested at the indicated time points and gene expression analysis was performed using qRT-PCR. Control plants were maintained at field capacity. Bars represent mean ± SE (n = 3). *, ** and *** = significance at $p \leq 0.05$, 0.01 and 0,001, respectively.

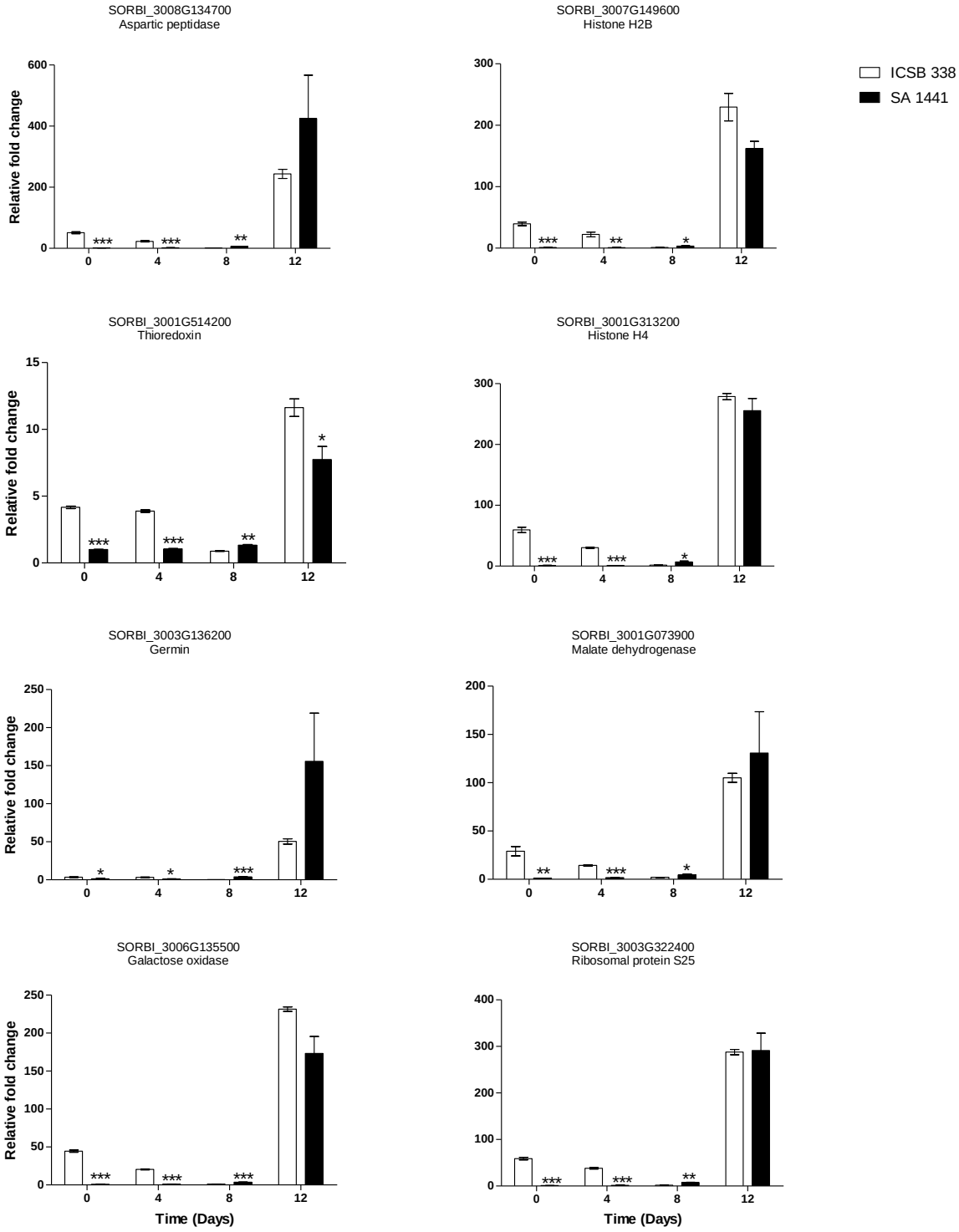

Figure 4.14: Drought stress-induced gene expression in sorghum leaf tissue. ICSB 338 (drought susceptible) and SA 1441 (drought tolerant) sorghum plants were exposed to drought by withholding water for 12 days. The leaf samples were harvested at the indicated time points and gene expression analysis was performed using RT-qPCR. Control plants were maintained at field capacity. Bars represent mean ± SE (n = 3). *, ** and *** = significance at $p \leq 0.05$, 0.01 and 0,001, respectively.

4.5 Discussion

Plants continuously synthesise proteins to maintain growth and development processes. When exposed to drought, stress response genes are activated which trigger a network of molecular responses in a bid to restore homeostasis and adapt to the imposed stress. In this study, a comparative root proteomic analysis of two sorghum varieties was conducted. The varieties used, ICSB 338 and SA 1441, had contrasting phenotypic traits to drought. ICSB 338 is drought susceptible while SA 1441 is drought tolerant. These varieties were used to identify changes in the total soluble protein profiles of roots following an 8-day drought stress treatment using iTRAQ analysis. This was followed by qRT-PCR analysis of 9 drought stress responsive target genes. Roots are important in that they are responsible for the primary perception of soil water deficits and subsequent signalling processes toward the shoots. This set of events results in the regulation of gene expression and subsequent modulation of drought stress response pathways (Ghatak *et al*., 2016). Fewer studies on root proteome profiles under drought stress have been performed on C_4 perennial grasses (Zhao *et al*., 2011), soybean (Mathesius *et al*., 2011), and tomato (Zhou *et al*., 2013). There has been no report on comparative sorghum root proteomics thus making this study relevant. This study also focuses on sorghum because it is an important naturally drought tolerant cereal crop with a wide genetic diversity.

A total of 237 and 184 unique root proteins were identified as drought responsive for ICSB 338 and SA 1441, respectively (Table 4.1 and 4.2). Of the iTRAQ identified drought responsive root protein, 76% and 72% were uncharacterised in ICSB 338 and SA 1441, respectively (Table 4.1 and 4.2). Uncharacterised proteins that are responsive to stress may be important is that they may possess relevant function, which can only be assessed through further experimentation via gene and protein function validation studies. It is therefore important to extend proteomics and genomics studies on sorghum under environmental

stresses. The drought responsive proteins were classified into functional groups on the basis of gene ontology, domain and protein family data obtained from the UniProt and InterPro databases.

In response to stress, plants recruit a network of pathways involved in energy and carbohydrate metabolism (Zadražnik *et al*., 2013). Energy is vital in plant growth and developmental processes. In this study, the expression of energy and metabolism proteins was altered by drought stress for both sorghum varieties. The main pathways affected by drought stress in ICSB 338 under the energy functional group were glycolysis, gluconeogenesis and the electron transport chain (Table 4.1). For SA 1441, the tricarboxylic acid (TCA) as well as glycolytic and the electron transport chain proteins were differentially expressed (Table 4.2) in response to the drought stress.

Glycolysis is responsible for converting glucose into pyruvate liberating ATP and NADH. Under drought stress, the glycolysis-related proteins were down-regulated for both sorghum varieties. Gluconeogenesis proteins, which are involved in the generation of glucose from substrates of a non-carbon origin, were down-regulated as well in ICSB 338 in this study. This is in agreement with Zhou *et al*. (2013), who reported the down-regulation of glycolytic and gluconeogenesis proteins in tomato root tissue under drought stress. A down-regulation of glycolytic proteins was also observed in wild wheat (*Triticum boeoticum*) root tissue in response to drought stress (Liu *et al*., 2015). Zhao *et al*. (2011) and Mathesius *et al*. (2011) also reported an up-regulation of glycolysis proteins in *Cynodon sp* and soybean (*Glycine max*) root tissue under drought stress, respectively. The results may suggest that sorghum or specifically sorghum root tissue conserves energy more efficiently in response to drought stress through reduced glucose catabolism.

The up-regulation of the drought responsive electron chain transport proteins was observed for both sorghum varieties in this study. The electron chain transport system is important for the generation of energy in the form of ATP. The TCA related proteins in the drought susceptible sorghum variety ICSB 338 were down-regulated. The TCA cycle is the primary driver of cellular respiration, which results in energy production through oxidative phosphorylation when the reduced NAD and FAD are fed in the electron transport chain (Stern *et al*., 2000). In this study, TCA related proteins were down-regulated in SA 1441 possibly as a way of limiting energy production under drought stress conditions.

As indicated in Figure 4.9, 25% and 21% of the drought responsive ICSB 338 and SA 1441 proteins respectively, were involved in metabolism. Of these, 13% and 24% are involved in carbohydrate metabolic processes for ICSB 338 and SA 1441 sorghum varieties, respectively. All these proteins were up-regulated. The up-regulation of carbohydrate metabolism proteins suggests that sorghum plants require a certain level of energy to fuel defence mechanisms and cellular repair in the root tissue in response to drought stress. The other up-regulated proteins for SA 1441 include those involved in glutathione, malate and protein metabolic processes. Lipoxygenase and other proteins involved in lipid metabolism were down-regulated for both sorghum varieties except ICSB 338 protein no. 111 which is an uncharacterised protein. The main functions of lipids in plants include membrane synthesis and energy storage. Of interest is the down-regulation of patatin, in both sorghum varieties in response to the drought stress. Papatin is a storage protein and also responsible for lipid catabolism (Andrews *et al*., 1988). Its down-regulation could be a mechanism for conserving cellular energy stores.

A total of 61 (26%) and 42 (23%) drought responsive proteins were disease and defence related for ICSB 338 and SA 1441 sorghum varieties, respectively (Figure 4.9). These proteins can further be classified into programmed cell death (PCD), redox homeostasis, and

molecular chaperones related proteins. Programmed cell death is an important component of defence (Lam, 2004), as it is selective and inactivates less useful cells and tissues in preference to life sustaining ones (Reape *et al*., 2008). Under PCD, the ubiquinone-6 biosynthetic process putative protein was up-regulated whilst the ubiquitin activating enzyme was down-regulated in SA 1441. Ubiquitin is responsible for tagging proteins for degradation prior to cellular repair (Gray and Estelle, 2000). A previous study of the grass *Sporobolus stapfianus* associated ubiquitin with desiccation tolerance mostly in the signalling processes and cellular protection and repair mechanisms (O'Mahony and Oliver, 1999). The down-regulation of the ubiquitin activating enzyme in this study may be due to the ability of the sorghum plant to limit cellular damage under drought stress. This would therefore result in less need of protein degradation for cellular repair processes. Zhou *et al*. (2013) observed that ubiquitin was induced only in drought tolerant tomato plants in comparison to the drought susceptible variety.

Drought stress disrupts cellular redox homeostasis resulting in excessive ROS accumulation (Mittler, 2002). This results in damage of cellular components. The production of antioxidant enzymes by plants acts as the main mechanism in the restoration of redox homeostasis. In this study, peroxidase enzymes, mainly responsible for the hydrogen peroxide catabolic process were highly represented in the disease and defence functional category for both sorghum varieties. For ICSB 338, some of the peroxidases were up-regulated (protein no. 173, 232, 235, 794) whilst others were down-regulated (protein no. 95, 148, 446, 708). On the other hand, only one peroxidase enzyme was down-regulated for SA 1441 (protein no.66) whilst the rest were up-regulated (protein no. 38, 97,130, 159, 187, 207, 287, 307, 437, 622, 641, 779). The up-regulation of peroxidases in response to abiotic stress was also reported in sorghum under salt stress (Swami *et al*., 2011). These results suggest that under drought

stress, the drought tolerant SA 1441 is able to synthesise more peroxidases to reduce cellular damage by ROS compared to the drought susceptible variety ICSB 338.

Heat shock proteins are known to be highly responsive to drought stress. In this study, one uncharacterised protein in the HSP20-like chaperone superfamily was up-regulated in both ICSB 338 (protein no. 214) and SA 1441 (protein no. 273) (Table 4.1 and 4.2). For SA 1441, the characterised small heat shock-like protein was up-regulated as well (protein no. 972). The up-regulation of the small heat shock proteins may play a role in preventing protein denaturation in response to stress thus improving the tolerance of sorghum to drought stress. Two uncharacterised proteins, which belong to the ricin-B like lectin family were assigned to the disease and defence functional category in ICSB 338. Lectins have been previously demonstrated to be responsive to abiotic stress in rice exposed to salt stress (Zhang *et al*., 2000). Lectins are carbohydrate binding proteins that agglutinate cells and glycoconjugates (Goldstein, 1980). One of their functions is defence against biotic and abiotic stresses (Etzler, 1986). In this study, the lectins were up-regulated in ICSB 338 possibly as a defence mechanism against drought stress.

Uricase is involved in liberating the much needed nitrogen to plants (Damsz *et al*., 1994; Capote-Mainez and Sánchez, 1997). The presence of different types of uricase enzymes has been previously established in roots of maize and tobacco (Theimer and Beevers, 1971). In this study, there was a down-regulation of this protein in ICSB 338. This could be for limiting the amount of nitrogen available to the plant as the plant lowers its metabolic activities in response to drought stress.

Pathogenesis related proteins are defined as proteins that are induced in plant defence against pathogens (Van Loon *et al*., 1994). The pathogenesis related protein 10b was down-regulated in ICSB 338 but up-regulated in SA 1441. This suggests that the drought tolerant sorghum

variety triggers a wide range of stress responses as an adaptive mechanism to increase chances of survival. Kim *et al*. (2014) also showed that pathogenesis related proteins were up-regulated in maize under drought stress. In another study, Mirzaei *et al*. (2011) demonstrated that pathogenesis-related proteins were generally increased in rice root tissue exposed to drought stress. Since their discovery, dirigent proteins have been shown to be involved in lignin biosynthesis through phenoxy-radical coupling (Davin and Lewis, 2000). In this study, dirigent proteins were differentially expressed and up-regulated in both sorghum varieties. This is essential in plants in maintaining cell wall integrity (Paniagua *et al*., 2017). LEA proteins function as cellular protectants under water loss (Chakrabortee *et al*., 2007). The LEA3 was up-regulated in SA 1441 in response to drought stress. This is in agreement with Xu *et al*. (1996), where the expression of LEA proteins in rice plants conferred both water and salinity stress tolerance. The LEA proteins were however, not identified in ICSB 338 in the current study.

Drought stress can repress protein synthesis (Good and Zaplachinski, 1994). A reduction in protein synthesis in response to heat (Duncan and Hershey, 1989) and drought (Good and Zaplachinski, 1994) stresses has been reported. In this study, all the characterised proteins involved in protein synthesis, that is, 60S ribosomal protein L13, 60S ribosomal protein L36, 40S ribosomal protein S6 and ribosomal protein L19 were down-regulated in ICSB 338 (Table 4.1). However, in SA 1441, the elongation factor 1-alpha was down-regulated whereas the 40S ribosomal protein S3a was up-regulated (Table 4.2). All the remaining proteins were uncharacterised and mainly predicted to be involved in translation and ribosome biogenesis and organisation.

The presence of protein destination and storage proteins in high abundance could signify protein mobility both within the cell and across the cell wall into the extracellular matrix.

Protein movement is also vital in cell-cell communication and signal transduction (O'Connor *et al*., 2010). Proteins involved in protein catabolic processes dominated the protein destination and storage functional group with 75% of the identified proteins being involved in proteolysis for ICSB 338 and 53% of these being up-regulated (Table 4.1).

The up-regulated proteolysis related proteins for ICSB 338 were uncharacterised proteins, but predicted to be involved in serine-type endopeptidase, dipeptidyl-peptidase, cysteine-type endopeptidase and aspartic type endopeptidase activities. On the other hand, only 33% of the proteins assigned to the protein destination and storage functional group were involved in proteolysis for SA 1441 with only the cysteine type endopeptidase being up-regulated (Table 4.2). These results are in agreement with Good and Zaplachinski (1994), who attributed the reduced protein synthesis in response to drought in oilseed rape (*Brassica napus*) to high protease activity and the enhanced synthesis of stress adaptive proteins at the expense of other proteins. The other protein destination and storage uncharacterised proteins in ICSB 338 and SA 1441 were involved in chaperone-mediated protein folding although all of them were down-regulated. Proteases, involved in the degradation of unfolded proteins were up-regulated, possibly to maintain homeostasis through the release of amino acids for recycling (Zou *et al*., 2011).

The initial perceived water deficits resulting from drought stress must be transmitted within the plant by signalling molecules. This occurs as a result of a process termed signal transduction. The transmission of signals to cellular machinery consequently triggers various signalling processes and transcription controls, which maintain homeostasis by activating adaptive stress responsive processes (Xiong and Zhu, 2001). These processes are directed towards cellular membrane and protein repair. In this study, purple acid phosphatase, which is involved in protein-protein interactions resulting in stress perception was down-regulated

in SA 1441 (Table 4.2). The other drought responsive proteins identified under this functional category for both sorghum varieties were mainly kinases and phosphatase activity proteins. Protein kinases and phosphatases are thought to be responsive to environmental stresses (Hardie, 1999). Membrane receptors receive signals and utilise receptor-coupled protein phosphorylation signalling modes resulting in a wide range of cellular processes including enzyme activation and protein degradation (Xiong and Zhu, 2001). It is however unclear why the purple acid phosphatase was down-regulated.

Cell structure related proteins play an important role in cell shape organisation and cellular signalling and have been reported to undergo rigorous changes when under abiotic stress (Abdrakhamanova *et al*., 2003). In this study, chitinase-B, involved in the chitin catabolic process, was up-regulated in ICSB 338 but absent in SA 1441. In drought stressed rice root tissue, chitinases were increased in response to drought stress (Mirzaei *et al*., 2011). The tubulin beta chain was down-regulated in SA 1441 but absent in ICSB 338. An up-regulation of profilin was observed in SA 1441 but absent in ICSB 338. Profilin is an important cell component that plays a role in actin microfilament growth both spatially and temporally resulting in cell shape alterations and locomotion (Gunning *et al*., 2015). In another study, actin was up-regulated in response to drought stress in Kentucky bluegrass in response to drought stress (Xu and Huang, 2010). The result of this study suggests that ICSB 338 may be unable to organise its cell cytoskeleton efficiently under drought stress resulting in its inability to confer drought tolerance compared to SA 1441.

Other proteins identified are those involved in transport and transcription. The mitochondrial protein carriers were up-regulated in ICSB 338. The rest of the differentially expressed proteins in this category were uncharacterised. The histone and nascent polypeptide-associated complex subunit beta proteins involved in chromatin silencing and regulation of

transcription, respectively were up-regulated in SA 1441. This suggests that drought stress was regulated at the transcription level in the drought tolerant sorghum variety.

Following the proteomic analysis, gene expression analysis of the eight targets with the largest fold changes selected from both ICSB 338 and SA 1441 was performed. RNA degradation was observed at 12 days in the leaf tissue of both sorghum varieties at 12 days of drought stress (Figure 4.11) possibly due to the observed leaf chlorosis. For the root tissue, ICSB 338 showed similar RNA degradation result on day 12 whilst in SA 1441 the RNA remained intact throughout the duration of the experiment. Despite the non-specific binding, the eight genes were used because the melt curves showed the presence of specific PCR product (Appendix, Figure C7, C8 and C9). Significant differences in expression profiles was noted between ICSB 338 and SA 1441 root and leaf tissue in all genes except *SORBI_3003G136200* in leaf tissue (Figures 4.13 and 4.14). The differential expression of the genes in the two sorghum varieties with contrasting responses to drought stress suggests that these genes can differentiate respective drought tolerance levels of the sorghum varieties. The gene expression levels were much higher in leaf tissue compared to root tissue for all of the genes analysed. The SA 1441 leaf tissue had an up-regulation of the genes starting at 8 days. The expression levels of most of these sorghum genes peaked at 12 days of drought stress, which could indicate a delayed drought stress response in aerial parts of the plant. This could be an advantage to the sorghum plants since an early response in mild drought stress unnecessarily consumes energy.

In conclusion, the two sorghum varieties showed different protein profiles for most of the assigned functional groups. This may be due to the differences in response mechanisms between the two sorghum varieties in response to drought stress. The results indicate that the drought tolerant variety SA 1441 expressed proteins aimed at establishing stability and also

conferring adaptive responses to drought stress to ensure continued function and survival in comparison to the drought susceptible ICSB 338. In addition, a greater proportion of the differentially expressed proteins were uncharacterised. As such, further experiments are recommended for the characterisation of these proteins since they may possess novel drought stress adaptive characteristics important to cereal crops. The gene expression analysis also validated the drought responsiveness of the protein targets selected from the two sorghum varieties. This suggests that the genes could be potentially utilised in developing drought markers for use in selecting drought tolerant varieties in plant breeding programs.

CHAPTER 5

DEVELOPING MOLECULAR MARKERS FOR DROUGHT TOLERANCE

5.1 Introduction

Classical plant breeding involves crossing closely or distantly related species in an effort to create variability and produce plants with desirable traits (Acquaah, 2012). Variability forms the basis for plant breeding (Messmer *et al*., 2015). In order to identify new traits, large populations of diverse germplasm are continuously crossed over several generations to achieve a certain combination of alleles (Poehlman *et al*., 1995). This is followed by screening of the progeny to identify individuals with the desired trait. This process is carried out in the field over several years. Thereafter, the plants with the desirable trait are crossbred to introduce the new trait into a widely accepted variety. Generations of backcrossing would then be performed to maintain the characteristics of the widely accepted variety (Acquaah, 2012).

As the duration and cost of the selection process is high, it is desirable to develop molecular markers which can assist in screening for a particular trait at the seedling stage to increase the efficiency and effectiveness of the process (Acquaah, 2012). Genes that would serve as high-fidelity molecular markers should have their expression tightly linked to the phenotype (Yang *et al*., 2015a). In the case of drought, the progeny of genetic crosses can be germinated in the confines of growth rooms or greenhouses and gene expression evaluated at the seedling stage. Only plants that pass the screen test will be transferred to the field to produce seed. This expedites the breeding program by reducing the space, time, water, agrochemical, and labour required to identify new crop varieties with desirable traits (Messmer *et al*., 2015).

Overall, this project aimed to develop a toolkit of drought marker genes to rapidly screen plants for drought tolerance at an early developmental stage. The objective of this chapter was to explore the utility of genes, identified in Chapter 4 and by Ngara *et al*. (2018), as putative marker genes for use as a screening tool in breeding platforms developing drought-tolerant crops.

5.2 Drought Marker Gene Expression in ICSB 338 and White Sorghum

Compared to other cereals, sorghum is highly drought tolerant, maintaining its yield potential under severe drought conditions. However, different sorghum varieties have different levels of drought tolerance, which can be physiologically distinguished (Chapter 3). The eight drought-responsive sorghum genes identified in Chapter 4 (Section 4.4) have already been shown to be differentially expressed between ICSB 338 and SA 1441 sorghum varieties (Figures 4.13 and 4.14). Expression of the same genes was then evaluated in another sorghum variety, White sorghum, relative to the ICSB 338 using cell suspension cultures developed by our research group (Ramulifho, 2017). Total RNA was extracted from ICSB 338 and White sorghum cell cultures grown under optimal conditions and analysis of gene expression was performed using real-time quantitative polymerase chain reaction (qRT-PCR).

According to the results, six genes, namely *SORBI_3001G514200, SORBI_3003G136200, SORBI_3007G149600, SORBI_3001G313200, SORBI_3001G073900* and *SORBI_3003G322400,* showed significant differences between the two sorghum varieties (Figure 5.1). Of these differentially expressed genes, *SORBI_3001G313200* and *SORBI_3001G073900* exhibited the highest difference in fold-change between White sorghum and ICSB 338 cell suspension cultures. *SORBI_3001G514200* and *SORBI_3003G322400* showed higher gene expression in White sorghum whilst the remaining 5 genes showed the opposite. Due to time constraints, physiological experiments to

verify this in whole plants could not be conducted within the PhD project. All the nine genes also showed significant differences between the two sorghum varieties in response to sorbitol-induced osmotic stress on at least one time point in a 72-hr time-course experiment (Appendix, Figure B1).

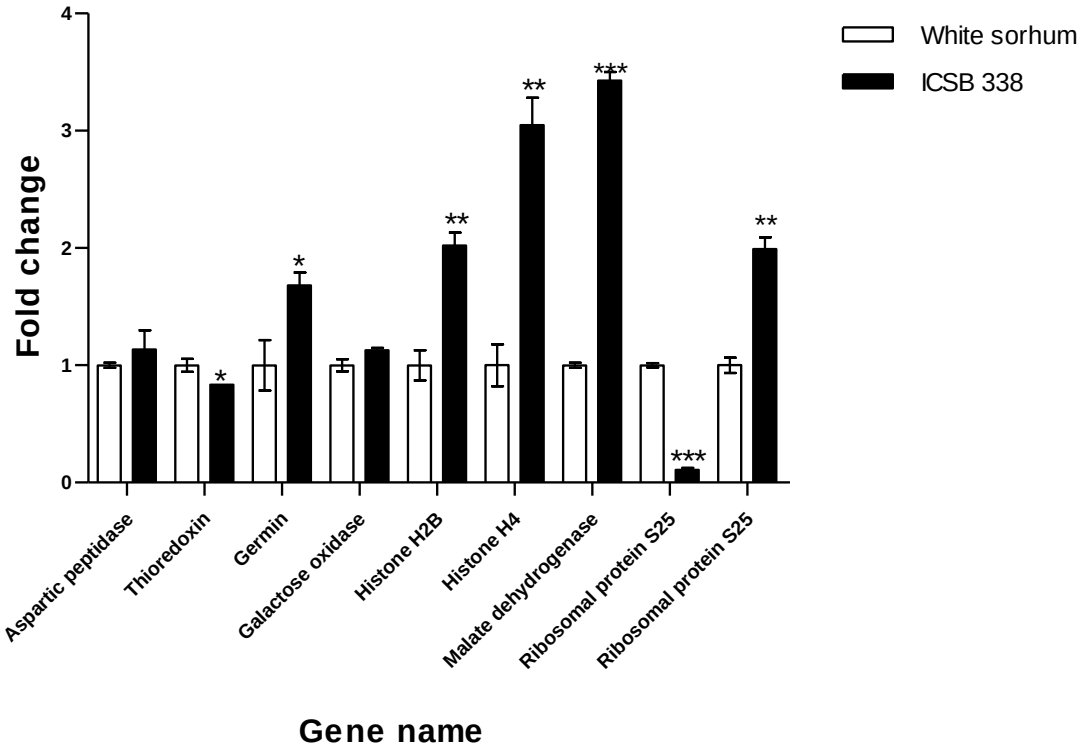

Figure 5.1: Gene expression in ICSB 338 and White sorghum cell cultures without osmotic stress. Gene identities are *SORBI_3008G134700* (Aspartic peptidase), *SORBI_3001G514200* (Thioredoxin), *SORBI_3002G217200* (Peptidase), *SORBI_3003G136200* (Germin), *SORBI_3006G135500* (Galactose oxidase), *SORBI_3007G149600* (Histone H2B), *SORBI_3001G313200* (Histone H4), *SORBI_3001G073900* (Malate dehydrogenase), *SORBI_3003G322400* (Ribosomal protein S25) and *SORBI_3002G049300* (Ribosomal protein S25) Gene expression analysis was performed using qRT-PCR. Bars represent mean ± SE (n = 3). *, ** and *** represent a significant difference between means at $p \leq 0.05$, 0.01, and 0.001, respectively.

Overall, the gene expression results (Figure 5.1 and Appendix, Figure B1) showed that the drought-responsive genes can be used to distinguish between two sorghum varieties, even in cell suspension cultures either with or without osmotic stress. Therefore, at least four of the genes (*SORBI_3003G136200, SORBI_3007G149600, SORBI_3001G313200,* and *SORBI_3001G073900)* can be possibly incorporated into a screen to identify sorghum seedlings likely to have better drought tolerance.

5.3 Heat Stress Activates Drought-Responsive Genes

Drought stress is inseparably associated with heat stress in most agro-ecological zones of sub-Sahara Africa. This raises the possibility that drought-responsive genes may also be responsive to temperature. Therefore, the effects of temperature on the expression of the nine sorghum drought responsive genes (Chapter 4, Section 4.4) were evaluated. White sorghum cell suspension cultures (Ngara *et al*., 2008; Ramulifho, 2017) were grown at either 22°C or 30°C for 8 days and cells harvested for RNA extraction. Gene expression analysis was conducted on the nine drought-responsive genes and sorghum homologues of Arabidopsis *DREB2A* and *ERD1* drought markergenes - *SbDREB2A-1* (*SORBI_3009G101400*), *SbERD1-1* (*SORBI_3004G162400*) and *SbERD1-2* (*SORBI_3006G065100*). Expression of all the genes was significantly different between the two temperatures, indicating that the genes were responsive to heat (Figure 5.2). All the genes were activated in response to heat except for *SORBI_3002G049300* (Figure 5.2), which was down-regulated. The nine sorghum genes except *SORBI_3002G049300* exhibited the same up-regulation expression trend as the three drought marker genes. Of all the genes evaluated *SORBI_3003G322400* showed the greatest gene expression. Overall, the results show that the majority of drought-responsive genes are triggered by heat stress as well.

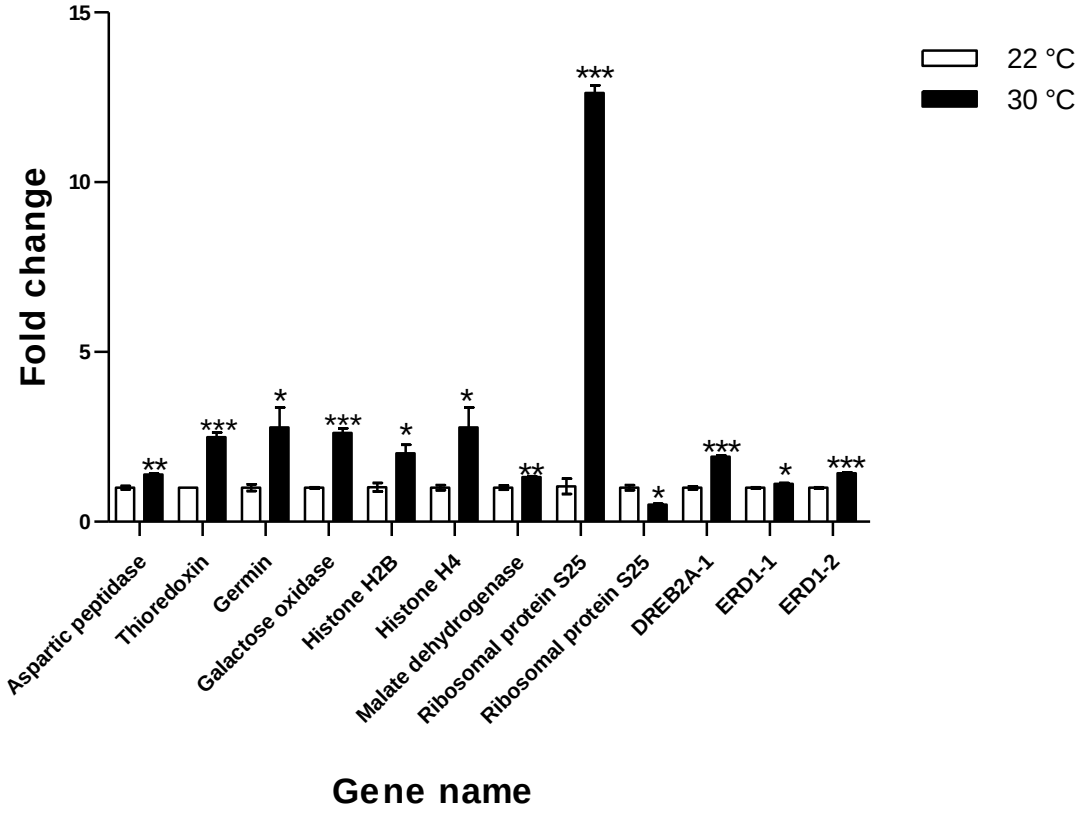

Figure 5.2: Drought-responsive genes [*SORBI_3008G134700* (Aspartic peptidase), *SORBI_3001G514200* (Thioredoxin), *SORBI_3002G217200* (Peptidase), *SORBI_3003G136200* (Germin), *SORBI_3006G135500* (Galactose oxidase), *SORBI_3007G149600* (Histone H2B), *SORBI_3001G313200* (Histone H4), *SORBI_3001G073900* (Malate dehydrogenase), *SORBI_3003G322400* (Ribosomal protein S25) and *SORBI_3002G049300* (Ribosomal protein S25)] are also responsive to high temperature. White sorghum cell cultures were grown at 22°C or 30°C and harvested 4 days later for RNA extraction. Gene expression analysis was performed using qRT-PCR. Bars represent mean ± SE (n = 3). *, ** and *** = a significant difference between means at $p \leq 0.05$, 0.01 and 0.001, respectively.

5.4: Identifying Homologues of Sorghum Drought Marker Genes in a Different Species

Because sorghum is a naturally drought tolerant crop, breeding platforms for drought tolerance tend to target other drought-sensitive crops, such as maize (*Zea mays*) and rice (*Oryza sativa*). Thus, the knowledge obtained from sorghum has to be transferred to other

species to improve their drought tolerance through classical breeding platforms or genetic engineering. To explore how this might be achieved, three sorghum drought genes previously identified by the Ngara and Chivasa research groups (Ngara *et al*., 2018) were selected for proof-of-concept using Arabidopsis (*Arabidopsis thaliana*). These are thioredoxin (*SORBI_3009G190800*), peptidase (*SORBI_3007G172100*) and xyloglucanase (*SORBI_3002G302000*). These genes are also responsive to sorbitol-induced osmotic stress in sorghum cell cultures and they are differentially expressed in ICSB 338 and SA 1441 sorghum plants exposed to drought stress (Ngara *et al*., 2018).

Putative Arabidopsis homologues of these genes were identified in the Arabidopsis Information Resource (TAIR) database (www.arabidopsis.org/Blast) using the sorghum protein sequences as bait in BLAST searches. It became clear that the equivalent gene families in Arabidopsis are very large, each consisting of over 50 genes (Appendix, Table B1). The top four hits per gene family were selected for further gene expression analysis.

Four-day-old Arabidopsis cell suspension cultures grown separately in continuous darkness or in a 16 hr-photoperiod were treated with 0.4 M sorbitol and samples for RNA extraction were collected at 0, 6, 24, 48 and 72 hrs (Section 2.1.2). The light and dark growth conditions were used to check if there are difference in gene expression under these conditions. The RNA was extracted and separated by electrophoresis in a 1.2% agarose gel. RNA of good integrity was obtained (Figure 5.3). This was followed by cDNA synthesis and standard PCR to assess the specificity of primers (Table 2.4) designed to amplify fragments of the target Arabidopsis genes. Primers that did not yield a product (*CEP2* and *XTH28*) were excluded from the study (Figure 5.4). Consequently, qRT-PCR was used to investigate the response of the selected Arabidopsis genes to osmotic stress using the eukaryotic Initiation Factor 4A (eIF4A) and Actin 2 as reference control genes.

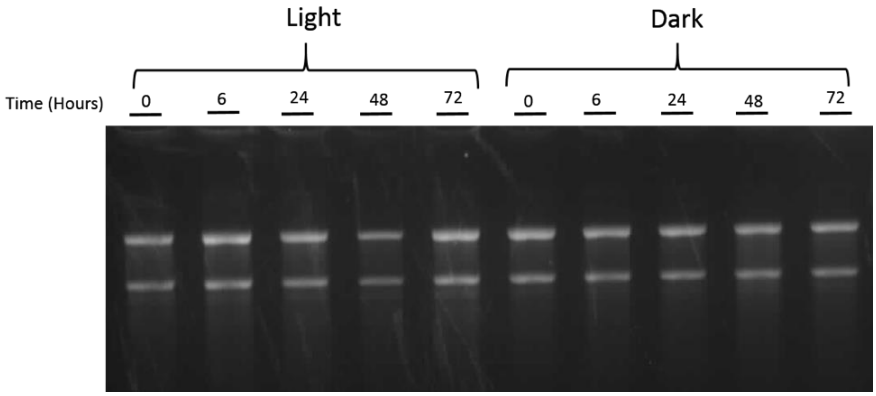

Figure 5.3: Arabidopsis RNA gel. Arabidopsis cells grown in total darkness (dark) or a 16 hr-photoperiod (light) were treated with 0.4 M sorbitol for the indicated time prior to harvesting and RNA extraction. Approximately 300 ng of RNA from each sample were separated in a 1.2% agarose gel.

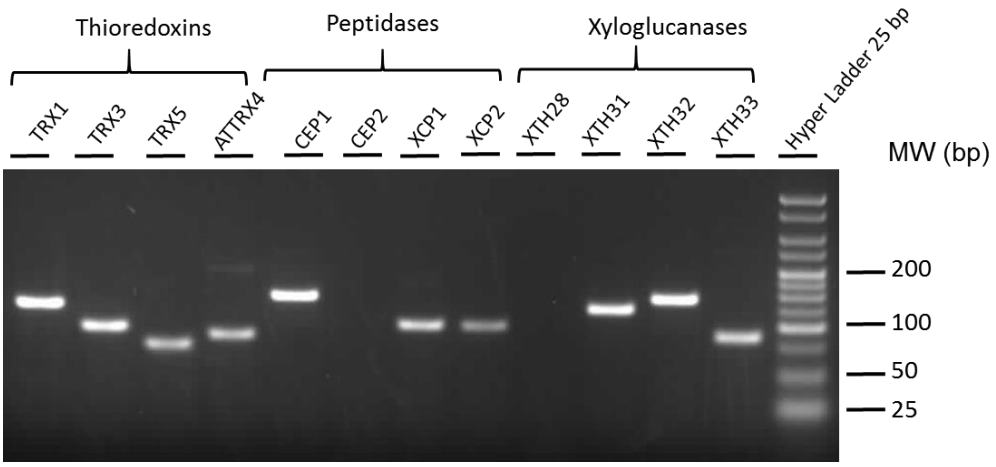

Figure 5.4: PCR-amplification of fragments of Arabidopsis genes. Arabidopsis cDNA was used as template to PCR-amplify the indicated genes to test the specificity of the primers. The PCR products were separated in a 3.5% agarose gel. The lane on the extreme right contain the HyperLadder™ 25 bp DNA marker.

5.4.1: Responses of Arabidopsis Thioredoxin Homologues to Sorbitol

A total of four Arabidopsis homologues of the sorghum thioredoxin gene with the highest sequence similarity were obtained from the TAIR database. The homologues were denoted *TRX1* (*AT3G51030.1*), *TRX3* (*AT5G42980.1*), *TRX5* (*AT1G45145.1*) and *ATTRX4* (*AT1G19730.1*). In cell cultures maintained in light, *TRX1* was suppressed from 6 hrs to 24 hrs followed by activation at 48 and 72 hrs (Figure 5.5). *TRX5* on the other hand exhibited gene activation at 6 hrs followed by suppression until the 72 hr time-point. *TRX3* was up-regulated only at 6 hrs whilst for *ATTRX4* there was gene activation at both 6 and 24 hrs. The cell cultures maintained in the dark also exhibited more or less the same trends as those

maintained in light (Figure 5.5). This shows that Arabidopsis thioredoxin homologues exhibited unique responses to osmotic stress.

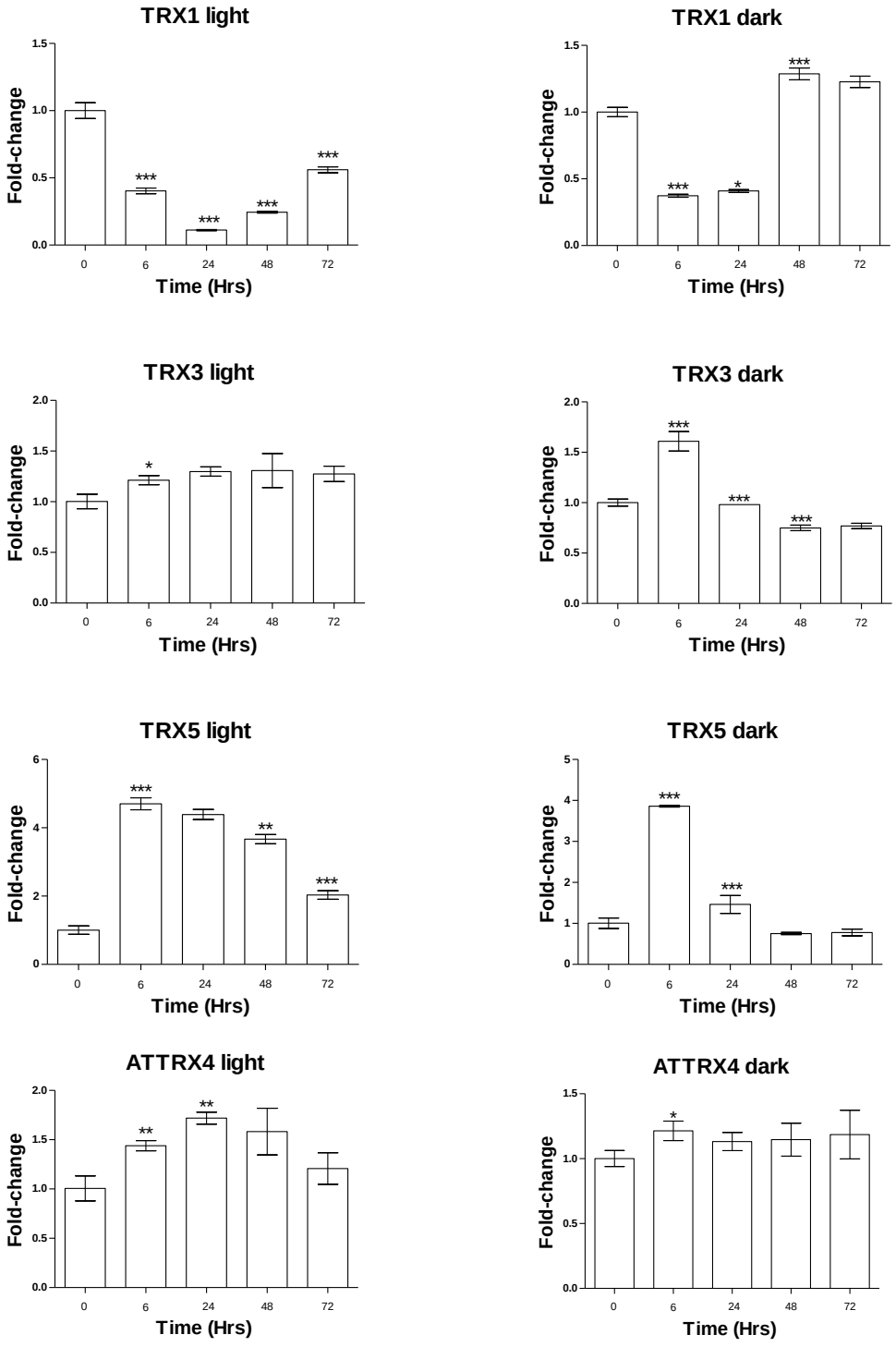

Figure 5.5: The transcriptional response of Arabidopsis thioredoxin genes to sorbitol. Arabidopsis cell suspension cultures were treated with 0.4 M sorbitol and samples for RNA extraction harvested at the indicated time-points. Gene expression analysis was conducted via qRT-PCR. Bars represent mean ± SE (n = 3). *, ** and *** = a significant difference between means at $p \leq 0.05$, 0.01 and 0.001, respectively.

5.4.2: Responses of Arabidopsis Peptidase Homologues to Sorbitol

Three Arabidopsis peptidase homologues from which RT-PCR amplified a product (Figure 5.4) were used for subsequent gene expression analysis. *CEP2* (*AT3G48340.1*) was excluded as the primers failed to yield a PCR product (Figure 5.4). In cell suspension cultures maintained in light, all the Arabidopsis peptidase homologues *CEP1* (*AT5G50260.1*), *XCP1* (*AT4G36880.1*) and *XCP2* (*AT1G20850.1*) showed an initial gene activation at 6 hrs followed by different expression patterns (Figure 5.6). *XCP1* gradually declined, while that of *CEP1* and *XCP2* dipped and 24 hrs before being re-activated again. This again is shows that gene expression of the homologues is generally different to one another. The general trends of gene expression in cell cultures maintained in light and dark conditions were similar except for *CEP1*. This gene exhibited a general gradual activation in light conditions with suppression under dark conditions (Figure 5.6).

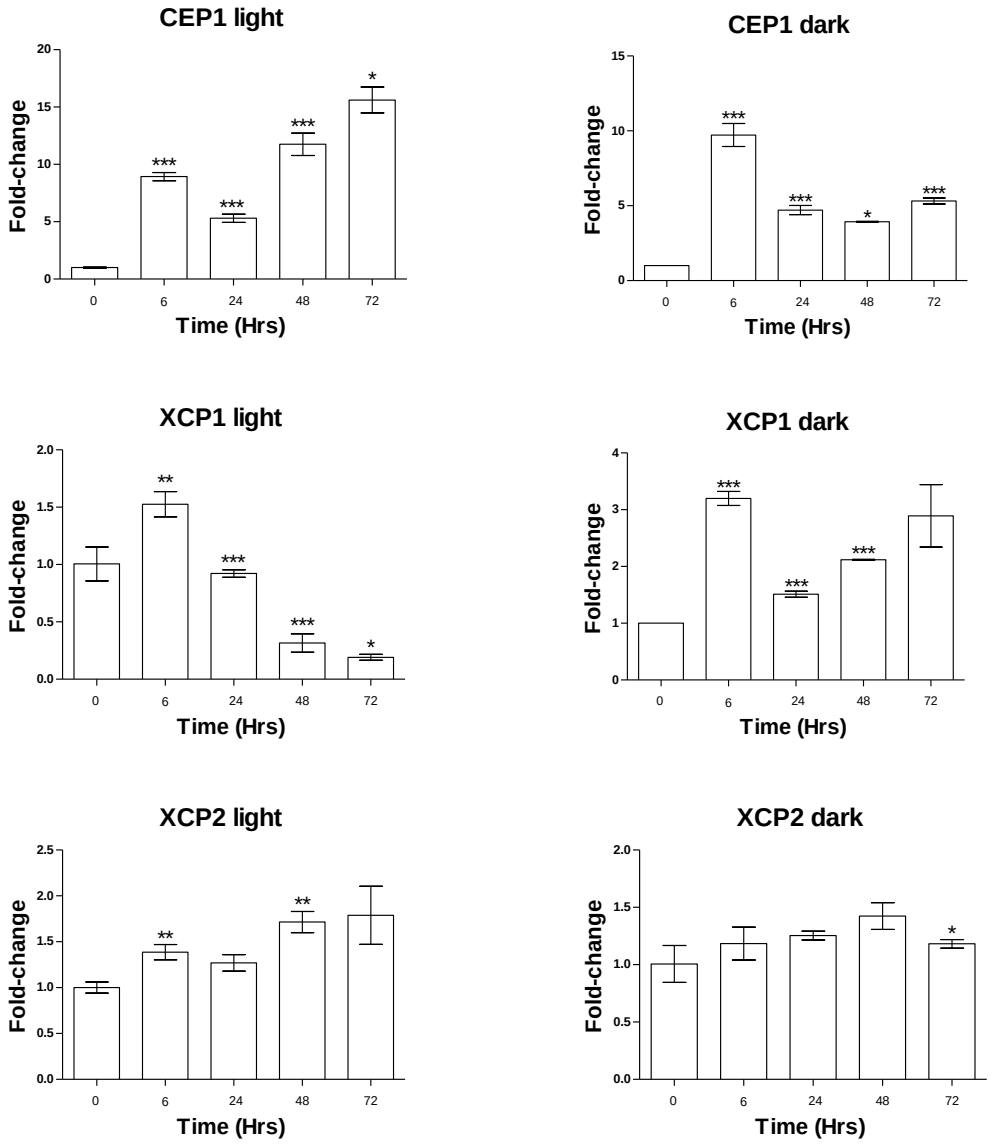

Figure 5.6: The transcriptional response of Arabidopsis peptidase genes to sorbitol. Arabidopsis cell suspension cultures were treated with 0.4 M sorbitol and samples for RNA extraction harvested at the indicated time-points. Gene expression analysis was conducted via qRT-PCR. Bars represent mean ± SE (n = 3). *, ** and *** = a significant difference between means at $p \leq 0.05$, 0.01 and 0.001, respectively.

5.4.3: Response of Arabidopsis Xyloglucanase Homologues to Sorbitol

A total of three Arabidopsis xyloglucanase homologues - *XTH31* (*AT3G44990.1*), *XTH32* (*AT2G36870.1*) and *XTH33* (*AT1G10550.1)* were successfully PCR-amplified (Figure 5.4). However PCR-amplifaction of *XTH28* (*AT1G14720.1*) failed. In Arabidopsis cell suspension cultures maintained in light conditions, *XTH31* & *XTH32* had gene activation peaking at 48 and 24 hrs, respectively, while *XTH33* was generally suppressed throughout the time-course (Figure 5.7). A comparison between the gene expression of cell cultures maintained in light and dark conditions showed generally different expression trends for all the genes.

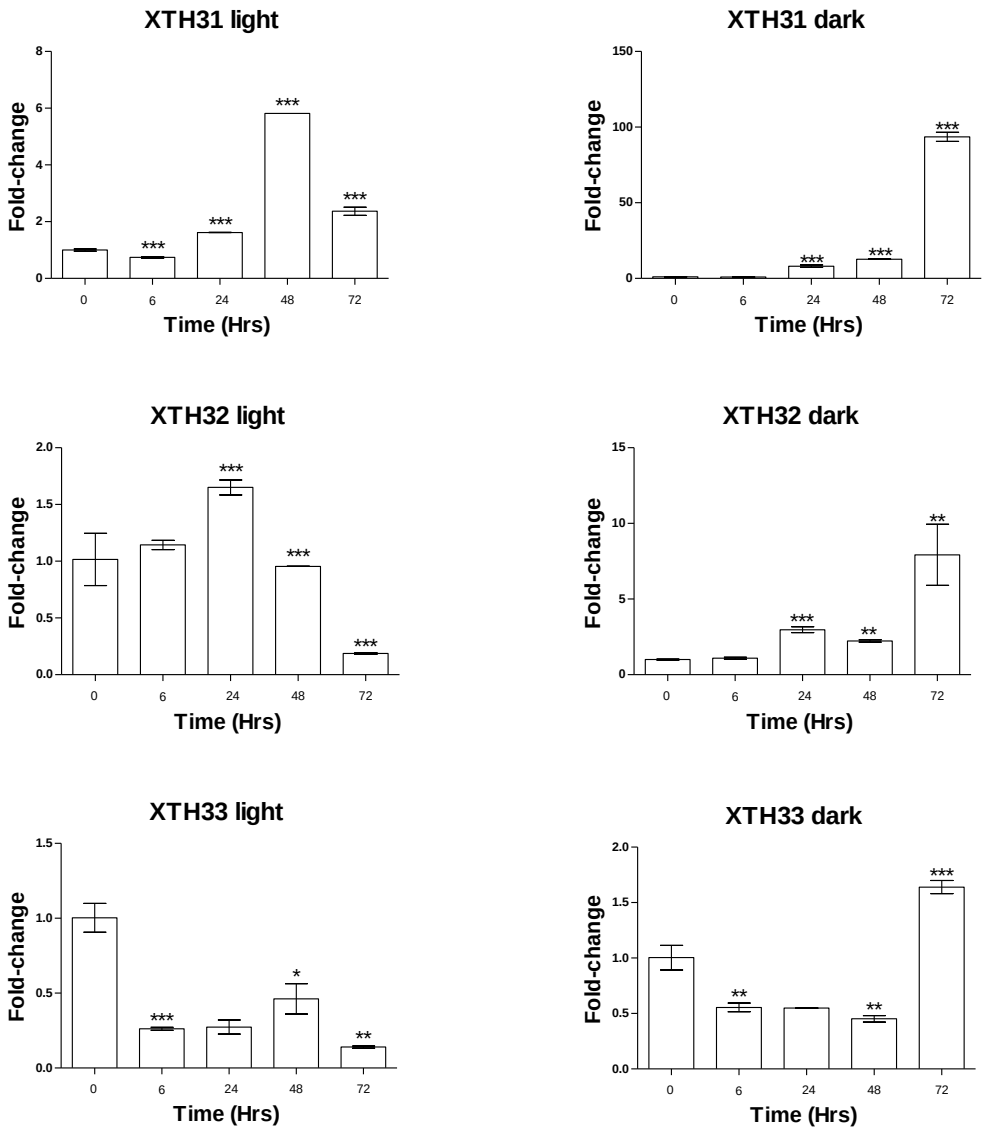

Figure 5.7: The transcriptional response of Arabidopsis xyloglucanase genes to sorbitol. Arabidopsis cell suspension cultures were treated with 0.4 M sorbitol and samples for RNA extraction harvested at the indicated time-points. Gene expression analysis was conducted via RT-qPCR. Bars represent mean ± SE (n = 3). *, ** and *** = a significant difference between means at $p \leq 0.05$, 0.01 and 0.001 respectively.

Overall, these results show that Arabidopsis homologues of sorghum drought genes can be identified through database searches and that at least some of these similarly respond to osmotic stress-simulated drought.

5.5 Discussion

Marker assisted selection (MAS) refers to any selection system that depends on the selection of desired traits through markers linked to them (Eckenstorfer *et al*., 2014). This selection system is more reliable than the traditional visual phenotypic assessment and selection done in classical plant breeding (Eckenstorfer *et al*., 2014). This is because molecular markers are both tightly associated with the desirable trait and also highly heritable (Bernardo, 2002). In addition, molecular markers are not affected by environmental factors or plant developmental stages (Winter and Kahl, 1995), whereas the phenotype changes in response to changing environments. Molecular markers are thus useful in plant breeding as they reduce the duration of the selection process in the classical plant breeding method (Acquaah, 2012).

The development of drought markers requires the identification and validation of drought tolerance phenotype linked genes. Most studies in molecular marker development are focusing on PCR based markers mainly for genetic diversity studies. These include random amplified polymorphic DNA (RAPD), simple sequence repeats (SSRs) and restriction fragment length polymorphism (RFLP). Some of these molecular markers can also be used for determining stress tolerant phenotypes. For example, genetic diversity analyses for drought tolerance have been carried out on sorghum using SSR markers (Rajarajan and Ganeshamurthy, 2011). In the study, the drought tolerant and drought susceptible varieties were grouped into different clusters on a molecular level of genetic diversity using SSR markers.

In the current study, a different approach for the development of drought molecular markers was used. The method involves the identification of the sorghum drought stress responsive proteins (Section 4.3) and validating the expression of corresponding gene under drought conditions (Section 4.4). The proteins were identified in sorghum, a naturally drought tolerant

crop (Rosenow *et al*., 1983). Messmer *et al*. (2015) also suggested the use of protein targets as a reliable method of identifying effective molecular markers. Drought stress responsive genes identified in Chapter 4 as well as three genes from a previous study by Ngara *et al*. (2018) were assessed for their utility as putative drought markers for use as a screening tool on breeding platforms developing drought-tolerant crops. Two sorghum cell suspension cultures systems were used for the proof-of-concept. Expression analysis of the nine genes in the two sorghum cell culture lines indicated that seven of the genes showed significant expression differences between the two sorghum varieties (Figure 5.1; Appendix, Figure B1) and thus could be used to distinguish the cell lines. Although ICSB 338 is a drought susceptible sorghum variety (Table 2.1), the corresponding phenotype of White sorghum is unknown.

The four genes identified in this study (*SORBI_3003G136200, SORBI_3007G149600, SORBI_3001G313200* and *SORBI_3001G073900*) (Figure 5.1) could be incorporated into breeding programs to screen for potentially drought tolerant crop varieties. Other studies have also developed drought marker genes for use in plant breeding. For example, Arabidopsis homologues of the ABA-independent pathway genes, namely, *GmaxRD20A*-like, *GmaxRD22*-like and *GmaxERD1*-like, were analysed under drought stress in soybean root tissue (Neves-Borges *et al*., 2012). The results showed that the three genes were responsive to drought stress. The authors recommended these genes for use as drought markers in soybean.

Heat stress is naturally associated with drought stress, especially in agro-ecological zones like the sub-Saharan Africa. Plant also respond to heat and drought stress using common response mechanisms (Wilkins *et al*., 2016). Furthermore, drought stress responsive genes such as *DREB2A* and *OsMYB55* have been shown to be heat responsive in previous studies (Sakuma *et al.*, 2006; Casaretto *et al*., 2016). Therefore, it is imperative to also evaluate the drought

stress responsive sorghum genes for heat stress response. In this study, eight of the nine drought responsive genes evaluated were also heat responsive (Figure 5.2). Therefore, during MAS, the markers could be used to select for drought and heat tolerant plants.

A gene with a known function in one species is likely to have a homologue with similar function in another plant species (Yang *et al*., 2015a). Homologous genes in other species may have slight differences in gene sequence but have similar protein structure and function supporting the development of molecular markers based on one species and used in another.

In this study, Arabidopsis was used to show the transcriptional responses of homologous genes found in sorghum. Arabidopsis homologues of three sorghum drought responsive genes validated by Ngara *et al*. (2018) were analysed. The results showed at least one homologue was up-regulated in response to simulated drought (Figures 5.5 - 5.7). The use of homologues of a gene with known function in another plant system has been practiced previously in many studies. These include the use of *DREB 1* gene homologues in wheat in a drought stress experiment (Huseynova and Rustamova, 2010). Similar studies were conducted where sorghum homologues of the Arabidopsis sodium proton antiporter (*NHX*) and the human sodium proton exchanger (*NHE*) genes were evaluated under multiple stresses of drought, cold, salt and heat (Kumari *et al*., 2018). The study concluded that the *SbNHX*s and *SbNHE*s were up-regulated by at least one of these stresses.

In a selection process for the identification of drought responsive homologues in another plant, the genes must be evaluated so that the best performing ones under drought stress are advanced to the next stage. These functional homologues would be overexpressed under stress to validate their response. Over-expression analyses have been done previously to confirm gene function (Baima *et al*., 2001; Pontier *et al*., 2001; Fan and Dong, 2002). The

other alternative would be to transfer the gene to the new species to create a transgenic plant with the gene of interest.

In conclusion, four genes (*SORBI_3003G136200, SORBI_3007G149600, SORBI_3001G313200* and *SORBI_3001G073900*) can be used in a classical plant breeding selection process to distinguish between sorghum varieties for drought tolerance (Figure 5.1). A total of eight genes (*SORBI_3008G134700, SORBI_3001G514200, SORBI_3003G136200, SORBI_3006G135500, SORBI_3007G149600, SORBI_3001G313200, SORBI_3001G073900, SORBI_3003G322400*) can also be used to screen sorghum plants for heat tolerance. Furthermore, sorghum homologues can be identified in other agriculturally important crops like maize and analysed for drought tolerance. This would assist plant breeders in MAS for drought tolerance.

CHAPTER 6

GENERAL DISCUSSION, CONCLUSION AND RECOMMEDATIONS

Drought stress is one of the abiotic factors that is detrimental to plant growth and development. As such, it is imperative that studies are carried out to develop crops that are tolerant to drought stress. To achieve this, various studies have utilised plant model systems such as Arabidopsis (*Arabidopsis thaliana*) and rice (*Oryza sativa*) among others. These plants are however, susceptible to drought stress. Sorghum (*Sorghum bicolor*), a naturally drought tolerant crop (Rosenow *et al*., 1983), with a wide genetic diversity (Motlhaodi *et al*., 2017), is also an ideal model system in drought stress studies.

The aim of this research was to evaluate the physiological, biochemical and molecular responses of two sorghum varieties to drought stress with the ultimate goal of working towards the development of drought markers. These drought markers would be vital in the selection of drought tolerant varieties by plant breeders at the seedling stage. The two sorghum varieties used in this study, ICSB 338 and SA 1441, are drought susceptible and drought tolerant, respectively. These phenotypic traits were assigned by plant breeders. However, no published data on their drought tolerance is currently available. This study therefore analysed various growth and physiological parameters in an effort to confirm the drought stress response phenotypes of the two sorghum varieties prior to the proteomic and genomic analyses. This evaluation confirmed that the two sorghum varieties indeed have contrasting responses to drought stress.

Striking differences were observed between the two sorghum varieties for all the growth and physiological parameters evaluated. For example, the chlorophyll content was higher in the drought tolerant variety compared to the drought susceptible variety following 8 days of

drought stress. Furthermore, the chlorophyll content was restored 24 hrs after re-watering (Figure 3.7). This could indicate that the drought tolerant variety possesses the ability to stay green and photosynthesise under drought stress. In addition, stomatal conductance was lower in the drought tolerant variety (Figure 3.6), signifying the closure of stoma to conserve water under drought stress. This stomatal closure is reciprocated by an increase in surface temperature (Figure 3.6), since the evaporative transpiration normally dissipates heat. Collectively, the leaf surface temperature and stomatal conductance reveal that SA 1441 has superior drought performance than ICSB 338. Furthermore, the decrease in stomatal conductance of the drought tolerant SA 1441 at 5 days suggests an active mechanism of drought tolerance.

Proline and glycine betaine content, which play important roles as osmoprotectants in plant cells (Hamilton and Heckathorn, 2001), increased in root and leaf tissues of both sorghum varieties in response to drought stress (Figure 3.9). Proline has an added role of scavenging for reactive oxygen species (ROS) (Smirnoff and Cumbes, 1989). This possibly reduces oxidative cellular damage in plants during periods of drought stress. Noteworthy was that the drought tolerant sorghum variety showed an early accumulation of these compatible osmolytes following stress and also accumulated higher levels compared to the drought susceptible variety (Figure 3.9). These osmolytes ultimately protect plant cells from the harmful effects of drought stress. Furthermore, the overall higher levels of proline in leaf tissue compared to roots and the inverse for glycine betaine possibly indicates the tissue specific responses of sorghum to drought stress.

After confirming the drought stress phenotype of the two sorghum varieties using a range of growth, morphological and biochemical parameters, the contrasting drought tolerance responses between the two varieties was further observed at the proteome level in root tissue.

Only the root tissue was used for the analysis because roots are the first organs to sense water deficits in the soil before sending signals to the rest of the plant (Ghatak *et al*., 2016). Furthermore, no other comparative root proteome studies have been carried out in sorghum to date. Therefore, the current study will provide a foundation for comparative sorghum root proteomic analyses. The proteomic analysis was conducted using the isobaric Tags for Relative and Absolute Quantitation (iTRAQ) analysis. In this study, the 8-plex iTRAQ kit, which labels 8 samples simultaneously (Ross *et al*., 2004), was used. Some of the advantages of using iTRAQ analysis are that it is a more efficient way of protein identification and quantitation compared to two-dimensional gel electrophoresis (2DE). This is because it is able to identify low abundant and hydrophobic proteins compared to 2DE (Zieske, 2006).

Briefly, the two sorghum varieties were exposed to drought stress by withholding water for 8 days and total soluble root protein was extracted from the control and drought stresses plants. Four biological replicates were used to increase reproducibility of the results. A total of 1169 and 1043 proteins were identified in ICSB 338 and SA 1441, respectively. Of these, 237 and 184 were drought responsive for ICSB 338 and SA 1441, respectively (Tables 4.1 and 4.2). However, a large percentage of protein were uncharacterised for both sorghum varieties, with proportions of 76% and 72% for ICSB 338 and SA 1441, respectively. The three most highly represented drought responsive proteins after functional annotation were related to disease/defence (26%), metabolism (25%) and energy (9%) for ICSB 338 (Figure 4.9). For SA 1441, these were disease/defence (23%), metabolism (21%) and protein synthesis (14%). Metabolism and disease/defence proteins were also identified as the highly represented functional categories in a wheat grain comparative proteomic study under drought stress (Ge *et al*., 2012).

Peroxidases were highly represented in both sorghum varieties in the disease/defence functional category. Their role was possibly to scavenge for, detoxify and reduce the harmful effects of ROS, thereby restoring cellular homeostasis (Elstner, 1987). Carbohydrate metabolism related proteins were highly represented in the metabolism functional category. High numbers of carbohydrate related proteins were also identified in a comparative root proteome study of two tomato (*Solanum spp.*) varieties (Zhou *et al.*, 2013). The results signify that the sorghum plants dedicated cellular resources towards disease/defence and metabolism to a greater extent in root tissue in response to drought stress. The ability to synthesise disease/defence and metabolism related proteins may be one of the reasons why sorghum is highly adapted to drought stress compared to other crops. However, more functional validation studies would need to be performed.

Following the comparative root proteome analysis between the two sorghum varieties, a total of 10 proteins were selected for validation by gene expression analysis (Table 4.3). The 10 target genes corresponding to these proteins were then analysed using qRT-PCR in a time-course experiment. A primer pair of one gene did not yield any PCR product and was subsequently excluded from the analysis (Figure 4.12). The gene expression analysis showed that all the nine genes were responsive to drought stress (Figures 4.13 and 4.14). In root tissue (Figure 4.13), four genes showed significantly higher gene expression in ICSB 338 at 12 days of drought stress in comparison to SA 1441 whilst two genes showed the opposite. In leaf tissue (Figure 4.14), ICSB 338 showed significantly higher gene expression at 0 and 4 days of drought stress for both root and leaf tissue. However, SA 1441 showed significantly higher gene expression at 8 days of drought stress for all genes in comparison to ICSB 338. This gene validation was an important step towards the development of drought marker genes.

The first step in the development of drought marker genes included expression analysis of the genes in sorghum cell suspension cultures of White sorghum and ICSB 338 varieties with and without sorbitol-induced osmotic stress stress. The result showed that seven of the genes could distinguish between the two sorghum varieties without osmotic stress (Figure 5.1). All the nine genes were also differentially expressed in the two sorghum cell suspension cultures in response to sorbitol-induced osmotic stress (Appendix, Figure B1). Since drought stress is closely associated with heat stress, the expression patterns of the 9 genes was further analysed on cell cultures maintained at 22°C and 30°C in White sorghum cell suspension cultures. The results showed that all the genes were responsive to heat stress at 30°C (Figure 5.2). This set of results led to the proposal for the use of these genes for the selection of drought tolerant varieties by plant breeders at the seedling stage. This could possibly save time, labour and space since the marker assisted selection can be carried out in a greenhouse using seedlings.

A workflow was proposed in which these drought marker genes can be utilised in other crops. The workflow involves the identification of the homologues of these genes in the target species. In this study, Arabidopsis (*Arabidopsis thaliana*) was used as a proof of concept. After the identification of four homologues per target gene, the results showed that the homologues behaved differently in response to osmotic stress in a time course experiment. Some genes were activated whilst some were suppressed under osmotic stress. Since large numbers of homologues were identified in Arabidopsis through bioinformatics, the osmotic stress responsive ones would be selected for gene overexpression as a way of assessing gene function in transgenic plants. These genes could be used by plant breeders through introgressing them into widely accepted varieties for drought stress tolerance improvement in target crops.

In future studies, the measurements of photosynthetic activities of sorghum under drought stress are recommended so that the changes in important photoreceptors such as chlorophyll *a* and *b* are determined. This is because chlorophyll is responsible for absorbing light during the photosynthetic process. Reciprocal gene expression analysis of some key genes such as delta1-pyrroline-5-carboxylate synthase 1 and 2 (*P5CS1* and *P5CS2*) and *gbsAB* in the biosynthetic pathways of proline and glycine betaine are also recommended. This is essential in understanding the activity of these compatible osmolytes in response to drought stress in different plant tissues. Furthermore, the use of bioinformatics and PCR to screen homologues of sorghum drought stress responsive genes in important crop species like maize (*Zea mays*) and wheat (*Triticum aestivum*) is recommended. This would assist in the transfer of knowledge obtained from sorghum to other crop species. A few target drought stress responsive homologues can then be overexpressed in the target crop parallel to the transgene in case sequence divergence in sorghum makes the gene non-functional in another species due to protein complexity. This would be important in developing drought stress tolerance in these target crops. In this study, *SORBI_3001G514200, SORBI_3003G136200, SORBI_3007G149600, SORBI_3001G313200, SORBI_3001G073900* and *SORBI_3003G322400* showed significant differences between the drought susceptible ICSB 338 and unknown phenotype White sorghum varieties in cell suspension cultures. Physiological experiments to verify this in whole plants are recommended. Overall, this study is important in that it created a foundation on comparative sorghum root proteomics under drought stress and developed drought marker genes for potential use by plant breeders in MAS for drought tolerance.

REFERENCES

Abdrakhamanova, A., Wang, Q.Y., Khokhlova, L., Nick, P., 2003. Is microtubule disassembly a trigger for cold acclimation? *Plant and Cell Physiology, 44*, 676-686.

Ackerson, R.C., Radin, J.W., 1983. Abscisic acid accumulation in cotton leaves in response to dehydration at high pressure. *Plant Physiology, 71*, 432-433.

Acquaah, G., 2012. *Principles of plant genetics and breeding*, (2nd. Ed). Wiley-Blackwell, Chichester.

Aebersold, R., Mann, M., 2003.Mass spectrometry based proteomics. *Nature, 422*, 198-202.

Ahmad, P., Prasad, M.N.V., 2011. *Environmental adaptations and stress tolerance of plants in the era of climate change*. Springer, New York..

Ahmed, M., 2013. Development of some molecular markers for drought tolerance in maize (*Zea mays* L.). *Asian Journal of Crop Science, 5*, 312-318.

Al Hassan, M., Chaura, J., Donat-Torres, M.P., Boscaiu, M., Vicente, O., 2017. Antioxidant responses under salinity and drought in three closely related wild monocots with different ecological optima. *AoB Plants, 9,* 1-20.

Alexandratos, N., Bruinsma, J., 2012. World agriculture towards 2030/2050: The 2012 revision. ESA Working paper, FAO, Rome.

Alexieva, V., Sergiev, I., Mapelli, S., Karanov, E., 2001. The effect of drought and ultraviolet radiation on growth and stress markers in pea and wheat. *Plant, Cell and Environment, 24*, 1337-1344.

Almolares, A., Abdy, M., Somani, R., Jilani, S., 1999. Comparative study of sorghum sudangarass hybrids and lines for forage. *Annals of Plant Physiology, 13*, 6–10.

Amrhein, N., Apel, K., Baginsky, S., Buchmann, N., Geisler, M., Keller, F., Körner, C., Martinoia, E., Merbold, L., Müller, C., 2013. *Plant Response to Stress*. Zurich-Basel Plant Science Center, Zurich.

Andrews, D., Beames, B., Summers, M., Park, W., 1988. Characterization of the lipid acyl hydrolase activity of the major potato (*Solanum tuberosum*) tuber protein, patatin, by cloning and abundant expression in a baculovirus vector. *Biochemical Journal, 252*, 199-206.

Anjum, S.A., Xie, X., Wang, L., Saleem, M.F., Man, C., Lei, W., 2011. Morphological, physiological and biochemical responses of plants to drought stress. *African Journal of Agricultural Research, 6*, 2026-2032.

Arimura, S., Aida, G.P., Fujimoto, M., Nakazono, M., Tsutsumi, N., 2004a. Arabidopsis dynamin-like protein 2a (ADL2a), like ADL2b, is involved in plant mitochondrial division. *Plant and Cell Physiology, 45,* 236-242.

Arimura, S., Yamamoto, J., Aida, G.P., Nakazono, M., Tsutsumi, N., 2004b. Frequent fusion and fission of plant mitochondria with unequal nucleoid distribution. *Proceedings of the National Academy of Sciences, 101,* 7805-7808.

Artlip, T., Funkhouser, E., 1995. *Protein synthetic responses to environmental stresses*. Handbook of plant and crop physiology. Marcel Dekker, New York.

Baima, S., Possenti, M., Matteucci, A., Wisman, E., Altamura, M.M., Ruberti, I., Morelli, G., 2001. The Arabidopsis ATHB-8 HD-zip protein acts as a differentiation-promoting transcription factor of the vascular meristems. *Plant Physiology, 126,* 643-655.

Baldocchi, D.D., Verma, S.B., Rosenberg, N.J., 1985. Water use efficiency in a soybean field: influence of plant water stress. *Agricultural and Forest Meteorology, 34*, 53-65.

Barrs, H., Weatherley, P., 1962. A re-examination of the relative turgidity technique for estimating water deficits in leaves. *Australian Journal of Biological Sciences, 15,* 413-428.

Beardsell, M.F., Cohen, D., 1975. Relationships between leaf water status, abscisic acid levels, and stomatal resistance in maize and sorghum. *Plant Physiology, 56,* 207-212.

Benešová, M., Holá, D., Fischer, L., Jedelský, P.L., Hnilička, F., Wilhelmová, N., Rothová, O., Kočová, M., Procházková, D., Honnerová, J., 2012. The physiology and proteomics of drought tolerance in maize: early stomatal closure as a cause of lower tolerance to short-term dehydration? *PLoS One, 7,* 1-17.

Bernardo, R., 2002. *Breeding for quantitative traits in plants*. Stemma Press, Woodbury.

Bevan, M., Bancroft, I., Bent, E., Love, K., Goodman, H., Dean, C., Bergkamp, R., Dirkse, W., Van Staveren, M., Stiekema, W., 1998. Analysis of 1.9 Mb of contiguous sequence from chromosome 4 of *Arabidopsis thaliana*. *Nature, 391,* 485-488.

Bhaskaran, S., Smith, R.H., Newton, R.J., 1985. Physiological changes in cultured sorghum cells in response to induced water stress. *Plant Physiology, 79*, 266-269.

Bindschedler, Cramer, 2010. Quantitative plant proteomics. *Proteomics, 11*, 756-775.

Blackstock, W., Weir, M., 1999. Proteomics: quantitative and physical mapping of cellular proteins. *Trends in Biotechnology, 17*, 121-127.

Blum, A., 2010. *Plant breeding for water-limited environments, life sciences*. Springer, New York.

Blum, A., 2009. Effective use of water (EUW) and not water-use efficiency (WUE) is the target of crop yield improvement under drought stress. *Field Crops Research, 112,* 119-123.

Blum, A., 2005. Drought resistance, water-use efficiency, and yield potential—are they compatible, dissonant, or mutually exclusive? *Australian Journal of Agricultural Research, 56,* 1159-1168.

Blum, A., Arkin, G.F., 1984. Sorghum root growth and water-use as affected by water supply and growth duration. *Field Crops Research, 9*, 131-142.

Boo, Y.C., Jung, J., 1999. Water deficit—induced oxidative stress and antioxidative defenses in rice plants. *Journal of Plant Physiology, 155*, 255-261.

Borrell, A., Hammer, G., Henzell, R., 1999. Does maintaining green leaf area in sorghum improve yield under drought? II. Dry matter production and yield. *Crop Science, 40*, 1037-1048.

Boudet, A.-M., 1998. A new view of lignification. *Trends in Plant Science, 3*, 67-71.

Bradford, M.M., 1976. A rapid and sensitive method for the quantitation of microgram quantities of protein utilizing the principle of protein-dye binding. *Analytical Biochemistry, 72*, 248-254.

Bradshaw, 2008. An introduction to proteomics: Applications to plant biology, in: *Plant proteomics: Strategies and applications*, Wiley, Hoboken, pp 1-6

Brash, A.R., 1999. Lipoxygenases: occurrence, functions, catalysis, and acquisition of substrate. *Journal of Biological Chemistry, 274*, 23679-23682.

Brossa, R., Pintó-Marijuan, M., Francisco, R., López-Carbonell, M., Chaves, M.M., Alegre, L., 2015. Redox proteomics and physiological responses in *Cistus albidus* shrubs subjected to long-term summer drought followed by recovery. *Planta, 241*, 803-822.

Burch, G., Smith, R., Mason, W., 1978. Agronomic and physiological responses of soybean and sorghum crops to water deficits II. Crop evaporation, soil water depletion and root distribution. *Functional Plant Biology. 5*, 169-177.

Burow, G.B., Franks, C.D., Acosta-Martinez, V., Xin, Z., 2009. Molecular mapping and characterization of BLMC, a locus for profuse wax (bloom) and enhanced cuticular features of Sorghum (*Sorghum bicolor* (L.) Moench.). *Theoretical and Applied Genetics, 118*, 423-431.

Cao, Y.-Y., Bian, X.-C., Chen, M.-X., Xia, L.-R., Zhang, J., Zhu, F.-Y., Wu, C.-F., 2017. iTRAQ-based quantitative proteomic analysis in vernalization-treated faba bean (*Vicia faba* L.). *PloS one, 12*, 1-18.

Capote-Mainez, N., Sánchez, F., 1997. Characterization of the common bean uricase II and its expression in organs other than nodules. *Plant Physiology, 115*, 1307-1317.

Carroll, A.J., Heazlewood, J.L., Ito, J., Millar, A.H., 2008. Analysis of the Arabidopsis cytosolic ribosome proteome provides detailed insights into its components and their post-translational modification. *Molecular and Cellular Proteomics, 7*, 347-369.

Casaretto, J.A., El-kereamy, A., Zeng, B., Stiegelmeyer, S.M., Chen, X., Bi, Y.-M., Rothstein, S.J., 2016. Expression of *OsMYB55* in maize activates stress-responsive genes and enhances heat and drought tolerance. *BMC Genomics, 17*, 1-15.

Chakrabortee, S., Boschetti, C., Walton, L.J., Sarkar, S., Rubinsztein, D.C., Tunnacliffe, A., 2007. Hydrophilic protein associated with desiccation tolerance exhibits broad protein

stabilization function. *Proceedings of the National Academy of Sciences, 104*, 18073-18078.

Chang, F., Szick-Miranda, K., Pan, S., Bailey-Serres, J., 2005. Proteomic characterization of evolutionarily conserved and variable proteins of Arabidopsis cytosolic ribosomes. *Plant Physiology, 137*, 848-862.

Chaves, M.M., Flexas, J., Pinheiro, C., 2009. Photosynthesis under drought and salt stress: regulation mechanisms from whole plant to cell. *Annals of Botany, 103*, 551-560.

Chen, L., Huang, Y., Xu, M., Cheng, Z., Zhang, D., Zheng, J., 2016. iTRAQ-based quantitative proteomics analysis of black rice grain development reveals metabolic pathways associated with anthocyanin biosynthesis. *PLoS ONE, 11*, 1-25.

Cornic, G., Massacci, A., 1996. Leaf photosynthesis under drought stress, in: *Photosynthesis and the environment*. Springer, Dordrecht. pp. 347-366.

Cramer, G.R., Nowak, R.S., 1992. Supplemental manganese improves the relative growth, net assimilation and photosynthetic rates of salt-stressed barley. *Physiologia Plantarum, 84*, 600-605.

Cruz, R., Jordan, W., Drew, M., 1992. Structural changes and associated reduction of hydraulic conductance in roots of *Sorghum bicolor* L. following exposure to water deficit. *Plant Physiology, 99*, 203-212.

Dahlberg, J., Berenji, J., Sikora, V., Latković, D., 2012. Assessing sorghum [*Sorghum bicolor* (L) Moench] germplasm for new traits: food, fuels & unique uses. *Maydica 56*, 85-92

Damsz, B., Dannenhoffer, J.M., Bell, J.A., Webb, M.A., 1994. Immunocytochemical localization of uricase in peroxisomes of soybean cotyledons. *Plant and Cell Physiology 35*, 979-982.

Davies, W., Metcalfe, J., Lodge, T., da Costa, A.R., 1986. Plant growth substances and the regulation of growth under drought. *Functional Plant Biology, 13*, 105-125.

Davin, L.B., Lewis, N.G., 2000. Dirigent proteins and dirigent sites explain the mystery of specificity of radical precursor coupling in lignan and lignin biosynthesis. *Plant Physiology, 123*, 453-462.

Di Martino, C., Delfine, S., Pizzuto, R., Loreto, F., Fuggi, A., 2003. Free amino acids and glycine betaine in leaf osmoregulation of spinach responding to increasing salt stress. *New Phytologist, 158*, 455-463.

do Carmo, L.S., Martins, A.C., Martins, C.C., Passos, M.A., Silva, L.P., Araujo, A.C., Brasileiro, A.C., Miller, R.N., Guimarães, P.M., Mehta, A., 2018. Comparative proteomics and gene expression analysis in Arachis duranensis reveal stress response proteins associated to drought tolerance. *Journal of Proteomics*, 1-12.

Duncan, R.F., Hershey, J.W., 1989. Protein synthesis and protein phosphorylation during heat stress, recovery, and adaptation. *Journal of Cell Biology, 109*, 1467-1481.

Eckenstorfer, M., Miklau, M., Gaugitsch, H., 2014. *New plant breeding techniques and risks associated with their application*. Umweltbundesamt, Vienna.

Edwards, G., Walker, D., 1983. *C_3, C_4: Mechanisms, and cellular and environmental regulation, of photosynthesis*. University of California Press, California.

Elstner, E.F., 1987. Metabolism of activated oxygen species, in: *Biochemistry of metabolism*. Elsevier, pp. 253-315.

Erickson, J.E., Soikaew, A., Sollenberger, L.E., Bennett, J.M., 2012. Water use and water-use efficiency of three perennial bioenergy grass crops in Florida. *Agriculture, 2*, 325-338.

Etzler, M.E., 1986. Distribution and function of plant lectins. *The lectins: Properties, Functions, and Applications in Biology and Medicine*, 371-435.

Fan, W., Dong, X., 2002. In vivo interaction between NPR1 and transcription factor TGA2 leads to salicylic acid–mediated gene activation in Arabidopsis. *The Plant Cell, 14*, 1377-1389.

Fan, X.K.L., Zhu, T.S., Soules, M.E., *et al*. 2010. NOTCH pathway blockade depletes CD133-positive glioblastoma cells and inhibits growth of tumor neurospheres and xenografts. *Stem Cells*, 28, 5-16.

Farooq, M., Wahid, A., Kobayashi, N., Fujita, D., Basra, S.M.A., 2009. Plant drought stress: effects, mechanisms and management, in: Lichtfouse, E., Navarrete, M., Debaeke, P., Véronique, S., Alberola, C. (Eds.), *Sustainable agriculture*. Springer Netherlands, Dordrecht, pp. 153-188.

Feussner, I., Wasternack, C., 2002. The lipoxygenase pathway. *Annual Reviews in Plant Biology, 53*, 275–297.

Finn, R.D., Bateman, A., Clements, J., Coggill, P., Eberhardt, R.Y., Eddy, S.R., Heger, A., Hetherington, K., Holm, L., Mistry, J., 2013. Pfam: the protein families database. *Nucleic Acids Research, 42*, D222-D230.

Ford, K.L., Cassin, A., Bacic, A.F., 2011. Quantitative proteomic analysis of wheat cultivars with differing drought stress tolerance. *Frontiers in Plant Science, 2*, 1-11.

Fracasso, A., Trindade. L.M and Amaducci, S., 2016. Drought stress tolerance strategies revealed by RNA-Seq in two sorghum genotypes with contrasting WUE. *BMC Plant Biology*, 16, 1-18.

Fraser, C.M., Rider, L.W., Chapple, C., 2005. An expression and bioinformatics analysis of the Arabidopsis serine carboxypeptidase-like gene family. *Plant Physiology, 138*, 1136-1148.

Fujimoto, M., Arimura, S., Nakazono, M., Tsutsumi, N., 2004. A rice dynamin-like protein, OsDRP3A, is involved in mitochondrial fission. *Breeding Science, 54*, 367-372.

Garfin, D., 1995. Electrophoretic methods, in: *Introduction to biophysical methods for protein and nucleic acid research*. Academic Press, San Diego, pp. 53-109.

Ge, P., Ma, C., Wang, S., Gao, L., Li, X., Guo, G., Ma, W., Yan, Y., 2012. Comparative proteomic analysis of grain development in two spring wheat varieties under drought stress. *Analytical and Bioanalytical Chemistry, 402*, 1297-1313.

Ghatak, A., Chaturvedi, P., Nagler, M., Roustan, V., Lyon, D., Bachmann, G., Postl, W., Schröfl, A., Desai, N., Varshney, R.K., 2016. Comprehensive tissue-specific proteome analysis of drought stress responses in *Pennisetum glaucum* (L.) R. Br.(Pearl millet). *Journal of Proteomics, 143*, 122-135.

Gill, S.S., Tuteja, N., 2010. Reactive oxygen species and antioxidant machinery in abiotic stress tolerance in crop plants. *Plant Physiology and Biochemistry, 48*, 909-930.

Goldstein, I.J., 1980. What should be called a lectin? *Nature*, 285, 66-66.

González, L., González-Vilar, M., 2001. Determination of relative water content, in: *Handbook of Plant Ecophysiology Techniques*. Springer, pp. 207-212.

González-Torralva, F., Brown, A.P., Chivasa, S., 2017. Comparative proteomic analysis of horseweed (*Conyza canadensis*) biotypes identifies candidate proteins for glyphosate resistance. *Scientific Reports, 7*, 1-11.

Good, A.G., Zaplachinski, S.T., 1994. The effects of drought stress on free amino acid accumulation and protein synthesis in *Brassica napus*. *Physiologia Plantarum, 90*, 9-14.

Goodlett, D.R., Keller, A., Watts, J.D., Newitt, R., Eugene, C.Y., Purvine, S., Eng, J.K., Von Haller, P., Aebersold, R., Kolker, E., 2001. Differential stable isotope labeling of peptides for quantitation and *de novo* sequence derivation. *Rapid Communications in Mass Spectrometry, 15*, 1214-1221.

Gray, W.M., Estelle, M., 2000. Function of the ubiquitin–proteasome pathway in auxin response. *Trends in Biochemical Sciences* 25, 133-138.

Grill, E and Ziegler, H, 1998. A plant's dilemma, *Science*, 282, 252-253.

Gunning, P.W., Ghoshdastider, U., Whitaker, S., Popp, D., Robinson, R.C., 2015. The evolution of compositionally and functionally distinct actin filaments. *Journal of Cell Science, 128*, 2009-2019.

Gygi, S.P., Rist, B., Gerber, S.A., Turecek, F., Gelb, M.H., Aebersold, R., 1999. Quantitative analysis of complex protein mixtures using isotope-coded affinity tags. *Nature Biotechnology, 17*, 994-999.

Hajheidari Mohsen, Abdollahian-Noghabi Mohammad, Askari Hossein, Heidari Manzar, Sadeghian Seyed Y., Ober Eric S., Hosseini Salekdeh Ghasem, 2005. Proteome analysis of sugar beet leaves under drought stress. *Proteomics, 5*, 950-960.

Hamilton, E.W., Heckathorn, S.A., 2001. Mitochondrial adaptations to NaCl. Complex I is protected by anti-oxidants and small heat shock proteins, whereas complex II is protected by proline and betaine. *Plant Physiology, 126*, 1266-1274.

Hamissou, M., Weibel, D.E., 2004. The effects of epicuticular wax cover on the rate of water loss of *Sorghum bicolor* L. Moench. *Asian Journal of Plant Sciience, 3*, 742-746.

Hardie, D., 1999. Plant protein serine/threonine kinases: classification and functions. *Annual Review of Plant Biology, 50,* 97-131.

Hare, P., Cress, W., 1997. Metabolic implications of stress-induced proline accumulation in plants. *Plant Growth Regulation, 21,* 79-102.

Harris, D., Tripathi, R., Joshi, A., 2002. On-farm seed priming to improve crop establishment and yield in dry direct-seeded rice. Direct seeding: Research Strategies and Opportunities, International Research Institute, Manila, 231-240.

Hartung, W., Sauter, A., Hose, E., 2002. Abscisic acid in the xylem: where does it come from, where does it go to? *Journal of Experimental Botany, 53,* 27-32.

Hasegawa, P.M., Bressan, R., Handa, A., 1986. *Cellular mechanisms of salinity tolerance*. ASHS Symposium on basic research ideas and opportunities for horticulturists in stress physiology. *HortScience, 21,* 1317-1324.

Haynes, P.A., Yates III, J.R., 2000. Proteome profiling—pitfalls and progress. *International Journal of Genomics, 1,* 81-87.

Hayyan, M., Hashim, M.A., AlNashef, I.M., 2016. Superoxide ion: generation and chemical implications. *Chemical Reviews, 116,* 3029-3085.

Hu, J., Rampitsch, C., Bykova, N., 2016. Advances in plant proteomics toward improvement of crop productivity and stress resistance. *Frontiers in Plant Science, 6,* 1-15.

Huseynova, I.M., Rustamova, S.M., 2010. *Screening for drought stress tolerance in wheat genotypes using molecular markers*. Presented at the Biol. Sci, pp. 132-139.

Ingle, R.A., Schmidt, U.G., Farrant, J.M., Thomson, J.A., Mundree, S.G., 2007. Proteomic analysis of leaf proteins during dehydration of the resurrection plant *Xerophyta viscosa*. *Plant, Cell & Environment, 30,* 435–446.

Isaacson, T., Rose, J.K., Finnie, C., 2006. Surveying the plant cell wall proteome, or secretome. *Annual Plant Reviews, Plant Proteomics 28,* 185.

Jackson, D.R., Arthur, M.F., 1980. Sweet sorghum: An alcohol crop for the US. *Gasohol USA, 2,* 12-12

Jagtap, V., Bhargava, S., Streb, P., Feierabend, J., 1998. Comparative effect of water, heat and light stresses on photosynthetic reactions in *Sorghum bicolor* (L.) Moench. *Journal of Experimental Botany, 49,* 1715-1721.

Jaleel, C.A., Manivannan, P., Wahid, A., Farooq, M., Al-Juburi, H.J., Somasundaram, R., Panneerselvam, R., 2009. Drought stress in plants: A review on morphological characteristics and pigments composition. *International Journal of Agricultural Biology, 11,* 100-105.

Jedmowski, C., Ashoub, A., Beckhaus, T., Berberich, T., Karas, M., Brüggemann, W., 2014. Comparative analysis of *Sorghum bicolor* proteome in response to drought stress and following recovery. *International Journal of Proteomics, 2014*, 1-10.

Ji, K., Wang, Y., Sun, W., Lou, Q., Mei, H., Shen, S., Chen, H., 2012. Drought-responsive mechanisms in rice genotypes with contrasting drought tolerance during reproductive stage. *Journal of Plant Physiology, 169*, 336-344.

Jiang, Y., Yang, B., Harris, N.S., Deyholos, M.K., 2007. Comparative proteomic analysis of NaCl stress-responsive proteins in Arabidopsis roots. *Journal of Experimental Botany, 58*, 3591-3607.

Johnson, D.A., Richards, R.A., Turner, N.C., 1983. Yield, water relations, gas exchange, and surface reflectances of near-isogenic wheat lines differing in glaucousness 1. *Crop Science, 23*, 318-325.

Johnson, S.M., Lim, F.-L., Finkler, A., Fromm, H., Slabas, A.R., Knight, M.R., 2014. Transcriptomic analysis of Sorghum bicolor responding to combined heat and drought stress. *BMC Genomics, 15*, 1-19.

Jordan, W., Shouse, P., Blum, A., Miller, F., Monk, R., 1984. Environmental physiology of sorghum. Epicuticular wax load and cuticular transpiration. *Crop Science, 24*, 1168-1173.

Jorrin-Novo, J., Pascual, J., Sanches-Lucas, R., Romero-Rodriguez, M., Rodriguez-Ortega, M., Lenz, C., Valledor, L., 2015. Fourteen years of plant proteomics reflected in proteomics: moving from model species and 2DE approaches to orphan species and gel-free platforms. *Proteomics, 15*, 1089-1112.

Kaida, R., Serada, S., Norioka, N., Norioka, S., Neumetzler, L., Pauly, M., Sampedro, J., Zarra, I., Hayashi, T., Kaneko, T.S., 2010. Potential role for purple acid phosphatase in the dephosphorylation of wall proteins in tobacco cells. *Plant Physiology, 153*, 603-610.

Kawano, T., 2003. Roles of the reactive oxygen species-generating peroxidase reactions in plant defense and growth induction. *Plant Cell Reports, 21*, 829-837.

Kim, S.G., Bae, H.H., Jung, H.J., Lee, J.-S., Kim, J.-T., Go, T.H., Son, B.-Y., Baek, S.-B., Kwon, Y.-U., Woo, M.-O., 2014. Physiological and protein profiling response to drought stress in KS141, a Korean maize inbred line. *Journal of Crop Science and Biotechnology, 17*, 273-280.

Kimber, C.T., Dahlberg, J.A., Kresovich, S., 2013. The gene pool of Sorghum bicolor and its improvement, in: *Genomics of the Saccharinae*. Springer, pp. 23-41.

Klose, J., Nock, C., Herrmann, M., Stuhler, K., Marcus, K., Bluggel, M., Krause, E., Schalkwyk, L.C., Rastan, S., Brown, S.D.M., Bussow, K., Himmelbauer, H., Lehrach, H., 2002. Genetic analysis of the mouse brain proteome. *Nature Genetics, 30*, 385-393.

Knight, H., Knight, M.R., 2001. Abiotic stress signalling pathways: specificity and cross-talk. *Trends in Plant Science, 6*, 262-267.

Koh, J., Chen, G., Yoo, M.-J., Zhu, N., Dufresne, D., Erickson, J.E., Shao, H., Chen, S., 2015. Comparative proteomic analysis of *Brassica napus* in response to drought stress. *Journal of Proteome Research, 14*, 3068-3081.

Koornneef, M., Meinke, D., 2010. The development of Arabidopsis as a model plant. *The Plant Journal, 61*, 909-921.

Kumar Swami, A., Alam, S.I., Sengupta, N., Sarin, R., 2011. Differential proteomic analysis of salt stress response in *Sorghum bicolor* leaves. *Environmental and Experimental Botany, 71*, 321-328.

Kumari, P., Anil, K., S., Ramesh, K., Sudhakar. R., P., Nagaraju, M., Bhanu, P., A., Shah, T., Henderson, A., Srivastava, R.K., Rajasheker, G., Chitikineni, A., Varshney, R.K., Rathnagiri, P., Lakshmi, N., M., Kavi, K., P.B., 2018. Genome-wide identification and analysis of arabidopsis sodium proton antiporter (NHX) and human sodium proton exchanger (NHE) homologs in *Sorghum bicolor*. *Genes, 9*, 1-18.

Laemmli, U.K., 1970. Cleavage of structural proteins during the assembly of the head of bacteriophage T4. *Nature, 227*, 680-685.

Lam, E., 2004. Controlled cell death, plant survival and development. *Nature Reviews: Molecular Cell Biology, 5*, 305-315.

Lambers, H., Chapin, F.S., Pons, T.L., 2008. Photosynthesis, in: *Plant Physiological Ecology*. Springer, pp. 11-99.

LeBansky, B.R., McKnight, T.D., Griffing, L.R., 1992. Purification and characterization of a secreted purple phosphatase from soybean suspension cultures. *Plant Physiology, 99*, 391-395.

Leroy, B., Houyoux, N., Matallana-Surget, S and Wattiez, R., 2012. Gel-free proteome analysis isotopic labelling vs label-free approaches for quantitative proteomics, In: Integrative Proteomics, 327-346.

Li, B., Carey, M., Workman, J.L., 2007. The role of chromatin during transcription. *Cell, 128*, 707-719.

Li, J., Ding, X., Han, S., He, T., Zhang, H., Yang, L., Yang, S., Gai, J., 2016a. Differential proteomics analysis to identify proteins and pathways associated with male sterility of soybean using iTRAQ-based strategy. *Journal of Proteomics, 138*, 72-82.

Li, Z., Zhang, Y., Xu, Y., Zhang, X., Peng, Y., Ma, X., Huang, L., Yan, Y., 2016b. Physiological and iTRAQ-based proteomic analyses reveal the function of spermidine on improving drought tolerance in white clover. *Journal of Proteome Research, 15*, 1563-1579.

Liu, H., Sultan, M.A.R.F., li Liu, X., Zhang, J., Yu, F., xian Zhao, H., 2015. Physiological and comparative proteomic analysis reveals different drought responses in roots and leaves of drought-tolerant wild wheat (*Triticum boeoticum*). *PLoS One, 10*, 1-29

Loggini, B., Scartazza, A., Brugnoli, E., Navari-Izzo, F., 1999. Antioxidative defense system, pigment composition, and photosynthetic efficiency in two wheat cultivars subjected to drought. *Plant Physiology, 119*, 1091-1100.

Ludlow, M., Muchow, R., 1990a. A critical evaluation of traits for improving crop yield in water-limited environments. *Advanced Agronomy, 43*, 107–153.

Macauley, H., 2015. Cereal crops: Rice, maize, millet, sorghum, wheat. United Nations Economic Commission for Africa, Dakar.

Mafakheri, A., Siosemardeh, A., Bahramnejad, B., Struik, P., Sohrabi, Y., 2010. Effect of drought stress on yield, proline and chlorophyll contents in three chickpea cultivars. *Australian Journal of Crop Science, 4*, 580-585.

Mahajan, S., Tuteja, N., 2005. Cold, salinity and drought stresses: An overview. *Archives of Biochemistry and Biophysics, 444*, 139-158.

Marchler-Bauer, A., Lu, S., Anderson, J.B., Chitsaz, F., Derbyshire, M.K., DeWeese-Scott, C., Fong, J.H., Geer, L.Y., Geer, R.C., Gonzales, N.R., 2010. CDD: a Conserved Domain Database for the functional annotation of proteins. *Nucleic Acids Research, 39*, D225-D229.

Martínez-Esteso, M.J., Casado-Vela, J., Sellés-Marchart, S., Pedreño, M.A., Bru-Martínez, R., 2014. Differential plant proteome analysis by isobaric tags for relative and absolute quantitation (iTRAQ), in: Jorrin-Novo, J.V., Komatsu, S., Weckwerth, W., Wienkoop, S. (Eds.), *Plant proteomics: Methods and protocols*. Humana Press, Totowa, pp. 155-169.

Mathesius, U., Djordjevic, M.A., Oakes, M., Goffard, N., Haerizadeh, F., Weiller, G.F., Singh, M.B., Bhalla, P.L., 2011. Comparative proteomic profiles of the soybean (*Glycine max*) root apex and differentiated root zone. *Proteomics, 11*, 1707-1719.

May, M.J., Leaver, C.J., 1993. Oxidative stimulation of glutathione synthesis in *Arabidopsis thaliana* suspension cultures. *Plant Physiology, 103*, 621-627.

Merrill, S.D., Rawlins, S., 1979. Distribution and growth of sorghum roots in response to irrigation frequency. *Agronomy Journal, 71*, 738-745.

Messmer, M., Wilbois, K.-P., Baier, C., Schäfer, F., Arncken, C., Drexler, D., Hildermann, I., 2015. Plant breeding techniques. An assessment for organic farming. Research Institute of Organic Agriculture, Switzerland.

Mirzaei, M., Soltani, N., Sarhadi, E., Pascovici, D., Keighley, T., Salekdeh, G.H., Haynes, P.A., Atwell, B.J., 2011. Shotgun proteomic analysis of long-distance drought signaling in rice roots. *Journal of Proteome Research, 11*, 348-358.

Mittler, R., 2002. Oxidative stress, antioxidants and stress tolerance. *Trends in Plant Science, 7*, 405-410.

Monson, R.K., Fall, R., 1989. Isoprene emission from aspen leaves: influence of environment and relation to photosynthesis and photorespiration. *Plant Physiology, 90*, 267-274.

Moran, J.F., Becana, M., Iturbe-Ormaetxe, I., Frechilla, S., Klucas, R.V., Aparicio-Tejo, P., 1994. Drought induces oxidative stress in pea plants. *Planta, 194*, 346-352.

Motlhaodi, T., Geleta, M., Chite, S., Fatih, M., Ortiz, R., Bryngelsson, T., 2017. Genetic diversity in sorghum [*Sorghum bicolor* (L.) Moench] germplasm from Southern Africa as revealed by microsatellite markers and agro-morphological traits. *Genetic Resources and Crop Evolution, 64*, 599-610.

Munns, R., Sharp, R., 1993. Involvement of abscisic acid in controlling plant growth in soil of low water potential. *Functional Plant Biology, 20*, 425-437.

Nathan, R.A., 1978. *Fuels from sugar crops: Systems study for sugarcane, sweet sorghum, and sugar beets.* Battelle Columbus Labs., Ohio.

Neves-Borges, A.C., Guimarães-Dias, F., Cruz, F., Mesquita, R.O., Nepomuceno, A.L., Romano, E., Loureiro, M.E., Grossi-de-Sá, M. de F., Alves-Ferreira, M., 2012. Expression pattern of drought stress marker genes in soybean roots under two water deficit systems. *Genetics and Molecular Biology, 35*, 212-221.

Ngara, R., 2009. A proteomic analysis of drought and salt stress responsive proteins of different sorghum varieties. PhD thesis. University of the Western Cape, South Africa.

Ngara, R., Ramulifho, E., Movahedi, M., Shargie, N.G., Brown, A.P., Chivasa, S., 2018. Identifying differentially expressed proteins in sorghum cell cultures exposed to osmotic stress. *Scientific Reports, 8*, 1-12.

Ngara, R., Rees, J., Ndimba, B.K., 2008. Establishment of sorghum cell suspension culture system for proteomics studies. *African Journal of Biotechnology, 7*, 744-749.

Ngara, Ndimba, 2014. Model plant systems in salinity and drought stress proteomics studies: a perspective on Arabidopsis and Sorghum. *Plant Biology, 16*, 1029-1032.

Noctor, G., Mhamdi, A., Foyer, C.H., 2014. The roles of reactive oxygen metabolism in drought: not so cut and dried. *Plant Physiology, 113*, 1636-1648

Nour, A.-E.M., Weibel, D., 1978. Evaluation of Root Characteristics in Grain Sorghum. *Agronomy Journal, 70*, 217-218.

Nxele, X., Klein, A., Ndimba, B.K., 2017. Drought and salinity stress alters ROS accumulation, water retention, and osmolyte content in sorghum plants. *South African Journal of Botany, 108*, 261-266.

O'Connor, C.M., Adams, J.U., Fairman, J., 2010. *Essentials of cell biology*. Cambridge, Massachusetts.

OECD/Food and Agriculture Organization of the United Nations, 2015. OECD-FAO agricultural outlook 2015.

O'Farrell, P., 1975. High resolution two-dimensional electrophoresisof proteins. *Journal of Biological Chemistry, 250*, 4007-4021.

O'Mahony, P.J., Oliver, M.J., 1999. The involvement of ubiquitin in vegetative desiccation tolerance. *Plant Molecular Biology, 41,* 657-667.

Palfi, G., Juhász, J., 1971. The theoretical basis and practical application of a new method of selection for determining water deficiency in plants. *Plant and Soil 34*, 503–507.

Paniagua, C., Bilkova, A., Jackson, P., Dabravolski, S., Riber, W., Didi, V., Houser, J., Gigli-Bisceglia, N., Wimmerova, M., Budínská, E., 2017. Dirigent proteins in plants: modulating cell wall metabolism during abiotic and biotic stress exposure. *Journal of Experimental Botany, 68,* 3287-3301.

Patel, J., Vora, A., 1985. Free proline accumulation in drought-stressed plants. *Plant and Soil 84*, 427-429.

Paterson, A.H., Bowers, J.E., Bruggmann, R., Dubchak, I., Grimwood, J., Gundlach, H., Haberer, G., Hellsten, U., Mitros, T., Poliakov, A., Schmutz, J., Spannagl, M., Tang, H., Wang, X., Wicker, T., Bharti, A.K., Chapman, J., Feltus, F.A., Gowik, U., Grigoriev, I.V., Lyons, E., Maher, C.A., Martis, M., Narechania, A., Otillar, R.P., Penning, B.W., Salamov, A.A., Wang, Y., Zhang, L., Carpita, N.C., Freeling, M., Gingle, A.R., Hash, C.T., Keller, B., Klein, P., Kresovich, S., McCann, M.C., Ming, R., Peterson, D.G., Mehboob-ur-Rahman, Ware, D., Westhoff, P., Mayer, K.F.X., Messing, J., Rokhsar, D.S., 2009. The *Sorghum bicolor* genome and the diversification of grasses. *Nature, 457,* 551-556.

Peng, Z., Wang, M., Li, F., Lv, H., Li, C., Xia, G., 2009. A proteomic study of the response to salinity and drought stress in an introgression strain of bread wheat. *Molecular & Cellular Proteomics, 8,* 2676-2686.

Pierce, A., Unwin, R.D., Evans, C.A., Griffiths, S., Carney, L., Zhang, L., Jaworska, E., Lee, C.-F., Blinco, D., Okoniewski, M.J., 2008. Eight-channel iTRAQ enables comparison of the activity of six leukemogenic tyrosine kinases. *Molecular & Cellular Proteomics, 7,* 853-863.

Plessis, A., Hafemeister, C., Wilkins, O., Gonzaga, Z.J., Meyer, R.S., Pires, I., Müller, C., Septiningsih, E.M., Bonneau, R., Purugganan, M., 2015. Multiple abiotic stimuli are integrated in the regulation of rice gene expression under field conditions. *Elife, 4,* 1-27

Pocketbook, F.S., 2015. World food and agriculture 2015. FAO, Rome.

Poehlman, J.M., Sleper, D.A., Rudd, J., 1995. *Breeding field crops*. Springer, Westport.

Pontier, D., Miao, Z., Lam, E., 2001. Trans-dominant suppression of plant TGA factors reveals their negative and positive roles in plant defense responses. *The Plant Journal, 27*, 529-538.

Prinsen, H.C.M.T., Schiebergen-Bronkhorst, B.G.M., Roeleveld, M.W., Jans, J.J.M., de Sain-van der Velden, M.G.M., Visser, G., van Hasselt, P.M., Verhoeven-Duif, N.M., 2016. Rapid quantification of underivatized amino acids in plasma by hydrophilic interaction liquid chromatography (HILIC) coupled with tandem mass-spectrometry. *Journal of Inherited Metabolic Disease, 39,* 651-660.

Quan, R., Shang, M., Zhang, H., Zhao, Y., Zhang, J., 2004. Engineering of enhanced glycine betaine synthesis improves drought tolerance in maize. *Plant Biotechnology Journal, 2,* 477-486.

Quilambo, O., Scott, P., 2004. Proline content, water retention capability and cell membrane integrity as parameters for drought tolerance in two peanut cultivars. *South African Journal of Botany, 70,* 227-234.

Rabilloud, T., Lelong, C., 2011. Two-dimensional gel electrophoresis in proteomics: A tutorial. *Journal of Proteomics, 74,* 1829-1841.

Rajarajan, K., Ganeshamurthy, K., 2011. Genetic diversity analysis of sorghum [*Sorghum bicolor* (L.) Moench] genotypes for drought tolerance using SSR markers. *Indian Journal of Genetics and Plant Breeding, 71,* 17-24

Ramulifho, E., 2017. Proteomic mapping of the *Sorghum bicolor* (L.) Moench cell suspension culture secretome and identification of its drought stress responsive proteins. Masters thesis. University of the Free State, South Africa.

Reape, T.J., Molony, E.M., McCabe, P.F., 2008. Programmed cell death in plants: distinguishing between different modes. *Journal of Experimental Botany, 59,* 435-444.

Rensink, W., Buell, C., 2004. Arabidopsis to rice. Applying knowledge from a weed to enhance our understanding of a crop species. *Plant Physiology, 135,* 622-629.

Rosenow, D., Quisenberry, J., Wndt, C., Clark, L., 1983. Drought tolerant sorghum and cotton germplasm. *Agricultural Water Management, 7,* 207-222.

Ross, P.L., Huang, Y.N., Marchese, J.N., Williamson, B., Parker, K., Hattan, S., Khainovski, N., Pillai, S., Dey, S., Daniels, S., 2004. Multiplexed protein quantitation in *Saccharomyces cerevisiae* using amine-reactive isobaric tagging reagents. *Molecular and Cellular Proteomics, 3,* 1154-1169.

Roychoudhury, A., Paul, S., Basu, S., 2013. Cross-talk between abscisic acid-dependent and abscisic acid-independent pathways during abiotic stress. *Plant Cell Reports, 32,* 985-1006.

Sakuma, Y., Maruyama, K., Qin, F., Osakabe, Y., Shinozaki, K., Yamaguchi-Shinozaki, K., 2006. Dual function of an Arabidopsis transcription factor *DREB2A* in water-stress-responsive and heat-stress-responsive gene expression. *Proceedings of the National Academy of Sciences, 103,* 18822-18827.

Salekdeh, G., Komatsu, S., 2007. Crop proteomics: aim at sustainable agriculture of tomorrow. *Proteomics, 7,* 2976–2996.

Salekdeh, G.H., Reynolds, M., Bennett, J., Boyer, J., 2009. Conceptual framework for drought phenotyping during molecular breeding. *Trends in Plant Science, 14,* 488-496.

Salekdeh Gh. Hosseini, Siopongco Joel, Wade Leonard J., Ghareyazie Behzad, Bennett John, 2002. Proteomic analysis of rice leaves during drought stress and recovery. *Proteomics, 2,* 1131-1145.

Santamaria, J., Ludlow, M., Fukai, S., 1990. Contribution of osmotic adjustment to grain yield in *Sorghum bicolor* (L.) Moench under water-limited conditions. I. Water stress before anthesis. *Australian Journal of Agricultural Research, 41,* 51-65.

Schittenhelm, S., Schroetter, S., 2014. Comparison of drought tolerance of maize, sweet sorghum and sorghum-sudangrass hybrids. *Journal of Agronomy and Crop Science, 200,* 46-53.

Seiler, C., Harshavardhan, V.T., Rajesh, K., Reddy, P.S., Strickert, M., Rolletschek, H., Scholz, U., Wobus, U., Sreenivasulu, N., 2011. ABA biosynthesis and degradation contributing to ABA homeostasis during barley seed development under control and terminal drought-stress conditions. *Journal of Experimental Botany, 62,* 2615-2632.

Seki, M., Narusaka, M., Abe, H., Kasuga, M., Yamaguchi-Shinozaki, K., Carninci, P., Hayashizaki, Y., Shinozaki, K., 2001. Monitoring the expression pattern of 1300 Arabidopsis genes under drought and cold stresses by using a full-length cDNA microarray. *Plant Cell, 13,* 61-72.

Seki, M., Narusaka, M., Ishida, J., Nanjo, T., Fujita, M., Oono, Y., Kamiya, A., Nakajima, M, Enju, A., Sakurai, T., Satou, M., Akiyama, K., Taji, T., Yamaguchi-Shinozaki, K., Carninci, P., Kawai, J., Hayashizaki, Y., Shinozaki, K., 2002. Monitoring the expression profiles of 7000 Arabidopsis genes under drought, cold and high-salinity stresses using a full-length cDNA microarray. *The Plant Journal, 31,* 279-292.

Sgherri, C.L.M., Navari-Izzo, F., 1995. Sunflower seedlings subjected to increasing water deficit stress: oxidative stress and defence mechanisms. *Physiologia Plantarum, 93,* 25-30.

Shi, J., Chen, Y., Xu, Y., Ji, D., Chen, C., Xie, C., 2017. Differential proteomic analysis by iTRAQ reveals the mechanism of *Pyropia haitanensis* responding to high temperature stress. *Scientific Reports, 7,* 1-11.

Shinozaki, K., Yamaguchi-Shinozaki, K., 2007. Gene networks involved in drought stress response and tolerance. *Journal of Experimental Botany, 58,* 221-227.

Shinozaki, K., Yamaguchi-Shinozaki, K., 2000. Molecular responses to dehydration and low temperature: differences and cross-talk between two stress signaling pathways. *Current Opinion in Plant Biology, 3,* 217-223.

Shinozaki, K., Yamaguchi-Shinozaki, K., 1997. Gene expression and signal transduction in water-stress response. *Plant Physiology, 115,* 327-334.

Shinozaki, K., Yamaguchi-Shinozaki, K., Seki, M., 2003. Regulatory network of gene expression in the drought and cold stress responses. *Current Opinion in Plant Biology, 6,* 410–417.

Siddique, M., Hamid, A., Islam, M., 2000. Drought stress effects on water relations of wheat. *Botanical Bulletin of Academia Sinica. 41,* 35-39.

Silva, J.C., Gorenstein, M.V., Li, G.Z., Vissers, J.P and Geromanos, 2006. Absolute quantification of proteins by LCMSE; a virtue of parallel MS acquisition, *Molecular Cell Proteomics,* 5, 144-156.

Sivaramakrishnan, S., Patell, V.Z., Flower, D. J., Peacock, J. M., 1988. Proline accumulation and nitrate reductase activity in contrasting sorghum lines during mid-season drought stress. *Physiologia Plantarum, 74*, 418-426.

Smirnoff, N., Cumbes, Q.J., 1989. Hydroxyl radical scavenging activity of compatible solutes. *Phytochemistry, 28,* 1057-1060.

Smith, S.J., Kroon, J.T., Simon, W.J., Slabas, A.R., Chivasa, S., 2015. A novel function for Arabidopsis *CYCLASE1* in programmed cell death revealed by isobaric tags for relative and absolute quantitation (iTRAQ) analysis of extracellular matrix proteins. *Molecular & Cellular Proteomics, 14,* 1556-1568.

Śniegowska-Świerk, K., Dubas, E., Rapacz, M., 2015. Drought-induced changes in the actin cytoskeleton of barley (*Hordeum vulgare* L.) leaves. *Acta Physiologiae Plantarum, 37*, 1-13

Stern, K.R., Bidlack, J.E., Jansky, S., Uno, G., 2000. *Introductory Plant Biology*. McGraw-Hill, Iowa.

Swami, A.K., Alam, S.I., Sengupta, N., Sarin, R., 2011. Differential proteomic analysis of salt stress response in *Sorghum bicolor* leaves. *Environmental and Experimental Botany, 71*, 321-328.

The Arabidopsis Genome Initiative, 2000. Analysis of the genome sequence of flowering plant *Arabidopsis thaliana*. *Nature, 408*, 796-815.

Theimer, R., Beevers, H., 1971. Uricase and allantoinase in glyoxysomes. *Plant Physiology, 47*, 246–251.

Thomas, M.C., Chiang, C.-M., 2006. The general transcription machinery and general cofactors. *Critical Reviews in Biochemistry and Molecular Biology, 41*, 105-178.

Thompson, A., Schäfer, J., Kuhn, K., Kienle, S., Schwarz, J., Schmidt, G., Neumann, T., Hamon, C., 2003. Tandem mass tags: a novel quantification strategy for comparative analysis of complex protein mixtures by MS/MS. *Analytical Chemistry, 75*, 1895-1904.

Tully, R.E., Hanson, A.D., Nelsen, C.E., 1979. Proline accumulation in water-stressed barley leaves in relation to translocation and the nitrogen budget. *Plant Physiology, 63,* 518-523.

Vahdati, K., Leslie, C., 2013. Abiotic stresses, plant responses and applications in agriculture. *InTech*, Rijeka.

Valadez-Bustos, M.G., Aguado-Santacruz, G.A., Tiessen-Favier, A., Robledo-Paz, A., Muñoz-Orozco, A., Rascón-Cruz, Q., Santacruz-Varela, A., 2016. A reliable method

for spectrophotometric determination of glycine betaine in cell suspension and other systems. *Analytical Biochemistry, 498,* 47-52.

Van Loon, L., Pierpoint, W., Boller, T., Conejero, V., 1994. Recommendations for naming plant pathogenesis-related proteins. *Plant Molecular Biology Reporter, 12,* 245–264.

Van Wijk, K., 2001. Challenges and Prospects of Plant Proteomics. *Plant Physiology 126,* 501-508.

Verslues, P.E., Agarwal, M., Katiyar-Agarwal, S., Zhu, J., Zhu, J., 2006. Methods and concepts in quantifying resistance to drought, salt and freezing, abiotic stresses that affect plant water status. *The Plant Journal, 45,* 523-539.

Vidal, N., Barbosa, H., Jacob, S., Arruda, M., 2015. Comparative study of transgenic and non-transgenic maize (*Zea mays*) flours commercialized in Brazil, focussing on proteomic analyses. *Food Chemistry, 180,* 288-294.

Vineeth, T., Kumar, P., Krishna, G., 2016. Bioregulators protected photosynthetic machinery by inducing expression of photorespiratory genes under water stress in chickpea. *Photosynthetica, 54,* 234-242.

Vranova, E., Inzé, D., Van Breusegem, F., 2002. Signal transduction during oxidative stress. *Journal of Experimental Botany, 53,* 1227-1236.

Waldren, R.P., Teare, I.D., 1974. Free proline accumulation in drought-stressed plants under laboratory conditions. *Plant and Soil, 40,* 689-692.

Wang, H., Miyazaki, S., Kawai, K., Deyholos, M., Galbraith, D.W., Bohnert, H.J., 2003a. Temporal progression of gene expression responses to salt shock in maize roots. *Plant Molecular Biology, 52,* 873-891.

Wang, W., Vinocur, B., Altman, A., 2003b. Plant responses to drought, salinity and extreme temperatures: Towards genetic engineering for stress tolerance. *Planta, 218,* 1-14.

Wang, W., Vinocur, B., Shoseyov, O., Altman, A., 2004. Role of plant heat-shock proteins and molecular chaperones in the abiotic stress response. *Trends in Plant Science 9,* 244-252.

Wang, Z.Q., Xu, X.Y., Gong, Q.Q., Xie, C., Fan, W., Yang, J.L., Lin, Q.S., Zheng, S.J., 2014. Root proteome of rice studied by iTRAQ provides integrated insight into aluminum stress tolerance mechanisms in plants. *Journal of Proteomics, 98,* 189-205.

Wei, P., Yang, Y., Wang, F., Chen, H., 2015. Effects of drought stress on the antioxidant systems in three species of *Diospyros* L. *Horticulture, Environment, and Biotechnology, 56,* 597-605.

Weigel, D., 2012. Natural variation in Arabidopsis: from molecular genetics to ecological genomics. *Plant Physiology, 158,* 2-22.

Wendelboe-Nelson, C., Morris, P.C., 2012. Proteins linked to drought tolerance revealed by DIGE analysis of drought resistant and susceptible barley varieties. *Proteomics, 12,* 3374-3385.

Wilkins, O., Hafemeister, C., Plessis, A., Holloway-Phillips, M.-M., Pham, G.M., Nicotra, A.B., Gregorio, G.B., Jagadish, K., Septiningsih, E.M., Bonneau, R., 2016. EGRINs (Environmental Gene Regulatory Influence Networks) in rice that function in the response to water deficit, high temperature, and agricultural environments. *The Plant Cell, 28*, 2365-2384.

Winter, P., Kahl, G., 1995. Molecular marker technologies for plant improvement. *World Journal of Microbiology and Biotechnology, 11,* 438-448.

Xie, H., Yang, D.-H., Yao, H., Bai, G., Zhang, Y.-H., Xiao, B.-G., 2016. iTRAQ-based quantitative proteomic analysis reveals proteomic changes in leaves of cultivated tobacco (*Nicotiana tabacum*) in response to drought stress. *Biochemical and Biophysical Research Communications, 469*, 768-775.

Xiong, L., Zhu, J., 2001. Abiotic stress signal transduction in plants: molecular and genetic perspectives. *Physiologia Plantarum, 112*, 152-166.

Xu, C., Huang, B., 2010. Comparative analysis of drought responsive proteins in Kentucky bluegrass cultivars contrasting in drought tolerance. *Crop Science, 50,* 2543-2552.

Xu, D., Duan, X., Wang, B., Hong, B., Ho, T.-H.D., Wu, R., 1996. Expression of a late embryogenesis abundant protein gene, *HVA1*, from barley confers tolerance to water deficit and salt stress in transgenic rice. *Plant Physiology, 110,* 249-257.

Xu, X., Bland, W.L., 1993. Reverse water flow in sorghum roots. *Agronomy Journal, 85,* 384-388.

Yamaguchi-Shinozaki, K., Shinozaki, K., 2006. Transcriptional regulatory networks in cellular responses and tolerance to dehydration and cold stresses. *Annual Review of Plant Biology, 57,* 781-803.

Yan, J.X., Devenish, A.T., Wait, R., Stone, T., Lewis, S., Fowler, S., 2002. Fluorescence two-dimensional difference gel electrophoresis and mass spectrometry based proteomic analysis of *Escherichia coli*. *Proteomics, 2,* 1682-1698.

Yang, H.-B., Kang, W.-H., Nahm, S.-H., Kang, B.-C., 2015. Methods for developing molecular markers, in: C*urrent technologies in plant molecular breeding*. Springer, pp. 15-50.

Yang, L., Fountain, J.C., Wang, H., Ni, X., Ji, P., Lee, R.D., Kemerait, R.C., Scully, B.T., Guo, B., 2015. Stress sensitivity is associated with differential accumulation of reactive oxygen and nitrogen species in maize genotypes with contrasting levels of drought tolerance. *International Journal of Molecular Sciences, 16*, 24791-24819.

Yang, W.-J., Rich, P.J., Axtell, J.D., Wood, K.V., Bonham, C.C., Ejeta, G., Mickelbart, M.V., Rhodes, D., 2003. Genotypic variation for glycinebetaine in sorghum. *Crop Science, 43,* 162-169.

Yokota, A., Kawasaki, S., Iwano, M., Nakamura, C., Miyake, C., Akashi, K., 2002. Citrulline and DRIP-1 protein (*ArgE* homologue) in drought tolerance of wild watermelon. *Annals of Botany, 89*, 825-832.

You, J., Chan, Z., 2015. ROS regulation during abiotic stress responses in crop plants. *Frontiers in Plant Science, 6*, 1-15.

Yu, T., Li, G., Dong, S., Liu, P., Zhang, J., Zhao, B., 2016. Proteomic analysis of maize grain development using iTRAQ reveals temporal programs of diverse metabolic processes. *BMC Plant Biology, 16,* 1-14.

Zadražnik, T., Hollung, K., Egge-Jacobsen, W., Meglič, V., Šuštar-Vozlič, J., 2013. Differential proteomic analysis of drought stress response in leaves of common bean (*Phaseolus vulgaris* L.). *Journal of Proteomics, 78,* 254-272.

Zhang, J., Kirkham, M., 1996. Antioxidant responses to drought in sunflower and sorghum seedlings. *New Phytologist, 132,* 361-373.

Zhang, W., Peumans, W.J., Barre, A., Houles Astoul, C., Rovira, P., Rougé, P., Proost, P., Truffa-Bachi, P., Jalali, A.A.H., Van Damme, E.J.M., 2000. Isolation and characterization of a jacalin-related mannose-binding lectin from salt-stressed rice (*Oryza sativa*) plants. *Planta, 210,* 970-978.

Zhao, Y., Du, H., Wang, Z., Huang, B., 2011. Identification of proteins associated with water-deficit tolerance in C_4 perennial grass species, *Cynodon dactylon*× *Cynodon transvaalensis* and *Cynodon dactylon*. *Physiologia Plantarum, 141*, 40-55.

Zhong, X., Wang, Z.Q., Xiao, R., Wang, Y., Xie, Y., Zhou, X., 2017. iTRAQ analysis of the tobacco leaf proteome reveals that RNA-directed DNA methylation (*RdDM*) has important roles in defense against geminivirus-betasatellite infection. *Journal of Proteomics, 152*, 88-101.

Zhou, D., Yang, Y., Zhang, J., Jiang, F., Craft, E., Thannhauser, T.W., Kochian, L.V., Liu, J., 2016. Quantitative iTRAQ proteomics revealed possible roles for antioxidant proteins in sorghum aluminum tolerance. *Frontiers in Plant Science, 7,* 1-14.

Zhou, S., Bailey, M.J., Dunn, M.J., Preedy, V.R., Emery, P.W., 2005. A quantitative investigation into the losses of proteins at different stages of a two-dimensional gel electrophoresis procedure. *Proteomics, 5,* 2739-2747.

Zhou, S., Palmer, M., Zhou, J., Bhatti, S., Howe, K.J., Fish, T., Thannhauser, T.W., 2013. Differential root proteome expression in tomato genotypes with contrasting drought tolerance exposed to dehydration. *Journal of the American Society for Horticultural Science, 138*, 131-141.

Zieske, L.R., 2006. A perspective on the use of iTRAQ^{TM} reagent technology for protein complex and profiling studies. *Journal of Experimental Botany, 57*, 1501–1508.

Zorca, S.M., Zorca, C.E., 2011. Bicentennial: The legacy of a founding father of modern cell biology: George Emil Palade (1912-2008). *The Yale Journal of Biology and Medicine, 84,* 113-116.

Zou, J., Liu, C., Chen, X., 2011. Proteomics of rice in response to heat stress and advances in genetic engineering for heat tolerance in rice. *Plant Cell Reports, 30,* 2155-2165.

APPENDICES

One-Dimensional (1D) Sodium Dodecyl Sulfate-Polyacrylamide Gel Electrophoresis (SDS-PAGE) preparation.

Table A1: Preparation of BSA standard solutions for protein quantification.

BSA final concentration (mg/ml)	BSA 5 mg/ml stock solution (µl)	Urea extraction buffer (µl)	0.1 M HCl (µl)	Distilled water (µl)
0*	0	10	10	80
5	1	9	10	80
10	2	8	10	80
20	4	6	10	80
40	8	2	10	80
50	10	0	10	80

*blank solution

Table A2: Preparation of resolving and stacking gels for gel electrophoresis.

	Resolving gel 12% (v/v)	Stacking gel 5% (v/v)
Distilled water	4.3mL	3.6mL
40% Acryl-bisacrylamide mix	3mL	0.625mL
0.5M Tris-HCL (pH 6.8)	-	0.63mL
1.5M Tris-HCL (pH 8.8)	2.5mL	-
10% SDS	0.1mL	0.05mL
10% APS	0.1mL	0.05mL
TEMED	0.006mL	0.005mL
Total volume	**10 mL**	**5 mL**

Heat-map showing the up-regulation and down-regulation of the 871 proteins common to both ICSB 338 and SA 1441.

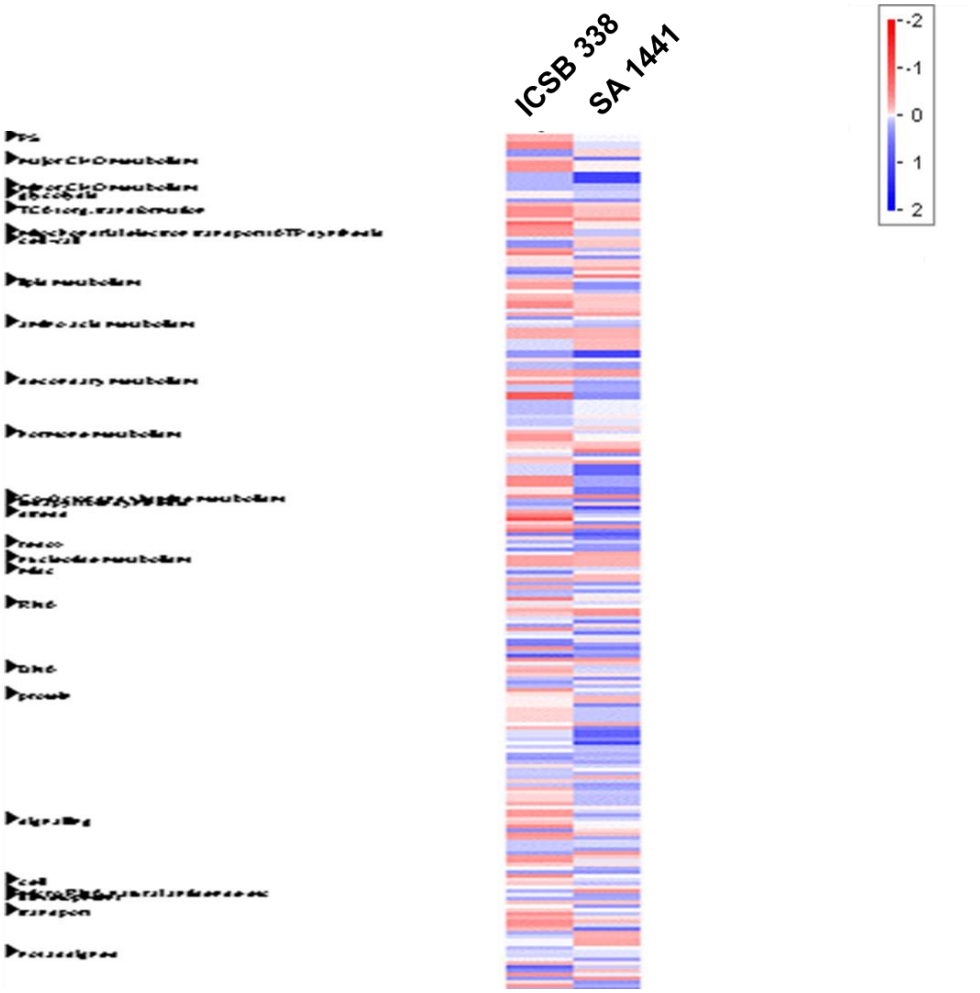

Figure A1: Heat-map showing the up-regulation and down-regulation of the 871 proteins common to both ICSB 338 and SA 1441. Each band shows a cluster of proteins in ICSB 338 and their corresponding SA 1441 proteins. The intensity of the red and blue colours represent down-regulation and up-regulation of proteins, respectively.

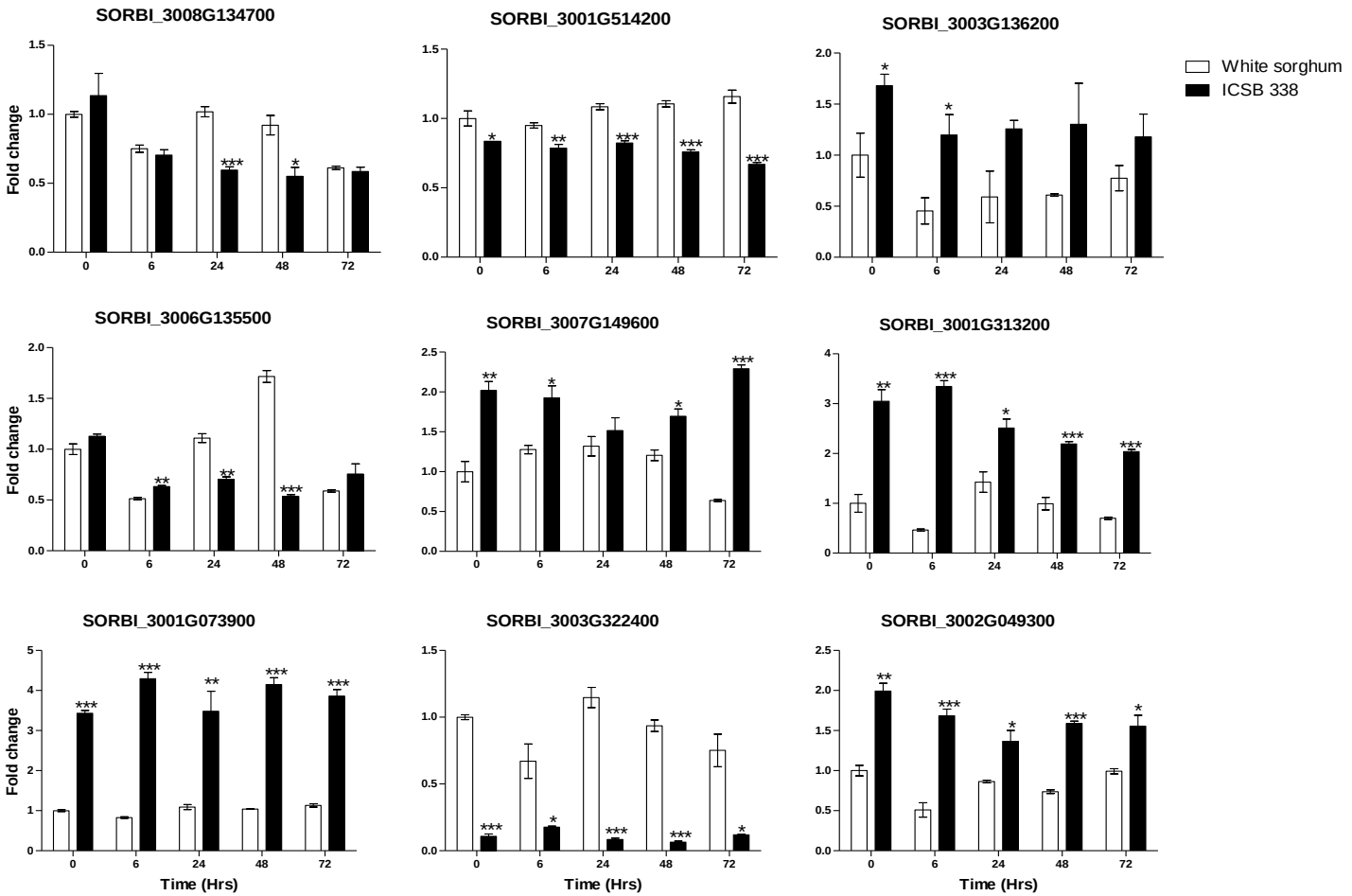

Figure B1: Sorbitol-induced gene expression in sorghum cell suspension cultures. The White sorghum (unknown) and ICSB 338 (drought susceptible) cell suspension cultures were exposed to osmotic stress by exposure to 0.4 M sorbitol and the cells were harvested at the indicated time points. Gene expression analysis was performed using RT-qPCR. Bars represent mean ± SE (n=3). *, ** and *** = significant differences between ICSB 338 and White sorghum means at each time point at $p \leq 0.05$, 0.01 and 0,001, respectively.

Arabidopsis homologues of sorghum genes.

Table B1: Arabidopsis homologues of sorghum genes.

Gene Code	Gene Name	Expected
Thioredoxin (SORBI_3009G190800)		
AT5G42980.1	TRX3	9e-39
AT1G45145.1	TRX5	3e-38
AT3G51030.1	TRX1	2e-34
AT1G19730.1	ATTRX4	2e-32
AT3G17880.2	ATTDX	1e-22
AT3G17880.1	ATTDX	2e-22
AT5G39950.1	TRX2	1e-21
AT3G56420.3	no symbol available	1e-21
AT3G56420.2	no symbol available	1e-21
AT3G08710.3	ATH9	2e-21
AT3G08710.2	ATH9	2e-21
AT3G08710.1	ATH9	2e-21
AT1G59730.1	TH7	2e-19
AT2G40790.2	CXXS2	2e-18
AT2G40790.1	CXXS2	2e-18
AT1G11530.1	CXXS1	3e-18
AT1G69880.1	ATH8	1e-17
AT2G35010.2	ATO1	9e-15
AT2G35010.1	ATO1	9e-15
AT4G26160.1	no symbol available	2e-14
AT1G31020.1	ATO2	3e-13
AT4G29670.2	ACHT2	6e-13
AT4G29670.1	ACHT2	6e-13
AT1G43560.1	Aty2	1e-12
AT5G16400.1	TRXF2	1e-12
AT3G15360.1	ATM4	5e-12
AT1G03680.1	ATHM1	6e-12
AT3G02730.1	TRXF1	6e-12
AT1G76760.1	ATY1	4e-11
AT5G61440.1	ACHT5	4e-11
AT4G04950.1	AtGRXS17	6e-11

AT1G76080.1	CDSP32	8e-11
AT4G03520.1	ATHM2	8e-11
AT5G61440.2	ACHT5	1e-10
AT3G53220.1	no symbol available	3e-10
AT4G32580.1	no symbol available	4e-09
AT4G37200.1	HCF164	7e-09
AT1G52990.1	no symbol available	8e-09
AT2G33270.1	ACHT3	2e-08
AT5G60640.3	PDI2	2e-08
AT1G08570.1	ACHT4	3e-08
AT1G08570.2	ACHT4	4e-08
AT1G08570.4	ACHT4	4e-08
AT1G08570.3	ACHT4	4e-08
AT5G60640.2	PDI2	4e-08
AT5G60640.1	PDI2	5e-08
AT1G07700.4	no symbol available	8e-08
AT1G07700.2	no symbol available	8e-08
AT1G07700.1	no symbol available	8e-08
AT1G50320.1	ATHX	8e-08
AT1G07700.3	no symbol available	1e-07
AT5G06690.1	WCRKC1	4e-07
AT2G47470.1	UNE5	4e-07
AT2G15570.2	ATHM3	5e-07
AT2G47470.4	UNE5	5e-07
AT2G47470.3	UNE5	6e-07
AT2G15570.1	ATHM3	6e-07
AT2G47470.2	UNE5	7e-07
AT1G53300.1	TTL1	9e-07
AT3G06730.1	TRX z	3e-06
AT1G77510.1	ATPDI6	5e-06
AT1G21750.1	PDIL1-1	1e-05
AT1G21750.2	PDIL1-1	4e-05
AT5G04260.1	WCRKC2	5e-05
AT2G42580.1	TTL3	2e-04
AT2G01270.1	QSOX2	5e-04
AT2G41680.1	NTRC	5e-04

AT3G25580.1	no symbol available	6e-04
AT4G12170.1	no symbol available	6e-04
AT3G54960.2	PDI1	6e-04
AT1G04980.1	PDIL2-2	6e-04
AT3G54960.1	PDI1	6e-04
AT3G25580.2	no symbol available	6e-04
AT4G03520.2	ATHM2	7e-04
AT3G58620.1	TTL4	7e-04
AT1G35620.1	ATPDIL5-2	7e-04
AT2G18990.1	TXND9	0.002
AT2G32920.1	PDIL2-3	0.002
AT3G14950.1	TTL2	0.003
AT3G16110.1	ATPDIL1-6	0.005
AT5G18120.2	ATAPRL7	0.007
AT5G18120.3	ATAPRL7	0.007
AT5G18120.1	ATAPRL7	0.008
AT3G03860.1	ATAPRL5	0.010
AT1G60420.1	AtNRX1	0.011
AT4G27080.2	PDIL5-4	0.011
AT4G27080.1	PDIL5-4	0.011
AT1G15020.2	QSOX1	0.012
AT1G15020.3	QSOX1	0.015
AT1G15020.1	QSOX1	0.015
AT1G52260.1	PDI3	0.074
AT4G08930.1	ATAPRL6	0.077
AT3G50960.2	PLP3a	0.11
AT3G50960.1	PLP3a	0.11
AT1G34780.1	ATAPRL4	0.17
AT5G66410.1	PLP3b	0.17
AT1G07960.4	ATPDIL5-1	0.45
AT1G07960.3	ATPDIL5-1	0.45
AT1G07960.2	ATPDIL5-1	0.45
AT1G07960.1	ATPDIL5-1	0.45
AT4G31240.2	NRX2	0.45
AT4G31240.1	NRX2	0.45
AT4G21990.1	PRH26	0.66

AT4G04610.1	APR	0.94
AT1G62180.2	APSR	2.0
AT1G62180.1	APSR	2.1
AT5G08290.1	YLS8	3.8
AT3G48170.1	ALDH10A9	4.2
AT3G44680.1	HDA09	4.5
AT1G56500.3	SOQ1	5.0
AT1G56500.2	SOQ1	5.0
AT1G56500.1	SOQ1	5.3
AT1G45100.1	no symbol available	9.9

Peptidase (SORBI_3007G172100)

AT5G50260.1	CEP1	e-134
AT3G48350.1	CEP3	e-119
AT3G48340.1	CEP2	e-118
AT4G35350.1	XCP1	e-100
AT1G20850.1	XCP2	2e-99
AT4G36880.1	CP1	6e-99
AT1G47128.1	RD21	2e-97
AT5G43060.1	RD21B	4e-97
AT3G19390.1	no symbol available	6e-92
AT5G45890.1	SAG12	8e-90
AT3G19400.1	no symbol available	7e-86
AT4G23520.1	no symbol available	2e-85
AT3G48350.2	CEP3	3e-84
AT1G06260.1	no symbol available	5e-84
AT2G27420.1	no symbol available	8e-84
AT3G49340.1	no symbol available	1e-82
AT4G11320.2	AtCP2	1e-81
AT4G11320.1	AtCP2	1e-81
AT4G11310.1	CP1	2e-81
AT2G34080.1	no symbol available	1e-77
AT1G29080.1	no symbol available	3e-77
AT1G09850.1	XBCP3	6e-77
AT1G29090.1	no symbol available	3e-76
AT4G35350.2	XCP1	4e-71

AT3G43960.1	no symbol available	5e-70
AT1G29110.1	no symbol available	2e-62
AT3G19400.2	no symbol available	7e-61
AT3G45310.1	no symbol available	3e-54
AT5G60360.1	AALP	3e-54
AT3G45310.2	no symbol available	3e-52
AT5G60360.2	AALP	3e-52
AT5G60360.3	AALP	7e-51
AT4G16190.1	no symbol available	7e-48
AT4G39090.1	RD19	5e-47
AT3G54940.2	no symbol available	3e-46
AT2G21430.1	no symbol available	3e-46
AT3G54940.3	no symbol available	2e-33
AT4G01610.1	AtcathB3	4e-20
AT1G02305.1	AtcathB2	3e-19
AT4G01610.2	AtcathB3	2e-18
AT1G02300.	AtcathB1	1e-13
AT2G22160.1	no symbol available	2e-12
AT1G03720.2	no symbol available	6e-06
AT1G03720.1	no symbol available	2e-04
AT5G17140.1	no symbol available	4e-04
AT5G05050.1	no symbol available	5e-04
AT5G17080.1	no symbol available	0.12
AT3G44780.1	no symbol available	0.33
AT1G58250.1	HPS4	3.0
AT1G58250.2	HPS4	3.1
AT3G19720.1	ARC5	9.5

Xyloglucanase (SORBI_3002G302000)

AT2G36870.1	XTH32	e-103
AT3G44990.1	XTH31	3e-95
AT2G36870.2	XTH32	1e-56
AT1G14720.1	XTR2	1e-56
AT1G10550.1	XTH33	5e-55
AT1G32170.1	XTH30	2e-54
AT2G01850.1	XTH27	2e-54

AT3G25050.1	XTH3	3e-51
AT1G11545.1	XTH8	4e-51
AT2G06850.1	EXT	6e-51
AT4G18990.1	XTH29	2e-50
AT5G13870.3	EXGT-A4	3e-50
AT5G13870.2	EXGT-A4	3e-50
AT5G13870.1	XTH16	3e-50
AT3G23730.1	XTH13	3e-50
AT5G57540.1	XTR7	5e-50
AT4G14130.1	XTH12	2e-49
AT5G57530.1	XTH6	3e-49
AT5G65730.1	ATXTH14	4e-49
AT4G25820.1	XTH22	5e-49
AT5G57560.1	XTR6	7e-49
AT4G25810.1	MERI5B	2e-48
AT4G30270.1	ATXTH21	2e-47
AT2G18800.1	XTH25	2e-47
AT5G57550.1	XTH9	8e-47
AT4G03210.1	EXT	4e-46
AT2G06850.2	ATXTH20	2e-45
AT5G48070.1	XTH7	9e-45
AT4G37800.1	XTH2	9e-45
AT4G13090.1	XTH9	2e-44
AT4G03210.2	XTH1	1e-43
AT4G13080.1	ATXTH18	3e-43
AT4G30280.1	XTH26	5e-43
AT4G28850.1	XTH10	5e-43
AT2G14620.1	ATXTH19	3e-42
AT4G30290.1	XTH17	5e-42
AT1G65310.2	XTH17	4e-40
AT1G65310.1	XTH10	5e-40
AT2G14620.2	XTH29	1e-37
AT4G18990.2	XTH10	2e-35
AT2G14620.3	XTH11	2e-35
AT3G48580.1	XTH11	2e-33
AT3G48580.3	XTH11	4e-30

AT3G48580.2	EXPRS	2e-21
AT2G32170.1	no symbol available	0.060
AT2G32160.2	no symbol available	0.39
AT2G32160.1	no symbol available	0.41
AT2G32160.3	no symbol available	0.42
AT2G32160.4	no symbol available	0.42
AT1G76810.1	no symbol available	0.62
AT4G02040.1	no symbol available	5.2

Melt curves of genes used in this study.

Arabidopsis sorbitol-induced osmotic stress.

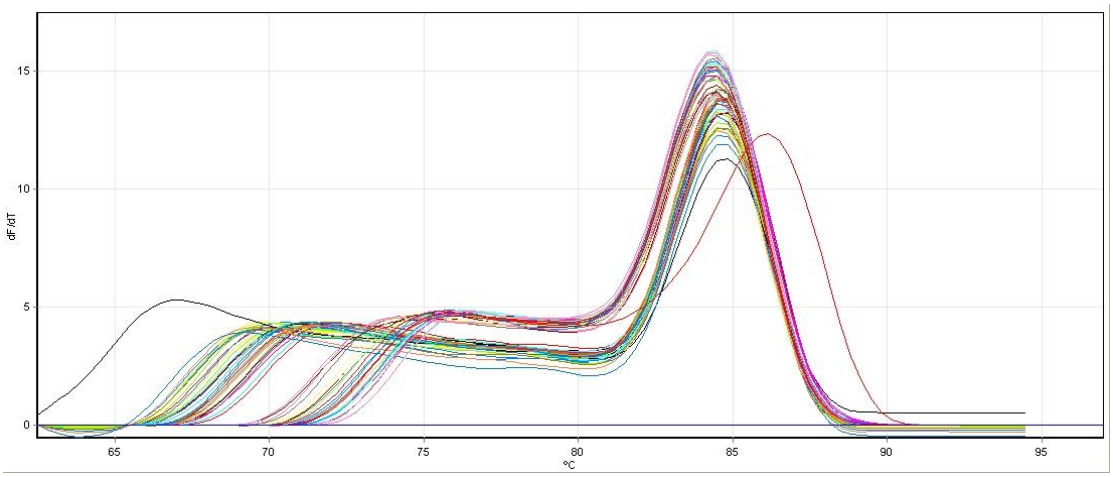

Figure C1: Act 2 and EIF4A

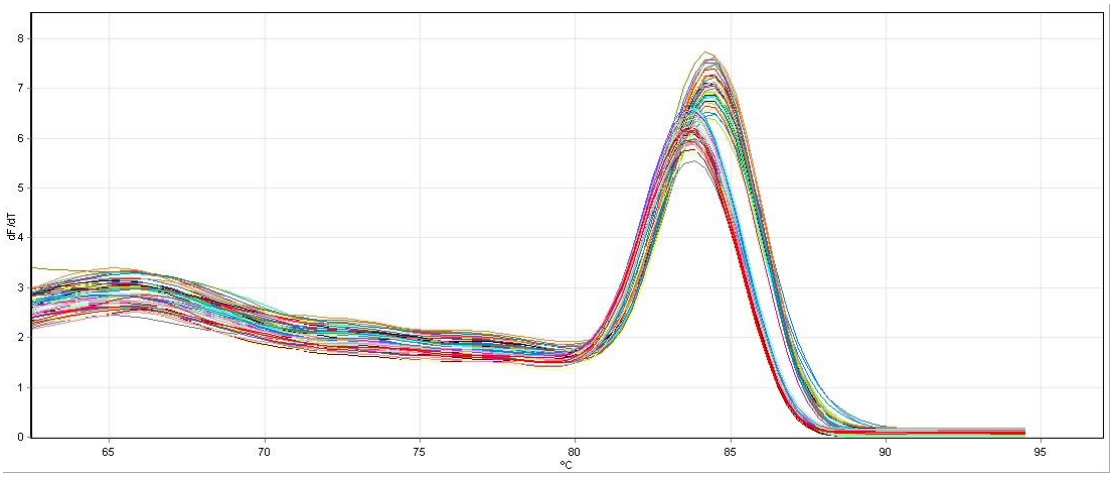

Figure C2: TRX1 and TRX3

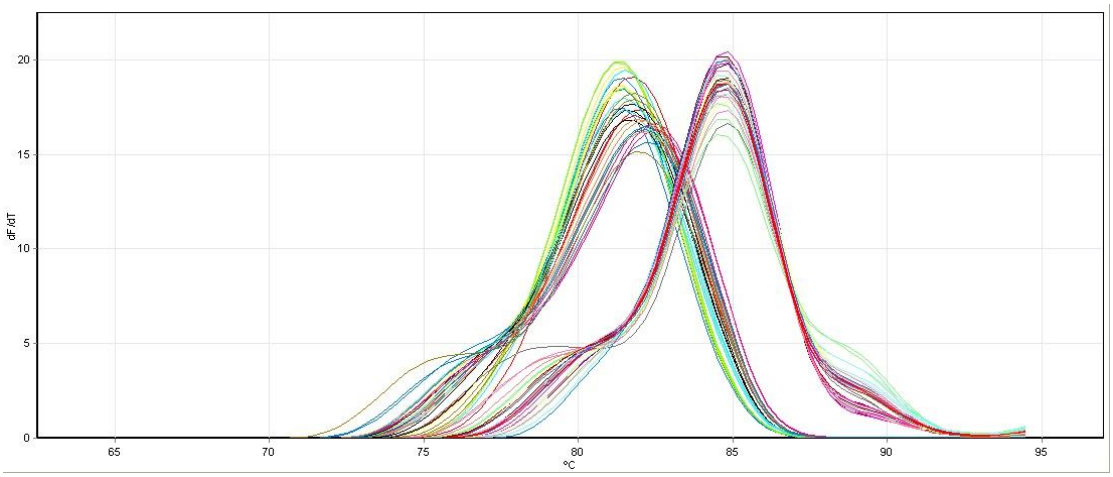

Figure C3:TRX5 and ATTRX4

Arabidopsis cell culture sorbitol-induced osmotic stress.

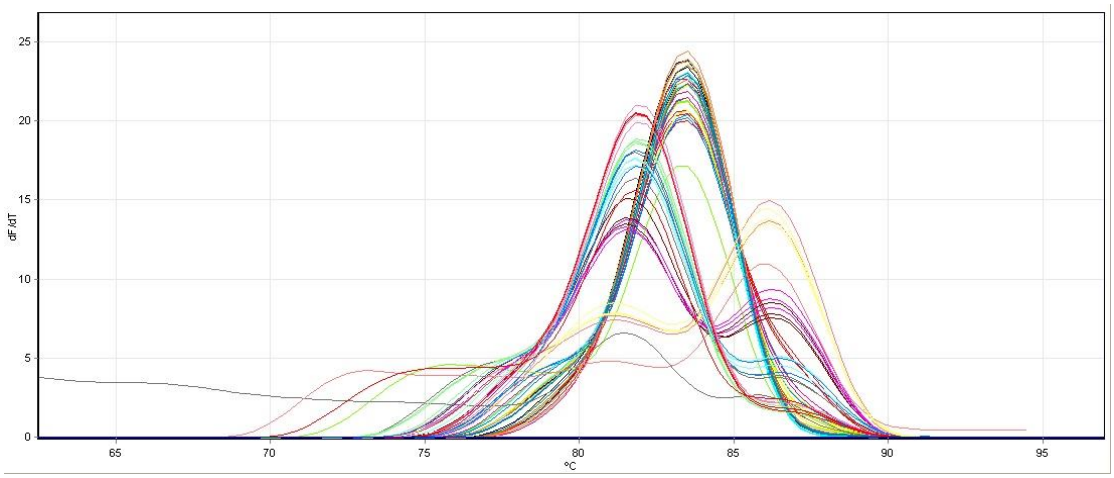

Figure C4: CEP1 and XCP1

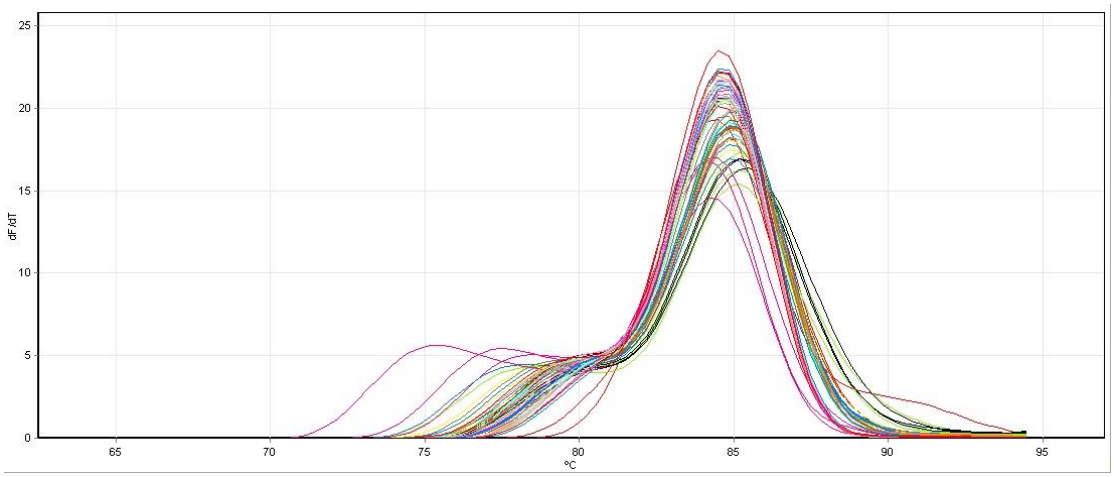

Figure C5: XCP2 and XTH31

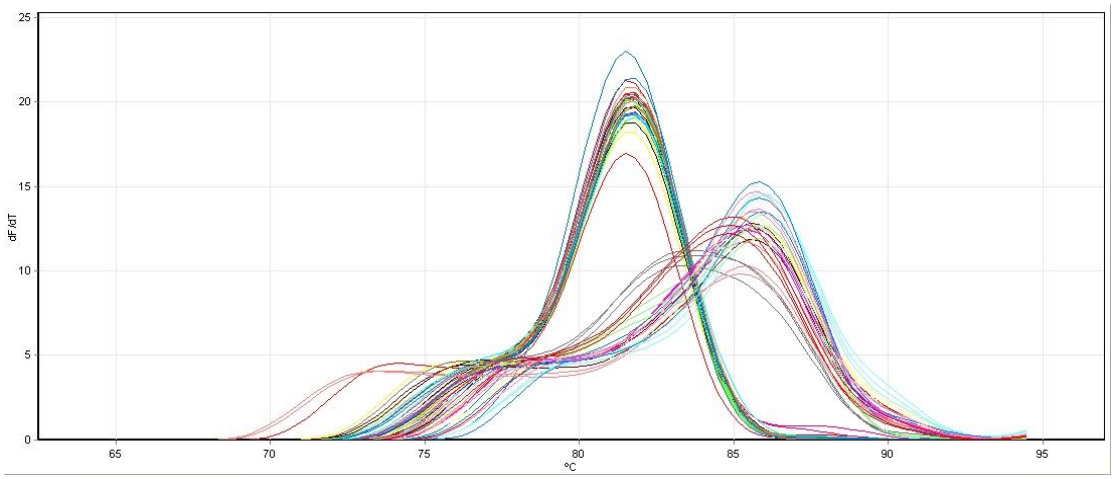

Figure C6: XTH32 and XTH33

Sorghum leaf tissue

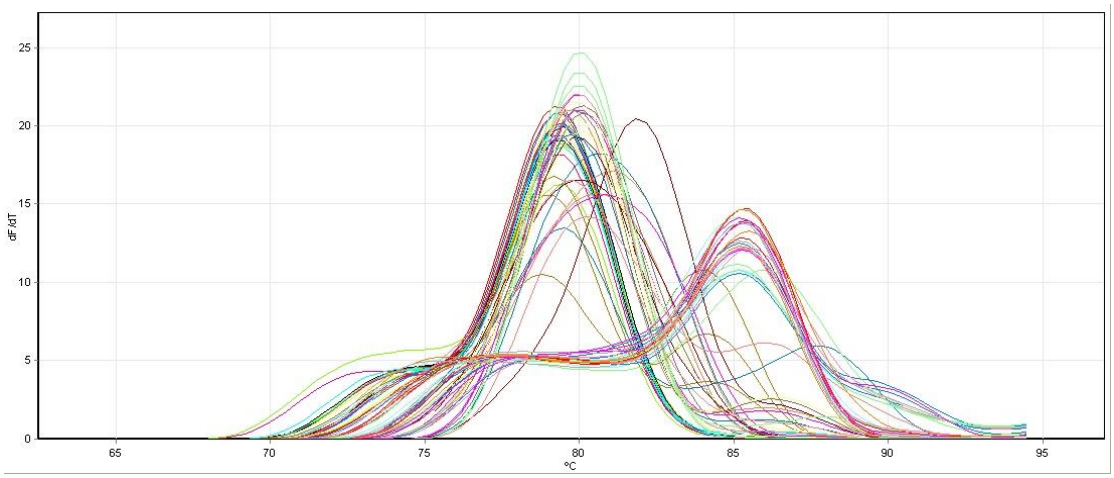

Figure C7: SORBI_3008G134700, SORBI_3001G514200 and SORBI_3003G136200

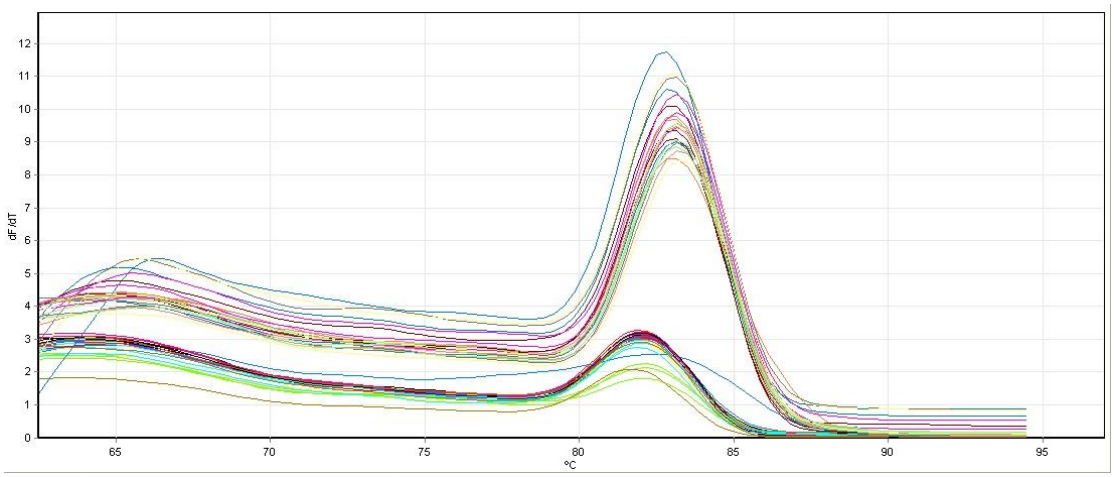

Figure C8: SORBI_3006G135500, SORBI_3007G149600 and SORBI_3001G313200

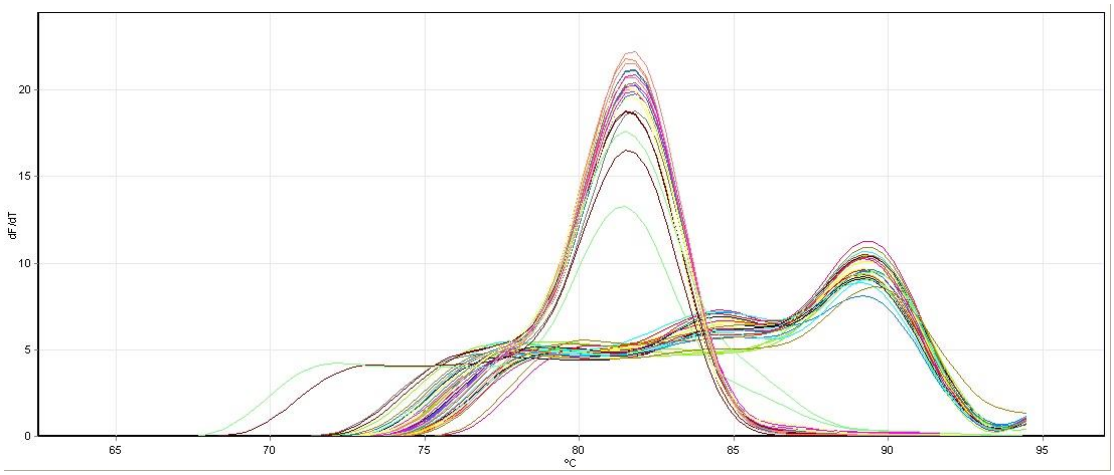

Figure C9: SORBI_3001G073900, SORBI_3003G322400 and SORBI_3002G049300

Sorghum root tissue

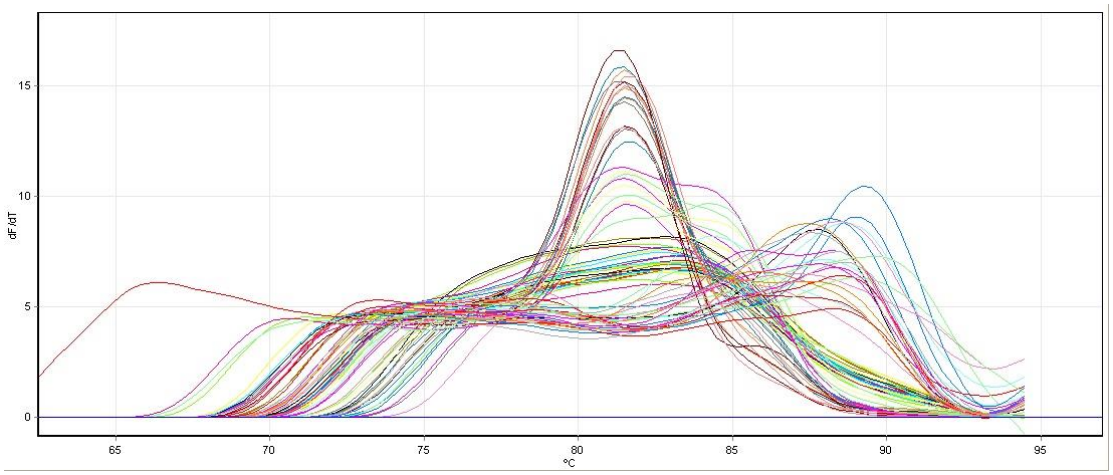

Figure C10: SORBI_3008G134700, SORBI_3001G514200 and SORBI_3003G136200

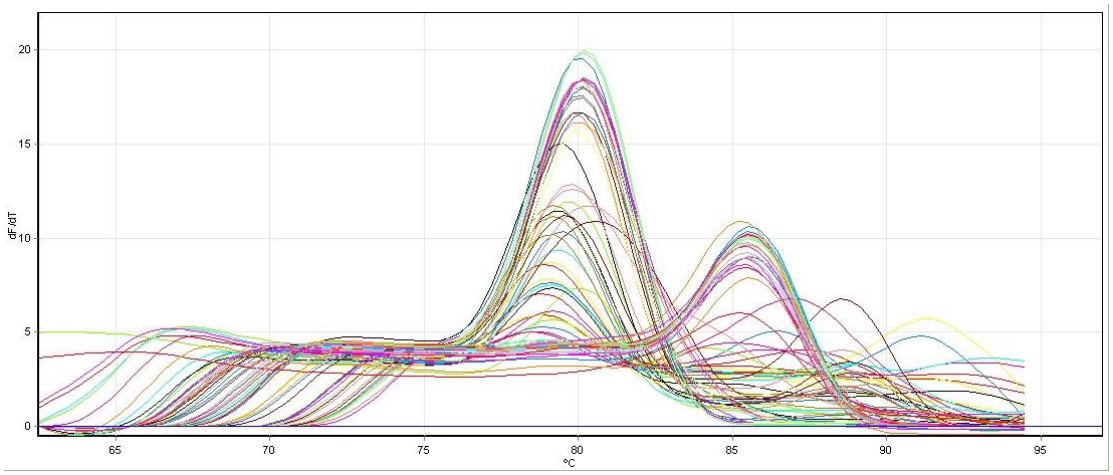

Figure C11: SORBI_3006G135500, SORBI_3007G149600 and SORBI_3001G313200

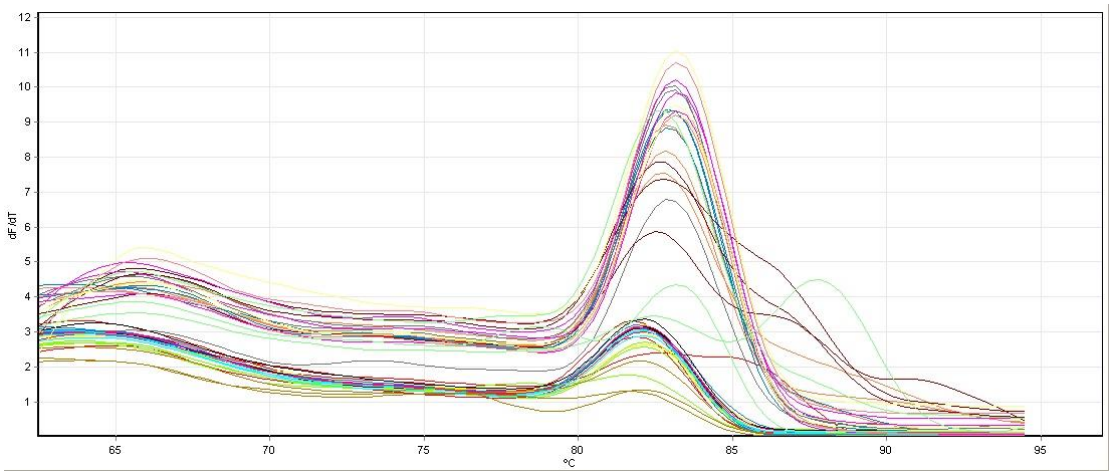

Figure C12: SORBI_3001G073900, SORBI_3003G322400 and SORBI_3002G049300

Sorghum cell cultures

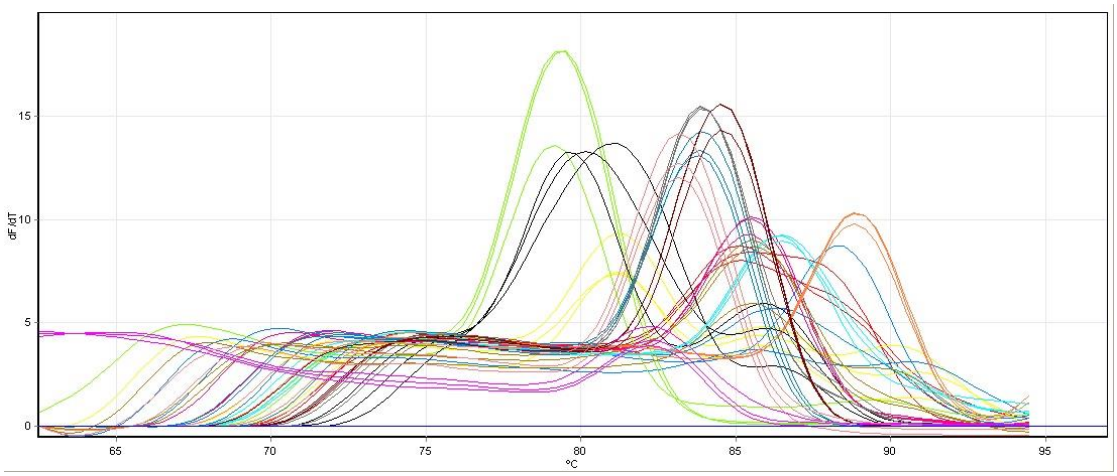

Figure C13: SORBI_3008G134700, SORBI_3001G514200, SORBI_3003G136200SORBI_3006G135500, SORBI_3007G149600, SORBI_3001G313200SORBI_3001G073900, SORBI_3003G322400, SORBI_3002G049300, DREB2A-1, ERD1-1, ERD1-2, Sb03g038910 and EIF4A.